The Dynamic Behaviour of Latch-Needles During Weft-Knitting

by

NEIL DEMPSTER BURNS B.Tech (Honours) (Brunel)

A Doctoral Thesis

Submitted in partial fulfilment of the requirements for the award of

the degree of Doctor of Philosophy of the Loughborough University of Technology.

April 1973.

Supervisor: Professor G.R. Wray, M.Sc.Tech., Ph.D (Manchester), C.Eng., M.I.Mech.E., A.M.C.S.T., F.T.I.

Department of Mechanical Engineering.

ACKNOWLEDGEMENTS

The author wishes to thank Professor Gordon R. Wray for his valued guidance, constructive criticisms, and helpful advice so readily made available throughout the course of the investigation. He also wishes to thank Mr. Peter M. Findlay, Mr. David Greenwood, and Mr. Graham Penny of Bentley Machine Development Company Limited, for their valued guidance and assistance at all times. He is indebted to Bentley Machine Development Company Limited, and to Professor B. Downs and the Department of Mechanical Engineering at Loughborough University of Technology, for making this combined and academic investigation possible, and for jointly providing comprehensive financial and technical support. It gives him pleasure to acknowledge the highly skilled help provided by Mr. P. Norton, Mr. K.M. Topley, Mr. B. Birch and many other members of the technical staffs of both the sponsoring company and the university; he is also indebted to his wife, Mrs. M. Burns, for typing the thesis.

ABSTRACT

The research described was initially concerned with the development, design, and manufacture of measuring instruments to facilitate a better understanding of the knitting process. Subsequently these instruments were used to measure the following physical properties :-

(i) the forces between a single needle and the cams during knitting;

(ii) the force exerted upon the verge and needle by the yarn during loop formation;

(iii) the impact forces when the needle first contacts the stitch and guard cams;

(vi) the frictional tension build-up as the yarn passes over the verges and needles;

and (v) the bounce of the needles on the cams. The steadier components of the cam-forces, impact forces, and yarn-tensions, were all theoretically analysed, and the subsequent predictions were compared with the experimental results.

The mechanism of needle fracture was examined. The wave propagation process in the needle shank, subsequent to impacts with the cams, was investigated using micro-miniature strain-gauges. A technique was developed which used dynamic photoelasticity to examine the wave passage through a needle model but the experimental work using the technique is uncomplete and will be continued as further work.

Non-linear stitch-cams and guard-cams were designed, within cam dimensions specified by the sponsoring company, so as to enable good quality fabric to be knitted at high speed whilst minimising the needle damage. Some recommendations were

made for the redesign of the needle elements, although it is expected that more comprehensive designs will evolve after the results of the dynamic photoelastic technique are available.

Finally, recommendations are made for extending the work to measurements on commercial cylinder and dial machines, using similar instrumentation to that developed in this investigation, with the intention of increasing knitting machine productivity.

CONTENTS

LIST OF ILLUSTRATIONS

Fig 20.3	Calibration of Strain-Gauges Bonded to Needle Sides.
Fig 20.4(a)	Parameters for traces shown in Fig 20.4(b),(c), and (d).
Fig 20.4(b)	Effect of Machine Speed Upon the Wave Propagated up the Needle Shank (169, 222 and 267 ft/min).
Fig 20.4(c)	As above (325 and 377 ft/min).
Fig 20.4(d)	As above (430 and 405 ft/min).
Fig 20.5	Force Magnitude Measured by Strain Gauges on Needle Shank.
Fig 20.6	Measurement of Bending Strains in the Needle Shank.
Fig 20.7	Measurement of Bending Strains following the Stitch Cam Impact.
Fig 20.8(a)	Strain-Wave at Hook (129 and 210 ft/min).
Fig 20.8(b)	Strain-Wave at Hook (264 and 402 ft/min).
Fig 20.8(c)	Strain-Wave at Hook (432 and 443 ft/min).
Fig 21.1	Dynamic Photo-Elastic Examination of Stress-Waves (Apparatus and Circuitry).
Fig 21.2	Dynamic Photo-Elastic Apparatus.
Fig 23.1	Cam-Width at Verge Height.
Fig 23.2	Dimensions for Non-Linear Cams.
Fig 23.3	The $\eta = 65^{\circ}$ Sine-Sine Cam Profile.
Fig 23.4	Co-ordinates for Sine-Sine Cams.
Fig 23.5	The $\eta = 60^{\circ}$ Sine-Sine Curves.
Fig 23.6	The $\eta = 60^{\circ}$ Sine-Sine Cams designed for Cam-Force Transducer Mark III.
Fig 23.7	0.675 in. Sine-Circular Cam.
Fig 23.8	0.585 in. Sine-Circular Cam.
Fig 23.9	A 60° continuous Sine curved Cam-Track with Tuck and Miss Stitch Facility.
Fig 24.1	Low Mass Needles.
Fig 24.2	Needle Head Design,

REFERENCES

1. The Production and Properties of Knitted and Woven Fabrics, M.S. Burnip, Textile Progress, Volume 1, No. 3.

2. Textile Progress, Volume 3, No. 3, 1971, J.D. Turner.

3. Friction as a Technological Problem in Textiles, G. Pflüger, Textil-Praxis, 1968, Volume 23, No. 11, 741 -745, and No. 12, 813 - 816.

4. Amonton's Law and Fibre Friction, J. Text Institute, 1953, 44, T59, H.G. Howell & J. Mazur.

5. The General Case of Friction of a String round a Cylinder, Journal Text Institute, 1953, 44, T359.

6. The Friction of a Fibre round a Cylinder and its Dependence upon Cylinder Radius, Journal Text Inst., 1954, 45, T575.

7. The Friction & Lubrication of Yarns, C. Rubenstein, Journal Text Inst., Volume 49, 1958, T13 - *32.

8. Characterstics of Fibre Friction Nature, March 4, 1967, James J.F. Knapton.

9. Whitney J.M., Textile Research Journal., 35, 281, (1965).

10. Gralén N., Proc Roy Soc., A, 212, 491 (1952).

11. A Study of the Mechanism of Loop Formation on Weft-Knitting Machinery, 1966, Part I, The Effect of Input Tension and Cam Setting on Loop formation, J.J.F. Knapton and D.L. Munden.

12. Making the Most of Knitting with Wool, J.J.F. Knapton, Textile Research Journal, May, 1965.

13. The Dynamics of Weft-Knitting Further Theoretical and Mechanical Analyses, J.J.F. Knapton, Textile Res. Journal, Jan., Dec., 1968.

14. The Dynamics of Weft-Knitting: A Mathematical Analysis, 1966, J.J.F. Knapton, Textile Research Journal, Vol. 36, No. 8, August, 1966.

15. The Mechanism of Loop Formation and the Dynamics of Weft-Knitting, J.J.F. Knapton, 1968, A.S.M.E. Paper 67 - tex 3 1967.

16. Knitting Performance of Wool Yarns Effects of Yarn/Metal Friction, Loop Length, and Cover Factor on Knitting Performance, J.J.F. Knapton, 1968, Textile Research Journal, Volume 38, Jan., Dec.

17. A Study of the Mechansim of Loop Formation on Weft-

Knitting Machinery, Part II, The Effect of Yarn Friction on Yarn Tensions in Knitting and Loop Formation, J.J.F. Knapton & D.L. Munden, 1966, Textile Research Journal, Volume 36, No. 12, December 1966, pp 1081 - 1091.

18. Knitting Performance of Wool Yarns, Instrumentation Studies Textile Research Journal, Volume 37, No. 7, July, 1967, J.J.F. Knapton, 1967.

19. New Design Aspects of Weft-Knitting Machinery, J.J.F. Knapton, Knitted Outerwear Times, 1967, 36, No. 8, p 21 - 2

20. Some Thoughts on the Continuous Operation of Weft-Knitting Machines, J.J.F. Knapton, 1971, Textile Institute and Industry, November, 1971.

21. Consideration of the Design of Knitting Cam Mechanisms, D.L. Munden, 1960, Journal Textile Inst., 1960, 51, P712.

22. Cam Action in Weft Knitting, Stephen C. Dangel, Knitted Outerwear Times, 37 (19), 1967, P 278 - 283.

23. The Art of Knitting by John Lawson, Knitted Outerwear Times, 37 (19) 1968, P 272 - 277.

24. Cam Forces in Weft Knitting, D.E. Henshaw, Textile Research Journal, P 592 - P 598, June, 1968.

25. Knapton J.J.F., PH.D Thesis, University of Leeds, (1963).

26. Measurement & Fundamental Theory of Knitting Tension, N. Aisaka, Textile Machinery Society of Japan, V22, 1969, No. 3.

27. Knitting Tension during Weft Knitting, Noboru Aisaka, Totsya Kawakami, and Tadashi Shindo Textile Machinery Society of Japan, Transactions, Volume 22, No. 3, T 39 - 50 (1969).

28. Knitting Tension in Loop Formation of Fancy Stitches, Noboru Aisaka, Totsya Kawakami and Tadashi Shindo, Journal of the Textile Machinery Society of Japan, English Edition, 1969, 15, No. 5, 171 - 185.

29. Ph.d Thesis, David H. Black, October 1968, University of Leeds.

30. Barth, J., Compressive Force between Cams and Knitting Elements, Deutsche Textiltechnik, 1969, Vol 19, Part 10, 639 - 47.

31. The Impact of Needles on a Knitting Cam, G.A.V. Leaf and F. Blackman, Textile Research, Journal, June, 1968, P 651 - 662.

32. Increasing the Speed of Knitting Machinery Textile Science and Research XII, J. Kopel (1972) National Textile Research Institute at Liberec, PP 72 - 87.

33. Petrow, E.I, The Working Conditions of the Knitting Needle,

Textil Praxis, 14 (1959), pp 803 to 806.

34. Petrow, J.I, Petrow E.I. Mashinostroenie, (Izv Vuz), 1959, No. 5, 11.

35. Petrow J.I, Petrow E.I., Textilnaja Promyslennost, 160, No. 5.

36. Petrow E.I., Textinaja Promyslennost, No. 3, 1959, Operating Conditions of the Knitting Needles.

37. Petrow E.I., Legkaja Promyslennost, 1958, No. 1.

38. B. Beddoe, Propagation of Elastic Stress Waves in Necked Rod, Journal of Sound & Vibration, Vol 2, No. 2, April, 1965, P 150 - 66.

39. Elastic Wave Propagation in Rods of Arbitrary Cross Section, R.L. Rosenfeld, J. Miklowitz, A.S.M.E. - Paper 65, - APM - 12, for meeting June 7 - 9, 1965.

40. Stress-Wave effects in Design of Long Bars and Stepped Shafts, N. Davids, N.E. Kesti, Int., J. Mech., Sciences, Vol. 7 No. 11, Nov., 1965, P759 - 69.

41. Damping of a Rectangular Stress Pulse in a thin elastic rod by External Coulomb Friction, Wilms, 1968, Journal of the Acoustical Society of America Volume, 45, No. 4, 1969, 1049 - 1050.

42. One Dimensional Wave Propagation through a short Discontinuity, V.H. Kenner and Werner Goldsmith, 1969, Journal of the Acoustical Society of America, Volume, 45, No. 1, 1969, 115 - 118.

43. Stress-Wave Propagation in Truncated Cones against a Rigid Wall, Nam P. Suh, 1967, Experimental Mechanics, Vol 7, No. 12, December, 1967.

44. Internal-Strain Measurements of Longitudinal Pulses in Conical Bars, J.L. Lewis, W. Goldsmith and D.M. Cunningham, Experimental Mechanics, Vol 9, No. 6, June 1969.

45. Bentley Machine Development Company Limited Report - Analysis and Design of Cams for use in Hosiery Knitting, May, 1963, Rothbart Associates.

46. Automatic-Slider Type of Knitting Needle, S. Ito, Journal Textile Machinery Society of Japan, 1968, 21, No. 2, PP 126 to 129.

47. J. Garside, Ph.d thesis, 1972, Loughborough University of Technology.

48. Johannes Barth, Theoretical Relationships for the Forces between the Needle Elements and Cams, and the Needle Follow-Up, Wissen Z.d.T.H. Karl-Marx-Stadt, Yr. 11, 1969, Vol. 1, PP 95 - 122.

49. An Investigation into the Frictional Forces arising over Needles and Sinkers of a Circular knitting Machine, Final

Year Undergraduate Project, D.E. Smith, Loughborough University, 1971 to 1972.

50. Dynamic Motion Analysis of the Cam Action of a Circular Knitting Machine, Final Year Undergraduate Project, C. Neal, 1968 to 1969.

51. Buckingham π theorem and other methods of non-dimensional plotting are discussed in many text-books a typical example in A Textbook of Fluid Mechanics. J.R.D. Francis, Edward Arnole (London), Chapter 10.

52. Vibrating Cams Patent., United States 3,690,124, Sept 12,1972

53. Some Recent Developments in Dynamic Photoelasticity, Dr. P.D. Flynn, J.T. Gilbert, A.A. Roll, S.P.I.E. Journal, Vol. 2, May 1964, Pages 128 - 131.

54. Equipment for "Watching" Propagating Stress Waves- Herbert Becker, The Review of Scientific Instruments, Vol. 30, No. 12, December 1959, 1107 to 1109.

55. Data Analysis in Dynamic Photoelasticity Experimental Mechanics, Vol. 7 No. 8, Aug. 1967, 332 to 338.

56. High-Speed Photographic Studies of Dynamic Stresses in Low Modulus Photoelastic Materials, Dr. P.D. Flynn, J.T. Gilbert, A.A. Roll, S.P.I.E. Journal, Vol. 1, March, 1963, 75 to 79.

57. A Recording Photoelastic Stress Meter, R. Gordon, R.W. Bayma, A. Warnick, Experimental Mechanics, Nov, 1966, 567 to 570.

58. Some Exploratory Photoelastic Studies in Stress Wave Propagation, M.L. Williams, M.E. Jessey, R.R. Parmester, Guggenheim Aeronautical Laboratory of the California Institute of Technology, Technical Report.

59. Sutton, G.W., Study of the Application of Photoelasticity to the Investigation of Stress Waves. Thesis in Mechanical Engineering, California Institute of Technology, June, 1955.

60. High-Speed Photography in Textiles, P.R. Lord, The Photo - graphic Journal, February, 1963, 33 to 37.

61. Application of Two-dimensional Photoelasticity to the Study of Acceleration Stresses under Quasi-Static Conditions, Judson R. Griffin, May, 1969, Experimental Mechanics, Vol. 9, 220 to 224.

62. Slow Motion Pictures of Impact Tests by means of Photoelasticity, L. Föppl, J. Appl. Mech., Vol. 16, 1949.

UNITS USED IN THE TEXT

mm	Millimetres
m	Metres
cm	Centimetres
in.	Inch
lbf	Pound-force
gf	Gramme-force
g	Gramme-mass
kgf	Kilogramme-force
kg	Kilogramme-mass
lb	Pound mass
Hz	Frequency (cycles per second)
ft	Feet
sec	Second
min	Minute

PART A

PRELIMINARY STUDIES

CHAPTER 1

INTRODUCTION

Technological improvements in knitting machinery, together with the development of new fibres and yarns, have been major factors in the increased demand for knitted fabrics. Machines are now capable of producing a wide range of good quality fabric structures at high production rates. However, there are difficulties in increasing the production rates still further. A limit has been reached where, unless there is a clearer understanding of the knitting process, very little progress can be made in the design of future knitting machinery.

This project was primarily concerned with the development of measuring instruments that could be used to obtain a better understanding of the knitting process over a wide range of operating conditions.

1.1 Brief Resume of Weft Knitting.

The type of needle used in most circular knitting machines is the latch needle. This needle, illustrated in Fig 1.1 consists of three major parts, the shank, the butt, and a pivoting latch. The unique advantage of the needle is that the yarn opens and closes the latch during the loop formation process. The mechanical simplicity of its action enables higher machine speeds to be achieved. A large number of these needles operate with their butts acting as a multi-follower system against a cylindrical cam-track known in the trade as a "cam-box".

Weft Knitting on Circular Machines can be carried out either with the cylinder rotating and the cam-box stationary or with the cam-box rotating and the cylinder stationary. Whichever system is used the knitting action is the same, but

the most usual is the rotating cylinder machine to which this work is confined. The cylinder has vertical guides (tricks) machined in the outer circumference; in each guide a latch knitting needle is fitted which is free to move vertically while being horizontally constrained by the trick walls. At the base of the needle a butt projects into the stationary cylindrical cam track, the cylinder-needle combination rotates, and each needle element is reciprocated vertically by the track. Initially, in the running position, yarn is held in the needle hook. When the needle hits the clearing cam, it ascends vertically, and the yarn loop effectively moves down the shank to open the latch. The needle, at position (A) in Fig 1.2, then contacts the stitch cam and begins to descend so that the old yarn loop, which is held around the shank, is effectively forced up to close the latch. New yarn, which is fed to the needle, is drawn over the cylinder verge and pulled through the old loop, as shown at (B) in Fig 1.2. The needle rises when it contacts the guard cam, and finally reaches a running position at (C) in Fig 1.2. The process is repeated at every yarn feeding station. The loop forming process for simple plain stitch knitting, togcther with the motion of the needles over the stitch and guard cam are shown in more detail in Fig 1.3.

Two modifications to the basic plain loop formation are shown in Fig 1.4. These are the float (or miss) stitch and thc tuck stitch. Plain, float and tuck stitches form the bases for a wide range of commercial fabrics. Moreover, they can be extended into more complex knitted structures by the incorporation of a corresponding set of interacting needles acting normally to those in the vertical tricks. These secondary needles are in radially-disposed tricks in a

further stationary cam-box system shaped like a disc and known as the "dial"; such machines are generally known as cylinder-and-dial machines.

1.2 Limitations to Production Rates of Current Types of Weft Knitting Machinery.

As the rotational speed of a knitting machine is increased, the incidence of needle fracture at the head and at the butt also increases. Consequently a limiting speed is reached beyond which it is not economic to proceed, increasing production rates being more than offset by poor quality fabric and the greater time required to replace broken elements. The traditional method of increasing production rates has been to keep the rotational speed relatively low and to increase the number of yarn feeding stations around the cylinder circumference. The circumferential length of the cams possible at each station is controlled by the operatable cam angles, and these have a practical limit whereby it is impossible to fit any more feeders.

1.3 Objects of Present Investigation.

The current research has the following objectives :-

1) Instrumentation is to be developed to measure the forces during knitting, and in particular to measure the following parameters :-

a) The forces between a single needle and the cams.

b) The forces exerted upon both the needle and the verge by the yarn during loop formation.

c) The impact force when the needle first contacts the stitch-cam and guard-cam.

d) The frictional tension build-up as yarn passes over the verges and needles.

e) The bounce of the needles on the cams during knitting and non-knitting.

Initially the instrumentation is to be fitted to a ten-inch diameter circular knitting machine having a cylinder but no dial. The instrumentation on the machine could then be used to analyse the knitting forces and to test possible modifications to cam needle design.

2) The mechanism of needle fracture is to be examined. Apparatus should be devised to measure the stress-wave propagation in the needle during knitting.

3) Systems might then be redesigned to facilitate high-speed operation whilst maintaining fabric quality. Such systems could possibly be tested on a thoroughly instrumented modern commercial knitting machine of the cylinder and dial type.

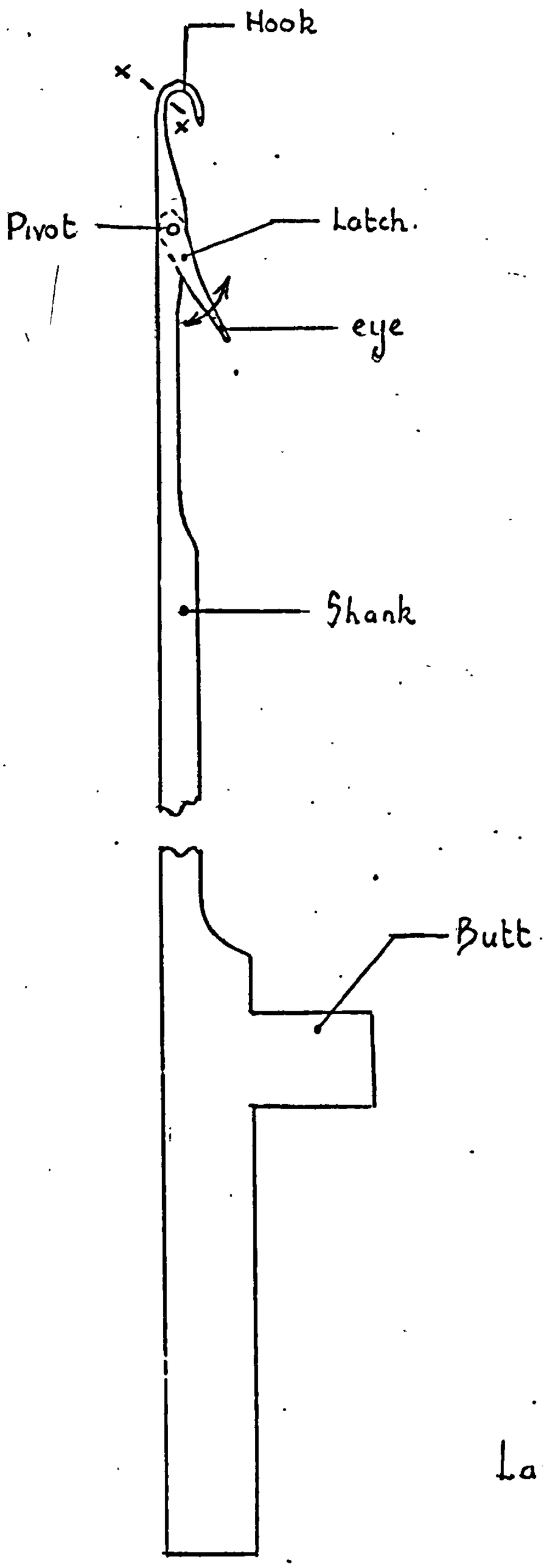

FIG 1.1

A

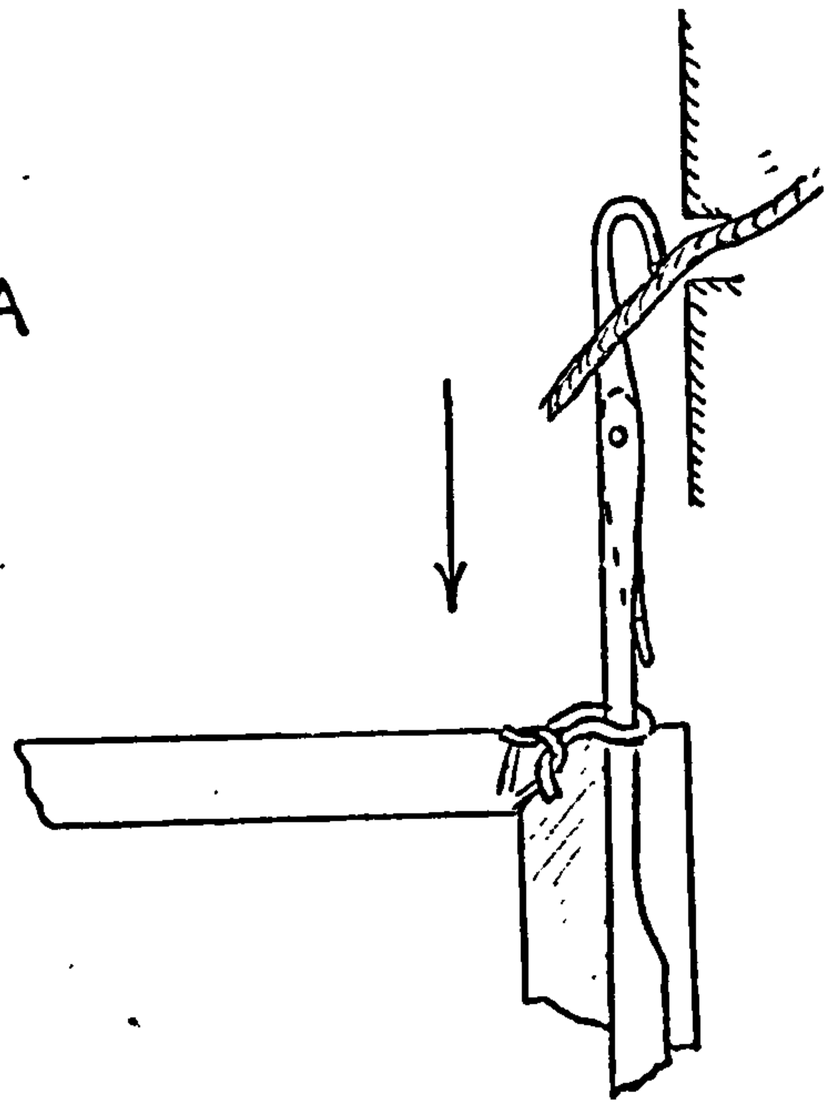

B

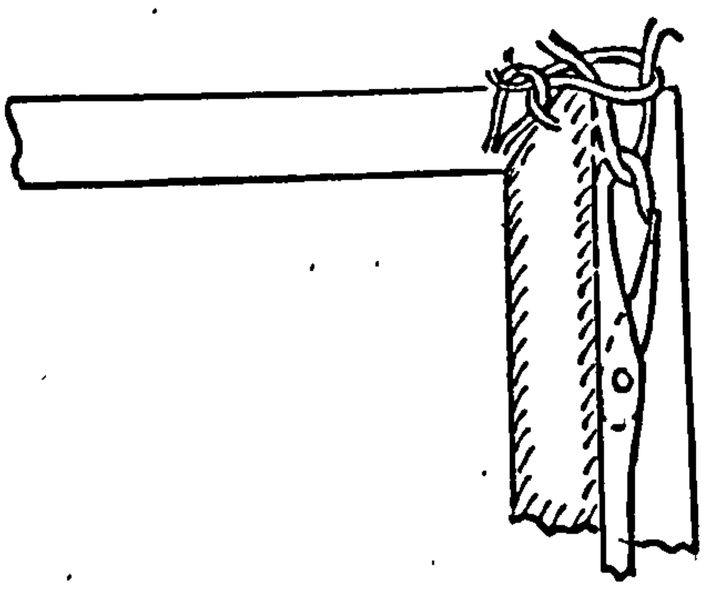

C

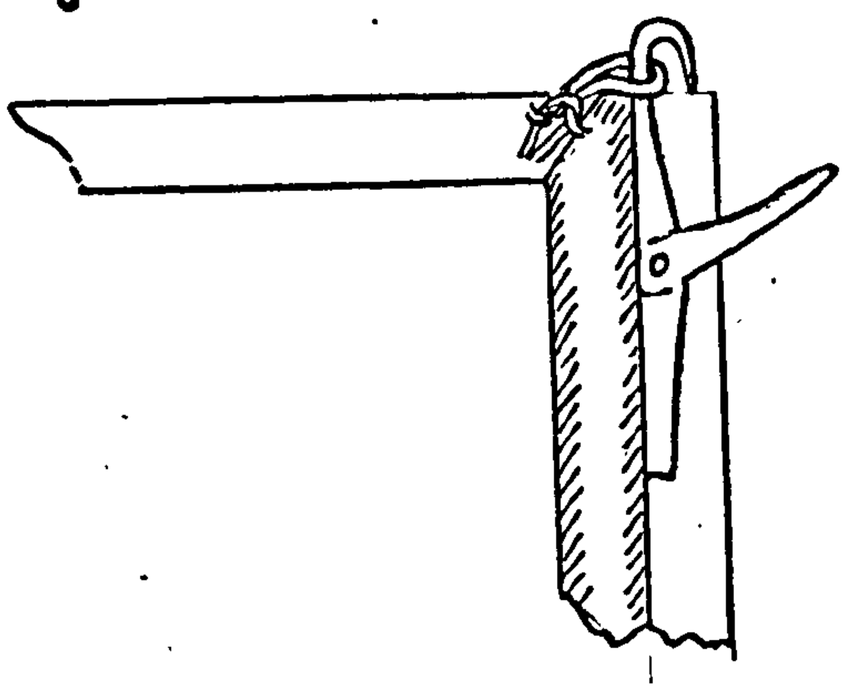

(only one needle shown)

THE PROCESS OF FORMING A PLAIN KNITTED STITCH.

FIG 1.2

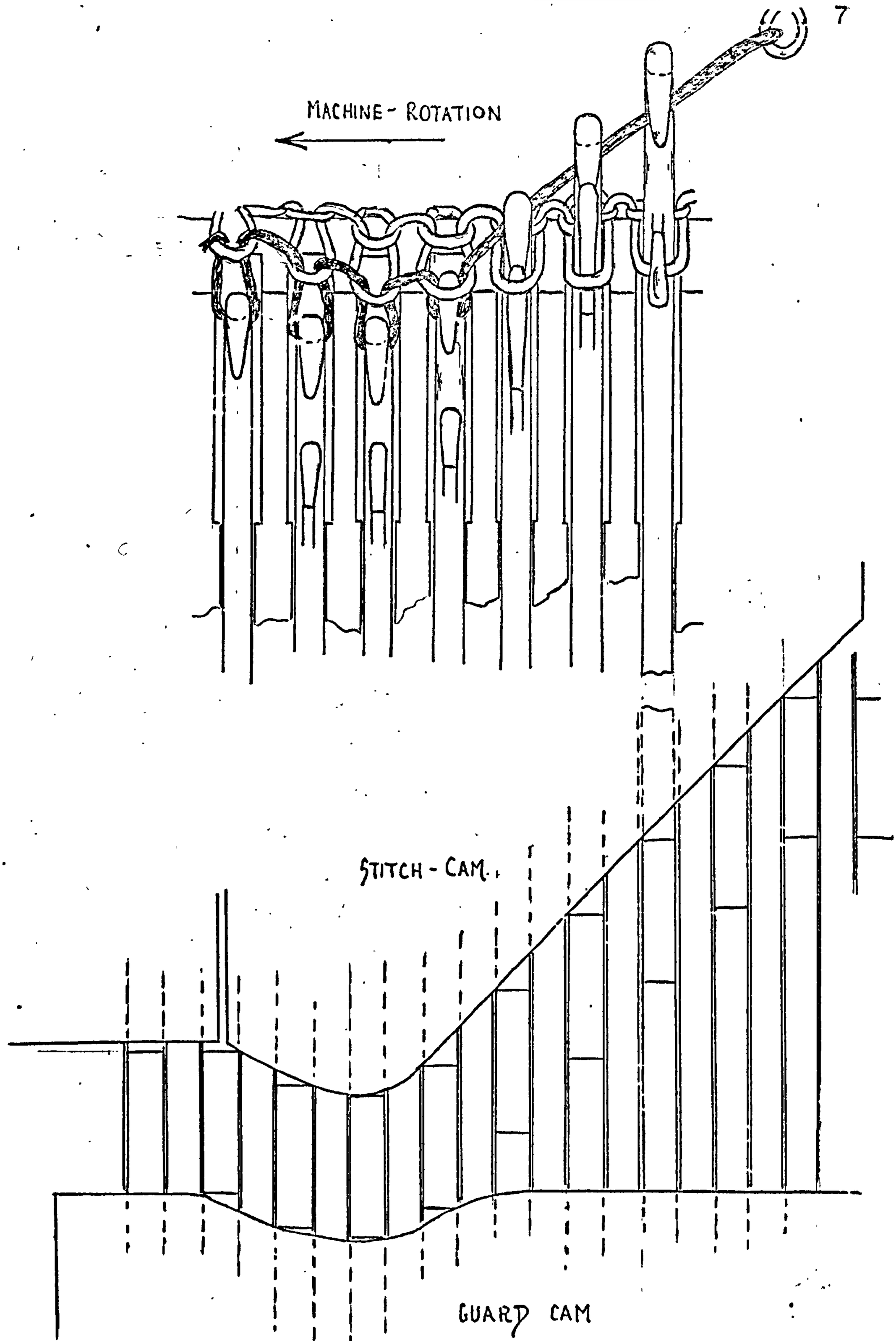

THE CONTINUOUS KNITTING OF PLAIN STITCHES AS THE NEEDLE BUTTS MOVE THROUGH THE KNITTING CAMS

FIG 1.3

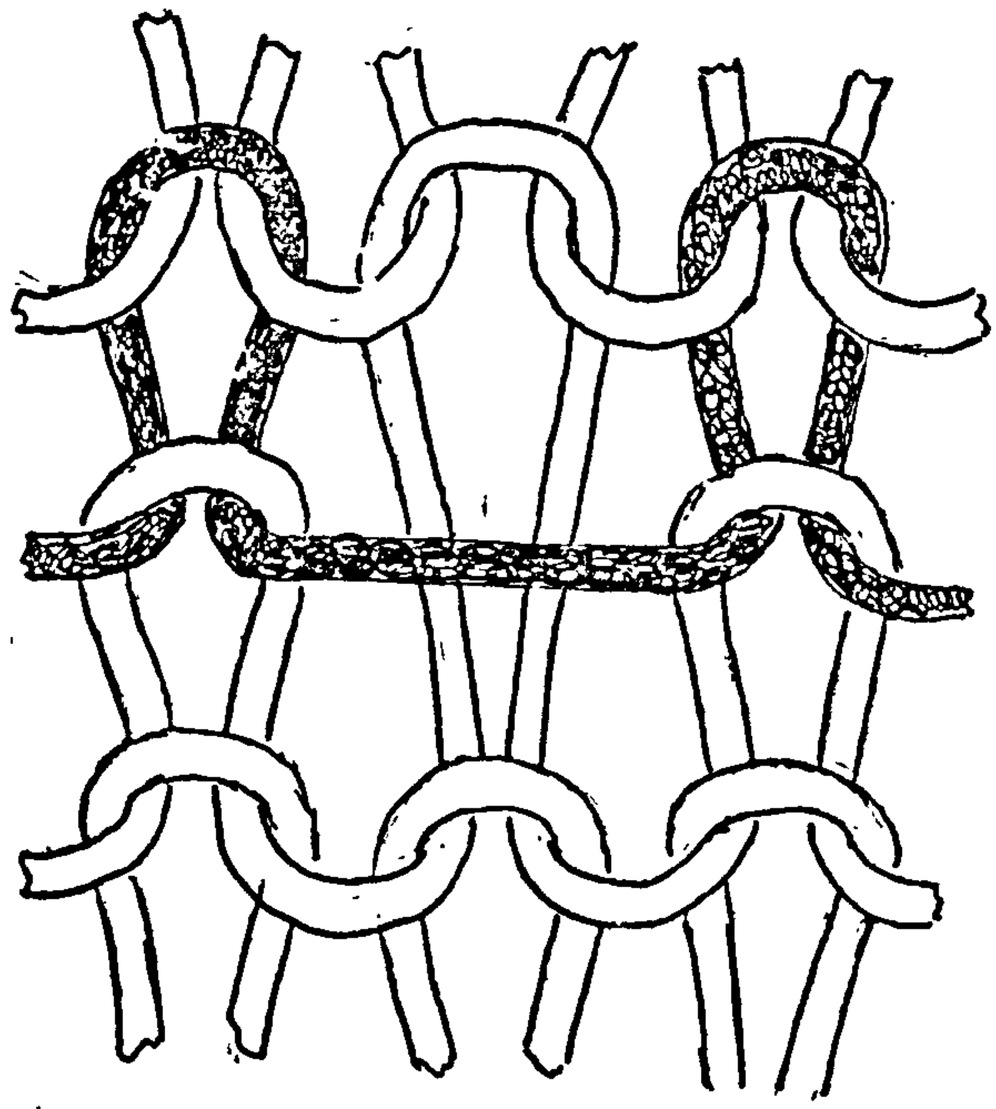

FLOAT - STITCH.

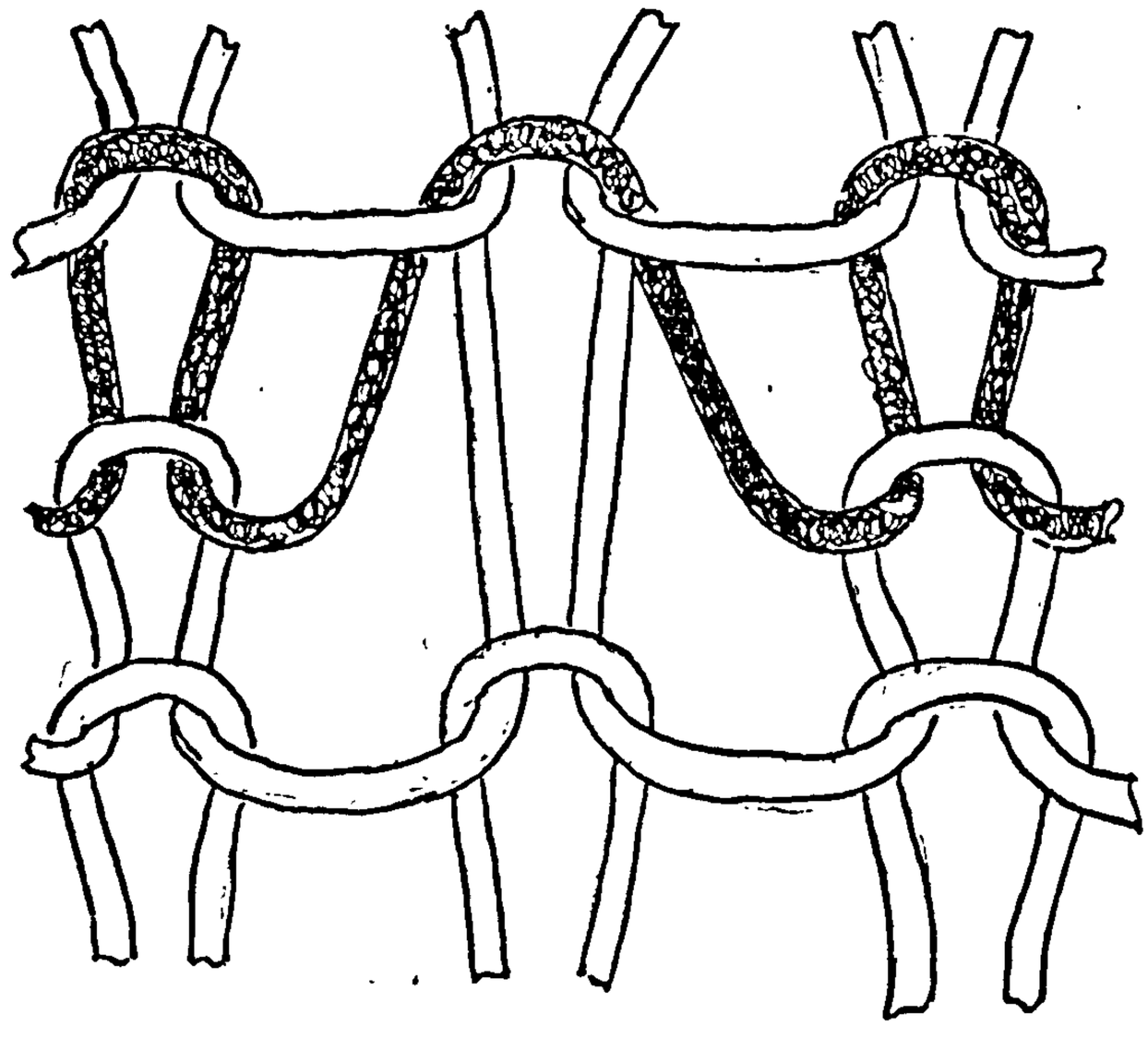

TUCK - STITCH.

MODIFIED KNITTED STITCH STRUCTURES.

Fig 1.4.

CHAPTER 2

REVIEW OF LITERATURE

2.1 A summary of the Present State of Published Knowledge regarding the Weft-Knitting Process.

Surveys of recent knitting research are contained in reference (1) and (2) and these between them contain 1,319 references to publications! Similarly, reference (3) contains a list of contributions to the understanding of yarn friction.

2.1.1 The loop forming process.

As yarn passes over each of the needle and verge elements there is a tension increase due to frictional resistance. The classical equation for the tension increase is derived from Amonton's Law[4] :-

$$\frac{T_2}{T_1} = e^{\mu\theta} \quad \ldots \quad (1)$$

where T_2 = yarn outgoing tension,
T_1 = yarn ingoing tension,
θ = yarn wrap angle around the bollard,
and μ = coefficient of friction between the bollard material and the yarn.

Howell[4,5,6] and Rubenstein[7] showed that equation (1) was inaccurate insofar as a strictly scientific investigation of the behaviour of textile fibres was concerned. Howell proposed an equation of the form :-

$$F = kW^n \quad \ldots \quad (2)$$

$$T_2^{1-n} - T_1^{1-n} = k(1-n)r^{1-n}\theta \quad \ldots \quad (3)$$

where : T_2 = yarn outgoing tension,
T_1 = yarn ingoing tension,
θ = yarn wrap angle around the bollard,
r = bollard radius,
F = limiting frictional force,
W = normal reaction force,
and k and n = constants.

Knapton[8] tested a 92 tex worsted yarn by running it over a 1.1 cm diameter bollard. He discovered a non-linear

relationship between n, k, and Θ that was not compatable with equation (3) and suggested that the frictional force was related to the normal load by the equation :-

$$F = \rho W^n - q n W^n \quad . \quad . \quad . \quad (4)$$

where F = limiting frictional force,
W = normal reaction force,
and ρ, q and n = constants.

Whitney[9] and Gralen[10] have proposed an equation for nylon and polypropylene monofilaments of the form :-

$$F = aW + bW^c \quad . \quad . \quad . \quad (5)$$

where F = limiting frictional force,
W = normal reaction force,
and a, b and c = constants.

Relatively little research has been carried out on bollards as small as practical needles and verges, where the effects of yarn rigidity[11] might well be of considerable importance for such small elements. For tension calculations through the knitting cycle Amonton's equation is a much easier expression to use than the equations (2) to (5), but it would be useful to have precise information on the degree of accuracy of Amonton's law under particular situations.

The loop-forming process and the yarn tensions during loop formation were explained theoretically by Knapton[12,13,15,16,18,25] and Knapton and Munden[11,17]. Dangel[22] summarised the results obtained from the researches of Lawson[23] and his model of the loop-forming prccess is shown in Fig 2.1. He proposed a numerical method where a digital computer could be used to solve the equations which are given below :-

$$T_{max} = T_i e^{\mu \beta_1} \quad . \quad . \quad . \quad . \quad (6)$$

$$T_{max} = T_f e^{\mu(\beta_2 - \beta_1)}, \quad . \quad . \quad . \quad (7)$$

$$\gamma_k = \gamma_R, \quad . \quad . \quad . \quad . \quad (8)$$

$$\gamma_R = f(\beta_1), \quad . \quad . \quad . \quad . \quad (9)$$

$$\gamma_R = f(\beta_2), \quad . \quad . \quad . \quad . \quad (10)$$

where T_{max} = the maximum tension in the system; this occurs on the stitch-cam at a depth of γ_k,
T_i = the input tension,
T_f = the take-down tension,
γ_R = the needle depth at which the loop is released,
μ = the coefficient of yarn-metal friction,
β_1 = the wrap angle to the position of T_{max},
and β_2 = the total wrap angle in the system.

The essential assumption of Dangel's work is that the maximum tension is related to the effective loop length produced, and that the needle depth at the knitting point is equal to the needle depth at the release point. Allowance must also be made for yarn extension.

Henshaw[24] attempted to assess the yarn tension during loop formation by measuring the needle butt reaction forces on the cam. His measured yarn tensions were much greater than those theoretically predicted by Knapton and Mundon[11,17] using Amonton's laws, and his suggested reason for this discrepancy related to the effect of yarn count. Henshaw showed that a flat-bottomed cam greatly reduced stitch-length variations because it prevented the process of robbing back of yarn from previously formed stitches, from interfering with the drawing of the new-loop. He concluded that flat-bottomed cams may have some real advantages in terms of stitch uniformity but that the extra cam space for a flat bottom, requiring five or six extra needle spaces, has the disadvantage of a reduction of the number of yarn feeds on many multi-feeder circular machines.

Similar work was done by Aisaka,[26,27,28] using a cantilever stain-gauge detector fitted to the base of the stitch-cam, and he showed that there was a definite trend for an increased reactive force when the number of needles held down by the stitch-cam was increased.

Both Henshaw and Aisaka measured the loop drawing forces by an instrumented cam-track. However, it is possible that other force contributions, for example, viscous forces, trick-needle clamping forces, and guard cam impacts, could all have contributed to the measured force levels.

2.1.2 The Reactive Force between the Cam and Needle during Knitting.

Munden[21] and Knapton[25,20,19,14] analysed the reactive forces between the cam and needle during knitting. Knapton evaluated the total cylinder torque required to move the needles through the cam system, and concluded that if a 60° cam system was used on present machines, the yarn knitting tensions would be less than one using conventional 45° cams. He argued that the total work required to knit the yarn into fabric would also be reduced and also showed that the use of friction-crimped needles increased the work required to knit a low friction yarn by as much as nine times above that required when using straight needles.

A much more rigorous theoretical analysis was carried out by Johannes Barth.[30,48] One interesting result in Barth's work is the predicted effect of the radial cam-cylinder spacing, i.e. if the knitting cams are set very close to the cylinder, the force between the cam and needles is less than when the cams are moved further away from the cylinder.

Black[29] built an instrument to measure the reactive force between the cam and needle. The cam-track was connected

to a strain-gauged cantilever system, and it responded to the total number of needles present in the track at any instant of time. With this instrument he obtained some interesting results, one being the effect of oil viscous resistance which acted so as to increase the reactive force as the machine speed was increased. Apart from Black's work, little attempt has been made to measure the reactive forces between the cam and needle during knitting.

2.1.3 The impact forces between the cam and needle during knitting.

Leaf and Blackman[31] carried out an analysis of needle behaviour after striking the stitch-cam. The analysis revealed critical cam angles defined in the paper as α_1 and α_3; if $\alpha \geqslant \alpha_1$, needle jamming occurs; if $\alpha < \alpha_3$ the needles bounce down the stitch-cam; and if $\alpha_1 > \alpha \geqslant \alpha_3$ the needles slide smoothly down the cam face. For given values of the coefficients of friction and the coefficients of restitution they computed values of α_1 and α_3 . Very small changes in the coefficients could lead to irregular needle behaviour.

Very recently (in fact during the final stages of submitting this thesis) an important research publication by J. Kopal[32] has emerged from Czechoslovakia in which he describes the use of a capacitance transducer, with a natural frequency of 9,500 Hz, for measuring the impact forces and normal reaction force between a needle butt and cam. His measurements show that cam impact increases linearly with machine speed and exponentially with cam-angle. The impact magnitude is highly variable; fifty needles were tested consecutively in the same needle guide and it was found that the impact force varied between 1,300 gf and 2,150 gf. Similarly, after testing the same needle in fifty guides, the impact

force was shown to vary between 1,050 gf and 2,750 gf.

Kopal recommended that yarn should be fed to the needles at a constant input tension of between 3 and 5 gf. High speeds, the cause of high tension vibrations in the yarn, lead to the suggestion that much greater attention should be given to the design of yarn guides. It is recommended that the problem of latch impact could be minimised by using elastic, high-damping materials in latch construction, and Kopal concludes that large diameter jaquard machines would soon be capable of cylinder speeds in the region of 60 m/min, whereas at present they are limited to about 50 m/min.

2.1.4 Stress Wave Propagation in the Needle Structure resulting from Needle Impact with the Cams.

J.I. Petrow and E.I. Petrow[33,34,35,36,37] carried out a detailed analysis of the stress-wave propagation in Groz-Beckert hosiery needles resulting from cam-needle impact. They mathematically predicted the passage of a plane longitudinal pressure wave through the needle structure which originated at the impact of the needle butt with the guard cam. They concentrated upon the effect of the tapered sections of the needle on the wave propagation and showed that as a pressure wave moved towards the top of the conical section a stress-strain wake remained. The force which was greater at the wake of the pressure impulse could exceed the ultimate strength of the material or lead to a fatigue situation. They concluded that the most dangerous cross-section of the straight needle was at the base of the needle hook, i.e. just at the beginning of the bend as denoted by X-X in Fig 1.1.

They redesigned some typical Groz-Beckert needles with the object of increasing their resistance to impact stresses. The designed needles had abrupt transitions and wedge-like

sections, and were shown to considerably reduce the wave transmission up the needle shank. During knitting tests at 380 revs/min of the cylinder, these needles had an average breakage rate of 0.5 needles per 15 minutes running time, while an ordinary needle had an average breakage rate of 40 needles over the same running time and at the same cylinder speed. The ordinary needle and the redesigned needle are compared in Fig 2.2.

The effects of step reductions and gradual reductions of area upon wave propagation through rods has been noted by several researchers.[38 to 44 inc.] In a paper by Davids and Kosti,[40] it is shown that a step reduction in area results in a maximum two-fold stress increase, while a gradual reduction in area, such as a tapered section, can result in a stress magnification greater than two. Whenever the stress level in a narrowed bar section is too high, a gradual entrance to the section is undesirable; a more abrupt change of section with small fillets is better as it tends to reflect more stress, so helping to exclude it from the section. Another interesting observation from the Petrow's work[33 to 37inc.] was the effect of butt length and hook radius. They experimentally demonstrated that the slightest changes in either of these parameters could lead to large increases (as high as 10 times) in the number of hook breakages.

2.2 Influence of the Literature Survey upon the Research Project.

A comprehensive literature survey is always essential to avoid duplication of work and form a foundation for further research and the author has investigated some 300 references in all. In his opinion, each of the transducers mentioned in the literature survey summarised above could be redesigned to

provide more useful information. For instance, only limited information can be obtained from a cam-force transducer that sums the total reactive force from a group of needles passing through the cam-track, and an improved transducer would be one that could separate out the force component from a single needle as it passed down the cam whilst undergoing realistic knitting conditions. With such an instrument it would be convenient to examine the cam-force at each stage of the loop forming process. Similarly, a more direct method could be used to measure the force involved in drawing the yarn loop. All the methods mentioned in the literature survey used an instrumented cam-track; this can lead to problems because it is not clear how much the cam and trick force components contribute to the measured force level. Work done on the frictional tension increase as the yarn passes over the needles and verges indicates that the theoretical relationship is limited in application to particular yarn types and surfaces. Rather that use a doubtful theory it would be better to build an experimental rig and measure the tension increase under realistic conditions for varying angles of wrap, and a range of yarn speeds. Such results could perhaps then be used as the basis of a theory which is applicable to the knitting experiments to be performed in this work.

The Petrows' research forms a useful theoretical basis for further experimental work on the stress-wave propagation in the needle structure, and this will complement the intended measurements of impact force.

2.3 Possible Future Trends in the Development of Knitting Machinery.

For high-speed machine operation some form of non-linear camming must be used. Black[29] proposes polynomial forms and

Rothbart[45] suggests the use of cosine-curved stitch-cams. The knitting industry necessarily imposes very tight constraints upon the design of cams; for example a non-linear cam must be capable of accepting needles presented to it at different heights; it must also have small circumferential dimensions, a low latch turnover angle, no separation at the stitch-cam base, a method of stitch draw adjustment. These are but a few of the constraints. It is difficult to see how a high-speed non-linear cam can be designed to extend circumferentially for no greater length than does a 55^{o} linear cam, and still have a low latch turnover angle. In the future a compromise will probably have to be made, i.e. towards high speed machinery which will run considerably faster but having fewer feeding stations on the circumference.

Researchers are now examining the latch needle to see whether this device is really the best practical form for high speed machinery. Black[29] suggests alternative needle forms, and Ito[46] has developed an automatic slider type needle. However, the needle with no moving parts, designed to replace the latch needle for high machine speed operation has yet to be discovered, and perhaps never will be!

A successful hydraulic knitting machine[47] which uses no cams at all, has recently been designed and built by J. Garside a research colleague in the Mechanical Engineering Department at Loughborough University of Technology. Although this machine operates at a very fast rate, the needle gauge is much coarser than that used in the majority of cammed knitting machines and for this and other reasons, the author is of the opinion that it cannot yet be considered as a viable competitor to most conventional circular knitting machines. Nevertheless, it has other inherent advantages, such as individual needle path control, as well as to little or no

back-robbing of stitches which could perhaps suit it for new types of knitting as yet unthought of. It is interesting to speculate that, with some considerable ingenuity in innovation, such individual control of needle paths, in magnitude and direction could perhaps be the basis of a refreshing breakaway from the conventional trick-guided and parallel needle systems which have persisted for over 400 years.

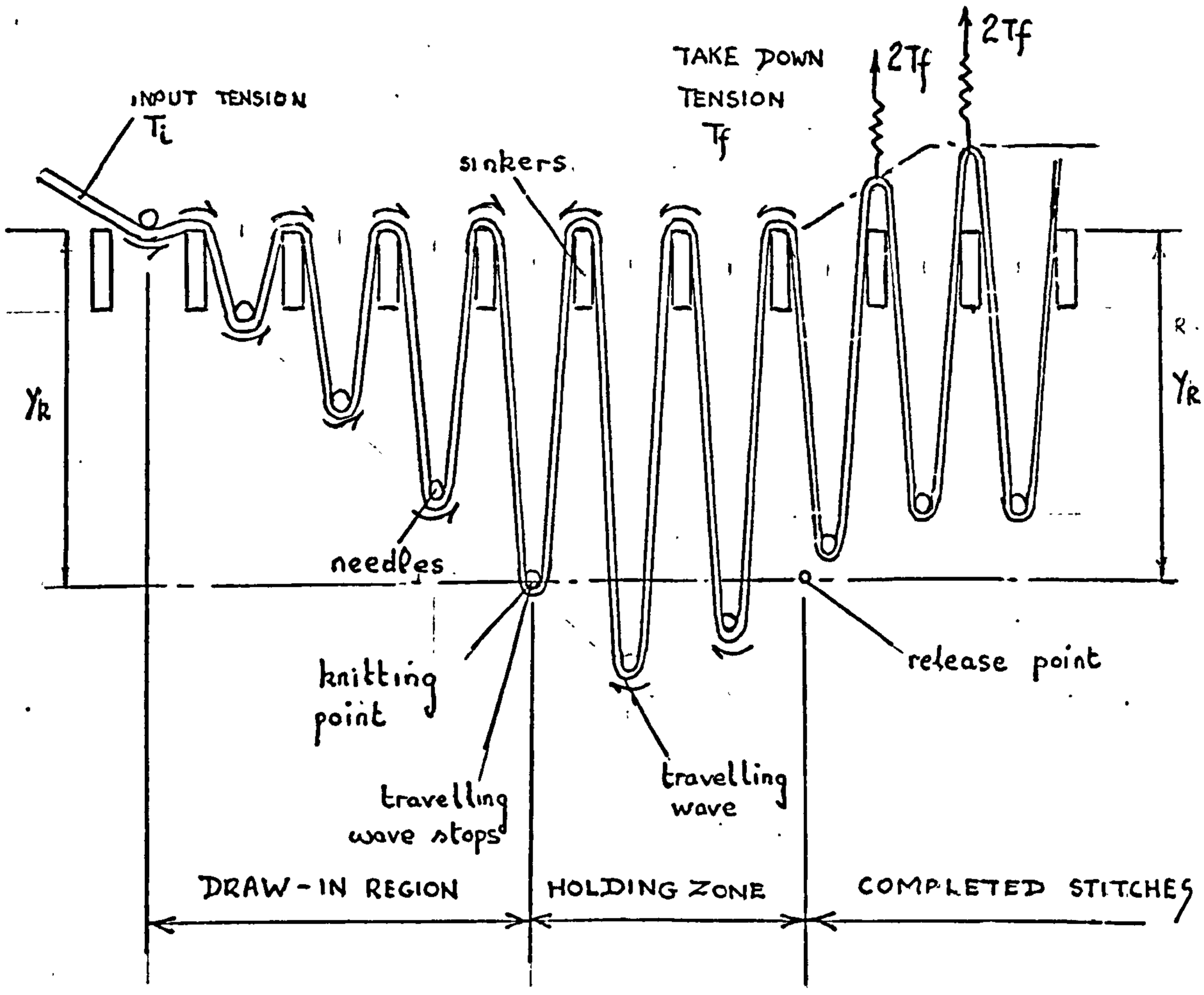

Y_k = needle depth to draw a stitch at the knitting point

Y_R = needle depth as a function of wrap.

for inextensible yarn $Y_k = Y_R$.

DANGEL'S MODEL OF THE LOOP FORMATION PROCESS

Fig 2.1

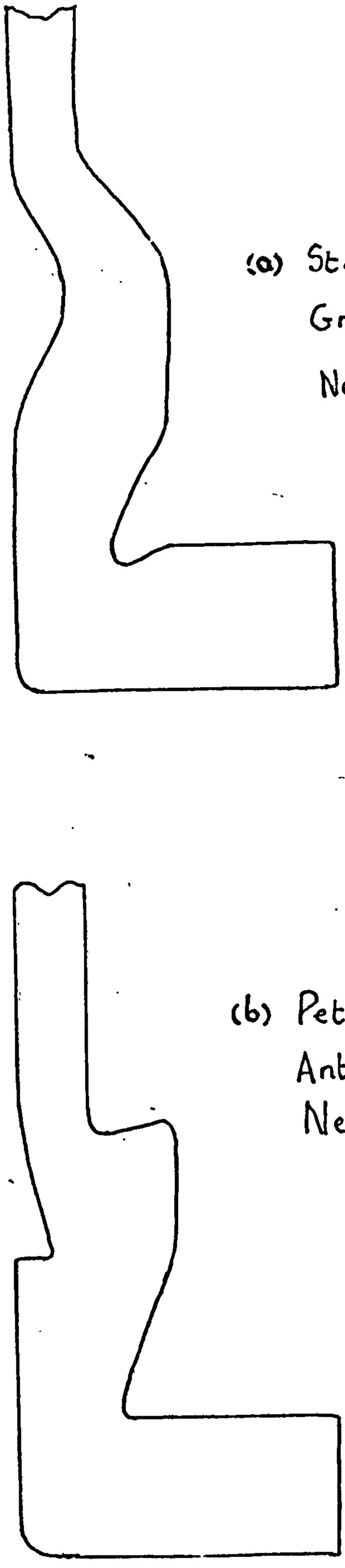

(a) Standard Groz-Beckert Needle.

(b) Petrow's Anti-impact Needle

The butt sections of Groz-Beckert needles (a) before and (b) after modification by Petrow[33,34,35,36,37]

FIG 2.2

CHAPTER 3

INITIAL CONSIDERATIONS IN THE MEASUREMENT OF KNITTING FORCES

3.1 Difficulties of making Precise Measurements.

Initially, two transducer systems were to be designed, one to measure the force between the needle butt and the cams and another to measure the force exerted upon the needle by the yarn during loop formation. In the text, these devices are referred to as the cam-force transducer, and the yarn-force transducer respectively. There were several distinct problems in designing sensitive instruments for use on a knitting machine. These had to be solved, because they fundamentally influenced (a) the structural design of the instrument; (b) the method of carrying out the measurements; and (c) the choice of the sensitive elements e.g. strain gauges, accelerometers, or other sensing devices. These problems are summarised in some detail below :-

(i) If the stitch and guard cams are approximately one-inch long and the machine is rotating at 60 m/min, then a needle moves from one end of the cam to the other in approximately 0.025 seconds. Inevitably the cam-force and yarn-force transducers would have to be designed to measure dynamic signals with high frequency components, and therefore to accurately record rapidly changing signals any measuring device must possess a natural frequency of at least five times the highest frequency component of the signal.

(ii) There were problems in fitting and using instruments on the knitting machine. The cam track, connected to the cam-force measuring device, had to fit closely in between the adjoining cams, and this meant that it had to

penetrate the cam-box and any other mechanisms on the machine near the measuring station. However, the device should not interfere in any way with the normal knitting mode of operation. The cam-force transducer had to be (a) resistant to oil; (b) able to operate at moderately high temperatures approximately 70°C maximum; (c) not sensitive to structural vibrations; (d) strong enough to withstand possible damage during normal operation; and (e) capable of calibration before and after tests.

(iii) If direct measurements were to be carried out it was highly probable that the yarn force transducer would have to be fitted near the loop-forming process. In addition to all the problems associated with the cam-force transducer, some means would have to be provided to transfer the signal from the rotating cylinder to the stationary signal display instrument. The yarn-force transducer would have to be structurally very small if it was fitted close to the loop forming process, and this meant that the sensitive element which would fit on the transducer would have to be even smaller.

(iv) The cam-force transducer was to be designed to measure the force between one needle and the cams during knitting. At any instant of time approximately eighteen needles would be passing through the cams, and if all these needles, except one, were not to register any output on the transducer, some means would have to be found to guide the needles through the normal knitting process with only one needle contacting the transducer cam track. In addition the instrument, when it was designed, needed to be capable of being fitted and removed easily. It should also be sufficiently versatile to test new cam shapes, and thus would need to include the facility for changing the stitch-draw.

3.1.1 The Particular Suitability of Semi-Conductor Strain-Gauges.

An examination of transducer sensitive elements revealed the particular suitability of semi-conductor strain gauges, for measurements on knitting machinery, for the reasons stated below :-

(i) High gauge factor, so enabling provision for a large voltage signal for a correspondingly small strain. Semi-conductor strain-gauges are, on average, almost sixty times as sensitive as foil strain gauges, thus fascilitating measuring systems of higher natural frequency to be built.

(ii) The gauges are very small, measuring only 3.5 mm long by 0.025 mm thick.

(iii) The gauges could be easily given an oil and water resistant coating.

(iv) The gauges are relatively easy to bond to a surface.

(v) Semi-conductor strain-gauges are no more expensive than foil gauges of similar size.

(vi) They are not easily damaged, if properly bonded to the surface.

3.2 The Knitting Machine used for the Investigation.

A 10 in. (25.4 cm) diameter 18-gauge circular knitting machine was used. One yarn feeding station was fitted, and this pulled yarn through various tensioning devices straight off the supply bobbin. Figure 3.1 is a photograph of the upper half of the knitting machine.

3.2.1 The Latch Needle Used.

For most of the experimental work, a 0.0175 in. (0.443 mm) thick latch needle was used; however, a 0.016 in. (0.406 mm) needle was used occasionally. The dimensions and shape of the

latch needle are shown in Fig 3.2. The needle was supported by a jack in the cylinder, and a view looking at the needle and jack in position, and also showing the cam track and band spring, is included in Fig 3.3.

3.2.2 The Type of Yarn Used.

The yarn used for the experimental work was Crimplene 150 den (17 tex)/30-fil polyester manufactured by P. Atkinson Co. Ltd. of Macclesfield. The sponsoring company stated that this was a typical commercial yarn, widely used on this type of machine. However, the instruments needed to be designed to operate with any suitable yarn, so that, if in future it was desired to measure the effect of yarn properties, this could be carried out easily.

3.2.3 Adaptation for Variable Speed Operation.

The motor was mounted on a Carter-gear variable speed unit. The system was designed so that the speed range of the knitting machine was variable between 0 and 135 m/min, the conventional maximum operating speed being approximately 60 m/min. The motor and Carter-gear unit were mounted on a platform completely separated from the knitting machine, the only connection to the machine being the belt drive. The purpose of isolating the drive in this way, was to minimise the vibration transmitted from the drive to the machine structure. Fig 3.4 is a diagram showing the motor mounting.

3.3 Relationship of the Investigation to other types of Knitting Machinery.

The simplified knitting machine would be used as an experimental rig for analysis of the forces involved during knitting, and for testing modifications and revised designs. Further information about dial and cylinder interaction and the effect of timing would have to be obtained later from

similar measurements on cylinder and dial machines. After designing instruments for the 10 ins single cylinder machine (section 3.2), and after gaining a thorough understanding of the nature of the forces involved, it would then be possible to optimise the instrument design before using such instrumentation on more complex commercial machinery.

THE 10 in. CIRCULAR KNITTING MACHINE

Fig 3.1

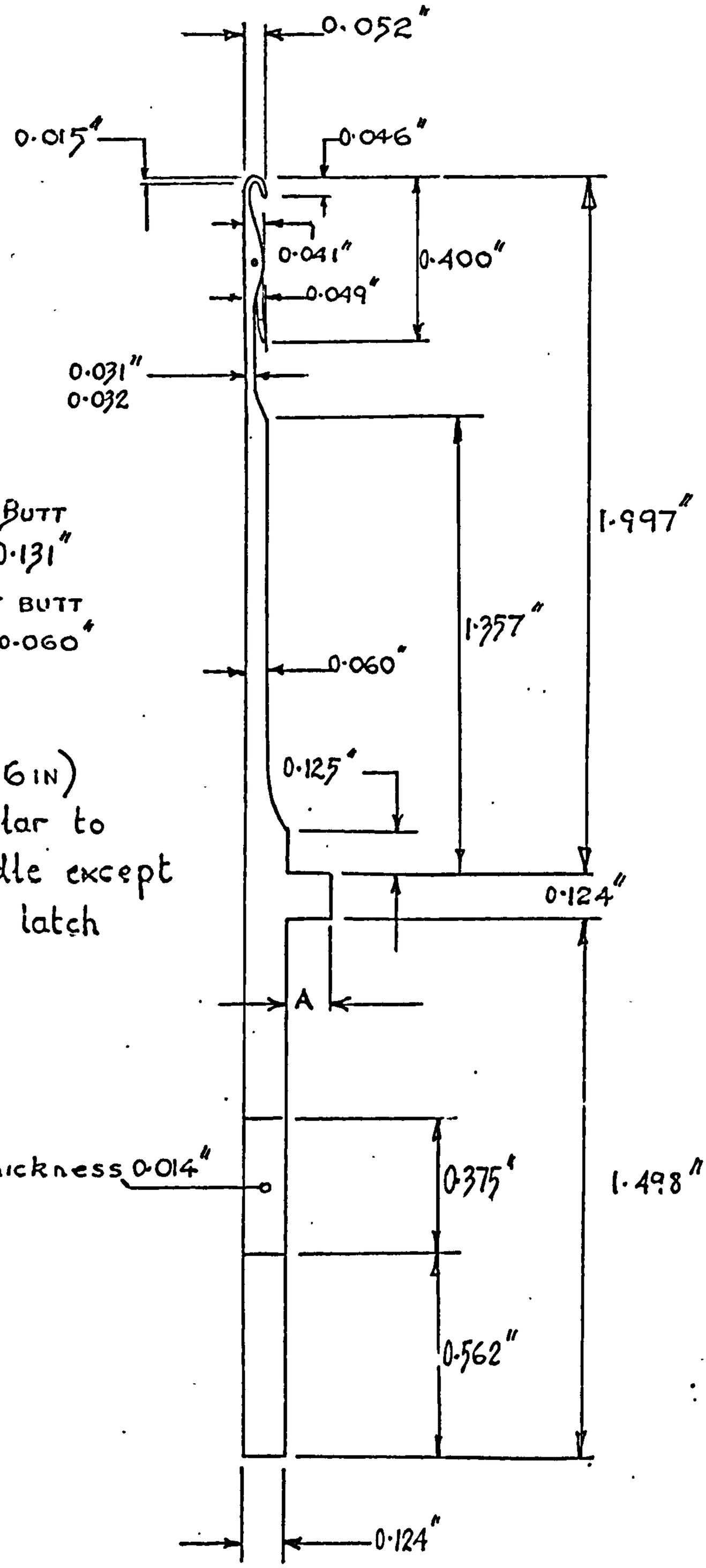

STANDARD LONG-BUTT
NEEDLE A = 0·131"

STANDARD SHORT BUTT
NEEDLE A = 0·060"

0·406 mm (0.016 IN)
Needle is similar to
0·443 mm needle except
for shortened latch
motion

Mill Thickness 0·014"

0·443 mm (0·0175) IN thick
Latch Needle

Fig 3.2

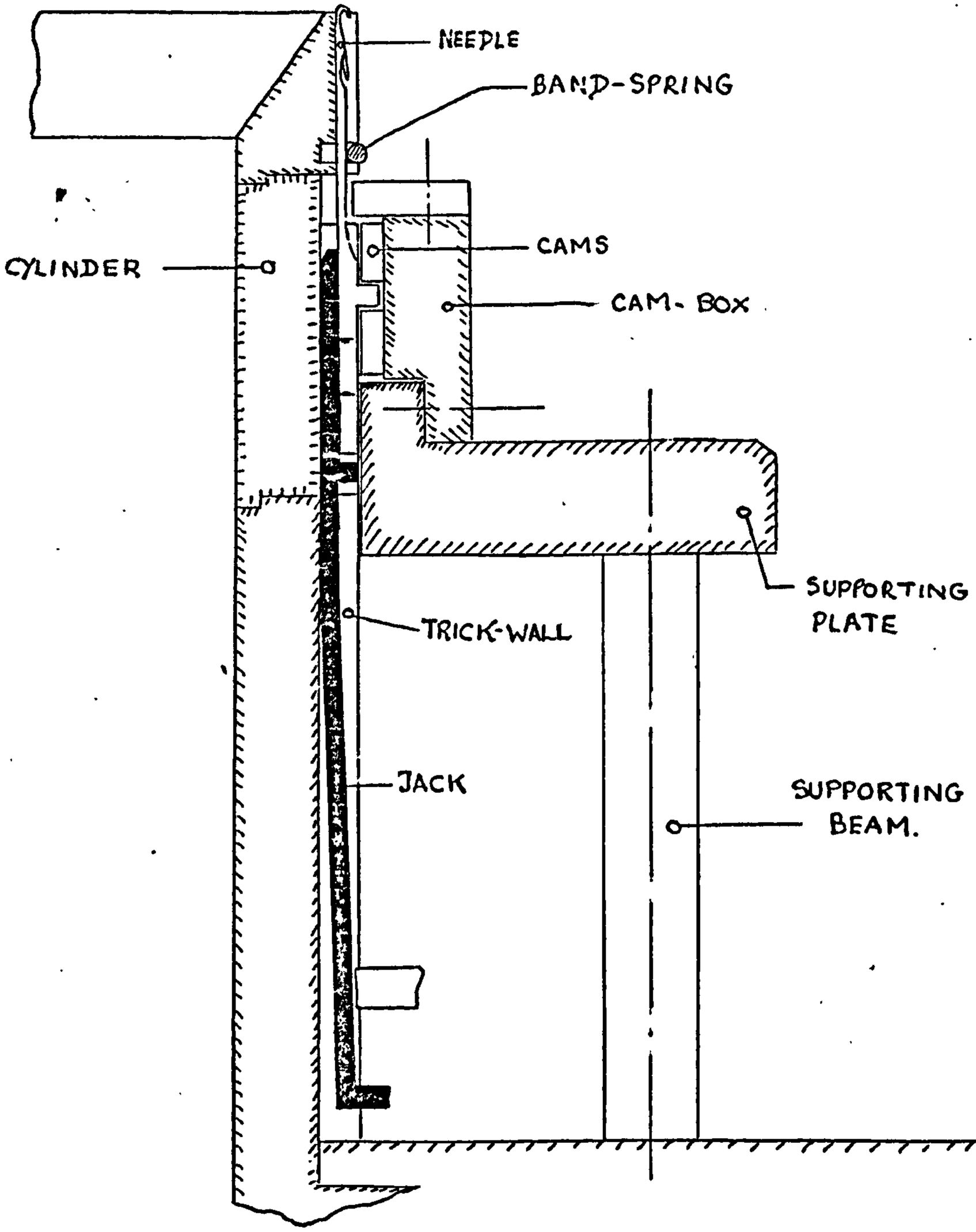

NEEDLE MOUNTING ON.
KNITTING MACHINE

Fig 3.3.

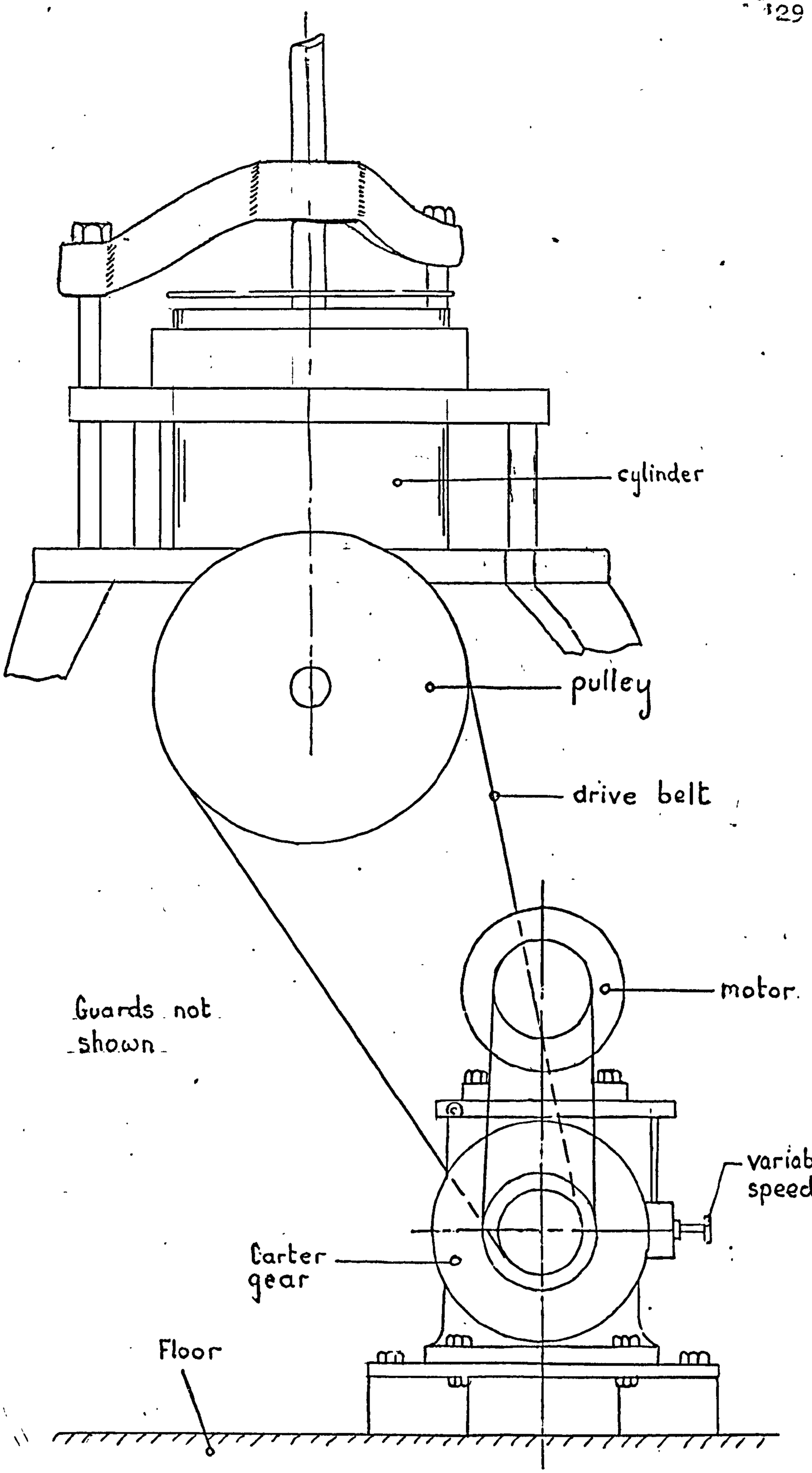

Motor and Carter Gear Mounting

Fig 3.4

PART B

INITIAL EXPERIMENTATION

CHAPTER 4

THE DESIGN, MANUFACTURE AND TESTING OF THE FIRST CAM-FORCE MEASURING SYSTEM

4.1 Selection of the System to be used for Force Measurement.

The measurement system selected was the transverse excitation of a stiff-beam as shown in Fig 4.1 (c). A cam track would be fitted to the end of the beam, and the force between the cams and the needle would produce a resulting strain, which semi-conductor strain-gauges, bonded to the beam surface would respond to. Provided that the beam natural frequency is considerably higher than the frequency of the highest discernable harmonic component of the force signal, the strain is directly proportional to the force, and static calibration is permissible. Before this system was selected many alternatives were examined, two feasible ones being a beam in compression (Fig 4.1 (a)), or a modified cam track (Fig 4.1. (b)). The merits and limitations of the three systems are also summarised in Fig 4.1. The masses of the beam and track would be minimised at the design stage, the only method of then increasing the natural frequency further would be to increase the beam stiffness by increasing its physical dimensions. This would reduce the cam track deflection to negligible proportions, but it had the serious disadvantage that the strain per unit force would become smaller, and more sensitive strain gauges would consequently be required. Semi-conductor strain gauges have a distinct advantage over wire and foil gauges, their increased output per unit strain meaning that much higher beam natural frequencies can be achieved.

4.2 Design and Manufacture of the Cam-Force Measuring Transducer Mark I.

The cam-force transducer Mark I was basically a double cam-track instrument, with one track fitted directly behind the other as illustrated in Fig 4.2. One needle had a butt so shaped that it only contacted the radially outer cams, which were carried on the force measuring cantilever. All the other needles ran in the radially inner cam-track. The impact point and the shape of the special needle is shown in Fig 4.2. At this stage before any measurements had been taken, the nature of the force input signal was unknown and it was impossible to predict the natural frequency necessary for the beam. Initially, the beam was designed to have a high natural frequency, approximately 2000 Hz, and if, after initial measurements, the frequency needed was seen to be higher, a new beam would then have been made. The dimensions of the initial beam were 0.35 ins (0.89 cm) square by 1.25 ins (3.17 cm) long and the strain sensitivity was calculated to be approximately 17.5 x 10^{-6} strain per unit kilogramme. The instrument had the following special features:-

(i) It allowed force measurements to be carried out on one needle without influencing the normal knitting process.

(ii) It required only a small amount of modification to the needle. The effect of this modification would be thoroughly analysed by a series of experiments before any detailed measurements were carried out.

(iii) The instrument could be easily removed and fitted to the knitting machine.

(iv) The stitch-draw could be adjusted easily.

(v) The mechanism could accomodate various cam-forms

4.2.1 The Cam-Shape used in Initial Experiments.

For initial experiments a typical widely used cam-form

was fitted to the beam, the dimensions and shape of the cams being shown in Fig 4.3.

4.3 Modification of Knitting Machine to Facilitate Measurements.

The knitting machine needed no alteration except that, to enable the instrument cam track to fit closely to the cylinder, the cam-box had to be modified. The existing stitch and guard-cams were removed and a slot was cut in the box sufficient to take the beam.

4.4 Electrical Circuitry.

Two strain gauges were bonded to each side of the beam, the gauges on the top and bottom were positioned so that they were responsive only to the vertical component of force. Similarly, the gauges on the beam sides were only responsive to horizontal components of force. Two Wheatstone bridge circuits were formed, one from the four gauges on the top and bottom, and the other, from the four gauges on the sides. The output from each Wheatstone bridge was passed to a Strain Stall type 91A D.C. amplifier. The bridge supply voltage was provided by the amplifier; however, since it was generally used with foil strain-gauges the stabilised voltage of 10.0 to 10.5 Volts was too large for semi-conductor strain-gauges, and dropping resistors (200Ω each) had to be placed in series with the bridge voltage supply terminals to reduce the voltage to approximately 6.0 Volts. For high frequency voltage amplification a D.C. amplifier had to be used since, although A.C. amplifiers are generally simpler and less prone to drift errors, they are not suitable for the amplification of rapidly changing signals with high frequency components. The output from each amplifier was taken to a four-channel type 564B Textronix storage oscilloscope, which was capable of displaying four separate inputs at the same time and also

had a triggering facility which, when fired, would enable one sweep of all four inputs to be stored on the screen. If desired this could be erased, and by pressing the single shot switch, another sweep would be recorded when the oscilloscope was triggered. The storage facility was extremely useful, since it meant that the trace could be examined closely before deciding whether a photograph was necessary. Throughout the circuitry, shielded wire was used wherever possible and the system was thoroughly earthed. Further information is shown in photograph Fig 4.4 and the circuit diagram in Fig 4.5.

4.4.1 Positioning the strain gauges.

It was important that the strain gauges should be bonded to the beam at a position where the strain was a maximum, and that the gauges responsive to vertical loads should be insensitive to horizontal loads. Conversely, the gauges sensitive to horizontal load, should be insensitive to vertical loads. The gauges were positioned as far from the cams as possible to maximise the bending moment and the strain; all the gauges were positioned a small equal distance from the beam neutral axis as shown in Fig 4.6. The effect of this was to ensure that the response to the undesired force cancelled out in the wheatstone bridge. This point is clarified in the next section (4.4.2).

4.4.2 The Four-Arm Wheatstone Bridge Circuit.

The gauges were connected into a four-arm wheatstone bridge circuit as shown in Fig 4.6.

The output voltage from the circuit is:

$$\Delta E = \frac{V R_1 R_2}{(R_1 + R_2)^2}\left(\frac{\Delta R_1}{R_1} - \frac{\Delta R_2}{R_2} + \frac{\Delta R_3}{R_3} - \frac{\Delta R_4}{R_4}\right) \cdot (1$$

$$\frac{\Delta R_n}{R_n} = G_n \epsilon_n \quad (n = 1 \text{ to } 4)$$

where $R_n\ (n=1\text{ to }4)$ = Resistance of the respective strain-gauges,
$G_n\ (n=1\text{ to }4)$ = Gauge factors of the respective strain-gauges,
$\epsilon_n\ (n=1\text{ to }4)$ = Strain at position where each respective gauge is positioned,
V = Voltage supply to bridge,
and ΔE = Voltage output from bridge.

The gauges were selected so that as nearly as possible :

$$R_1 \doteq R_2 = R_3 = R_4$$

and $$G_1 = G_2 = G_3 = G_4$$

Gauges 1 and 3 were bonded to the beam side experiencing tensile strains, while gauges 2 and 4 were bonded to the compressive side. If the gauges are properly aligned, gauges 1 and 3 experience positive strain of equal magnitude to the negative strain of gauges 2 and 4, i.e. $+\epsilon$ and $-\epsilon$ respectively.

The output voltage then becomes :-

$$\Delta E = VG\epsilon \quad . \quad . \quad . \quad . \quad (12)$$

Equation (12) shows the simple relationship governing the output from the bridge. One unique advantage of the bridge is that it produces a higher voltage output for a particular strain. It is twice as sensitive as the two-arm bridge and four times as sensitive as the single-arm bridge. However, it has other very important advantages, which are sumarised below :-

(i) If the gauges are positioned closely together and there are no temperature gradients from one gauge to another, then, for four matched gauges, complete temperature compensation is achieved, i.e.

$$\frac{\Delta R_1}{R_1} = \frac{\Delta R_2}{R_2} = \frac{\Delta R_3}{R_3} = \frac{\Delta R_4}{R_4}$$

and $$\Delta E = 0$$

(ii) If the gauges on each beam face are positioned a small distance on each side of the neutral axis, as shown in Fig 4.6, then when a load is applied at right angles to the direction of desired sensitivity, the strain on gauges 1 and 2 is $+\epsilon$ and on gauges 3 and 4 is $-\epsilon$, and hence :-

$$\Delta E = 0$$

It is impossible to obtain complete matching of strain-gauges and it was inevitable that there would be some small response to transverse loads. This response was minimised by the fact that the gauges were only a small distance offset from the neutral axis, and consequently bending strains produced by the undesired loading were very small.

4.4.3 The Triggering Circuit.

It was important that the oscilloscope should be triggered at the instant of time when the special needle was passing through the cam-track. A simple, battery micro-switch circuit was used. A small stud was attached to the cylinder and this closed the micro-switch as the cylinder rotated. The exact instant at which the stud closed the switch and fired the oscilloscope was set to correspond to the passage of the special needle through the transducer cam-track. The circuit diagram is shown in Fig 4.7.

4.5 The Calibration Procedure.

Before each experiment a calibration was carried out. This was designed to determine the relationship between the force applied to the cam-track and the deflection of the oscilloscope trace. All the apparatus was assembled on a bench and was wired and connected in exactly the same way as when fitted to the knitting machine. The cam-force transducer was then clamped upright in a vice and dead weights were hung on

the cam-track as shown in Fig 4.8. The response of the strain-gauges to each load was stored on the oscilloscope screen, and a graph was plotted of oscilloscope trace deflection against the vertical-force applied to the cam. A similar procedure was carried out for the horizontal force calibration, except that the cam-force transducer was turned on its side and then clamped in the vice. Dead weights were again applied and a calibration graph was plotted. The two graphs are shown in Fig 4.9

It was desirable that the cam-force transducer could be calibrated on the knitting machine, and, if possible, during and after the running of tests. The bench calibration meant that all the apparatus had to be removed from the machine and assembled on a bench before calibration could be carried out, and this was a time consuming operation. An apparatus as detailed in Fig 4.10 enabled very quick vertical force calibration, without any part of the apparatus having to be removed from the machine. Unfortunately, the horizontal force could not be calibrated in this manner because the cams on the transducer were horizontally inaccessible when mounted on the knitting machine. However, a technique was developed to enable frequent checks on the strain gauge response to horizontal loading. During bench calibration a spring balance was used to apply a known horizontal force to a part of the beam at a little distance from the cam track. The deflection of the oscilloscope trace in response to this force was noted. During experiments when the cam-force transducer was attached to the knitting machine, frequent checks were carried out by applying the same horizontal force to the beam and noting the oscilloscope trace deflection.

The calibration procedure was to carry out a full bench

calibration before an experiment, and then make frequent spot checks of vertical calibration and response to horizontal force during the experiment. At the conclusion of experimentation, a further bench-calibration was carried out.

4.5.1 The Effect of Off-Set Loads upon the Calibration.

Initially, when the needle contacts the stitch-cam, the moment-arm between the beam centre and the force application point is large. As the needle moves through the cam-track the moment arm reduces, and finally increases again as the needle moves towards the end of the guard cam. An experiment was carried out to determine the effect of offset forces on the strain-gauge output. Loads were applied to the cam track at positions and in directions shown by the arrows in Fig 4.11. The normal position for hanging the weights for vertical calibration was at A, and that for horizontal calibration was at B. Maximum errors in the calibration occured if the loads were applied at position 1, i.e. + 2.5% for vertical calibration and + 2.0% for horizontal calibration. However, this error was throught to be negligible, and it was therefore considered unnecessary to correct the experimental results to allow for the effect of off-set loading.

4.6 Experiments Designed to Examine the Output from the Cam-Force Transducer.

The special needle (section 4.2) had two basic modifications; it had a butt cut out, and the needle-cam impact point was approximately 2.24 mm (0.088 ins) from the cylinder. The impact point for the standard long butt needle, detailed in Fig 3.2 was between 0.076 mm (0.003 ins) and 0.304 mm (0.012 ins) from the cylinder. These experiments described below were designed to investigate the effect of these butt modifications. If the instrument was to be used successfully, the effects

would have to be small and predictable, so that the forces between the standard needle and the cams could easily be obtained from experiments using the special needle.

4.6.1 Experimental Method.

Some time before each experiment was carried out, the oscilloscope and amplifiers and triggering mechanism were switched on. This was to allow the instruments to warm up and the room temperature to stabilise before measurements were taken. The trick in which the special needle was fitted was cleaned with grease-removing solvent, the needle was fitted, and the machine was lightly oiled with Vicker's spotless B.N.O Needle Oil. It was found in early experiments, that immediately after fitting the needle in the trick, the cam-force was variable from one machine revolution to the next until the needle settled in the trick, and the force became stabilised. To ensure that the measurements were carried out when the forces had settled, the machine was run for a short time before taking a reading. The system was calibrated as detailed in section 4.5. The calibration factors were 35.3 gf horizontal load per 1 mm photograph trace deflection, and 13.4 gf vertical load per 1 mm photograph trace deflection.

4.6.2 Measurement Parameters.

For all of these initial experiments 0.443 mm (0.0175 in) thick needles were used. Traces were obtained under knitting conditions unless otherwise stated. The stitch-draw was approximately 1.78 mm (0.07 in).

The cam-cylinder clearance was fixed at 0.15 mm (0.006 in). A 0.15 mm thick shim was placed between the inner radial cam and the cylinder. The cam-force transducer was pushed up against the shim and the retaining screws were tightened, thus clamping the unit to the machine structure.

The tests were carried out at machine speeds of 27 and 57 revs per minute. The normal operational speed of the machine is 57 revs per minute.

The horizontal scale for the photographs is 5×10^{-3} seconds per unit division, one division on the photograph equalling 8.5mm.

4.6.3 Effect of Butt Cut-Out upon the Forces.

A special needle with a cut out of 0.20 mm depth at the top of the butt and one of 0.25 mm depth at the bottom, as shown in Fig 4.12.(1), was placed in a thoroughly cleaned trick. The machine was run for a short while and a trace was stored on the oscilloscope screen. The needle was then removed from the trick and the butt cut out was increased to 0.33 mm at the top and 0.25 mm at the bottom as shown in Fig 4.12.(2). The trick was re-cleaned and the machine was run for a short while. A trace was obtained and this was superimposed on top of the original trace. The process was repeated until five complete traces were stored on top of each other. A photograph of these was then taken and a typical record is shown at the top of Fig 4.12. On this can be seen both the vertical component of force between the butt and the cams, and the horizontal component of force. Initially the experiment was carried out at 27 R.P.M. and was then repeated at 57 R.P.M. Results obtained at the higher speed showed a similar trend to those obtained at the lower speed; however, the photographs showed severe distortion due to natural frequency oscillation of the beam. The oscillation appeared to be triggered by needle impact with the stitch-cam and guard-cam, since the oscillation was very large at these points on the cams.

The results indicated that, as the cut-out depth was increased, the force also increased, especially in the region

where the needle butt initially contacted the stitch-cam. However, at the bottom of the stitch cam, the force changed very little. Obviously the first trace, marked as No. 1 on Fig 4.12, showed that the cut-out depth was so small that the needle was contacting the radially inner track and not contacting the outer track at all.

The probable explanation for the increase of force at the beginning of the stitch-cam was that the butt was bending so much due to the displaced impact point, that for shallow depth cut-outs the radially inner cams were taking some proportion of the load, and hence reducing the force on the outer cam track attached to the beam.

4.6.4 Effect of Moving the Impact Point Radially away from the Cylinder.

A special needle (Fig 4.2) was positioned in a thoroughly cleaned trick, the apparatus being switched on and the knitting machine run for a short time. Initially a trace was taken with the cam transducer in the normal position, i.e. with the radially inner cams positioned 0.152 mm from the cylinder. The transducer was then moved outwards, so increasing the distance between the impact point and the cylinder. Further traces were taken and these were superimposed one upon the other. A typical photograph of the results is shown in Fig 4.13 , this giving added details concerning the distance, D, between the impact point and the cylinder for each trace. The results clearly show that the force increased as the impact point was moved radially outwards.

The inner radial cams were then removed from the cam force transducer. The cam-track connected to the beam was moved forward so that it was only 0.152 mm from the cylinder. A standard long butt needle was fitted in a cleaned trick, the

needles each side of it were removed so that only the one needle was running in the cam-track, the yarn was also removed from the needle, and a horizontal and vertical force trace record was obtained. The transducer was then moved back so that the needle impact point was 3.05 mm. from the cylinder, and another trace was taken. The traces were superimposed one on top of the other and an enlarged graphical representation of a typical record is shown in Fig 4.14. The machine speed was measured at 27 R.P.M. by means of a tacho-wheel pressed against the revolving cylinder. The experiment was repeated at 57 R.P.M. but due to resonant beam vibration, was somewhat difficult to interpret.

The results show a large increase in force as the impact point was moved away from the cylinder. Moving the impact point from 0.152 mm to 3.05 mm changed the max horizontal force from 265 gf to 490 gf and the max vertical force from 125 gf to 300 gf.

4.7 Conclusions to Part B.

The results indicated that moving the impact point further away from the cylinder increased the reaction force between the cam and the needle. The cut-out on the butt also had an effect upon the force; however, it seemed probable that this was caused by the inner radial cam sharing the load when the cut-out depth was small.

Due to the large effect of moving the impact point away from the cylinder, the forces on the special needles would be considerably larger than the force on a normal needle. Therefore, the designed cam-force transducer could not be used because the errors involved in carrying out the measurements on the special needle were far to large.

Johannes Barth[30,48] predicted a force increase as the

impact point was moved away from the cylinder. These results confirmed his opinion. The theory of Munden and Knapton[13,14,15,19,20,21] takes no account of the position of the impact point and it was not expected that the butt modification would produce such large differences in the force level; unfortunately Barth's paper was not available when this cam-force transducer was designed.

In these early experiments several modifications required in the circuitry became obvious :-

(i) As the machine speed was increased, the beam vibration tended to obscure the results, consequently, some means would need to be found either to reduce the beam vibration or to electronically remove the beam oscillation from the force signal.

(ii) Some basic difficulties occurred with the use of the trigger circuit. The contacting arm of the micro-switch tended to bounce as speed was increased, and this caused some damage tothe cylinder and the micro-switch. Similarly it would, if possible, be useful to combine speed measurement with the triggering function.

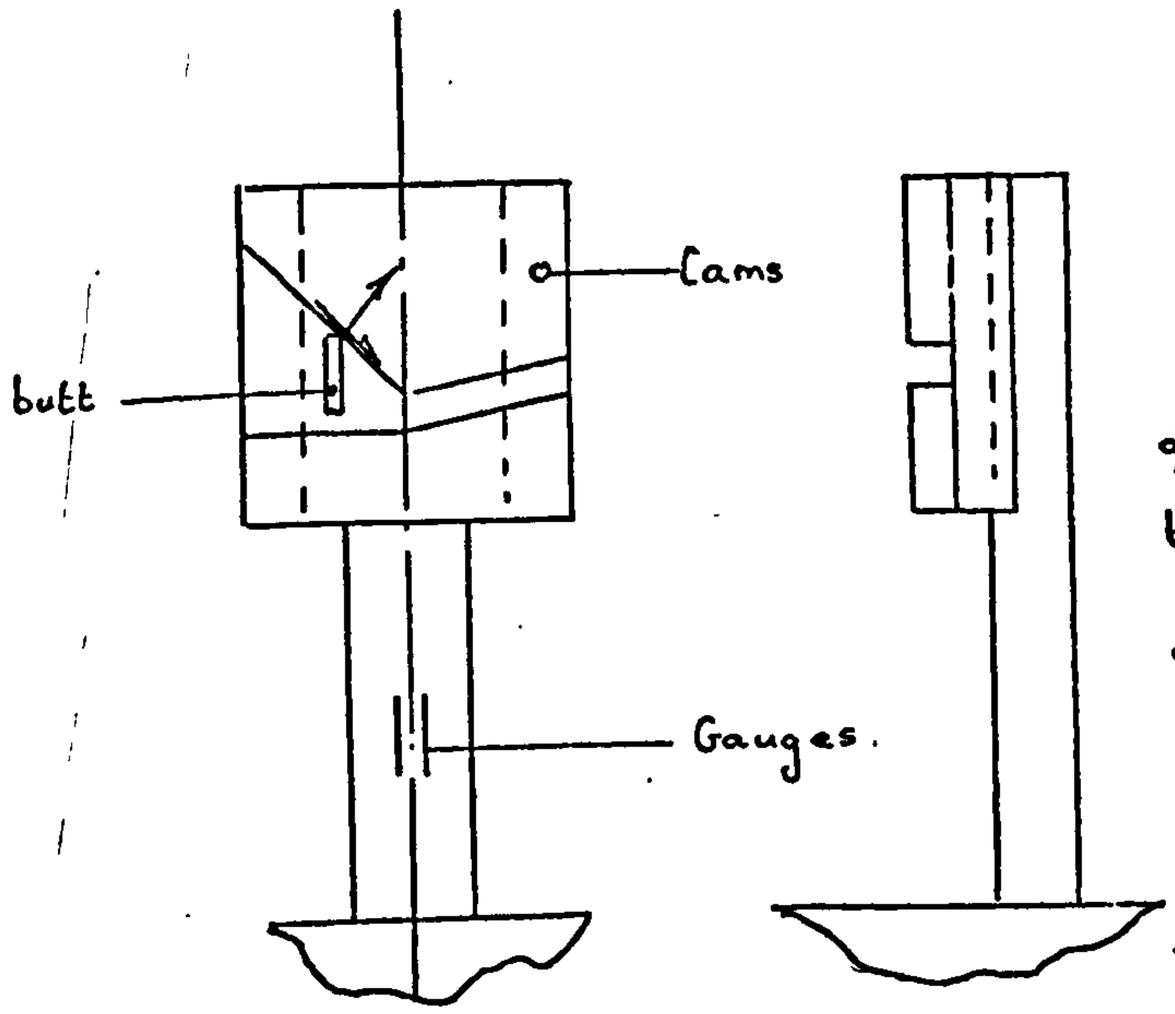

(a) COMPRESSION - BEAM.

a) Very Sensitive to Bending
b) Very difficult to fit in Cam-box.
c) Prone to Damage during normal running
d) Insensitive to Direct Loads.
e) Easy to fit gauges.
f) Cannot Measure Horizontal Forces.

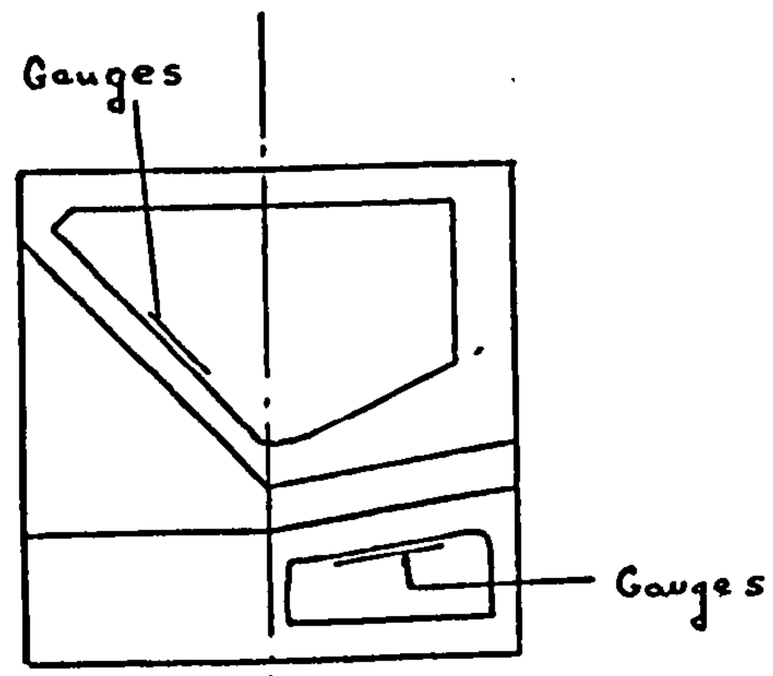

(b) MODIFIED - CAM.

a) Stiff and Insensitive
b) Very difficult to fit gauges
c) Very difficult to make
d) Difficult to Measure at base of Stitch cam.

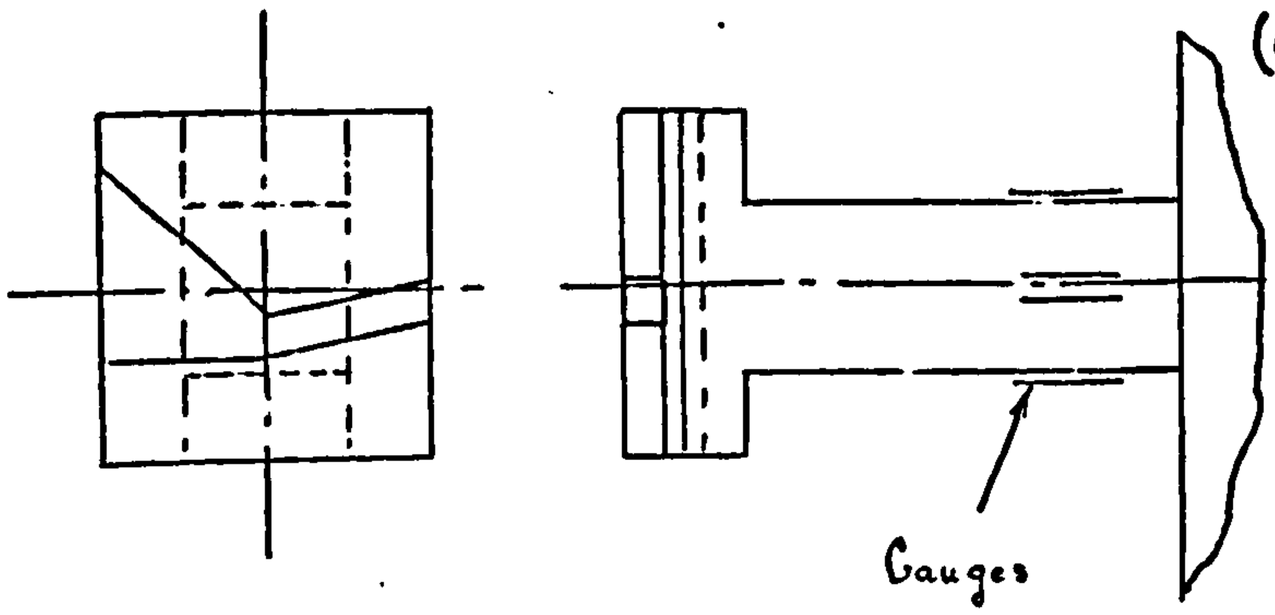

(c) - BEAM - IN - BENDING

a) No end-load on beam
b) Relatively easy to fit on machine
c) Easy to Strain-Gauge
d) Measure horizontal and Vertical forces
e) Not so sensitive to damage during normal running.

THREE POSSIBLE SYSTEMS FOR MEASURING CAM-FORCE

Fig 4.1

Com-force transducer material → Mild Steel.
Cams. → K200

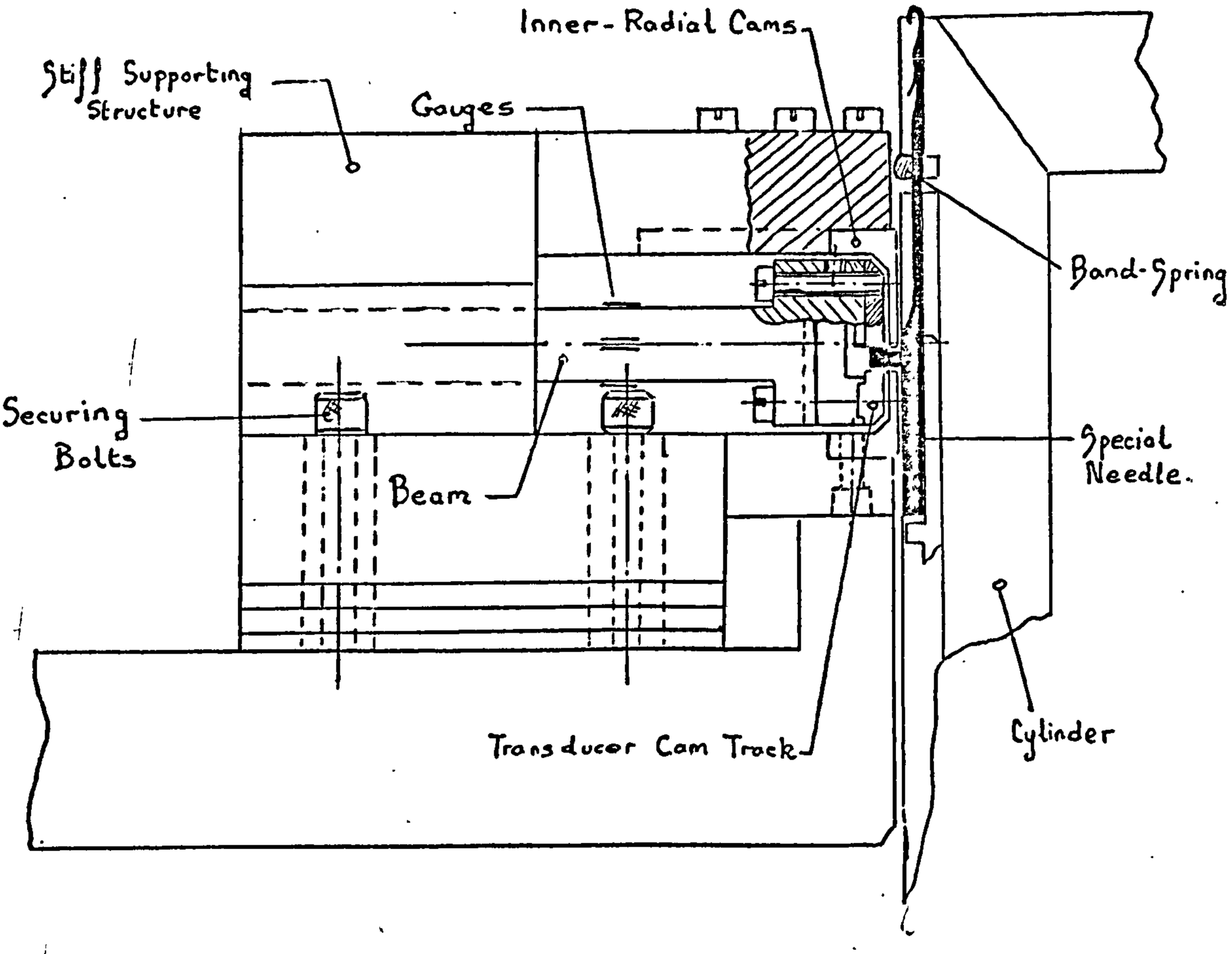

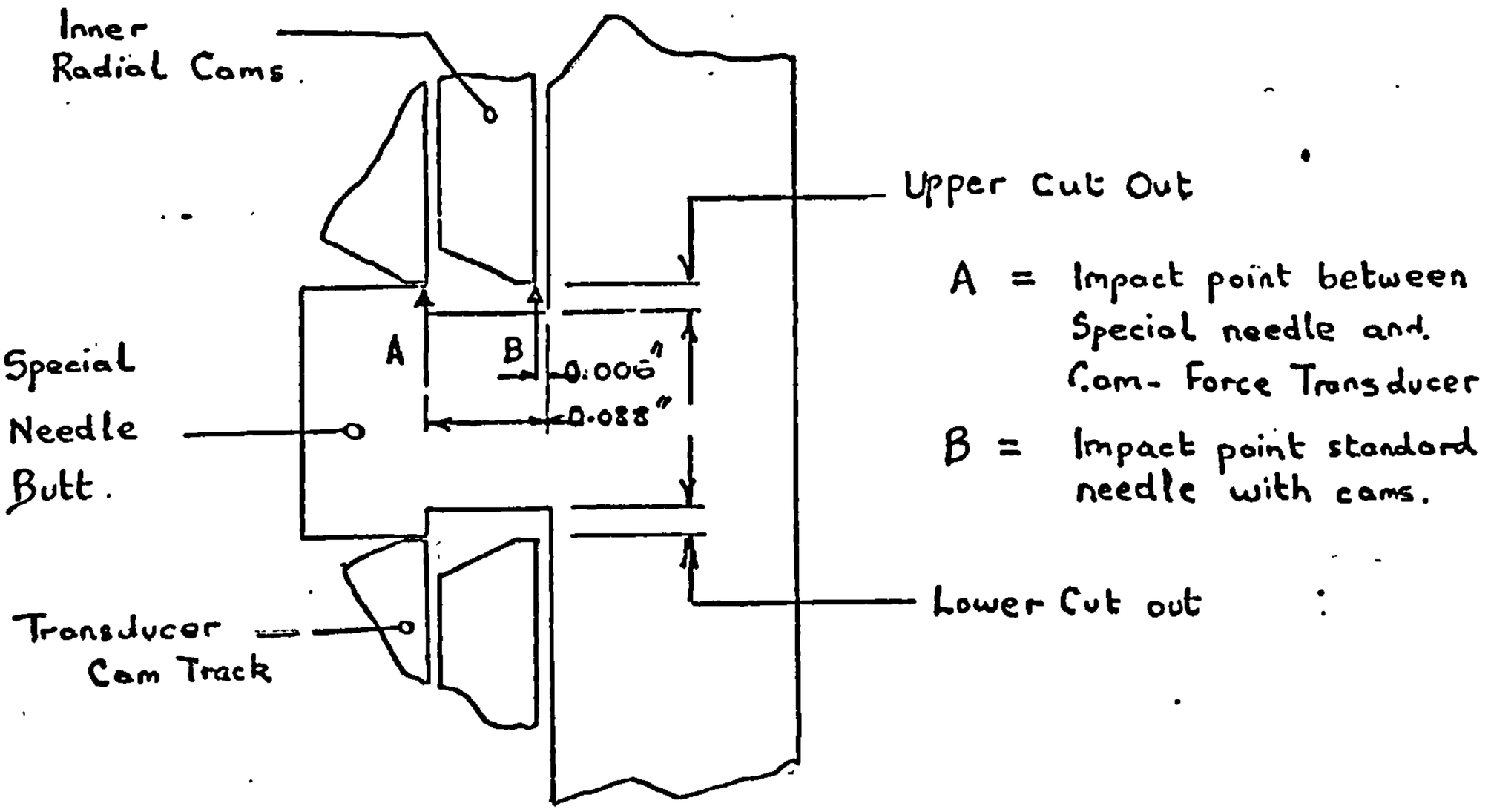

THE CAM-FORCE TRANSDUCER MARK I
AND SPECIAL NEEDLE

Fig 4.2

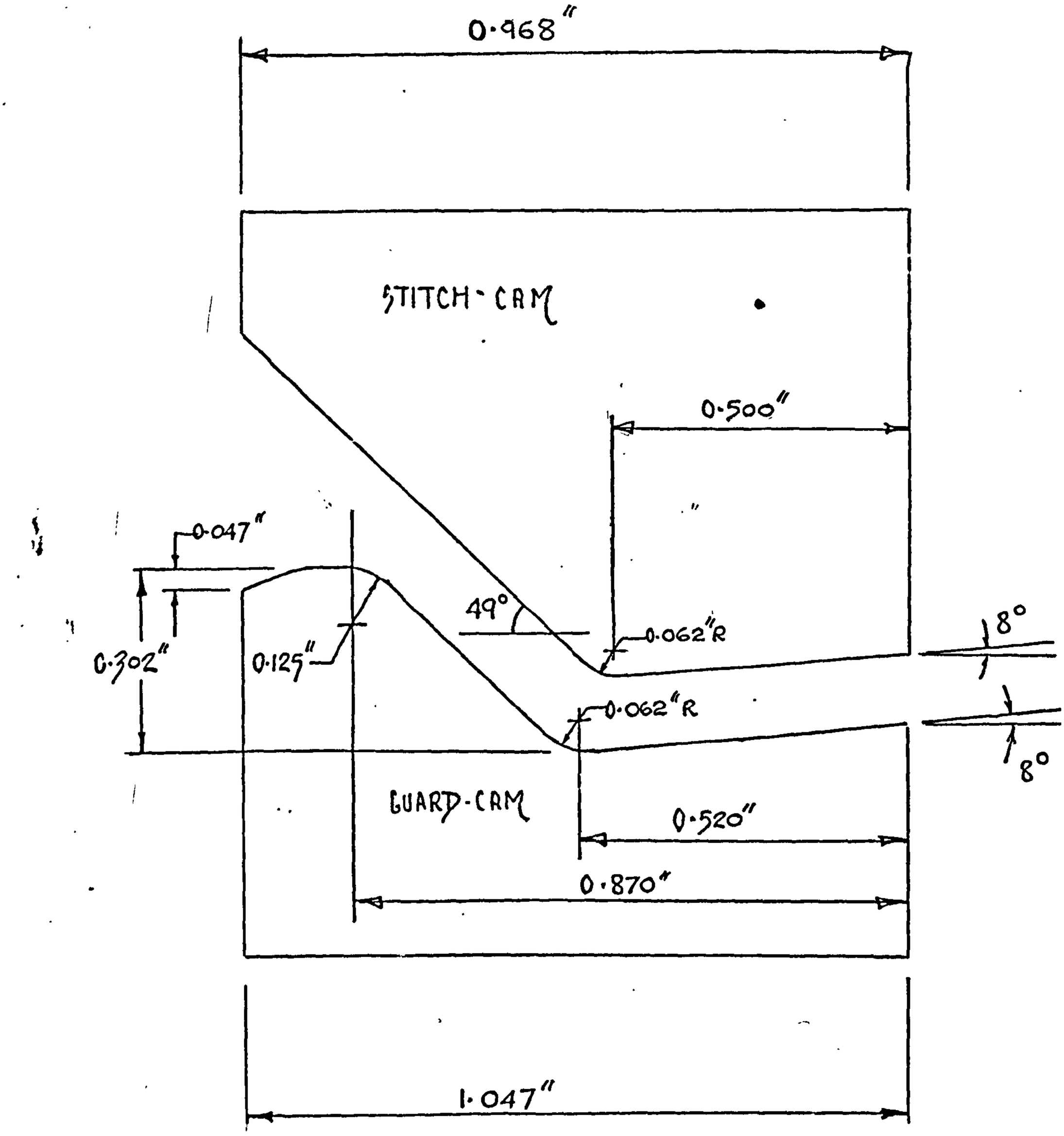

THE CAM-PROFILE

Fig 4.3

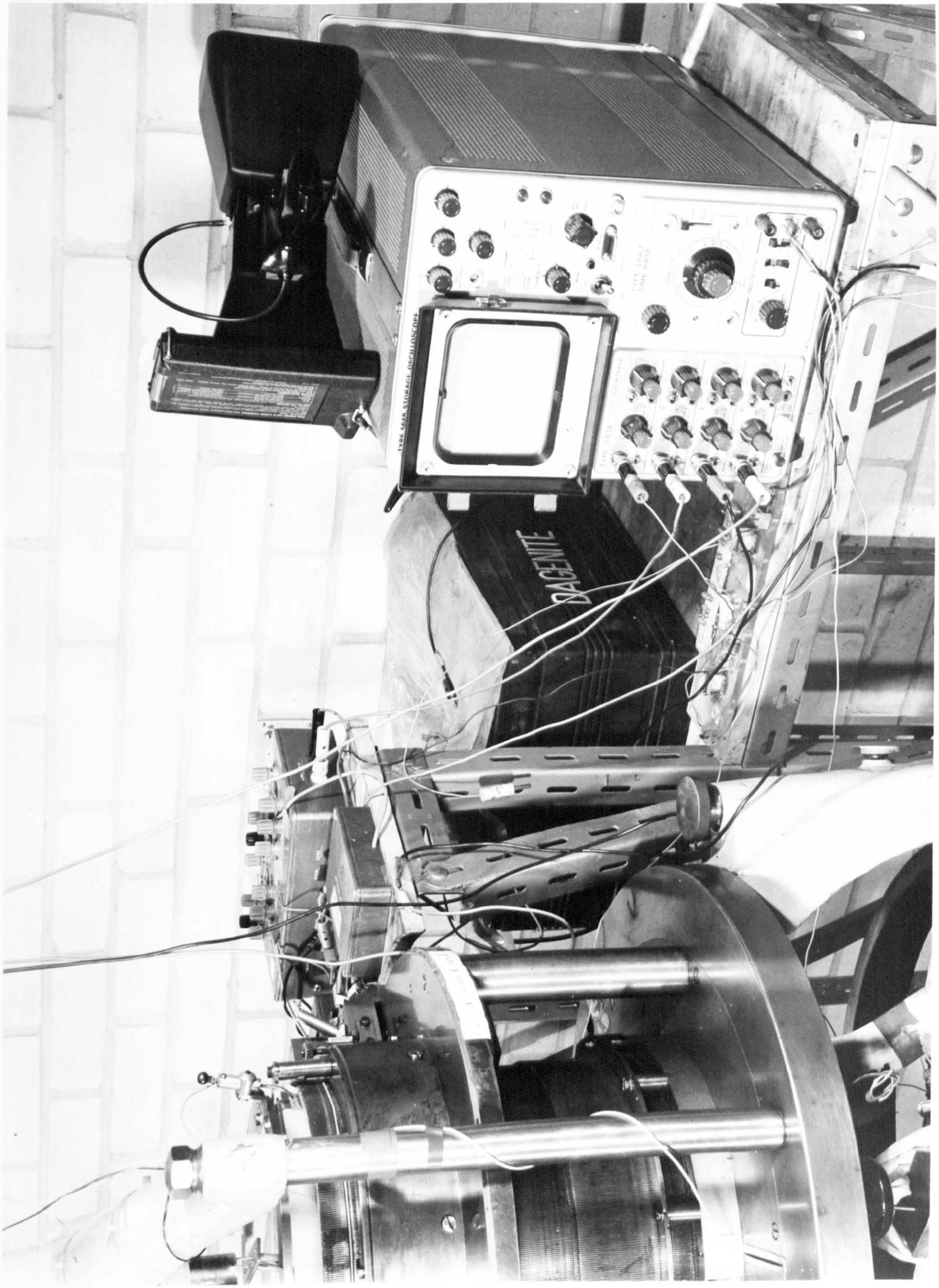

ELECTRICAL CIRCUITRY

Fig 4.4

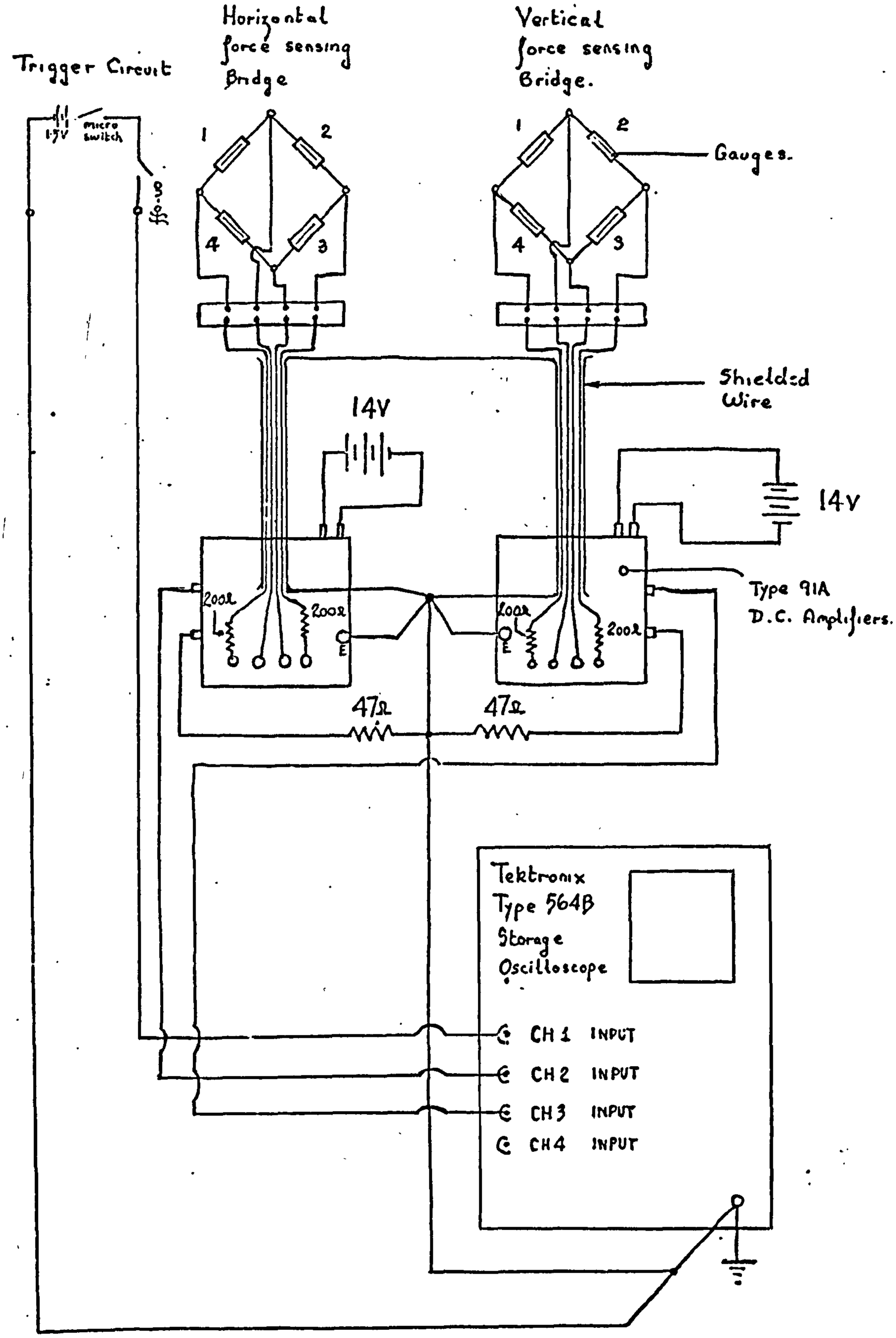

CIRCUIT DIAGRAM
CAM-FORCE TRANSDUCER.

Fig 4.5

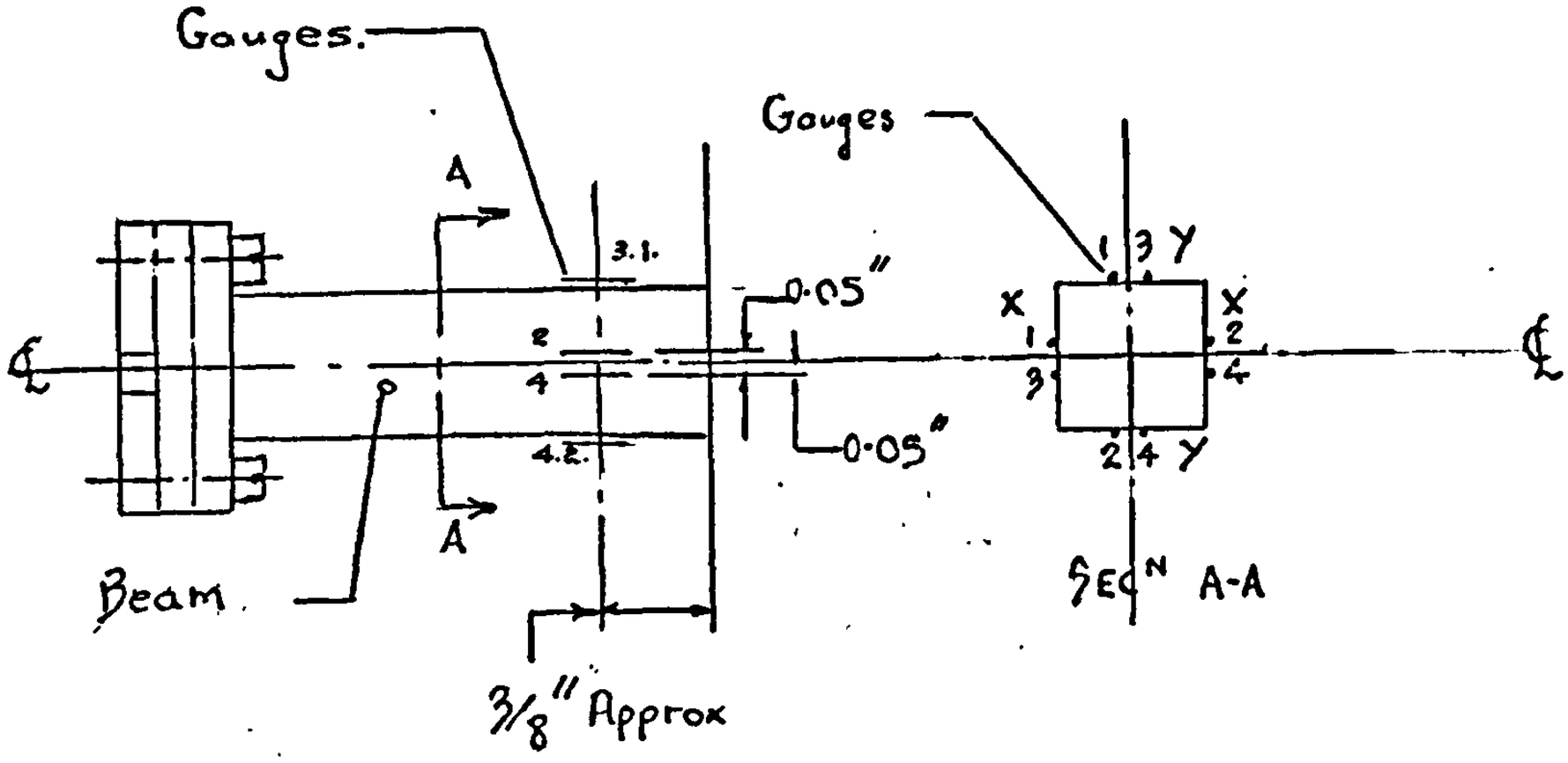

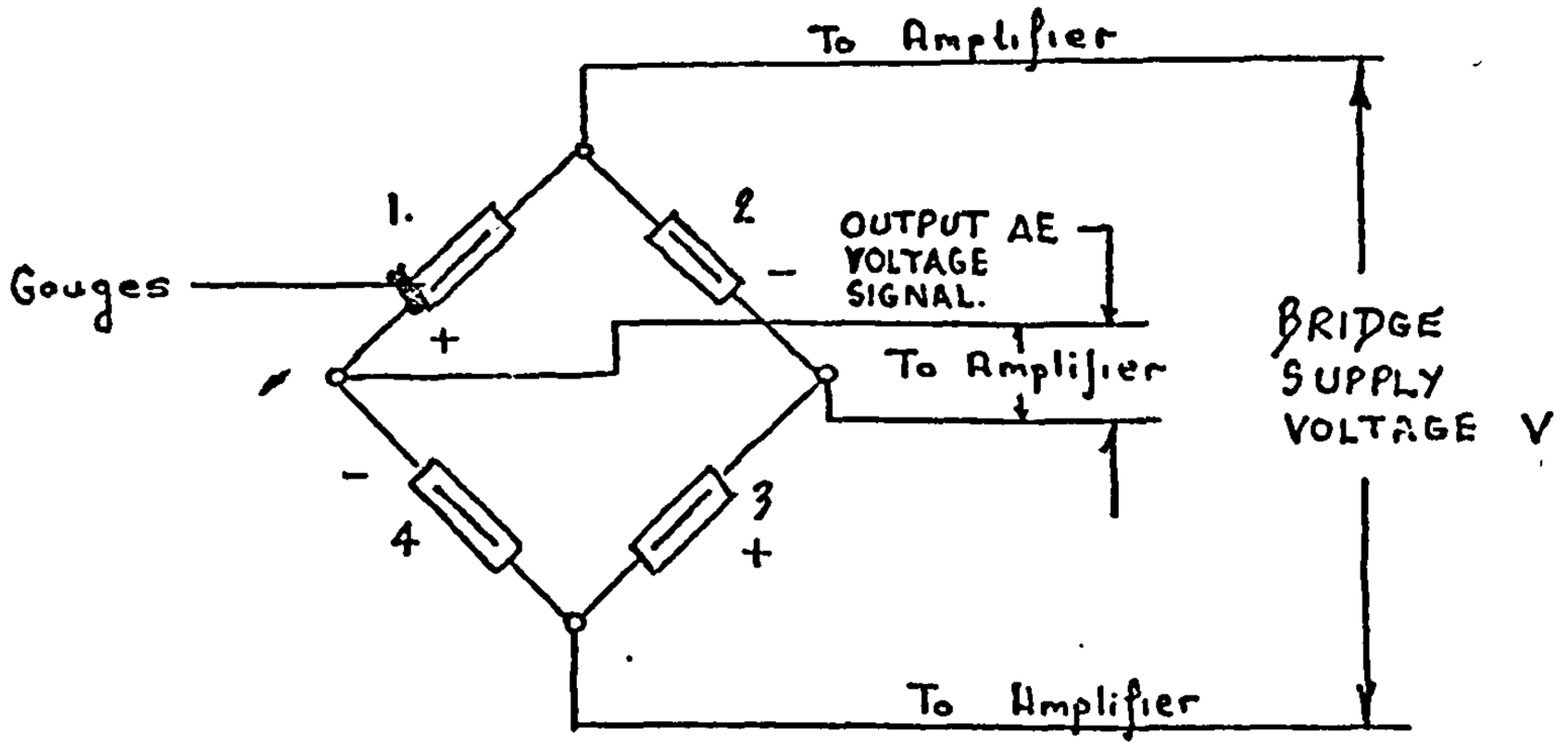

GAUGES NOMINAL RESISTANCE = 120Ω
P-TYPE SEMI-CONDUCTORS

VERTICAL FORCE SENSING GAUGES, FACES Y

HORIZONTAL FORCE SENSING GAUGES, FACES X.

POSITION OF STRAIN-GAUGES ON BEAM AND WHEATSTONE-BRIDGE CIRCUIT.

Fig 4.6

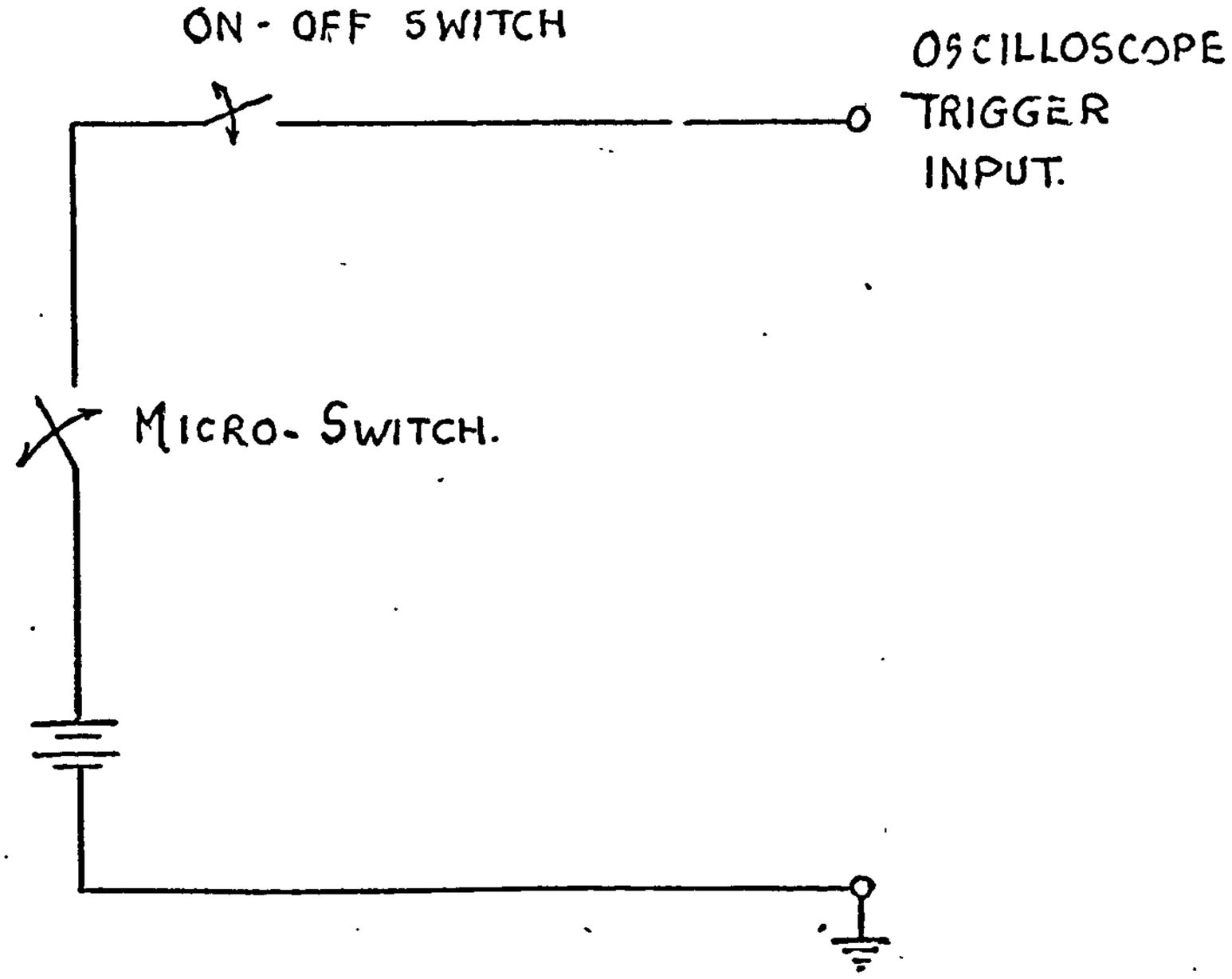

TRIGGER CIRCUIT.

Fig 4.7.

VERTICAL- FORCE
CALIBRATION

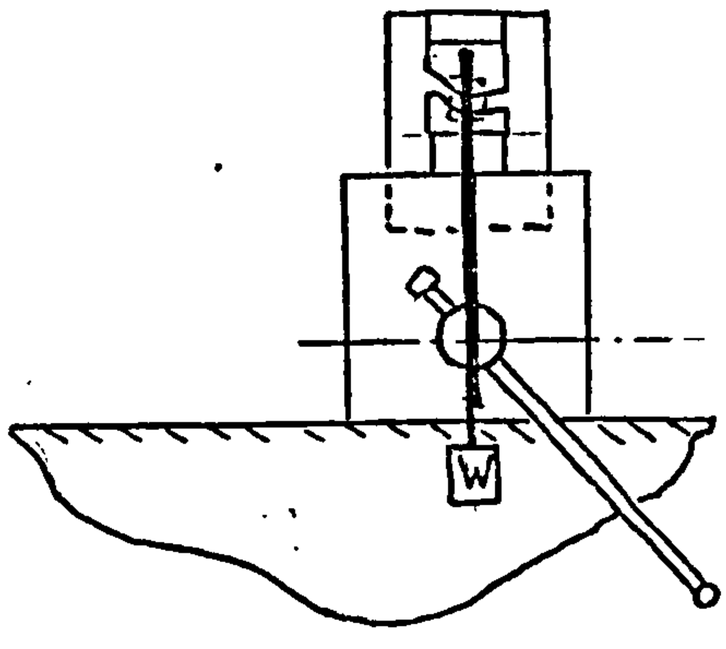

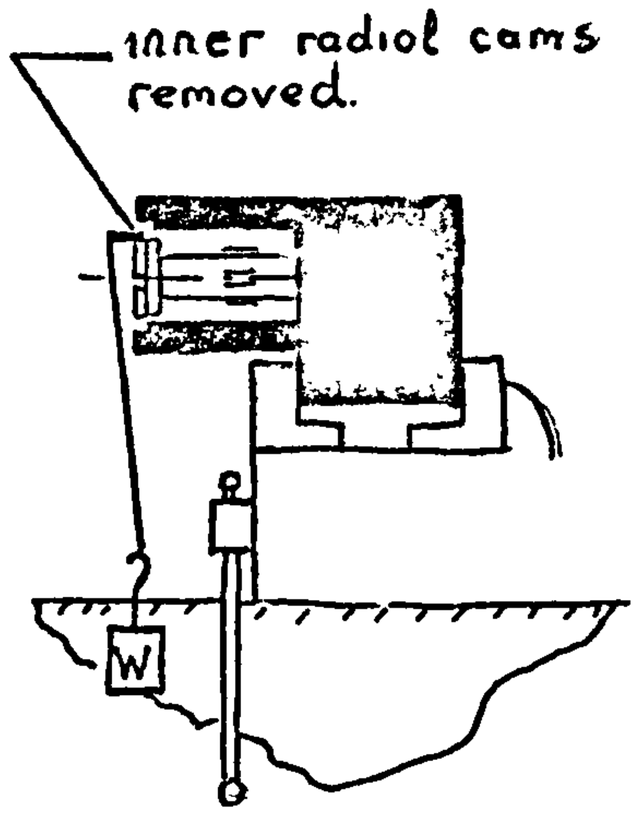

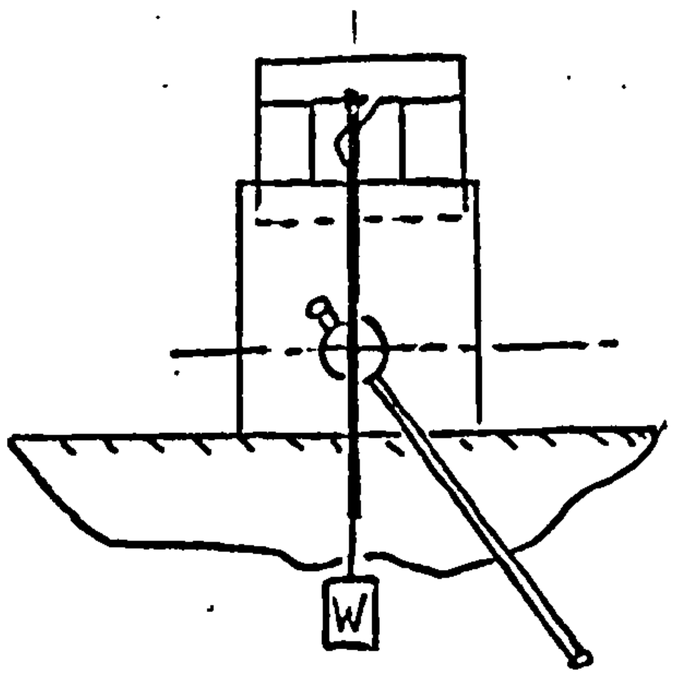

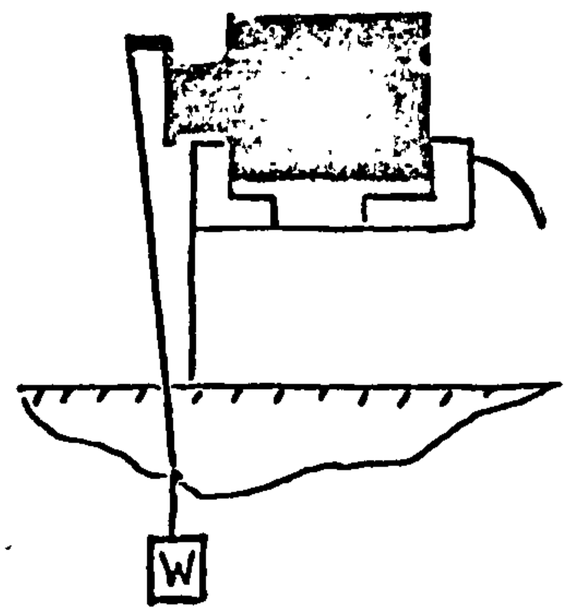

HORIZONTAL
FORCE CALIBRATION

BENCH CALIBRATION OF
CAM-FORCE TRANSDUCER

Fig 4.8

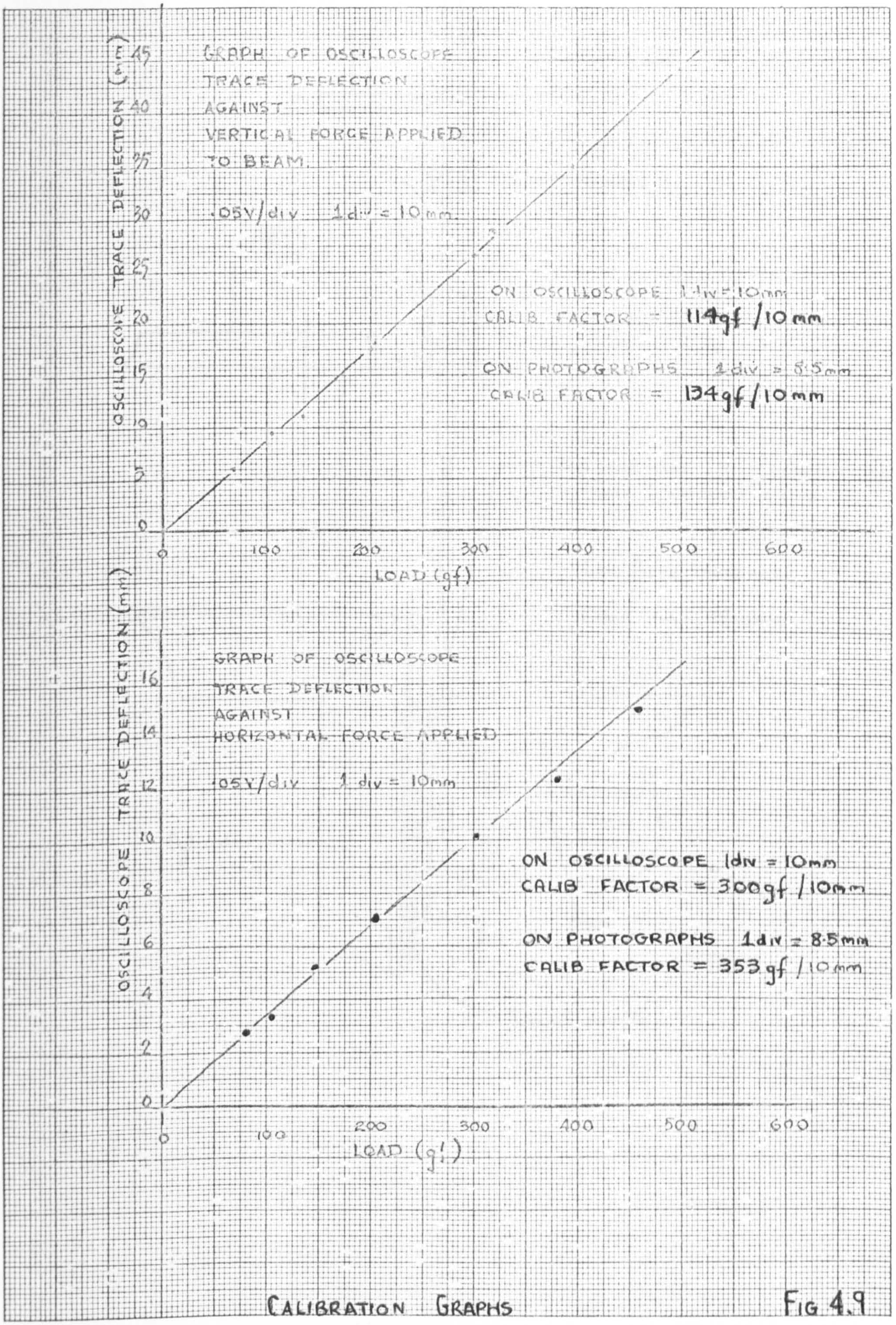

CALIBRATION GRAPHS

FIG 4.9

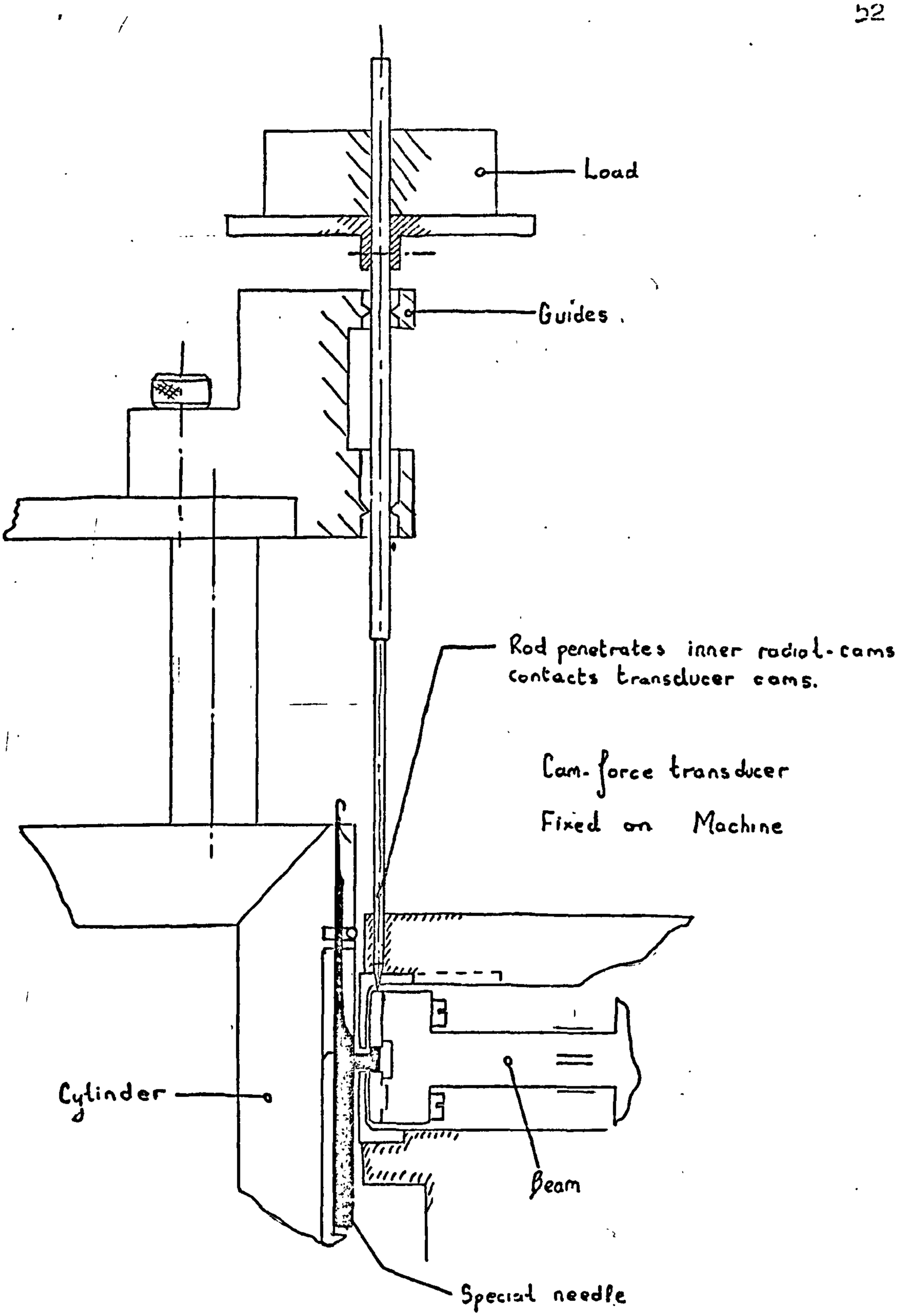

ON MACHINE VERTICAL
FORCE CALIBRATION

Fig 4.10

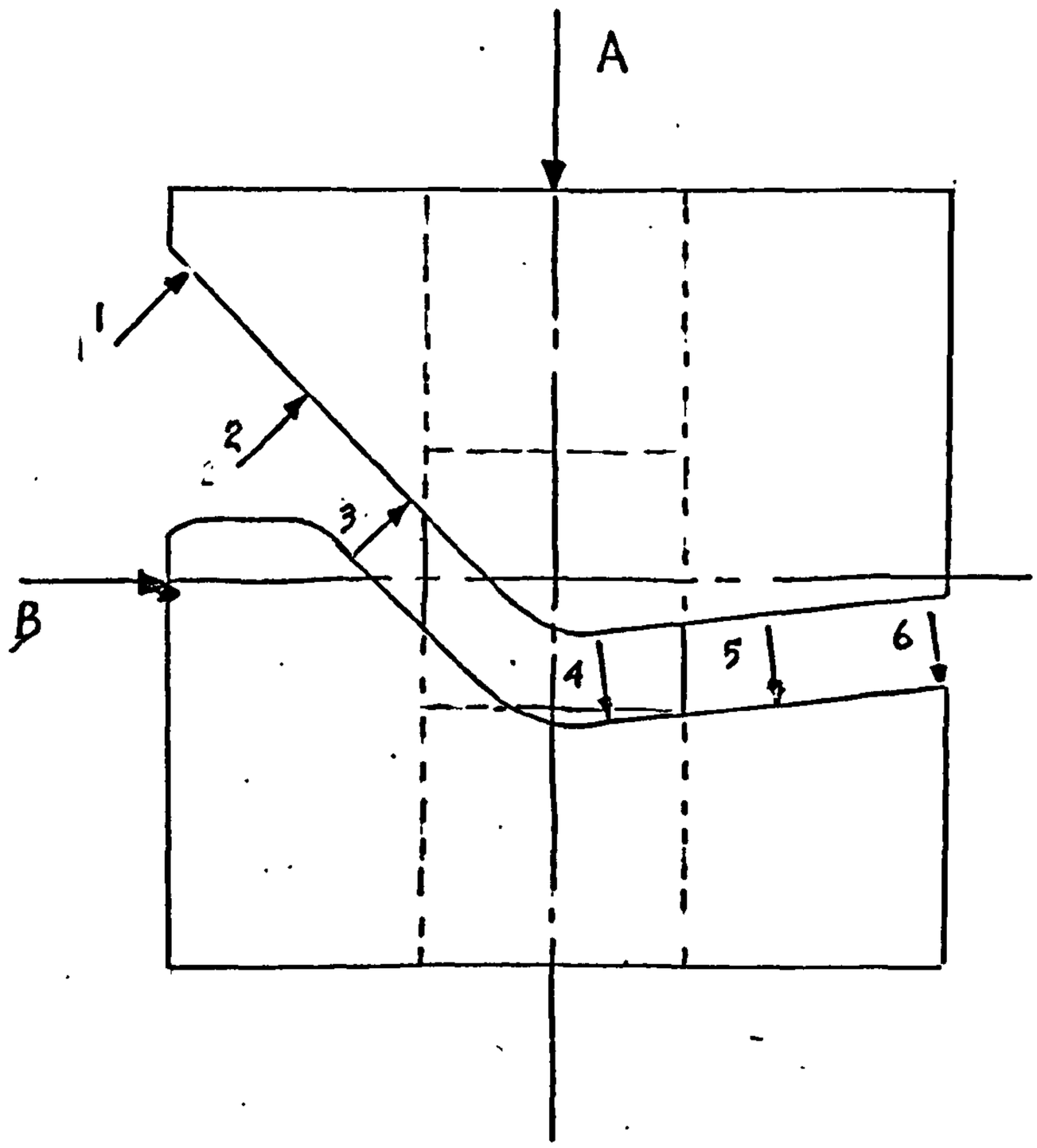

Arrows mark position and direction of offset loads.

THE EFFECT OF OFFSET LOADS UPON THE CALIBRATION

Fig 4.11

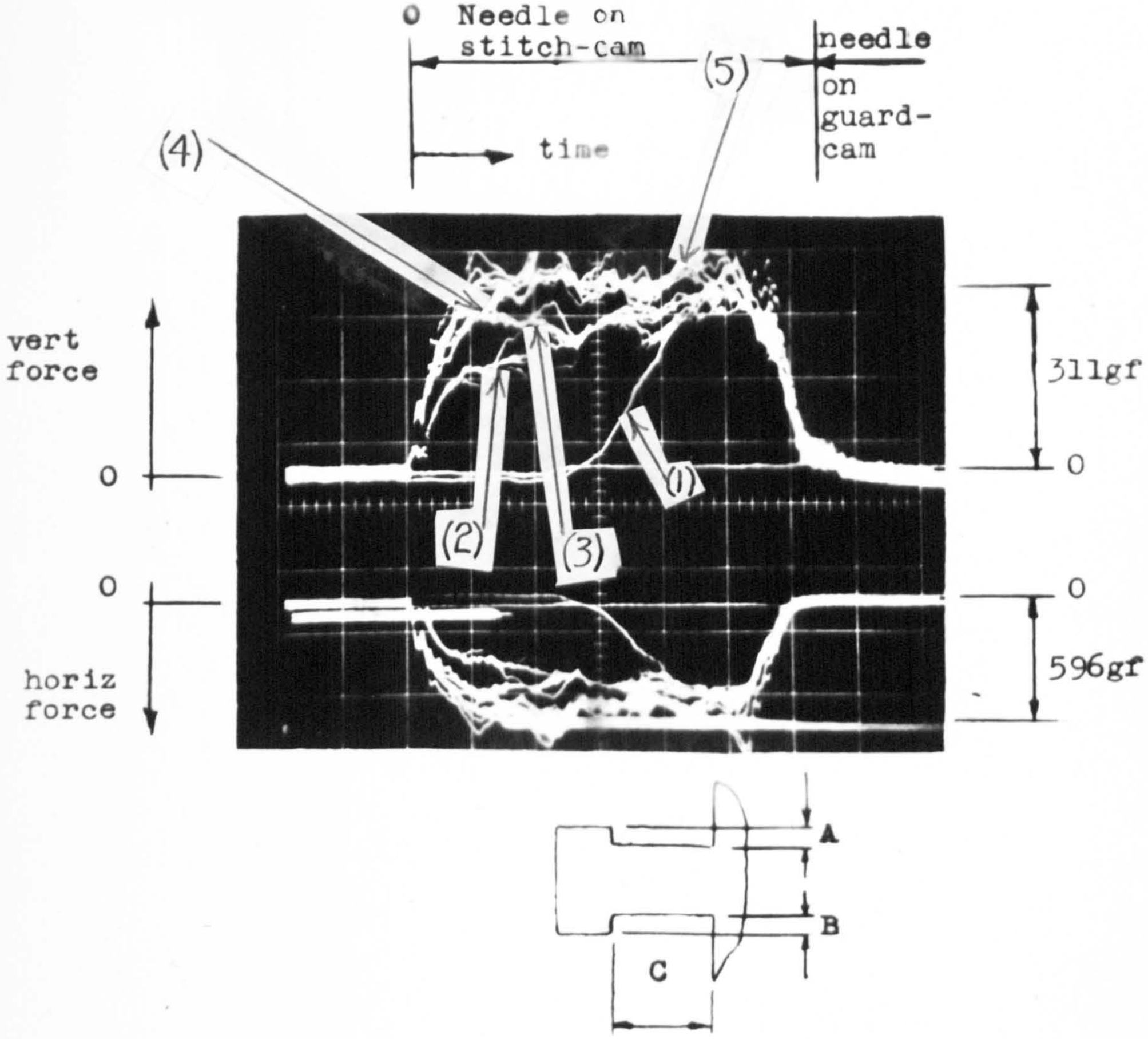

(1) A = 0.008 ins (0.203 mm)
B = 0.010 ins (0.254 mm)
C = 0.088 ins (2.24 mm)

(2) A = 0.013 ins (0.33 mm)
B and C same as (1)

(3) A = 0.016 ins (0.406 mm)
B and C same as (1)

(4) A = 0.025 ins (0.635 mm)
B and C same as (1)

(5) A = 0.050 ins (1.27 mm)
B and C same as (1)

Machine speed = 27 R.P.M.
Horiz force = 353 gf/10 mm
Vert force = 134 gf/10 mm
Time = 5 x 10-3sec/8.5 mm

Effect of butt cut-out on forces

EFFECT OF BUTT CUT-OUT ON FORCES Fig 4.12

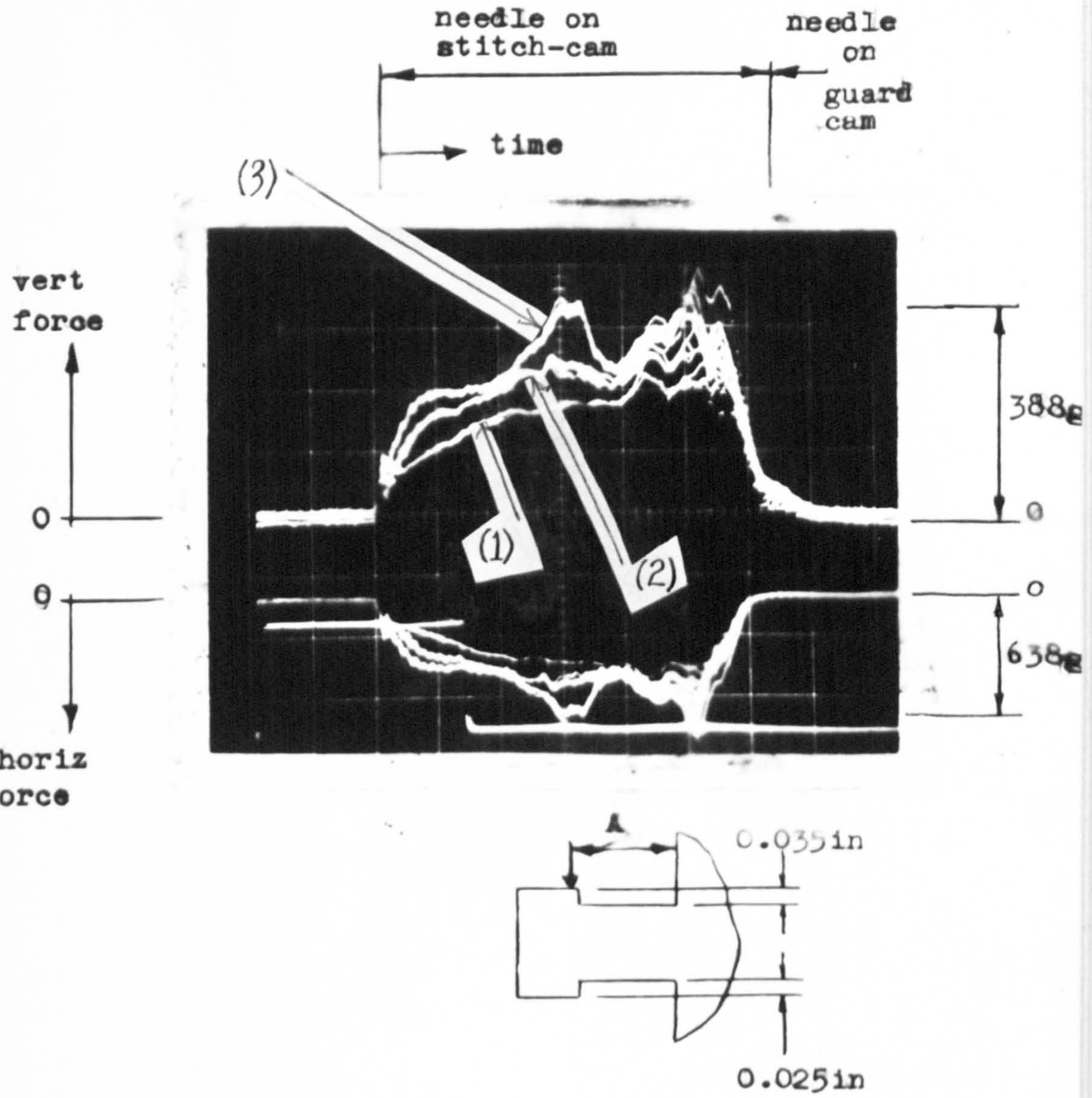

(1) A = 0.093in (2.36mm)

(2) A = 0.111in (2.82mm)

(3) A = 0.120in (3.04mm)

Vertical Force = 13.4 gf/mm

Horizontal Force = 35.3 gf/mm

Speed = 27rpm

Knitting Time = 5 m sec/8.5mm

EFFECT OF MOVING THE IMPACT POINT AWAY FROM THE CYLINDER Fig 4.13

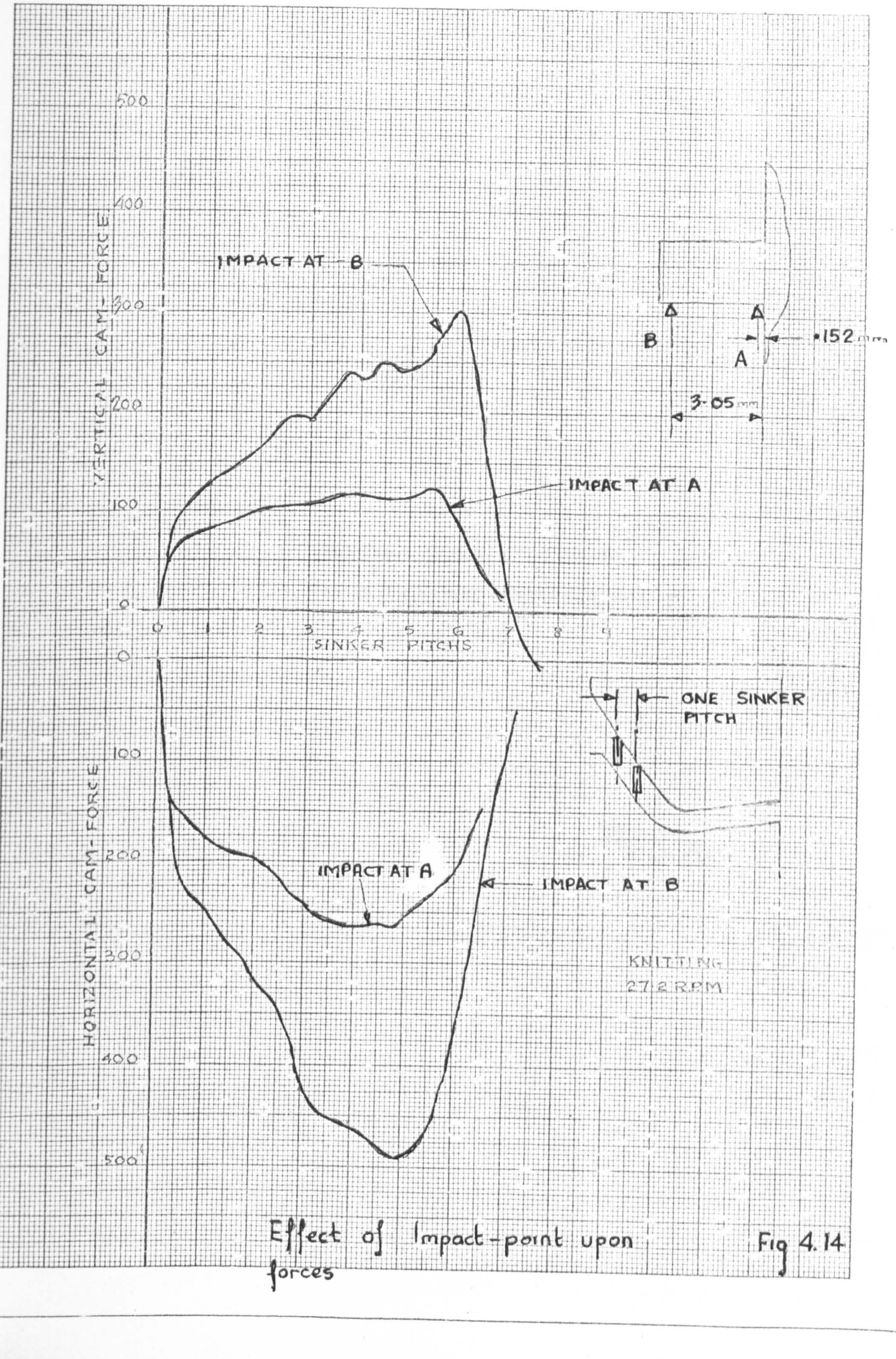

Effect of Impact-point upon forces

Fig 4.14

PART C

FURTHER EXPERIMENTATION USING IMPROVED MEASURING APPARATUS

CHAPTER 5

DESIGN OF AN IMPROVED CAM-FORCE MEASURING INSTRUMENT

5.1 Design and Manufacture of the Improved Cam-Force Transducer.

The special needle used for measurements with the original Mark I cam-force transducer had two basic modifications: (i) the butt was cut out so that it missed the inner radial cams, and (ii) the point of contact (impact point) between the butt and the transducer cam-track, was radially further from the cylinder then the corresponding impact point between a standard needle and the knitting cams. Experiments (section 4.6.4) showed that this movement of the impact point radially away from the cylinder had a large effect upon the cam-needle force, thereby making it impossible to predict the force that would be experienced by a standard needle during the knitting process, and any modifications made to a needle or to the cams in order to facilitate measurements might have a significant effect upon the forces. Obviously, a device needed to be designed to measure the force between one needle and the cams during knitting but it would have to be a system that did not require any modifications to the shape of the needle, or to the position of the cams, or to anything else that could possibly influence the knitting forces on the needle.

From the experience obtained during the design of the first (Mark I) transducer it was possible to reach a conclusion about the design of an improved measuring instrument quite quickly. Two possible systems emerged and these are treated seperately in the two following sections.

5.1.1 The Cam-Force Transducer-Mark II.

The Mark II transducer (as sketched in Fig 5.1), was a double cam-track instrument, rather similar in appearance to the original cam-force transducer. However, it differed in that the inner radial cams were now connected to the strain-gauged beam, whereas the outer radial cams were fixed. Twenty needles on each side of a standard long-butt needle had a modified butt, designed so that these needles only contacted the fixed outer radial cams, whereas the standard needle would only contact the inner cams. As the total stitch and guard cam length was approximately 18 needle pitches, then no matter where the standard long butt needle was in the cam-track, the other needles passing through the track at the same time would all be running on the outer cams, and not contacting the inner cams at all. The only modification required to the needles on either side of the standard needle, would be in their butt design. The needle heads would be identical, and providing the outer cam-track was well matched to the inner, the motion of all the needles would be the same. This meant that the knitting process would remain undisturbed by the measuring technique and that the standard needle would experience a completely normal set of circumstances. The remaining needles in the cylinder could all be standard needles running through the inner cam-track; this would not damage the beam cam-track because it was very stiff and it would not produce any spurious traces because the oscilloscope only recorded a trace when it was triggered.

There were considerable problems in manufacturing this instrument. If the standard long butt needle was not going to make unwanted contact with the rigidly supported outer cams, then they would have to be provided with a slightly wider track than the inner. Obviously, this would make

for extreme difficulties in matching the cams exactly, to ensure that all the needles, no matter what track they contacted, would all traverse through exactly the same motion paths; these difficulties were the reason for a further redesign i.e. the mark III transducer system described immediately below.

5.1.2 The Cam-Force Transducer Mark III.

The cam-force transducer mark III was a double cam-track device with one track fitted beneath the other as can be seen from Fig 5.2. Twenty needles, lengthened by a special jack, were fitted on each side of a standard long-butt needle. The standard needle was guided through the upper track connected to the strain-gauged beam, while the longer needles were guided through the lower rigid cam-track. The needles to each side of the standard needle were supported on a jack which had a butt at its base. The needle-butt was slightly reduced in width so that it would pass through the upper track without contacting it. The butt on the jack was the same as that of a standard needle butt and this ran in the lower track. If the upper and lower cams were set correctly, then all the needles would draw yarn to the same extent and there would be no modification to the loop forming process. The basic operation of the transducer was therefore similar to the mark II transducer in that, after the group of special needles had passed through the cams the remaining needles in the cylinder were all standard, these running through the upper track.

The only problem with this transducer was in the precise setting of the cams. The lower cam had to be set very accurately relatively to the upper cam, to ensure that the thinned upper butt had no contact with the upper measuring cam-track. Diagrams of the mark III transducer and the special needle are shown in Figs 5.2 and 5.3 respectively, Fig 5.4. is a sketch showing a radial view of the transducer

cam-track in position in the cam-box.

Adequate space was available on the experimental machine to fit a cam-force transducer with one track beneath the other so this overcame the serious practical limitation of the earlier mark I design, moreover, the mark III transducer was easier to manufacture and many parts that had existed on the original instrument could be used without any modification.

However, on commercial dial and cylinder machines it would be extremely difficult to fit an upper and lower cam track and in that case the mark III transducer would be inpractical. The author recommends, therefore, that any practical measurements to be undertaken at a later stage on more typical commercial machinery, should be undertaken using a transducer similar to mark II, despite the inherent difficulties in manufacture and operation stated in the ultimate paragraph of section 5.1.1.

5.2 Design of a L-C Filter Circuit.

Initial experiments using the original mark I cam-force transducer revealed a basic problem with the apparatus. As machine speed was increased, so the natural frequency oscillations of the beam increased, and these soon reached magnitudes that caused difficulties in interpreting the photographs. Two things could be done to elliminate this vibration, i.e:

(a) redesign the beam for higher natural frequencies,

or (b) design a simple L.C circuit to remove the oscillation frequency from the output signal.

An examination of photographs taken at high-speed showed that the frequency of horizontal oscillation was 1,390 Hz, and that of vertical oscillation was 1,360Hz.

These frequencies were lower than the predicted theoretical values. However, the calculations for these were based on simple bending theory and an estimate of the cam mass. The length-to-diameter ratio for the beam was rather too large for the simple bending theory used to be strictly accurate.

The cam-force transducer was primarily intended for measurements of the steadier components of cam-force, rather than for impact measurement. Obviously, for measurement of impact, a very high natural frequency instrument is desirable, but for the lower frequency measurements of the reaction forces involved as the needle passes through the track, a lower frequency has some advantages. For example, the transducer beam is more sensitive to small loads and the response to the impact is less, thus the disturbance to the relatively slow varying trace, caused by the impact, is less damaging.

For the above reasons, and because a L-C filter circuit is very simple to design and manufacture and certainly less expensive than would be the re-designing and strain gauging of a new beam, it was decided to build such a circuit.

The filter circuit is illustrated in Fig 5.5 and consists simply of an inductor, a capacitor and a resistor. Two filters were built, one for horizontal forces having frequency rejection at 1,390 Hz the other for vertical forces having frequency rejection at 1,360 Hz.

Referring to Fig 5.5 the following relationships can be derived :-

$$e_o = i\left(R_L + j\omega L - \frac{j}{\omega C}\right) \quad . \quad . \quad (13)$$

where: e_o = voltage across oscilloscope terminals,
i = current-neglecting the small current taken by oscilloscope,
R_L = inductor resistance,
j = $\sqrt{-1}$,
ω = circular frequency,
and L = inductance (henrys),
C = capacitance (farads),

also:

$$e_i = i\left(R + \left(j\omega L - \frac{j}{\omega C} + R_L\right)\right)$$

where e_i = voltage input signal,
and R = resistance.

Therefore:

$$\frac{e_o}{e_i} = \frac{1}{1 + \dfrac{R}{R_L + j\left(\omega L - \dfrac{1}{\omega C}\right)}} \qquad (14)$$

and when:

$$\omega^2 = \frac{1}{LC} \qquad (15)$$

then:

$$\frac{e_o}{e_i} = \frac{1}{1 + \dfrac{R}{R_L}}$$

and, since $R >> R_L$

then $\dfrac{e_o}{e_i} \simeq 0$

The filter circuit is designed using equation (15).

Obviously L and C can have a wide range of values and, provided equation (15) is satisfied, then frequency rejection will occur at the desired value of ω. However, it is desirable to have L large and C small. The Q factor of the filter defines the sharpness of its frequency cut-off; this depends upon the resistance of the inductor, which is less for large value of

inductance.

When ω is small, $\frac{1}{\omega C}$ is large, and $\frac{e_o}{e_i}$ approaches unity.

When ω is large, ωL is large, and $\frac{e_o}{e_i}$ approaches unity.

Suitable filter circuits were produced for the horizontal and vertical force signals with resistance R so designed to be variable so that the frequency rejection characteristic could be changed as desired. Experiments were carried out to measure the frequency responses of the filters at various resistances and these characteristics are shown in Fig 5.6.

It was very important to determine precisely the effect of the filter upon the force signal. Several experiments were carried out superimposing traces obtained with the filter first in and then out of the circuitry. No differences in the traces could be detected under a wide range of conditions. At high speed, the photographs from the unfiltered response were somewhat difficult to interpret, but by filtering it was possible to superimpose traces to observe that the filtered plot was equal to the mean level of the unfiltered signal.

The effect that the L-C filter had upon the cam-force traces is clearly illustrated by the photograph labelled Fig 5.7.

5.3 Design of a Photo-Diode Triggering Device.

For initial experiments a micro-switch unit was used to trigger the oscilloscope. Although the device was adequate for low machine speeds, it became more unstable and tended to bounce as the speed was increased; this caused damage to the micro-switch and the cylinder, and the triggering position became more uncertain.

An ideal triggering device would be one that did not physically contact the cylinder, had no moving parts, had a fast and repeatable response, and preferably could be used

for speed measurement. A photo-diode trigger satisfies all these requirements, and Fig 5.8 shows the essential construction of the device used.

A small mirror, painted black except for a thin vertical line, was clipped to the cylinder. As the cylinder rotated, the mirror passed the photo-diode, and, at the exact instant that they were opposite each other, a beam of light was reflected off the mirror at the diode, this causing a large voltage signal to appear across the oscilloscope, terminals. The signal was large enough to trigger the oscilloscope without any pre-amplification.

The mirror could be moved and therefore the triggering position was easily adjustable. Tests carried out using the device at high machine speeds showed it to be completely reliable and very convenient to use.

5.3.1 Use of Photo-Diode Trigger for Machine Speed Measurement.

The photo-diode trigger could easily be used for speed measurements. The mirror was painted black except for two thin vertical parallel lines. The first line was positioned opposite the diode so that the voltage output on the oscilloscope was a maximum. A fine mark was made on a stationary member opposite a projection on the cylinder. The cylinder was then turned until the second line on the mirror was opposite the diode, and the voltage output was again a maximum. A second mark was made opposite the cylinder projection. The distance between the two marks was then measured using a powerful magnifying glass and a steel ruler. During experiments the photo-diode voltage output was connected to channel 1 of the oscilloscope, when cam-force and yarn-force traces were recorded, the timing pulses from the trigger unit being also recorded. The exact time between

the two voltage peaks could be measured and this was used to determine the machine speed.

The two principal advantages of this system were :-

(i) speed measurement was carried out at the same time as the cam-force and yarn-force traces were being recorded,

and (ii) no extra measurement was required, the machine speed being simply read off the polaroid photographs.

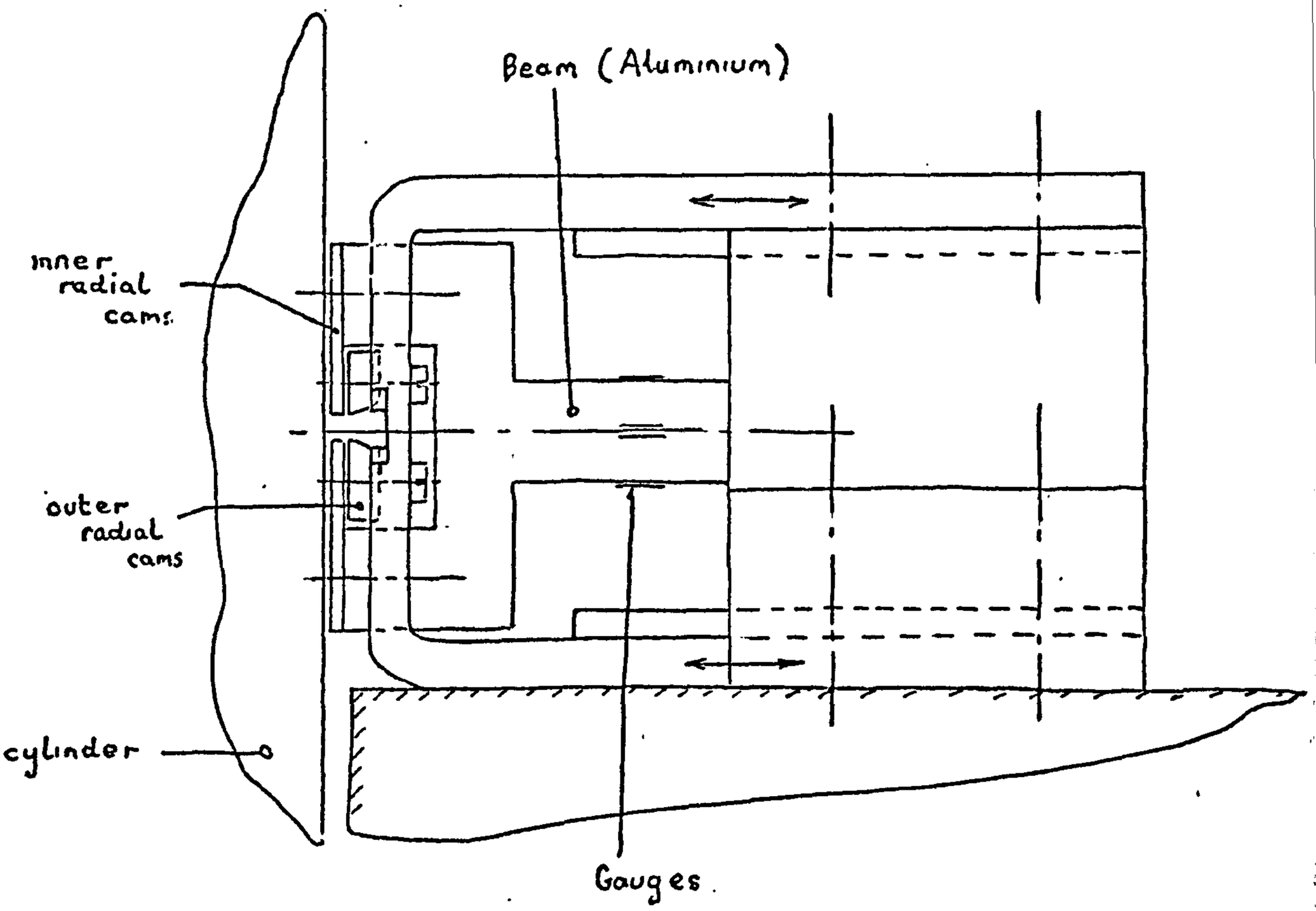

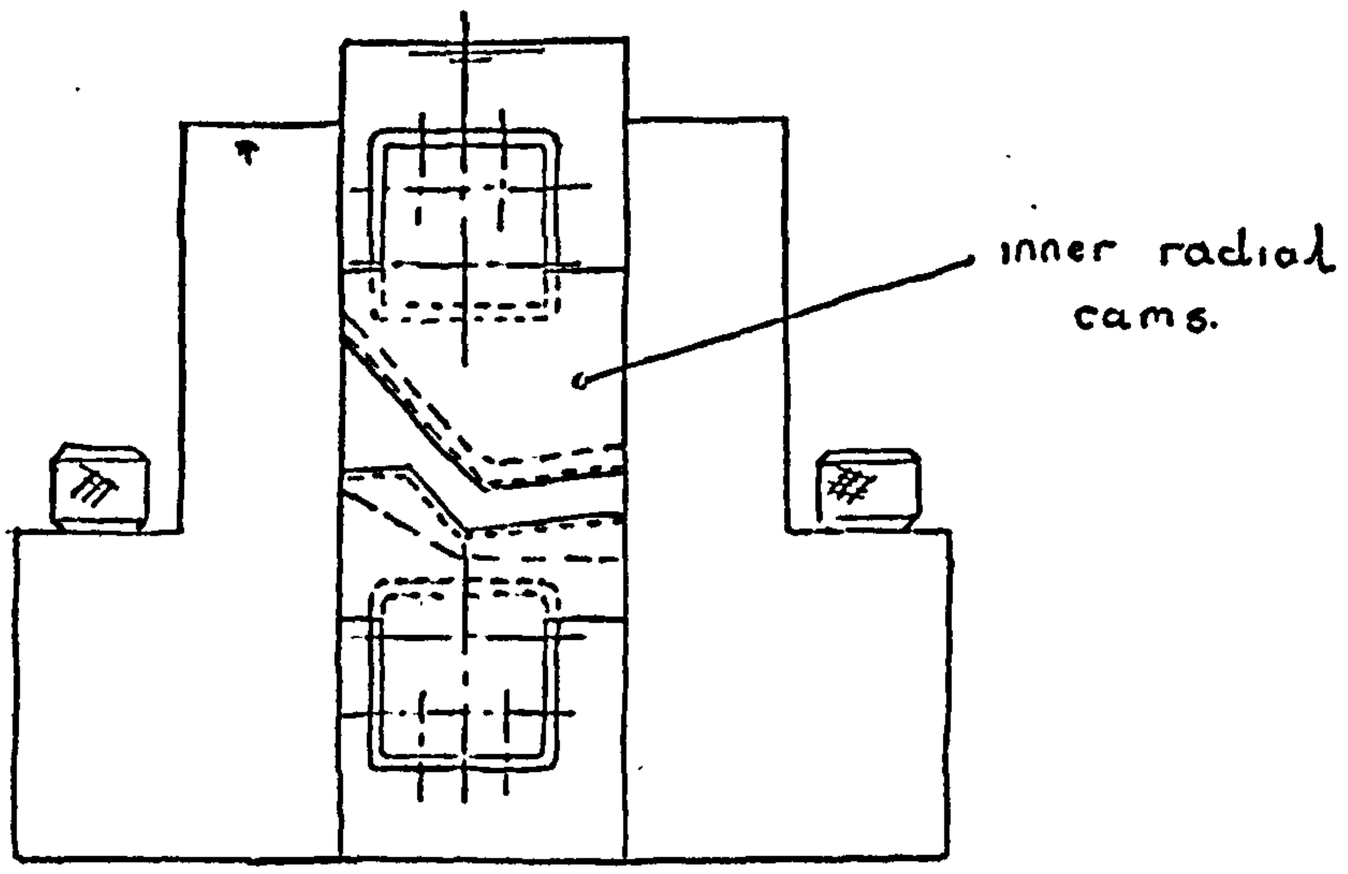

End on view of Transducer.

CAM-FORCE TRANSDUCER MARK II

FIG 5.1

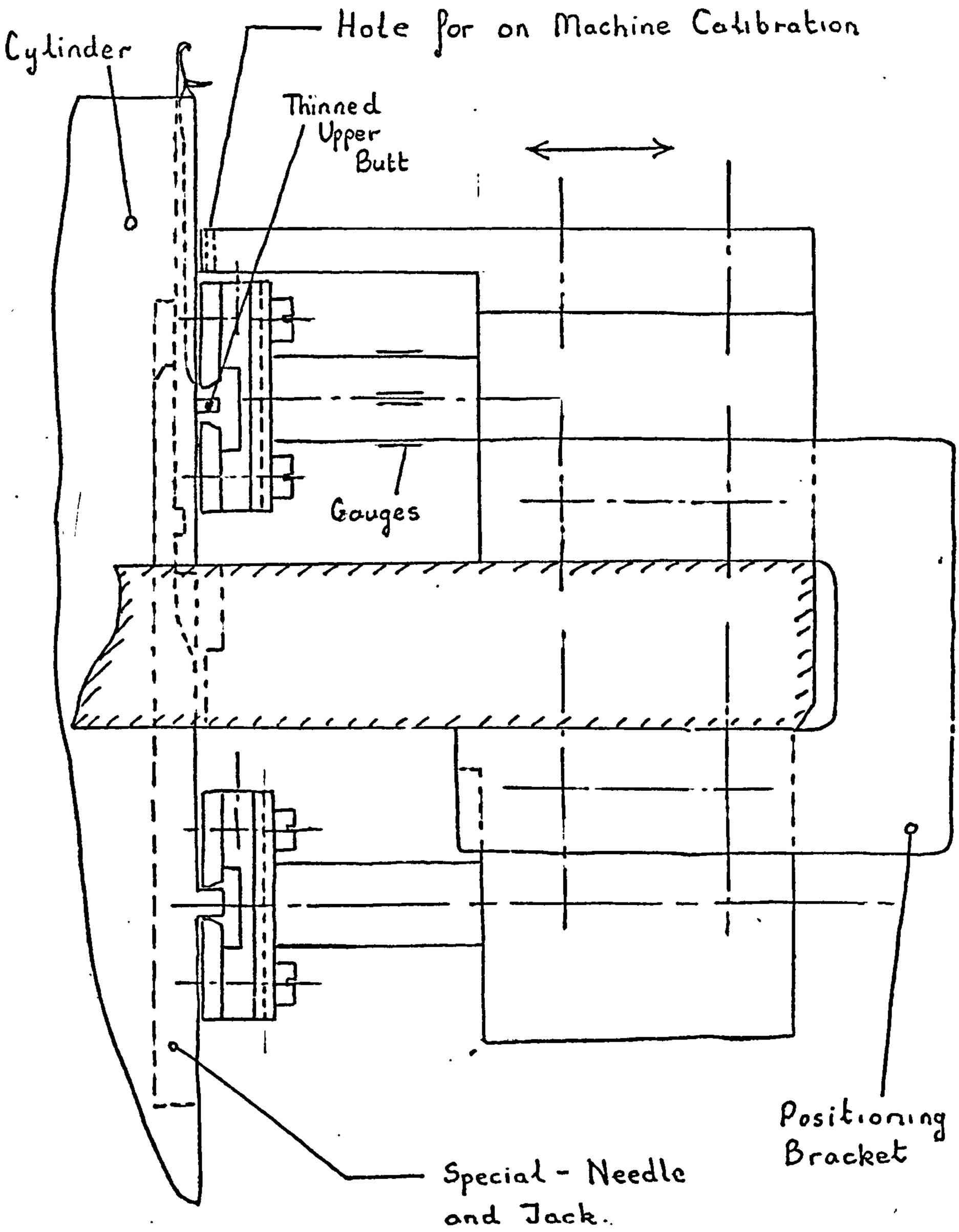

CAM- FORCE TRANSDUCER

MARK III

FIG 5.2

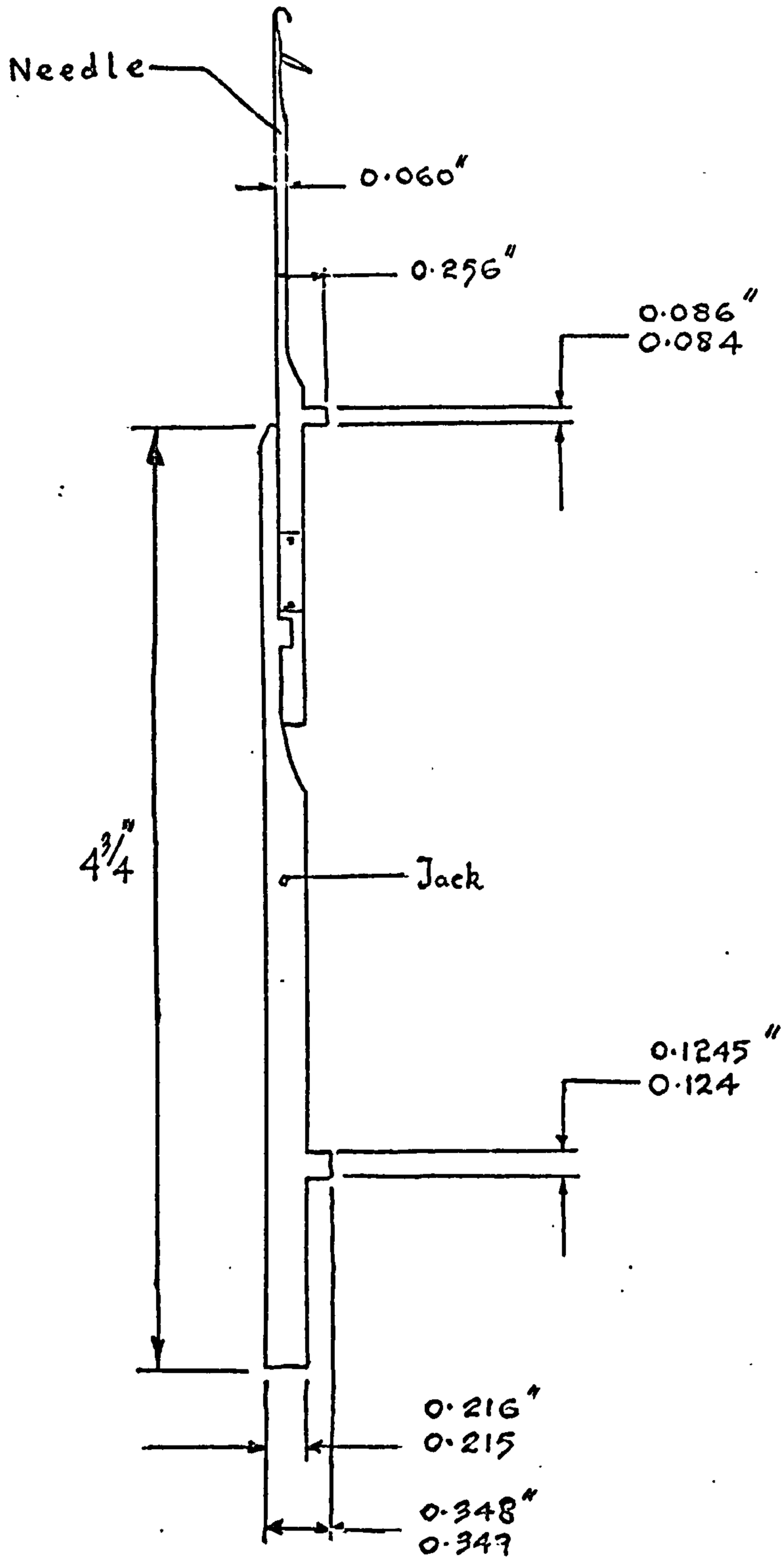

THE SPECIAL NEEDLE AND JACK.

FIG 5.3.

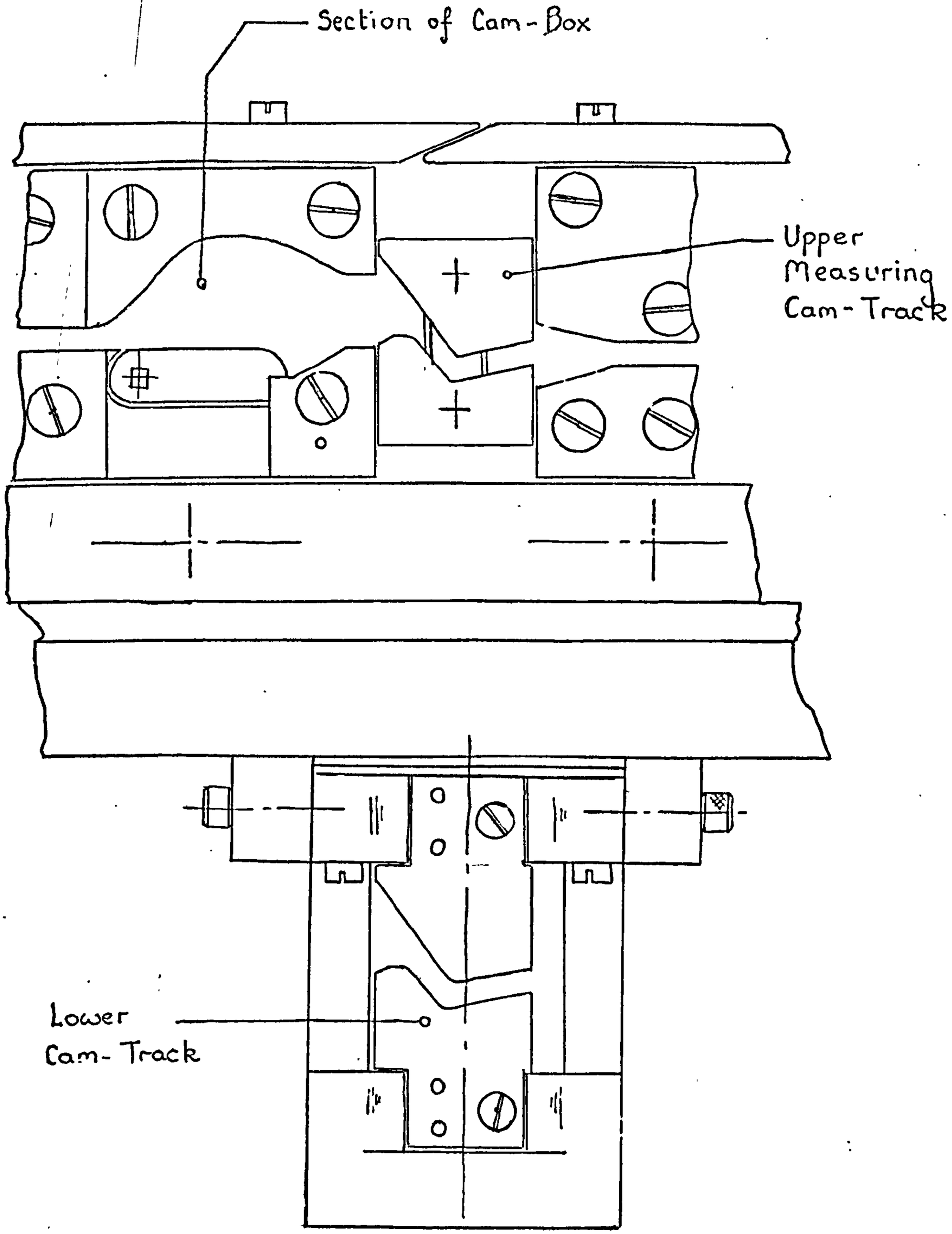

RADIAL OUTWARD VIEW OF
CAM-FORCE TRANSDUCER MARK III

FIG 5.4

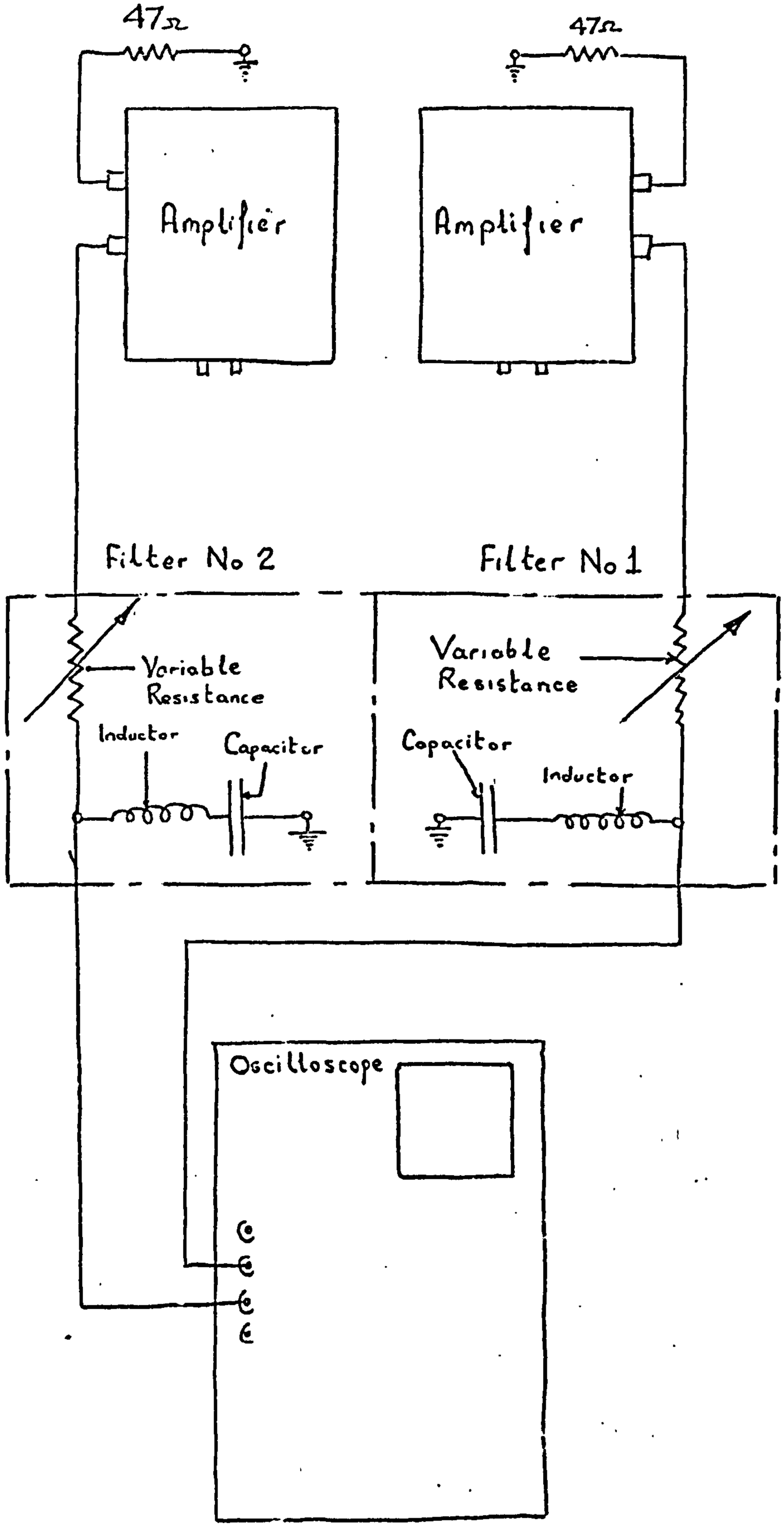

FILTER CIRCUITS

FIG 55

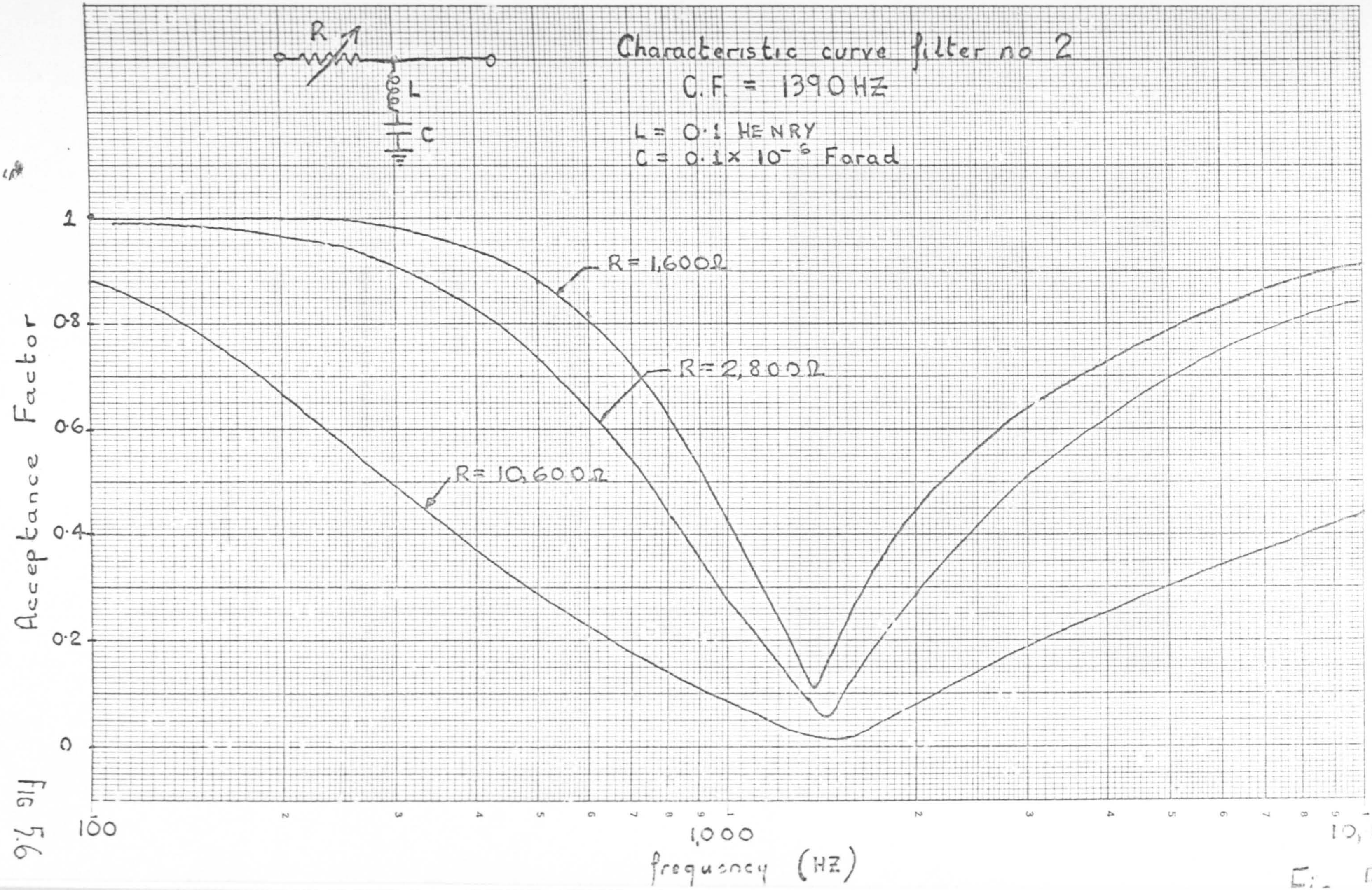
R
L
C
Characteristic curve filter no 2
C.F. = 1390 HZ
L = 0·1 HENRY
C = 0·1 × 10⁻⁶ Farad
R = 1,600Ω
R = 2,800Ω
R = 10,600Ω
Acceptance Factor
1
0·8
0·6
0·4
0·2
0
100
1,000
10,000
frequency (HZ)

Fig 7.6

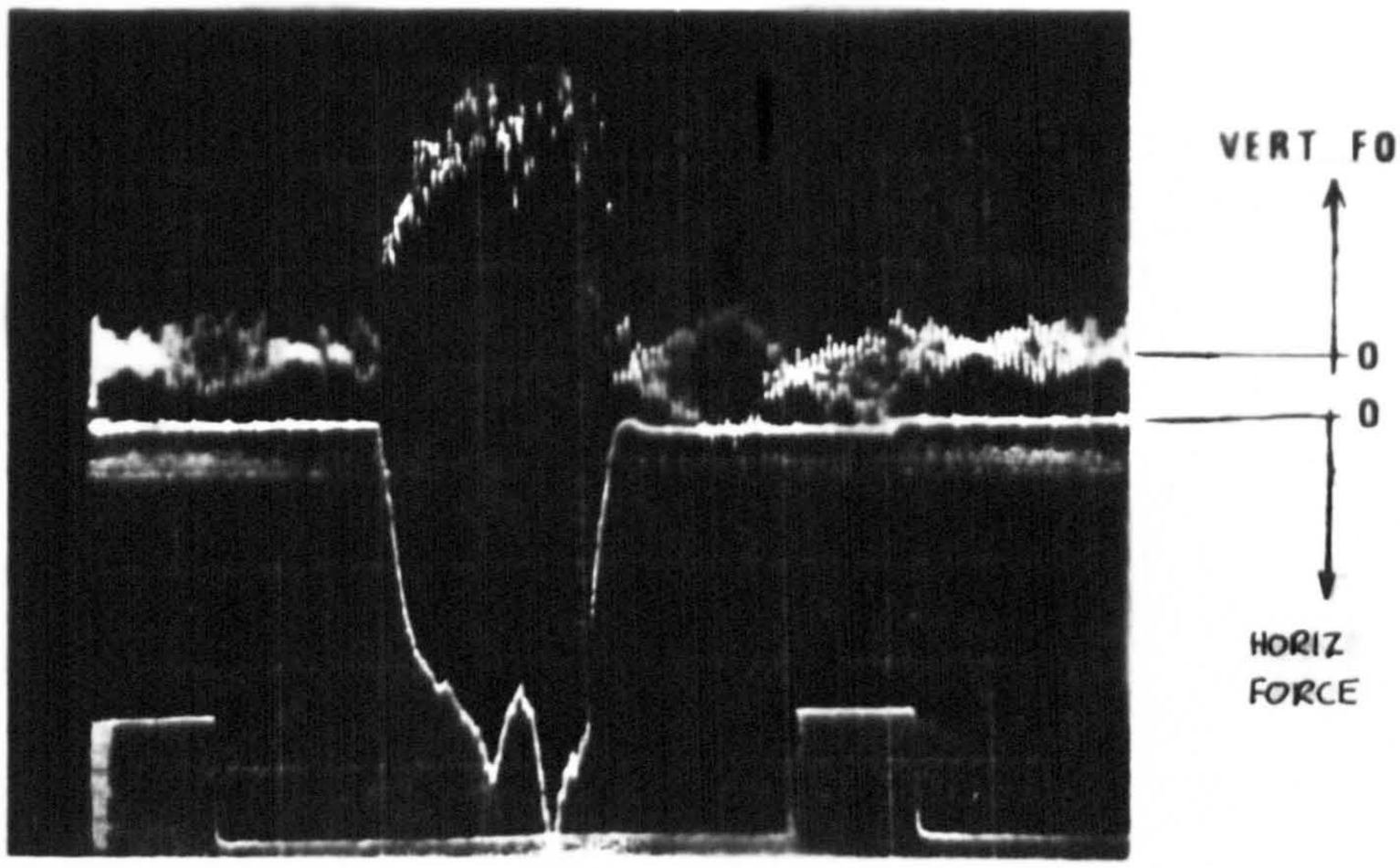

Horizontal-force trace filtered (1390Hz)

Vertical-force trace unfiltered

KNITTING

Speed = 40 R.P.M

Time-base 0·010 secs per div

1 div = 8·5 mm

EFFECT OF FILTER CIRCUIT UPON CAM-FORCE

FIG 5.7

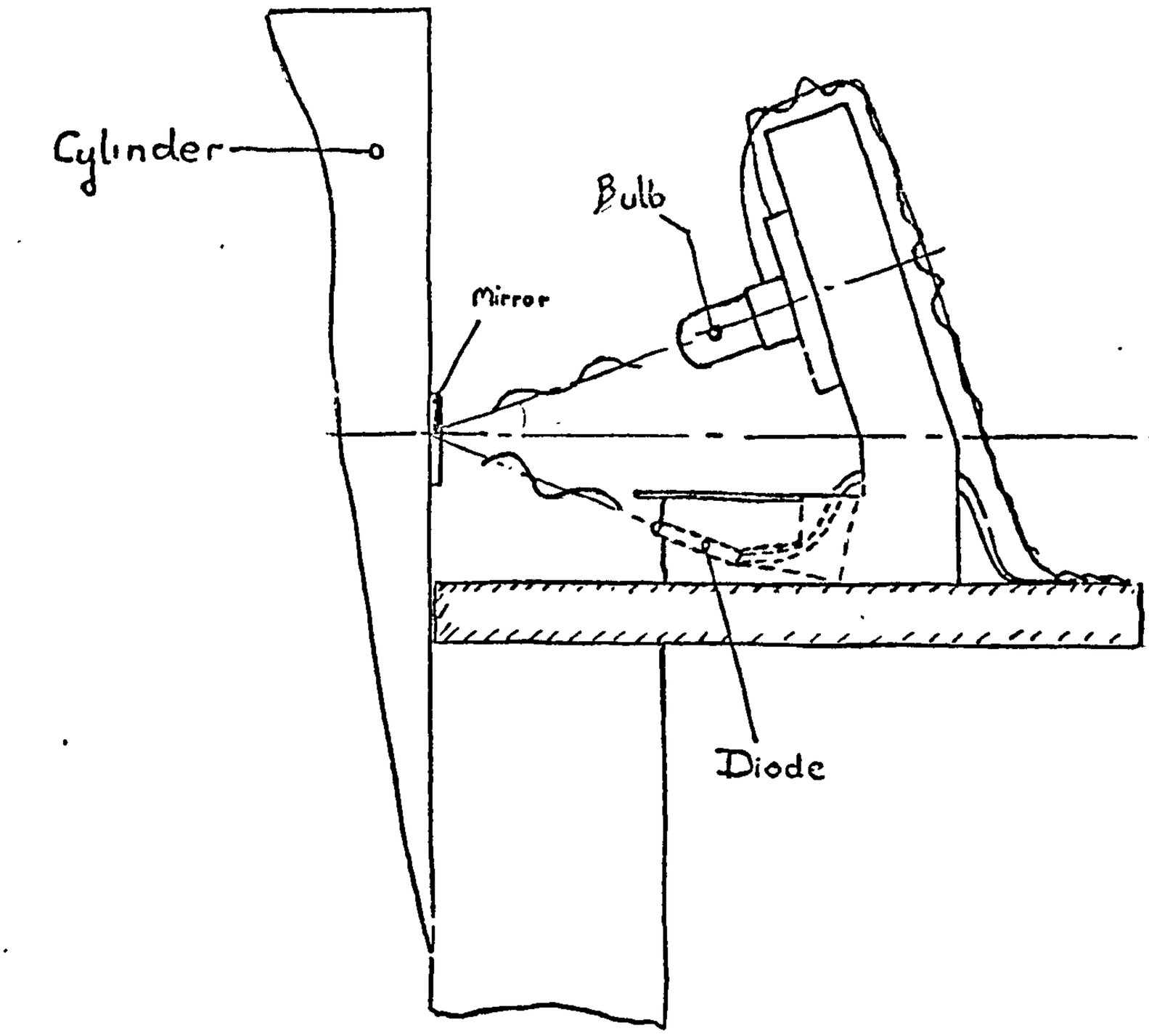

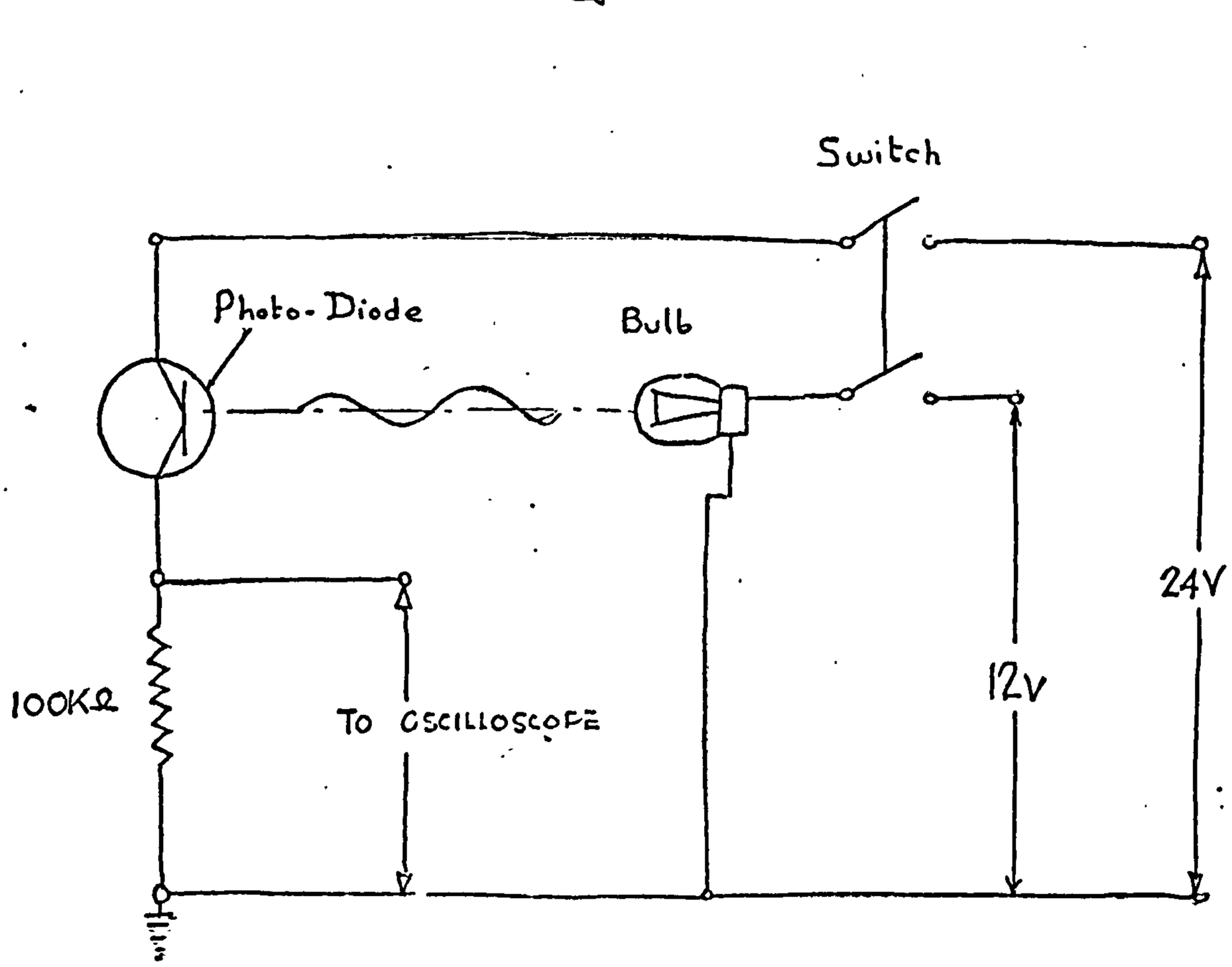

THE PHOTO-DIODE TRIGGER.

CONSTRUCTION AND CIRCUIT.

FIG 5.8

CHAPTER 6

A TRANSDUCER DESIGNED TO DETERMINE THE FORCE EXERTED BY THE YARN UPON THE NEEDLE AND VERGE

6.1 The Need for a Yarn Force Transducer.

The process of loop formation has been theoretically examined at some length, and theoretical expressions exist to predict the yarn tensions through-out the knitting process. However, very little work has been done experimentally to measure the yarn forces and determine the effect of various parameters upon the loop drawing process. With a thorough experimental knowledge, accepted theories such as those attributed to Howell[4,5,6] Knapton[11,15,16,17] and Dangel[22] could be tested, and the mechanism of robbing back could also be closely examined.

Previous researchers[32,24,26,29] have used instrumented cam-tracks to measure the forces, but with such a measurement technique it is difficult to judge effects due to trick-needle poperties and lubricating oils, and these probably exert effects which mask the true nature of the loop drawing forces. There is a need for a system that measures the yarn-force directly. It should only be responsive to the yarn-tension, and should not be affected by any other parameters unless these have influence on the loop drawing process.

6.2 Design and Manufacture.

The yarn-force transducer should be capable of measuring the tension in the yarn at each stage of the loop-forming process, since from such measurements the force exerted upon the needle by the yarn could be determined. After a consideration of measurement techniques three possible systems

emerged. The first, was to measure the tension by actually fitting a device in the yarn which would register a signal proportional to the force. Another method, was to fit some device to a needle that would register the forces imposed by the yarn. Finally, a small portion of the verge could be designed to measure the force exerted by the yarn upon the verge as it passed over it during loop formation.

The most direct method was to fix something in the yarn. However, considerable difficulties had to be overcome if a device of this type was to be successful, and it would require the following characteristics :-

(i) a firm contact with the yarn which would allow for some interfibre slip if it was used on multi-filament yarns,

(ii) it would have to be extremely small and certainly of the order of a few thousandths of an inch,

(iii) it would have to be sufficiently flexible to allow for bending as the yarn flowed over the needles and verges,

(iv) it should not influence in any way the normal process of loop formation and yarn friction,

and (v) some means would have to be found to obtain the force signal from the instrument.

No instrument could easily satisfy the above requirements, but recently the author has been told that it may now be possible to obtain a single filament of a special yarn which can be interspersed with a test yarn so that as the yarn tension increases, the filament changes colour and this can be photographed to obtain a direct tension indication. The method sounds rather imprecise, and the author has failed to find published information on this type of yarn.

The second method of measurement mentioned above was

to attach a device to the needle surface. It was possible to fit very tiny strain-gauges to the needle shank, but unfortunately the extra thickness of the gauges made it impossible to refit the needle in the normally close-fitting trick.

The remaining system of measurement was an instrumented verge. There were design problems with a device of this type, three of the most important are summarised below :-

(i) Any device would have to be very small because very little space exists in which to fit it if the fabric motion is to be undesturbed.

(ii) Very little movement should occur on the verge since any deflection would influence the yarn-force and the stitch-draw.

(iii) Some method had to be provided to transfer the signal from rotating system to a stationary display instrument.

The problems associated with the device for measuring the force exerted upon the verge by the yarn were not considered insurmountable. However, with a knowledge of the yarn-friction, which would need tobe determined for all three methods of measurement, it would be possible for this instrument to predict the yarn-tension and the force exerted upon the needle, and thus to thoroughly examine the accepted theories of loop formation.

A verge transducer was built, a diagram of the instrument being shown in Fig 6.1. It consisted of a small stiff beam having a natural frequency of approximately 4,000 Hz, made out of the same material and hardened to the same extent as that used for the machine verge. The cylinder was slightly modified at the top, as shown in Fig 6.1, to enable

the beam to be fitted. The existing verge was removed and the beam positioned and clamped in its place. A small polished cover was fitted over the instrument so that it did not disturb the fabric motion over the cylinder top.

A summary of the important features of the transducer are given below :-

(i) It was possible that during the knitting cycle the point of application of the yarn force would move a short distance over the verge. The cantilever beam was so designed that this did not alter the bending moment on the beam and this is shown in more detail in Fig 6.2.

(ii) Micro-minature semi-conductor strain-gauges were mounted on the beam, these being so small as to allow for the use of small stiff elements.

(iii) The beam deflection at the verge was only 0.02 mm per 500 gf load applied to the verge.

(iv) The beam had a high natural frequency.

(v) The complete transducer had only three basic parts, i.e. the beam itself and two other parts used as a clamp. The manufacturing process was therefore simplified.

(vi) It was possible to measure the yarn-force simultaneously with the horizontal and vertical cam-forces. This meant that all three signals could be displayed on the oscilloscope together.

Fig 6.3 shows the transducer with the polished cover removed, and Fig 6.4. shows the transducer verge (at the front of the cylinder), the cylinder, and fabric.

6.3 Design of Electrical Circuit.

The major problem with the design of the circuitry, was the transmission of the signal to the stationary oscilloscope from the transducer mounted on the rotating

cylinder. The standard method of solving this problem would have been to use a slip-ring device; this would have meant bringing the transducer output wires to the centre of the cylinder, and connecting them into a slip ring so that the stationary output wires could then be connected to the oscilloscope. In the past slip-rings have unfortunately been associated with a significant electrical noise output known as slip-ring hash. Although nowadays slip-rings can be produced relatively hash-free, it was considered at the time the work started that possibly a better system with less noise output would be a wire wind-up mechanism using a special British Insulated Callender Cables wire known as "8-ends tinsel".

The strain gauge wires from the transducer were passed to the amplifier. The amplifier, a Strain-Stall type 91A, and its voltage supply were all connected to the cylinder, and hence rotated with the transducer. It was considered that the major source of electrical noise in the circuit would be the wire wind-up mechanism. If the amplifier had been mounted subsequent to the wind-up mechanism, the signal and the electrical noise would be equally amplified and the resulting trace on the oscilloscope would be difficult to interpret due to the excessive noise disturbance.

By passing the signal first to the amplifier, the signal was amplified but the noise was not : therefore, the trace disturbance was much less and the consequent distortion on the photographs was also reduced. The output from the amplifier was passed to the wind-up mechanism which was basically three long tinsel wires wound in a helical spiral. More detail concerning the device is given in section 6.3.2. The wind-up mechanism allowed approximately 300 machine revolutions before it was necessary to release the wires,

allow them to unwind, and then re-connect them. The necessity of stopping the machine periodically during an experiment was no real disadvantage, since the machine had to be stopped at similar time intervals to readjust the constant take-down tension unit which is detailed in section 7.1. The output from the wind-up mechanism was passed straight to channel 4 of the Tektronix Storage Oscilloscope. The total system was thoroughly earthed, and shielded wire was uced wherever possible.

Fig 6.5 is the circuit diagram, and the diagram, Fig 6.6, shows the amplifier mounting.

6.3.1 Position of the Strain-Gauges on the Beam.

Two semi-conductor strain-gauges were mounted on each side of the beam and near to the clamping brackct to maximise the bending moment. The four gauges were connected into a wheatstone bridge circuit as shown in Fig 6.7, the wires from the bridge being then taken down around the cylinder to the amplifiers.

6.3.2 The Wind-Up Mechanism.

Inside the cylinder, about six-inches down from the top, a bracket was fitted and at the centre of the bracket a fine steel plate was clipped in position. The central axis of the plate corresponded as closely as possible to the vertical axis of cylinder rotation. In the plate, on a 1 inch pitch-circle diameter, a number of small holes were drilled and polished. The wires from the amplifier were taken up the cylinder, passed along the bracket and connected into a junction block fixed to the bracket. The output wires from the block were"8-end tinsel" each wire consisting of eight strands of fine tinsel wrapped around a nylon filament core. The wire had the property of being very flexible so that it could

easily be bent and twisted into complex shapes without any damage to the wire. From the junction block the tinsel wire was taken through the holes in the plate, vertically upwards for about four feet through a steel pipe. The purpose of the pipe was to limit any whip in the wires as the cylinder rotated and to act as anearthed shield to electrical noise pick-up. The steel pipe was also used as the main support for the yarn creel and stop motions. At the top the tinsel wire was taken through holes in another plate similar to the one below and passed over guides around a pivoting weight. As the cylinder rotated the tinsel wire was wound in a spiral and, if the wire had been fixed between the two plates, there would have been a large tension increase as it was wound up. Howeyer, the tension increase was relieved by drawing in some wire attached around the pivoting weight. This caused the weight to rise, a micro-switch and a light was fitted and when the weight had risen to a pre-set position it closed the switch, so that the warning light came on and the machine stopped. The lower plate was unclipped and the wires were allowed to unwind, this causing the weight to fall. When the lower plate was re-clipped in position the machine could be re-started. In all, the total process of disconnecting, and reconnecting the wires took only a few seconds. The micro-switch could be moved, so that the exact position at which the rising weight closed the switch was adjustable so that the machine could be stopped after a pre-set number of revolutions. The wires from the wind-up mechanism were taken straight tc the oscilloscope.

Fig 6.8 is a diagram showing the wire wind-up mechanism, and the photograph of the 10 in knitting machine ,

Fig 3.1, shows the steel pipe and pivoting weight assembly.

6.4 Calibration of Instrument on Knitting Machine.

A system was devised where it was possible to calibrate the yarn-force transducer without removing it from the knitting machine. The calibration could be carried out very quickly before and after every test. Thin cylindrical bars of known weight were carried in two guides just above the verges. When a calibration was required, the system was rotated until it was just above the verge of the force transducer. A weight was then passed through the guides until it rested on the verge, at the exact position in which the yarn passed over the verge during loop formation. The process was repeated using a range of weights and the output on the oscilloscope was recorded. A diagram of the calibration apparatus is shown in Fig 6.9.

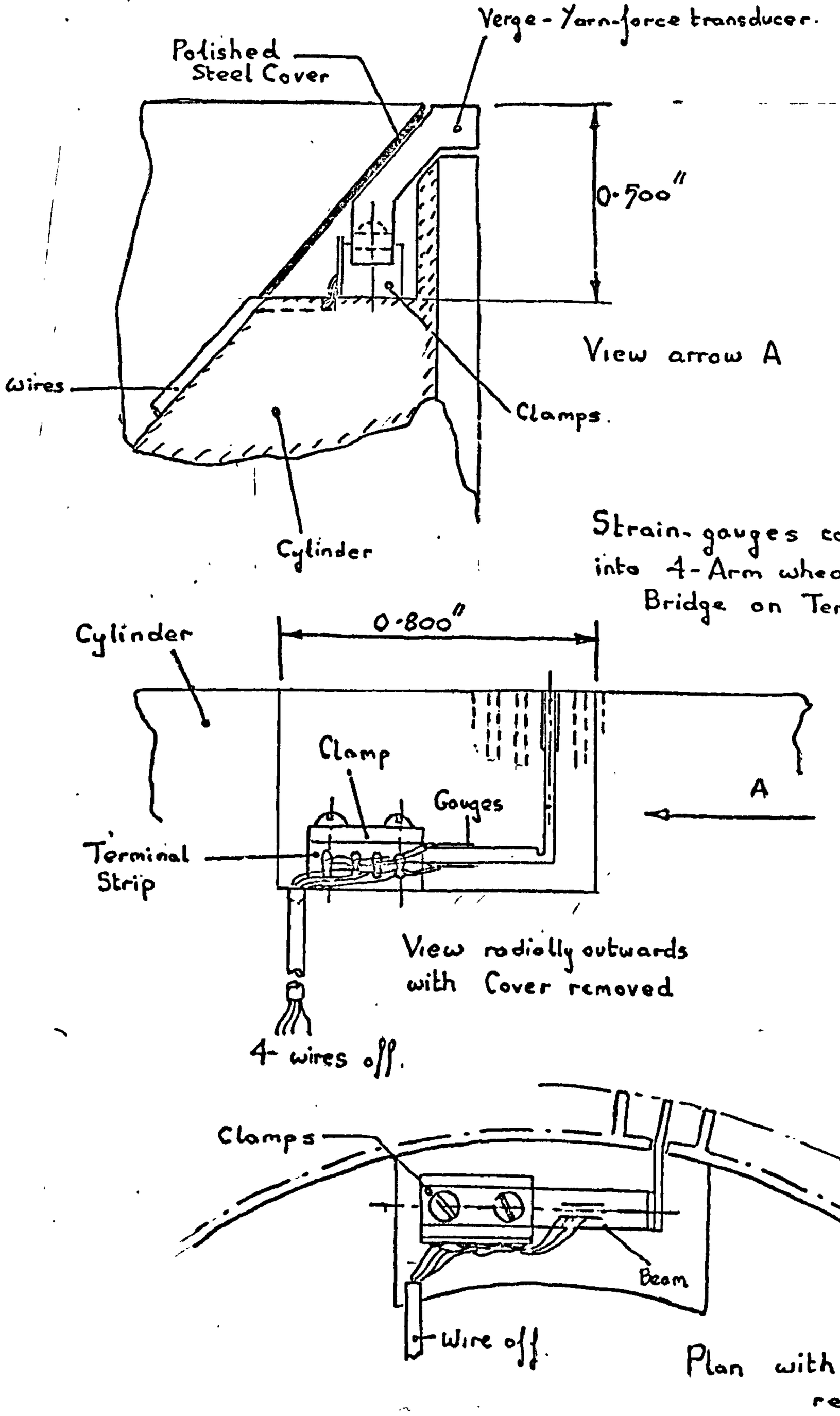

YARN - FORCE TRANSDUCER

FIG 6.1

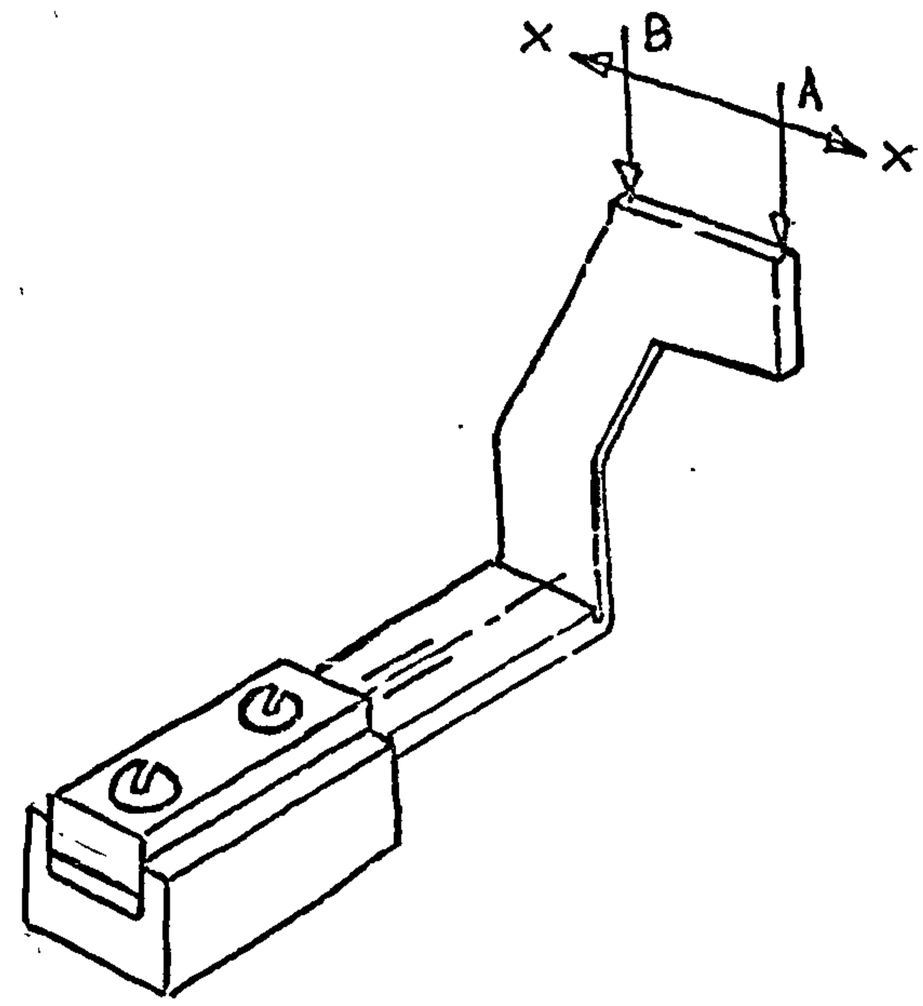

The beam is designed so that movement of moment arm X←→X should not effect the moment on beam.

Maximum movement of load on beam is from B to A.

EFFECT OF MOVING LOAD ON VERGE

FIG 6.2

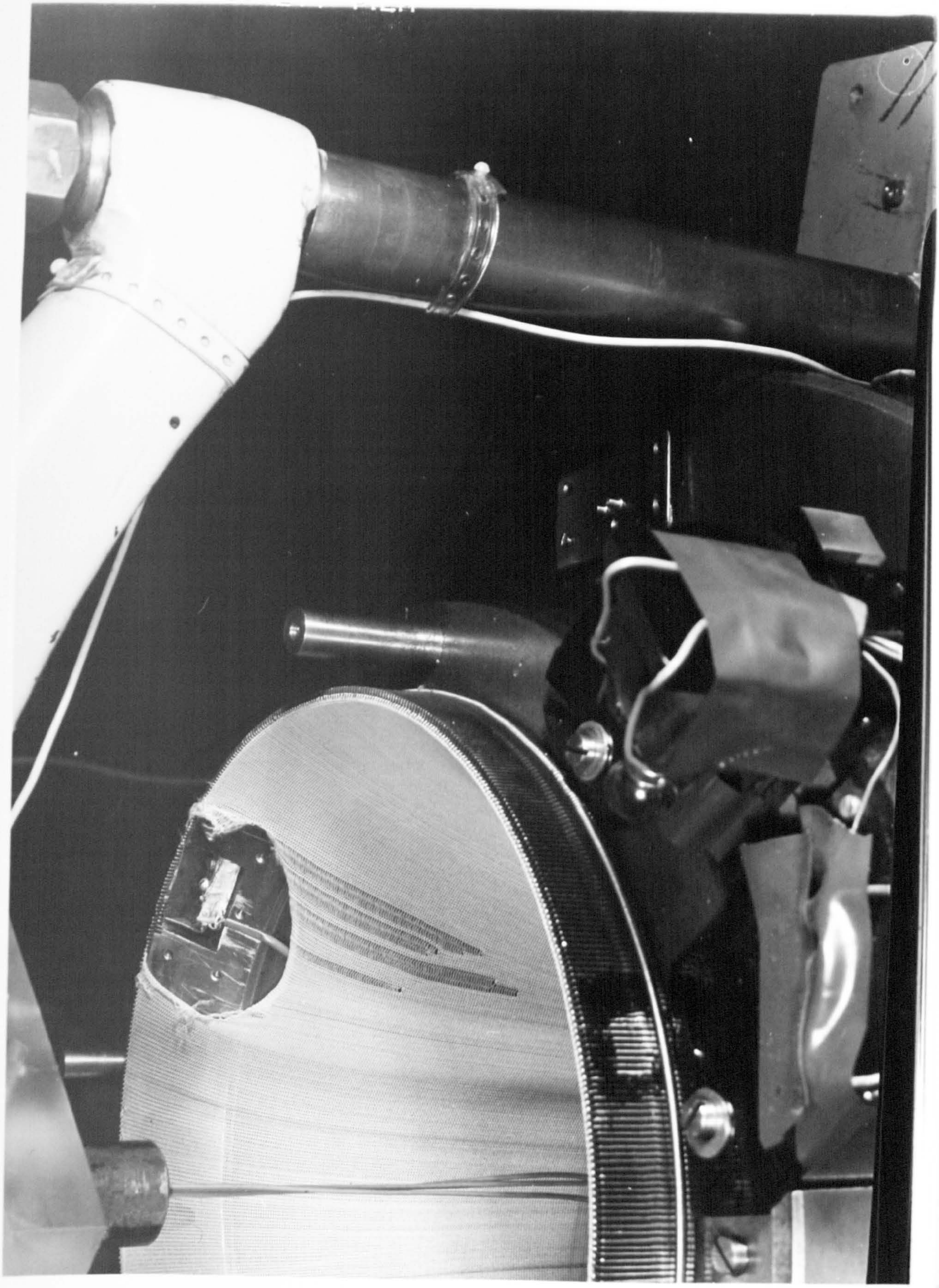

Yarn-Force Transducer with the Polished Cover Removed

Fig 6.3

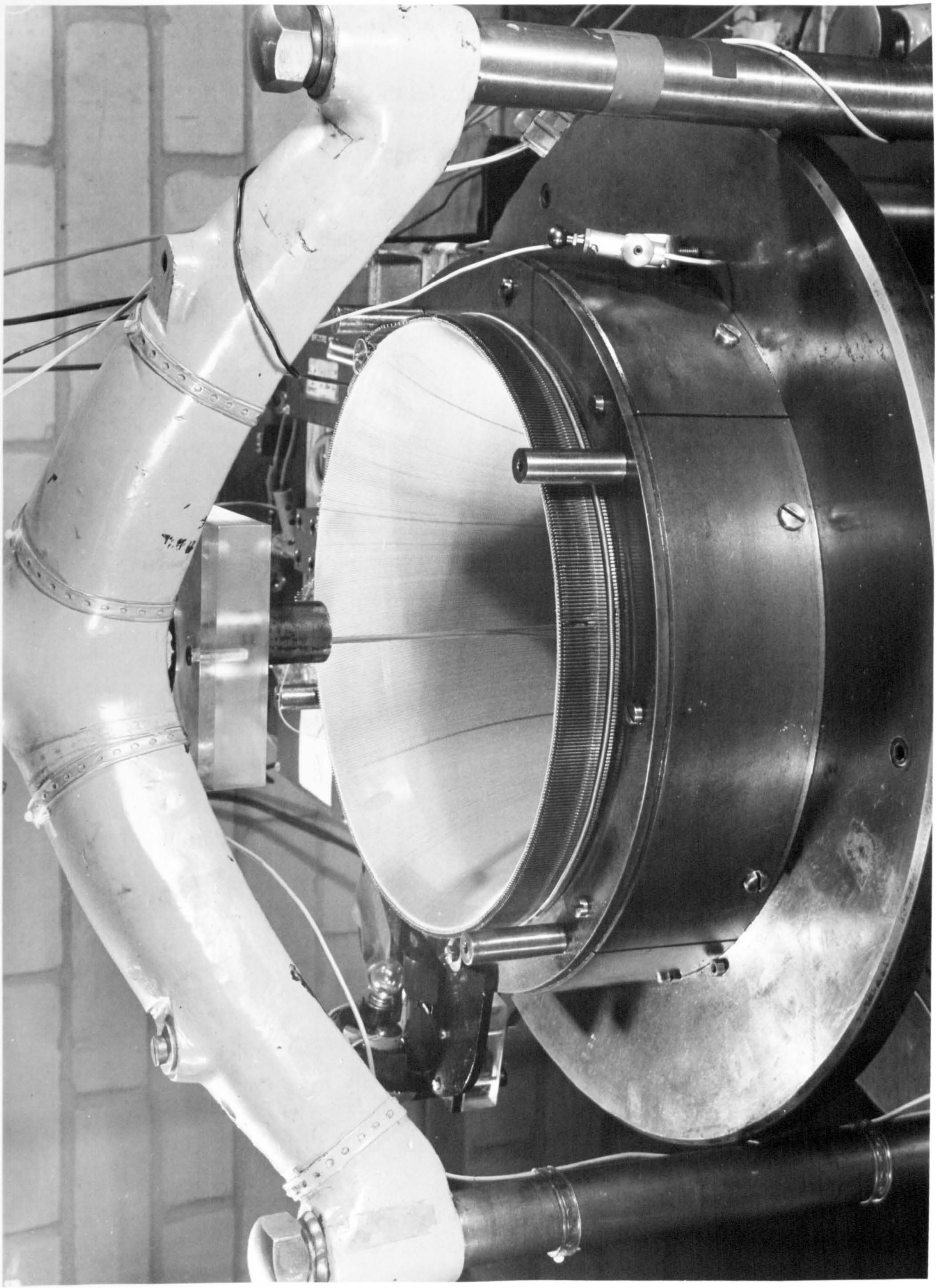

Yarn-Force Transducer,
(at Front of Cylinder)

Verge, Fabric and Cylinder

Fig 6.4

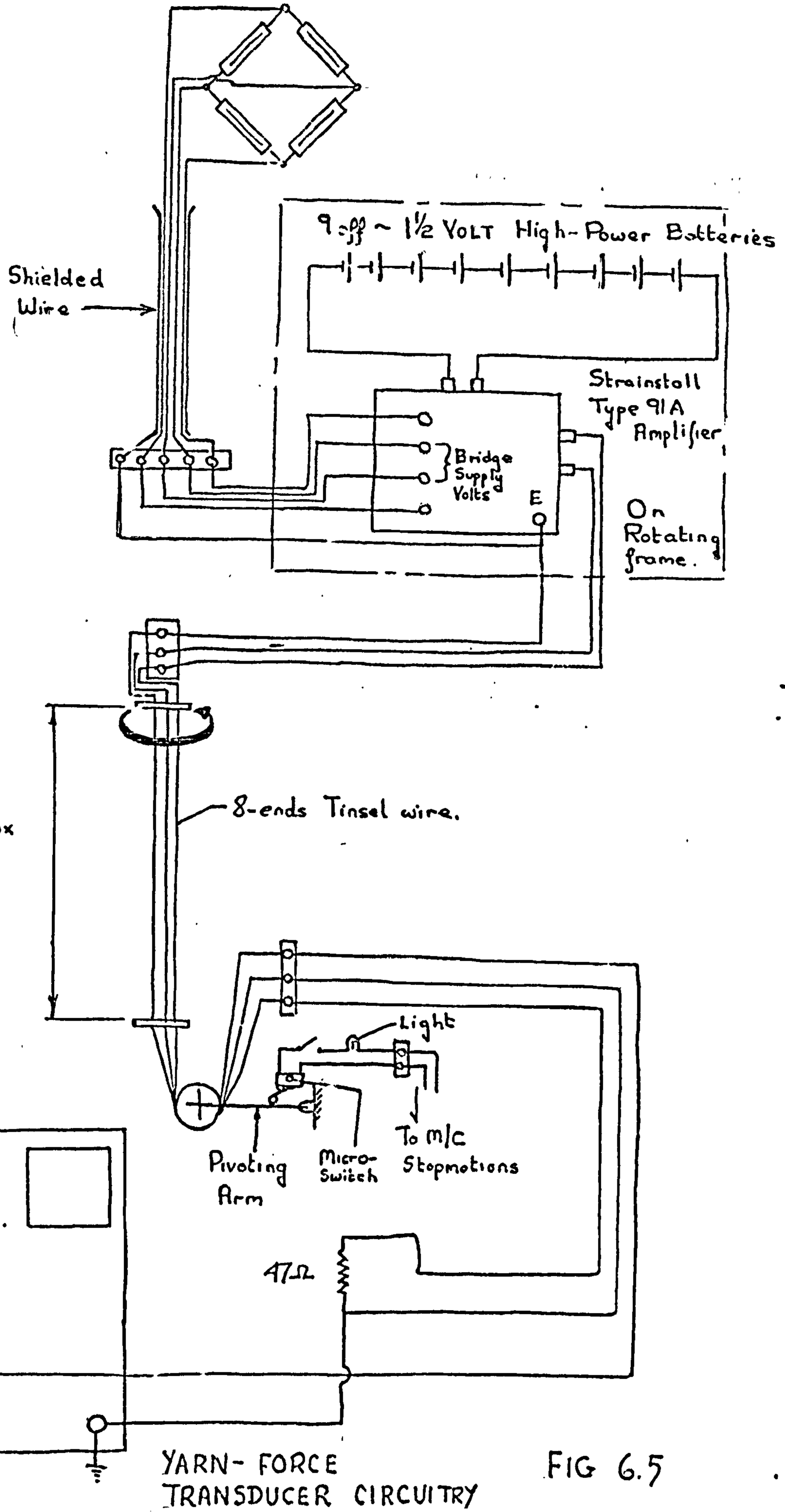

YARN-FORCE TRANSDUCER CIRCUITRY

FIG 6.5

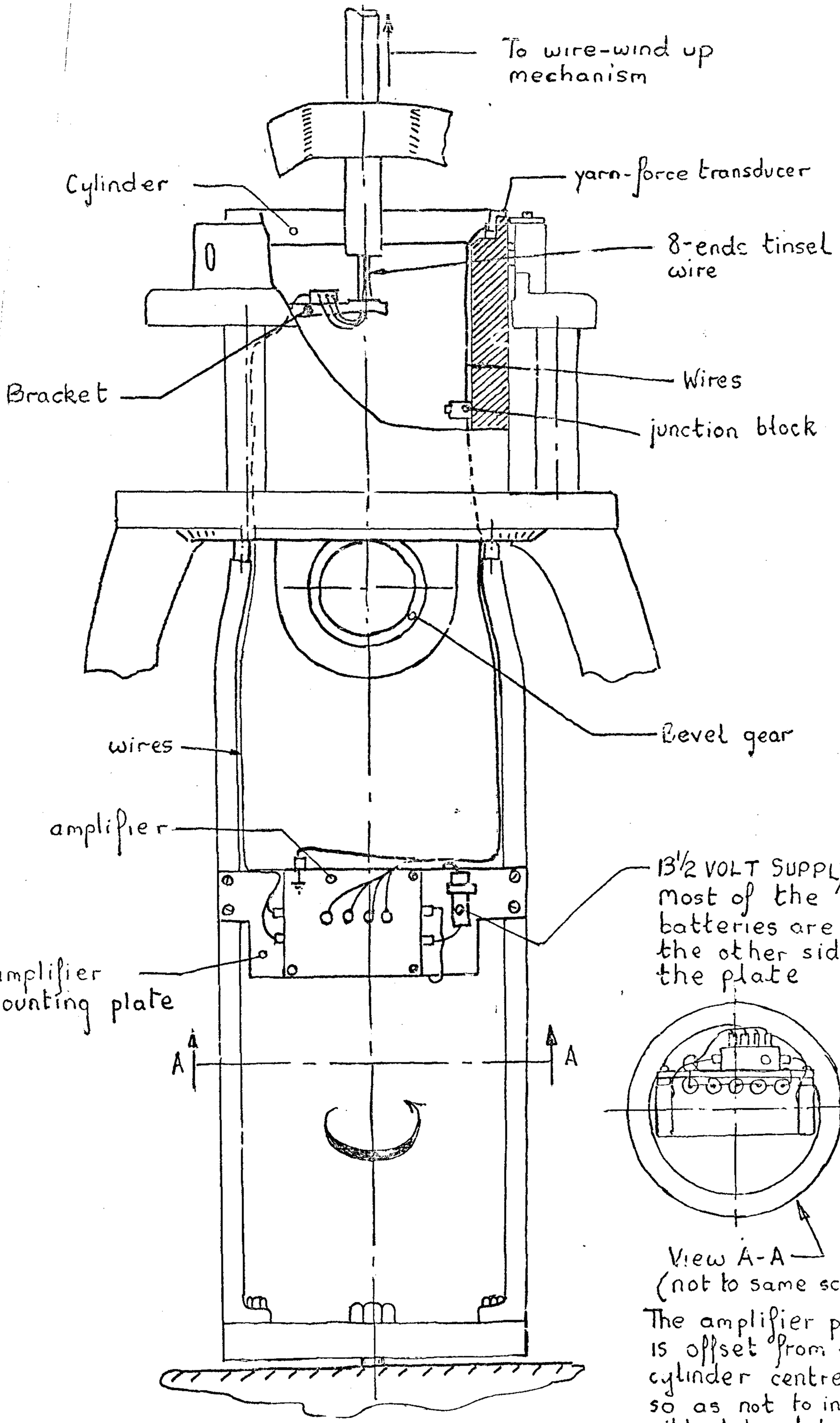

MOUNTING OF AMPLIFIER ON KNITTING MACHINE

FIG 6.6

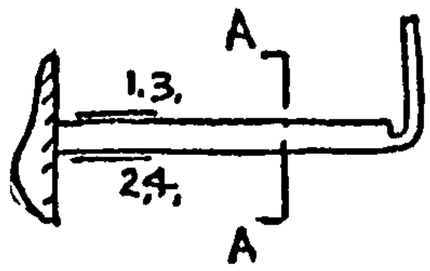

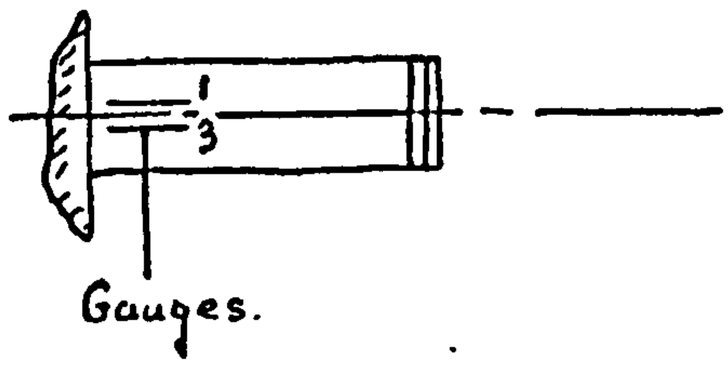

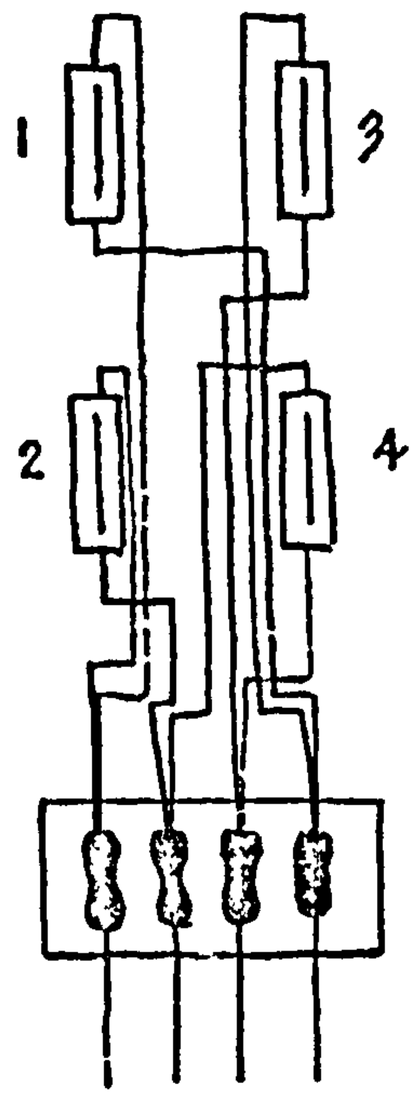

STRAIN- GAUGE POSITION AND WHEATSTONE BRIDGE

FIG 6.7

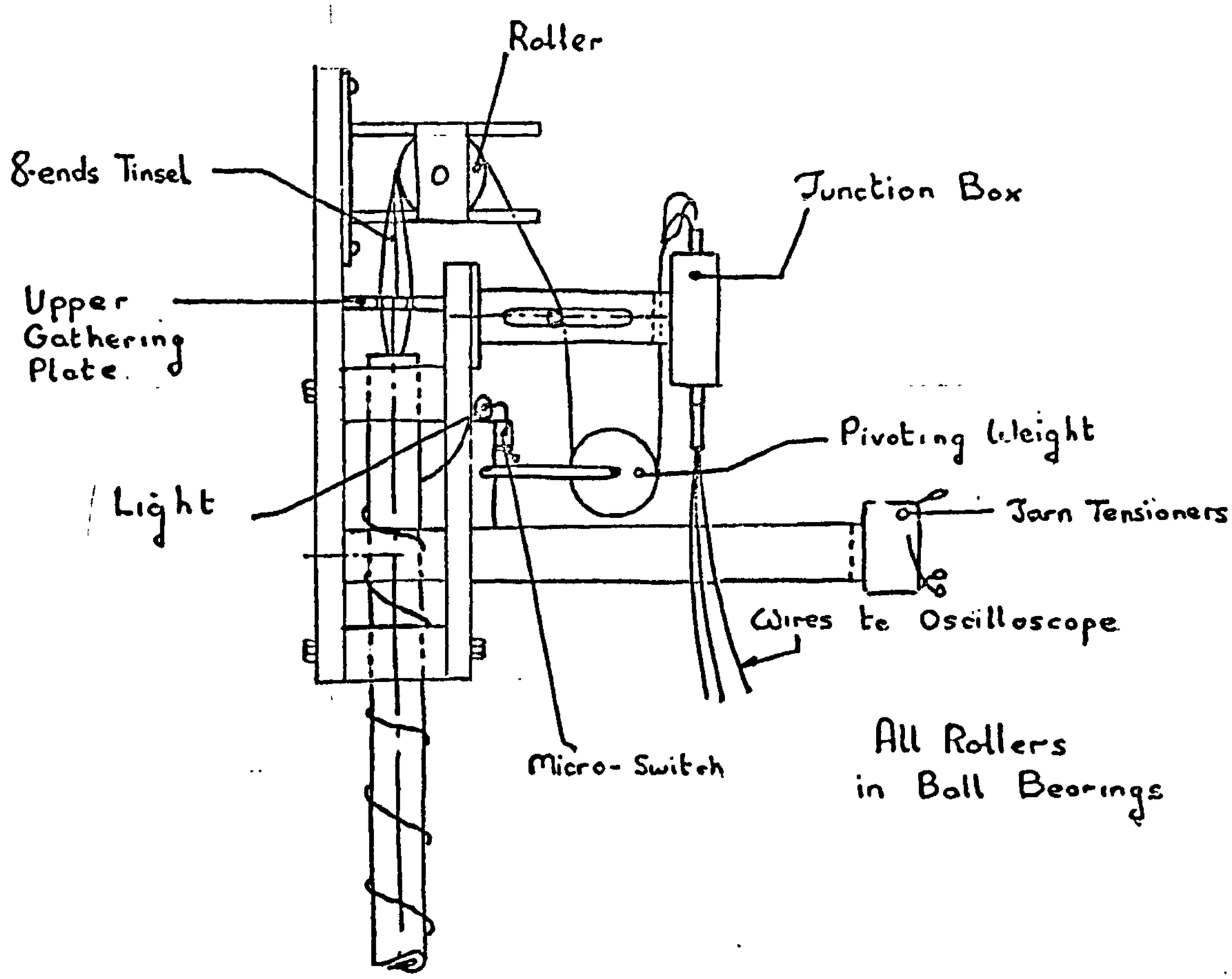

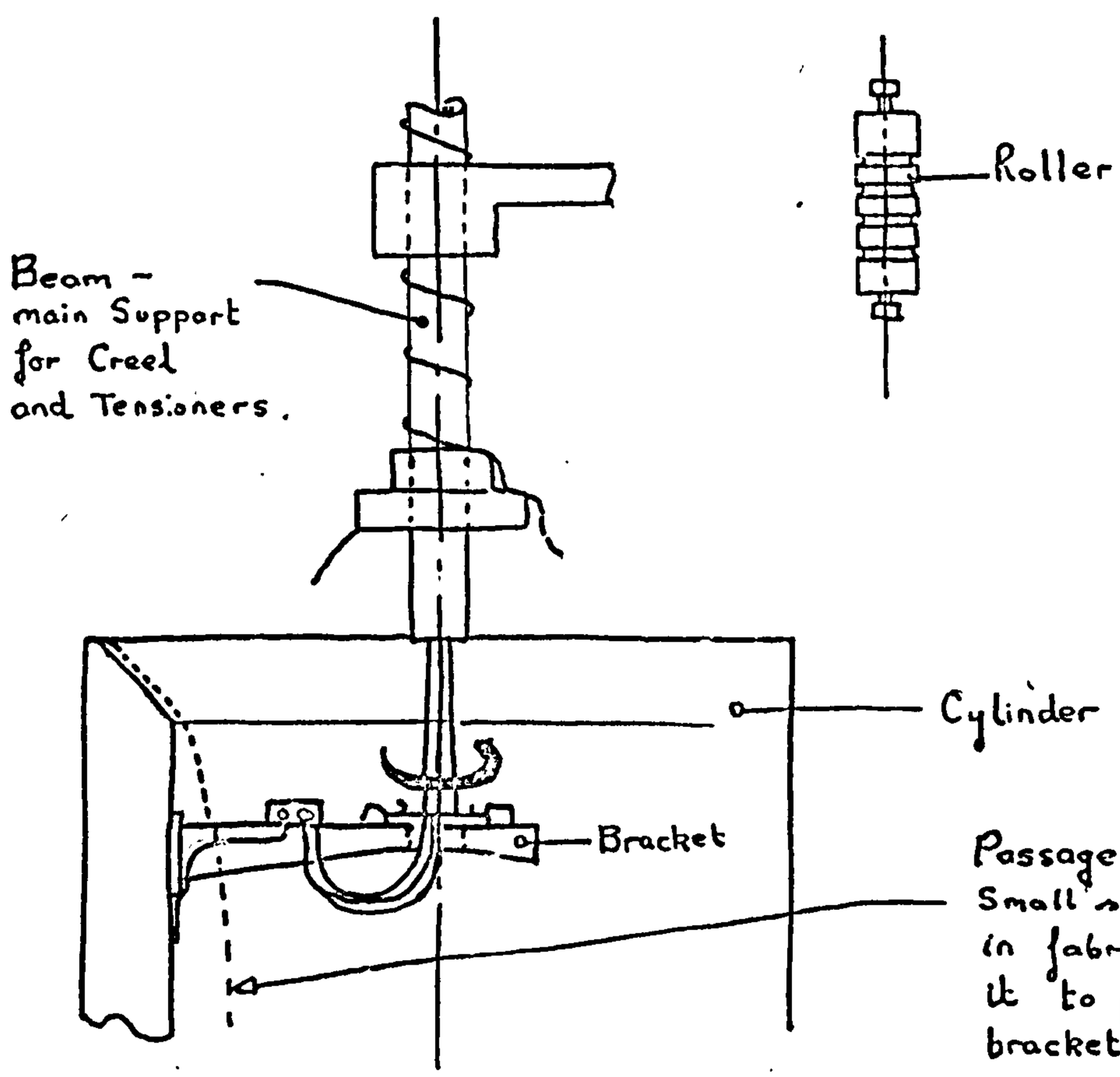

WIRE WIND-UP MECHANISM.

FIG 68

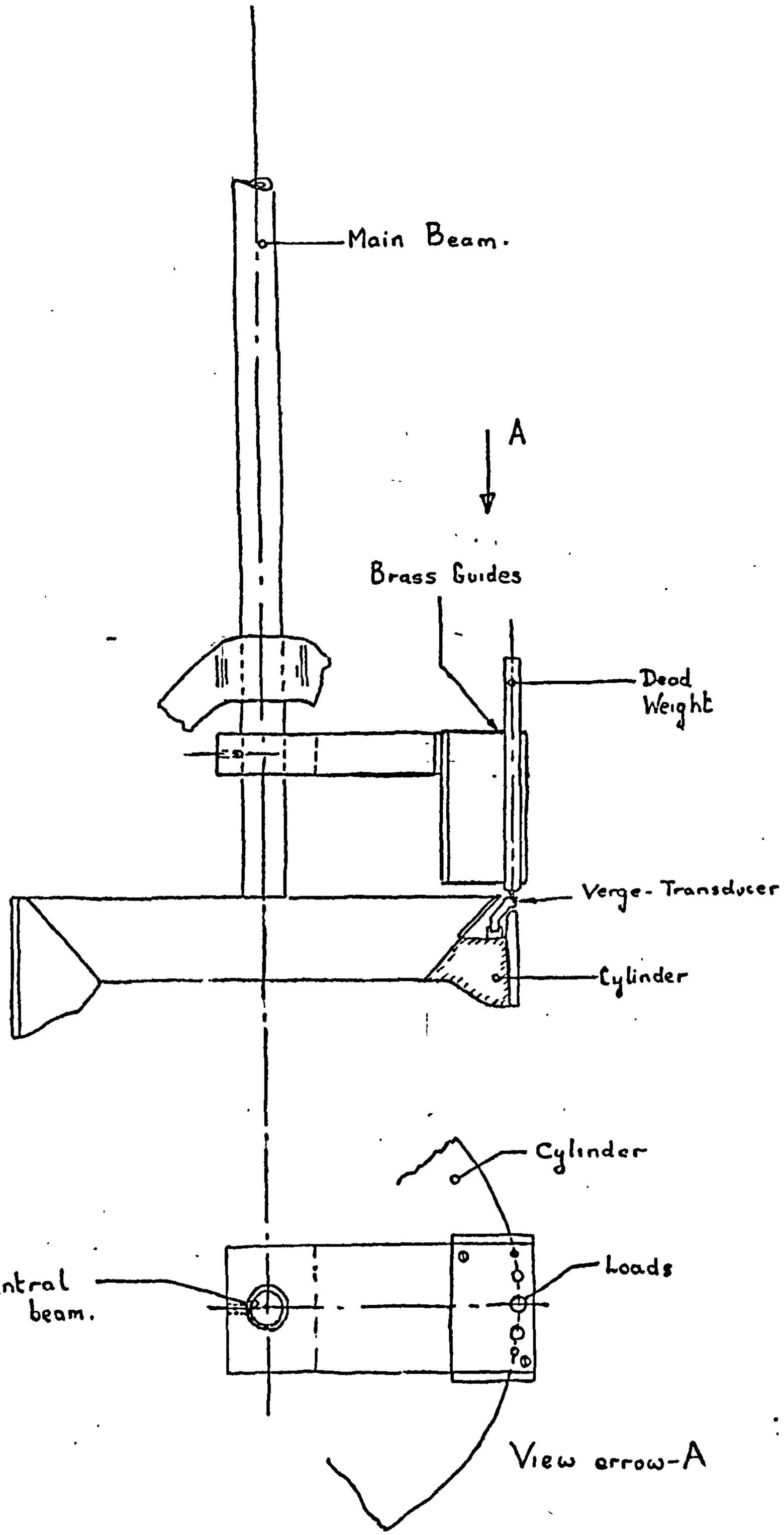

YARN - TENSION CALIBRATION APPARATUS.

FIG 6.9.

CHAPTER 7

ANCILLARY EQUIPMENT REQUIRED FOR MEASUREMENT

7.1 The Constant Take-Down Tension Device.

During yarn-force and cam-force experiments, it was seen to be essential that the fabric take-down tension should be constant and predictable.

A device was therefore built which applied a uniform tension to the fabric and the magnitude of this could be varied by simply adding or removing weights. The system is illustrated in Fig 7.1. A long thin spindle was fitted through a hole in the centre of an 6 inch diameter disc and was supported in two bearings. The upper part of the spindle was threaded, so that variable cylindrical loads provided with central holes could be fitted over this part of the spindle, and held in position by two nuts. The fabric was gathered around the disc and tied underneath by a loop of string.

During experimentation the spindle slowly moved down through the bearings. Periodically it was necessary to stop the machine, move the spindleup, cut-off a length of fabric, and re-tie the string. These periods of machine stoppage could be arranged to coincide with those required for releasing the twisted output wires carrying the yarn-force transducer signals (see section 6.3).

7.2 Monitoring of Input-Yarn Tension.

It was essential that, combined with the yarn-force and cam-force measurements, the input yarn tension should also be known. Using the standard machine yarn guide and latch guard arrangement, illustrated in Fig 7.2 (a), it

was very difficult to get any form of measuring device into the small confined space immediately prior to the yarn entry to the needles. It was important that measurements were made directly on entry to the needles, because the guides could have a large effect upon the forces generated, and any measurements undertaken prior to the final guide, could be considerably different from the actual force in the yarn directly before needle entry. Most of the measurements were taken with a modified guide that exposed more yarn, and enabled a measuring device to be fitted close to the needles. A diagram of the modified guide and latch-guard is shown in Fig 7.2 (b). The yarn input tension was measured with a 0 to 100 gf Rothschild Measuring Head, positioned as shown in Fig 7.2 (b). The output from the head was passed to the Rothschild amplifier, and the output from the amplifier was connected into one of the channels of the tektronix storage oscilloscope. The yarn-input tension was displayed on the oscilloscope simultaneously with the input signals in the other channels, since a great advantage of the system was that the yarn input tension display was obtained at exactly the same instant as the cam-force and yarn-force measurements were recorded. The variation of yarn input tension during the loop formation process and the measurement of the cam forces, could thus be easily determined.

The yarn was drawn through guides directly off the bobbin. For most experiments, a Disc-Tensioner was used but a Hysteresis Brake yarn tensioner was occasionally used. Fig 7.3 is a diagram showing the yarn path.

7.3 The Kinetic Yarn Friction Apparatus.

The yarn-force transducer measured the force exerted upon the verge by the yarn. However, it was impossible to

predict the tension in each arm of the yarn without a knowledge of the frictional build-up in tension as the yarn passes over the needle and verge elements. There were a number of theories relating to this problem, but it was still essential to build an experimental rig to measure the tension increase and to closely examine the theories under realistic conditions.

An apparatus was built to carry out the tests at varying speeds and varying wrap angles. Although during the course of this work only one type of yarn was used, the frictional properties of a range of yarns and elements could easily be examined with the apparatus. The essential components are illustrated in Fig 7.4. Yarn was wound off a bobbin at an adjustable tension, it was passed through the guides and around the measuring element which was clamped in the vice. The wrap angle could be read off from a protractor mounted behind the vice. The yarn was then taken to the supply drum, which was directly connected to the motor and Carter-gear unit.

Experiments were carried out using 0.443 mm (0.0175 in) needles, 0.406 mm (0.016 in) needles and a simulated verge element. The experimental verge was of the same material, and hardness as the standard machine verge. Additionaly, the verge surface was shaped to closely correspond to the surface of a machine verge.

A Rothschild 0. to 100 gf measuring head was applied to the yarn, just before it passed over the element. Similarly, another Rothschild 0 to 100 gf head was applied to the yarn just after it had passed over the element. In the Rothschild manual it was stated that the measuring heads had a negligible

braking effect on the yarn. It was very important during experiments that the yarn tension entering the element was the same, or at least only different by a known amount, from the tension measured by the head. A simple experiment was carried out to determine the braking effect of the Rothschild measuring head. Two 0-100 gf heads were calibrated in the normal manner recommended in the manual, by attaching a weight to a length of yarn and then steadily drawing the yarn through the head. The scale was adjusted to read the value of the weight. Two heads were then applied to the yarn one vertically above the other, a weight was hung on the yarn which was then steadily pulled through the heads. If there was no braking effect, then the reading for both heads should be the same. The experiment was repeated a large number of times with a range of weights. It was found that the tension measured by the upper head was significantly higher than the tension measured by the lower. A graph was plotted showing the output yarn tension from the head against the input yarn tension, for the particular test yarn, and this is shown in Fig 7.5. During experiments care was taken to see that the lower head was used on the input side of the element and the upper head the output side. The tension indicated on the input yarn head was then corrected using Fig 7.5.

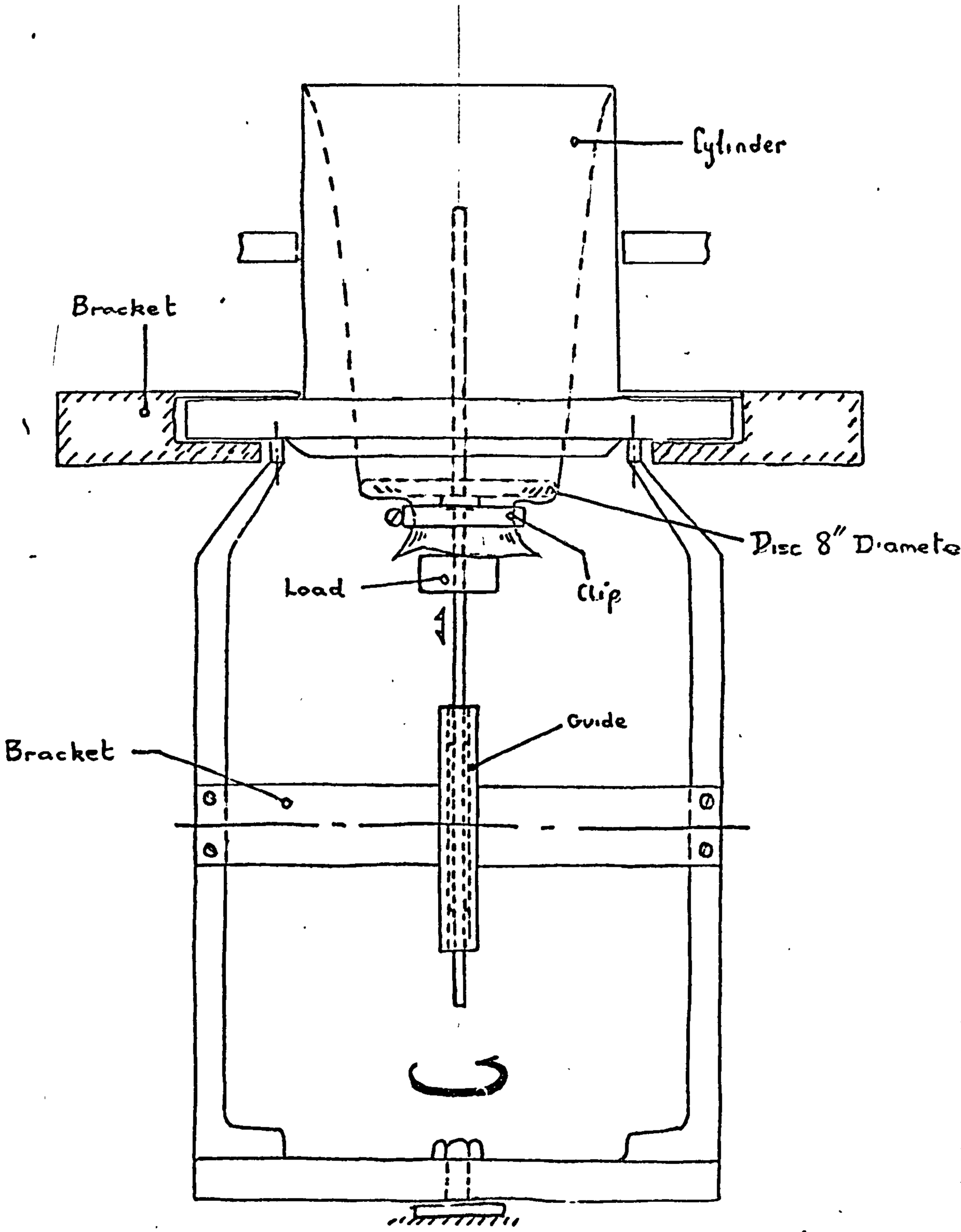

CONSTANT TAKE-DOWN TENSION DEVICE

FIG 7.1

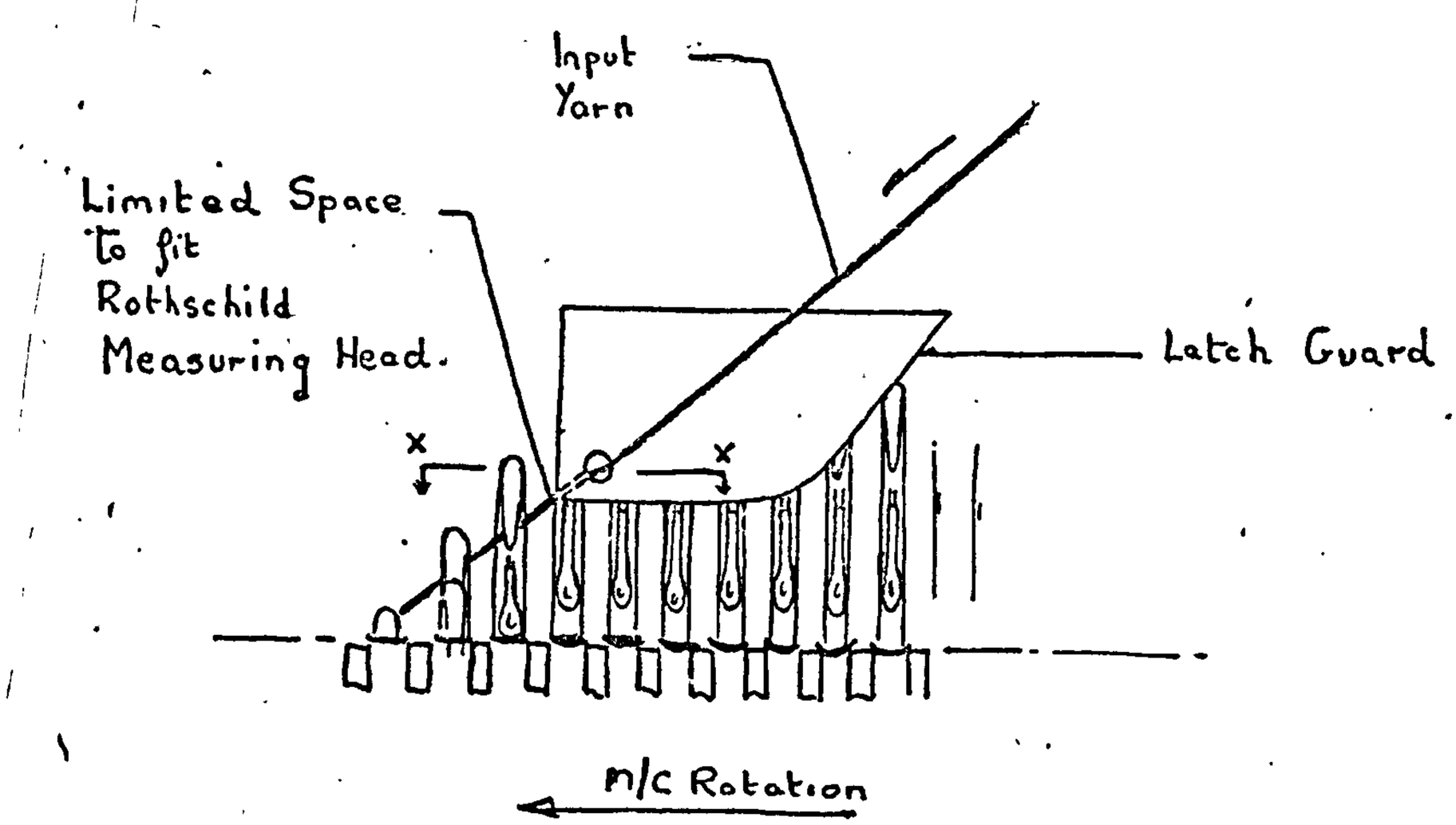

(a) Standard Latch - Guard – Yarn - feeding Cam.

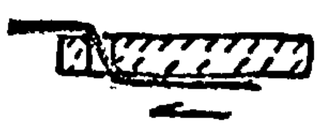

SECTION X-X
Showing Yarn path

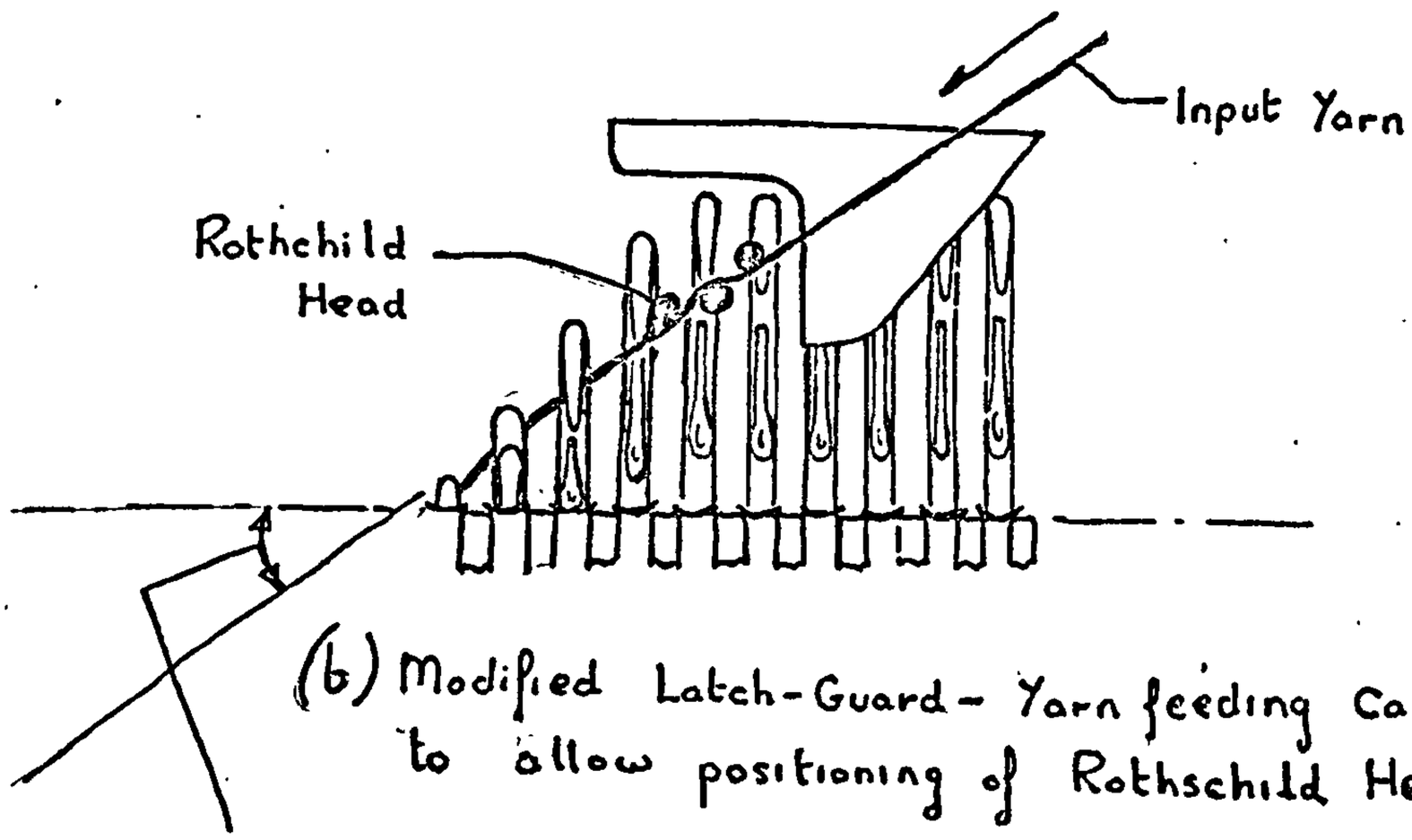

(b) Modified Latch-Guard- Yarn feeding Cam
to allow positioning of Rothschild Head.

(a) STANDARD AND
(b) MODIFIED LATCH-GUARD
AND YARN-FEED CAM.

FIG 7.2

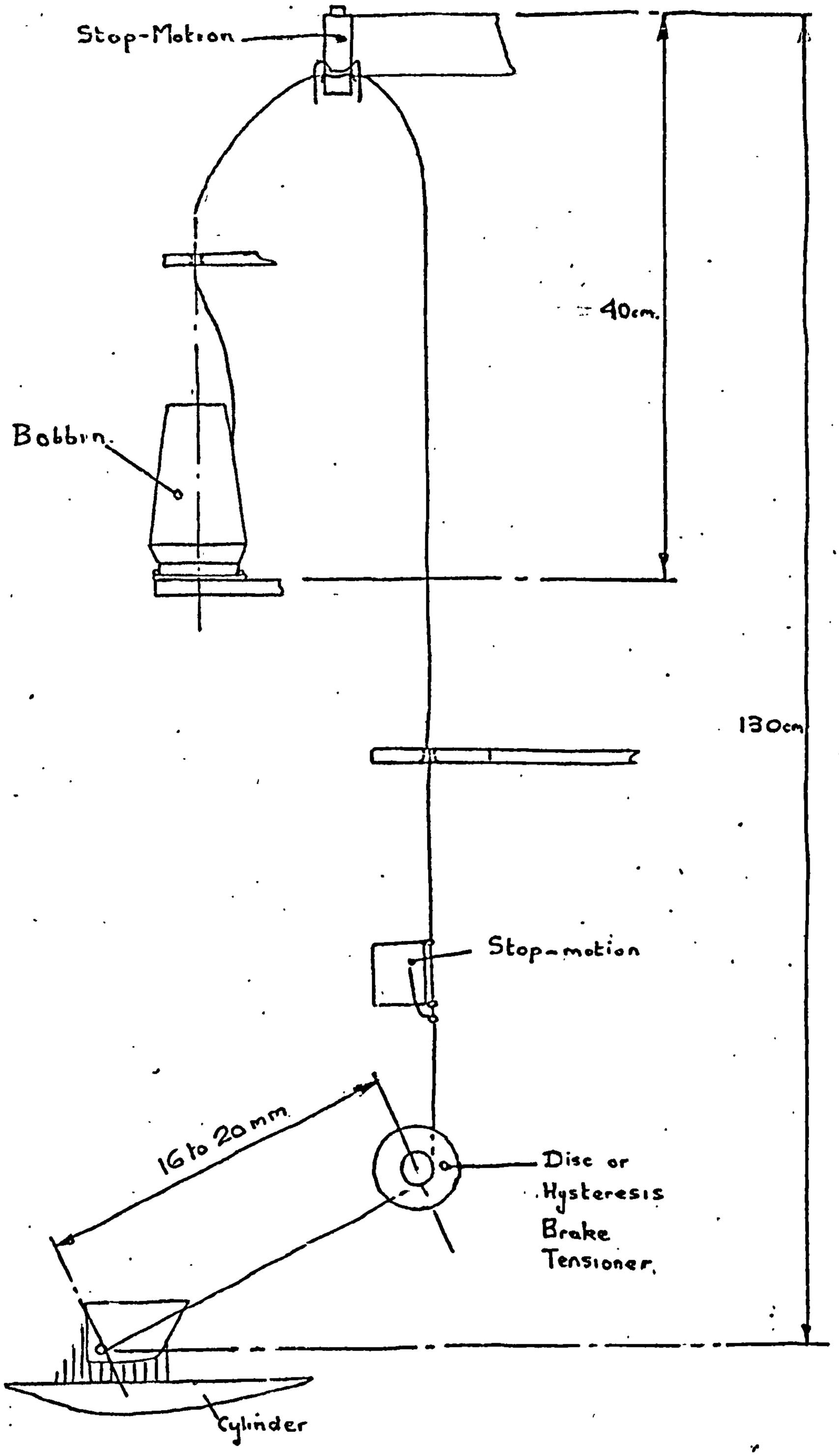

YARN-PATH AROUND
MACHINE

FIG 7.3

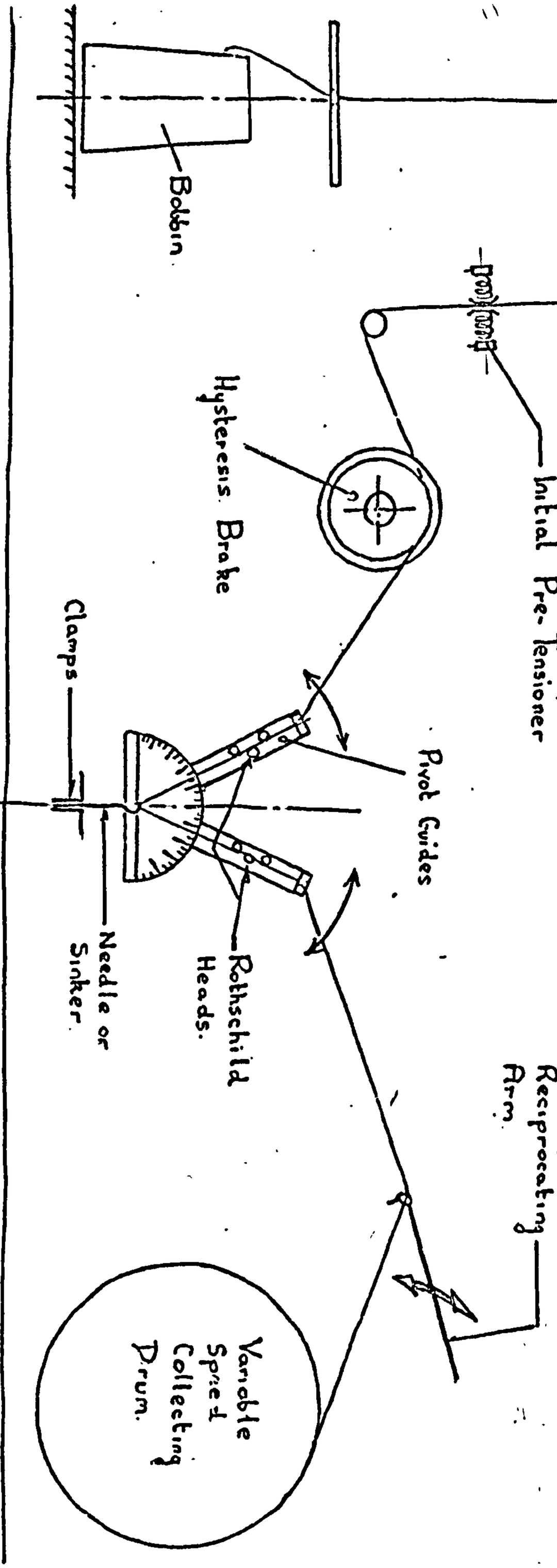

KINETIC YARN FRICTION APPARATUS FIG 7.4

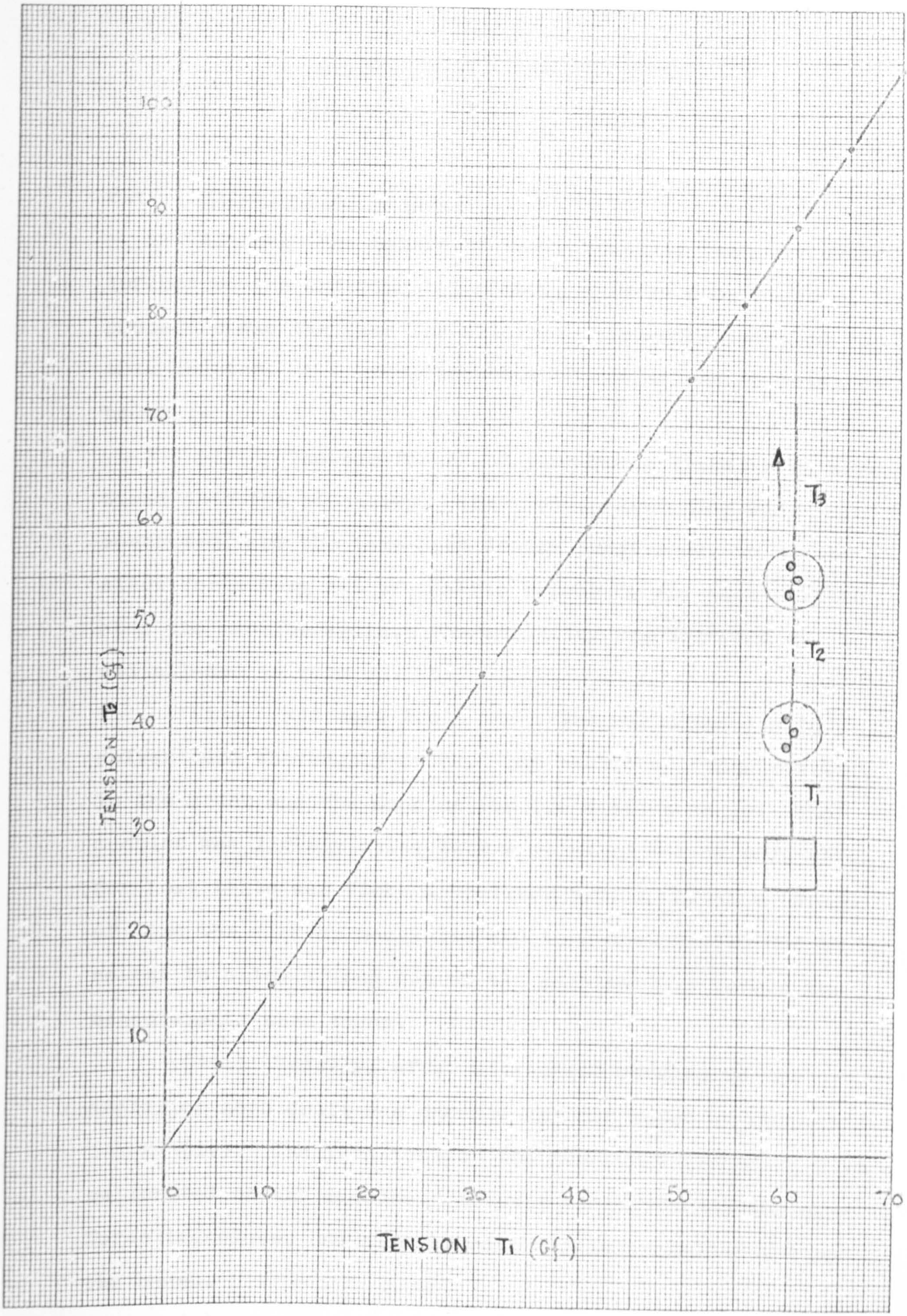

CALIBRATION CURVE FOR ROTHSCHILD HEADS

FIG 7.5

CHAPTER 8

EXPERIMENTATION ON THE FORCES PRESENT IN THE KNITTING OPERATION

8.1 Experimental Method.

Although the nature of the particular test obviously influenced the experimental method, a large proportion of the procedure was the same for all the experiments detailed in this chapter. A typical sequence of operations is detailed below :-

(i) The cam-force and yarn-force transducers were wired into the circuitry. The wind-up mechanism was connected, and the take-down device positioned, so as to allow for a long run of fabric before it was necessary to stop the machine again. The circuitry was switched on and allowed to warm up.

(ii) For most tests the trick was cleaned with solvent and thoroughly dried. The needle was then refitted in the trick and the machine run for a short while. The machine was lightly oiled with a standard needle oil, which for most tests was Vickers Spotless B.N.O. After a period of time the wind-up mechanism and take-down device had to be re-set to allow a long run on the machine just before the measurements were taken.

(iii) Usually, after sufficient warming up the amplifier zero drift was checked and corrected if necessary.

(iv) The yarn-tension and cam-force transducers were calibrated on the machine. In most circumstances the cam-force transducer had already been initially calibrated on the bench.

(v) The triggering point was set following the

procedure detailed in section 8.1.1.

(vi) The particular experiments were then carried out, the calibration being rechecked at frequent intervals.

8.1.1 Setting the Oscilloscope Trigger.

A procedure was adopted for setting the triggering circuit to fire the oscilloscope when the verge was at a known position in relation to the cams. The method is illustrated in Fig 8.1; a fine 0.18 mm wire was placed under a needle hook and the cylinder was turned slowly so that the needle was moved down the stitch-cam. At the exact position where the wire contacted the verge top and began to bend upwards, the cylinder was held stationary. The relative position of the needle to the cams was then fixed, and as the verge was a known distance behind the needle, the position of the verge in relation to the cams was also fixed and a known quantity. The trigger was set to fire when the needle was at this position.

When cam-force traces combined with the yarn-force traces were obtained the setting of the oscilloscope triggering circuit was not so critical, because the position of the verge relatively to the cams could be determined from the cam-force traces. The height of the needle at the instant of stitch-cam impact could be measured, and this point was also clearly marked on the polaroid photograph by the sudden rise in the force level. Knowing the machine speed and the oscilloscope time-scale, the exact position of the needle anywhere on the cam profile in relation to the force trace could be determined, and, since the verge was a known distance from the needle, the exact position of the verge in relation to the force was also known.

8.1.2 Measurement of Stitch-Draw.

Throughout the experiments, the stitch-draw refers to the distance between the verge top and the underside of the needle hook, as shown in Fig 8.2. A procedure was adopted for setting the stitch-draw at a precise value. For example, if it was desired to have a draw of 2.00 mm, spacers would be placed under the transducer having a thickness of 2.00 mm + 0.18 mm (the significance of the 0.18 mm dimension will be explained below). The transducer was raised until the needles at the lowest position on the cams were just above the level of the verge top. The transducer was then clamped down to the machine structure and the cylinder was turned slowly. A fine 0.18 mm wire was placed under the hook of a descending needle, and as the needle approached the lowest point on the cam the wire was closely observed; if it just began to bend as the needle clamped the wire against the verge top, then the lowest cam position was set at a known distance below the verge top. The procedure was somewhat similar to the method used for setting the oscilloscope trigger as was illustrated in Fig 8.1. If the wire under the hook did not bend at all, or bent too much, then the procedure had to be repeated using fine shims to raise or lower the transducer the required amount. When the correct height was reached, the transducer was unclamped and the 2.00 mm + 0.18 mm shims were removed. The transducer was then tightened-down, setting the stitch-draw at 2.00 mm.

8.2 Early Measurements using the Yarn-Force Transducer.

8.2.1 Effect of Variation in Yarn Moment Arm.

It was possible that during the loop forming process that the point of application of the force on the verge would vary a small amount, as was illustrated in Fig 6.2. Referring

to this illustration, an experiment was carried out by first placing a load at A and then again at B. The output signal with the load at A was approximately 4% higher than the signal with the load at B. Since the distance between A and B was much larger than the maximum possible movement of the yarn on the verge during normal operation, it was considered unnecessary to correct the output from the yarn-tension transducer to allow for any effects due to slight movements of the yarn on the verge.

8.2.2 Effect of Variation in Yarn-Input Angle.

The angle between the verge and the input yarn, as shown in Fig 7.2 (b) was variable between approximately 0^{o} to 35^{o}. It was important, before detailed experiments were carried out, that the effect of changes in angle upon the loop drawing force should be clearly understood. The input yarn angle was varied between 0^{o} and 35^{o}, and traces were obtained at each change in angle. Although the traces varied a small amount there was no definite relationship between the change in the trace and the input angle. There were similar variations in the trace from one machine revolution to the next without any alteration to the input angle or to any other parameters affecting the loop-drawing process. It was therefore concluded that the effect of variation in the input angle was negligible. For the majority of subsequent experiments the input angle was 30^{o}.

8.3 Measurement of the Variation of Yarn-Input Tension during Knitting.

The input yarn tension was measured just before the yarn entered the needles after it had left the final guide. The tension showed a cyclic variation of frequency double the needle passing frequency. For example, in Fig 8.9 (b) where

the machine speed was 50 ft/min, the tension frequency was 340 cycles/second and the needle passing frequency was 170 needle pitches per second.

It was difficult to match up exactly the position of the needle in relation to the tension fluctuation on the yarn. However, by setting the oscilloscope trigger in the manner detailed in section 8.1.1 it was possible to fix the needle position relatively to the yarn-force. From this, and knowing the needle height at which the input yarn was just touched by the descending needle, it was possible to work out approximately the position of the needle in relation to the input yarn tension. The results indicated that the input-yarn tension rose sharply just after the needle engaged the yarn.

From Fig 8.3, which shows the verges and needles in six different positions denoted as Diagrams I to VI, a plausible explanation for the build up in tension is given below:-

Diagram III :- The tensioner is unable to provide instantaneously the quantity of yarn suddenly demanded by needle C, the yarn stretches and the tension rises.

Diagram IV :- The high tension pulls a large quantity of yarn through the guide and the tension falls.

Diagram V :- The yarn is snatched by the verge which again stretches the yarn and produces a high tension.

Diagram VI :- Yarn is pulled through the guide under high tension, and the sudden inflow of yarn causes the tension to fall.

The process continues through Diagrams I and II and reaches the starting point again at Diagram III.

The yarn and tensioner appear to possess similar behaviour to that of a spring-mass system in oscillation. An attempt

was made to limit the fluctuation by moving the disc tensioner back, increasing the yarn length between the needles and the tensioner. This acted so as to reduce the tension fluctuation, but as soon as guides were placed between the tensioner and the needles the fluctuation increased again. A number of parameters influenced this fluctuation and these are Listed below :-

(i) The tension fluctuation increased markedly when the mean level of input tension was increased, for example, a change in mean level from 6.5 gf to 14 gf increased the max fluctuation from 6.5 $\pm$ 2 gf to 14 $\pm$ 5 gf. This is shown in more detail in Fig 8.9 (b).

(ii) Increasing the stitch-draw from 1.60 mm to 2.73 mm increased the maximum fluctuation of tension from 13 gf $\pm$ 2 gf to 13 gf $\pm$ 6.5 gf. Although a tension of 13 gf just prior to the needles may seem high, yarn friction measurements, which are explained in more detail in section 9.6, showed that a tension of 13 gf just before entering the needles was compatible with a tension of only 4 to 5 gf just before passing into the machine's final yarn guide.

8.3.1 <u>The Disc and Hysteresis Brake Yarn Tensioner.</u>

It was thought that the tension fluctuation may have been due to the particular tensioner being used. Experiments were carried out using Disc and Hysteresis brake tensioners but the tension fluctuation was virtually the same whichever device was used; however, the mean level of tension varied slightly more with the Hysteresis brake than with the Disc tensioner. The variation in the traces from the yarn-force transducer seemed closely related to the mean-level variation in input yarn tension. The output from the verge transducer responded in direct unison with the input yarn tension, and

if the tension was highly variable then the yarn-force was also highly variable.

The Disc tensioner held the mean level of input yarn tension more constant than the Hysteresis brake, and for this reason it was used for the majority of the experiments.

8.4 <u>A Description and Tentative Explanation of the Shape of the Cam-Force Plot.</u>

Fig 8.4 is a reproduction of a photograph of cam-force and yarn-force at the particular conditions specified on the diagram. The horizontal scale relates the forces to the position of the needle on the cams and the upper sketch shows the position of the yarn on the needle head, at each of the needle positions.

A detailed analysis of cam and yarn force is carried out in Chapter 9; however, a tentative explanation for the build up of cam forces is as follows :-

Referring to Fig 8.4 the respective needle positions during the knitting process are defined as S1 to S9 and the verge positions N1 to N9. The needle impacts the cam at position S1.

<u>Needle Position.</u>

Between S1 and S2 :- The force in this region is largely the force required to overcome trick and spring resistance to motion.

Between S2 and S3 :- The force increases rapidly as the old loop expands over the widening needle section just below the rivet

Between S3 and S4 :- The force reaches a maximum when the old loop is at the thickest section of the needle. The force then decreases sharply as the loop passes on to the decreasing section of the needle above the latch rivet.

Between S4 and S5 :- Abruptly the loop rises on to the latch. At first the rise in force is rapid as the yarn expands over a relatively

steep latch slope, but as the unfavourable slope decreases, the loop expansion becomes more constant and the force stabilises at a high value.

Between S5 and S6 :- The needle reaches such a position within the knitting cycle that it is possible to rob-back yarn from the cast-off loop one or two needles ahead. As soon as robbing back commences the force rapidly decreases.

Between S6 and S7 :- The force remains at a constant value until the needle passes below the verge and begins to draw the new loop.

Between S7 and S8 :- High force exists as the yarn is held in the hook at high tension, the tension drops suddenly as soon as it becomes possible to rob yarn from previously formed loops.

After S8 :- The force drops to zero as the needle moves from the stitch cam to the lower cam. The force then assumes a smaller constant value until the needle leaves that cam.

8.5 Effects of Various Parameters upon Cam and Yarn Force During Knitting.

A wide range of experiments were carried out for investigating the effects of knitting parameters upon the cam and yarn-forces. The results of these experiments are displayed in the respective sub-sections. Detailed analysis of the results and a comparison with theoretical solutions is carried out in Chapter 9.

8.5.1 Effect of Stitch-Draw upon Cam and Yarn Force.

Many researchers[11,15,16,23,25,26,28,29] have shown theoretically that the yarn-force increases as the stitch-draw becomes deeper and this result was confirmed by this experiment. A sample of the results obtained is shown in Fig 8.7 (a) and (b). Similarly, as the yarn force becomes larger the cam-force in the region where the loop is being drawn must also increase. A large loop easily passes over the needle head during casting-off, and as there is very

little yarn stretch, there is almost no vertical resisting force on the cams. When the loop size is reduced to a value where some yarn stretch must occur if the loop is to pass over the head, then the vertical resistance grows in magnitude. This force increases rapidly as the loop is further reduced in size until the machine can no longer satisfactorily knit.

Further information is contained on the graphs Figs 8.5 and 8.6. Peaks 1 to 4 are defined on Fig 8.5. The graphs show that the force required to draw the yarn into a loop limits the maximum value of stitch-draw, while the force required to stretch the yarn-loop over the needle head sets the lower limit on the stitch-draw.

8.5.2 Effect of Input Yarn Tension Upon the Cam and Yarn Forces.

The experimental results clearly demonstrated that the input yarn tension had a large effect upon both the yarn-forces and the cam-forces in the stitch-formation zone. The graph shown in Fig 8.8 summarises the experimental results. A typical sample of results is shown in the traces labelled Fig 8.9 (a) and (b) and Fig 8.10 (a) and (b). The graphs show that the maximum-yarn force linearly increases as the yarn input tension increases. Theoretically, a linear relationship would be expected and Dangel[22] expresses the well known frictional relationship :-

$$T_{max} = T_i \, e^{\mu \beta_1}$$

where T_{max} = max yarn tension during the loop forming process,

T_i = initial yarn-tension,

μ = coefficient of friction over needle and verge,

and β_1 = total yarn wrap angle around needle and verge.

if β_1 and μ is not varied,

then $T_{max} = K T_i$

where K = Constant.

Therefore the maximum yarn tension during the loop forming zone is linearly related to the input yarn tension.

8.5.3 Effect of Fabric Take-Down Tension upon the Cam and Yarn-Force during Knitting.

The yarn-force is a twin-peaked plot, the photographic traces clearly showing that the effect of increasing the take-down tension is to raise the magnitude of the second peak. Fig 8.11 and Fig 8.12 are graphical plots of the results obtained during the experiment. The traces given by Fig 8.13 (a) and (b) are samples of the results obtained.

8.5.4 Effect of Machine Speed.

The yarn-force appeared to be largely uninfluenced by the machine speed. The cam-force varied more in shape, rather than in overall magnitude, as the speed was increased. The precise effect of the speed increase depended upon the amount of oil applied to the machine cylinder, and, although this is covered in more detail in section 8.5.9, some of the results are expressed in the graph Fig 8.15. A sample of the traces of cam-force obtained during the experiment is included in Fig 8.16 (a) and (b). Fig 8.14 is a reproduction of the vertical forces on the traces shown in Fig 8.16 (b). A sample of the traces showing the effect on yarn-force as the machine speed is increased is given in Fig 8.17 (a) and (b).

There was clear evidence from the photographic records that, as machine speed was increased, an impact force due to the needle contacting the stitch cam grew in magnitude. This is clearly illustrated in Fig 8.16 (b) on the photograph taken at higher speed (200 ft/min).

8.5.5 Effect of the Needle Thickness upon the Non-Knitting Cam-Force.

The heads of the needles were removed so that the yarn had no influence upon the cam-forces, and in fact all that was measured in this test was the frictional resistance to motion caused by the band-spring and trick. The force was much lower for thinner needles but it was observed that frequently these needles would tip out of the trick and foul the cams.

Fig 8.19 (b) is a sample of the traces taken in this experiment and Fig 8.18 is a graph showing the effect of needle thickness upon the vertical cam-force.

8.5.6 Effect of the Clearance between the Cylinder and the Cams on the Cam-Force.

The effect of moving the cams radially away from the cylinder has been examined in some detail in section 4.6.4. This experiment was primarily concerned with the effect upon the knitting cam-force, of moving the cams a small distance from the cylinder. For most commercial machines the clearance between the cylinder and cams is between 0.15 mm and 0.36 mm (0.006 in and 0.014 in). The results in Fig 8.20 show that for such small movements, there is very little variation in the cam-force. A typical trace obtained during the experiments is given in Fig 8.21 (a) and (b).

8.5.7 Effect of Latch Frictional Resistance to Motion.

A trace was obtained of yarn-force and cam-force under the conditions specified in Fig 8.22 (a). The needle shank near the latch-pivot was then squeezed with a pair of pliers to increase the latch resistance to motion. The subsequent trace is shown in Fig 8.22 (b). As the old loop rose over the needle head, the yarn was trapped under the latch, and

the force increased until it reached a value such that the latch resistance could be overcome, and the loop could continue to move up the needle shank. However, needle manufacturers who subsequently examined the needle, considered that the latch was very stiff and the needle would have been removed from the cylinder before it had got into this particular state.

8.5.8 Effect of the Resistance to Needle Motion in the Trick.

The trick resistance to needle motion varied a great deal from one trick to another. The two traces shown in Fig 8.23 (a) and (b) are typical of results obtained. Diagram I shows the cam force for a needle in a relatively free trick and Diagram II shows the cam-force for the same needle in a stiffer trick. A similar variability in trick properties was noted by Kopel[32] in his research.

8.5.9 Effect of the Oil in the Trick.

The head of a needle was removed so that the yarn had no effect upon the cam-force. Experiments were carried out to examine the effect of the oil upon the force. If the machine was lightly oiled and traces were obtained some considerable time later, the force-level showed very little change as the machine speed was increased. However, if the machine was heavily soaked in oil and tested immediately after oiling, the force level showed a substantial increase as the machine speed was increased. Obviously if the machine was running at high speed and it was suddenly soaked in oil, the effect could be disastrous because there could be a rapid rise in force which could possibly fracture needle butts. The photographs, a sample of which is included in Fig 8.24 (a) and (b) clearly demonstrate the rise in force with increasing

speed, when the machine is heavily oiled. The graphical plot, Fig 8.25, summarises the results of another similar ~~this~~ experiment.

8.5.10 Effect of Temperature upon the Cam-Force and Yarn-Force.

In production, commercial machinery is run continuously for long periods of time and the working parts can become very hot. Primarily, it was expected that higher temperatures would mainly effect the viscosity of the oil. This was a very difficult experiment to carry out because the machine could not be run continuously for sufficient time for it to become really hot. An attempt was made to raise the temperature by enclosing the machine in a polythene tent and disposing electric heaters all around it. A temperature rise of approximately 15°C was achieved; from 21°C to 36°C, photographic traces were obtained at the low temperature and high temperature for varying amounts of oil. However, very little difference could be noted from the traces, a typical sample is included in Fig 8.26 (b).

8.5.11 Further Minor Experiments.

(i) Effect of Butt Width.

Traces were obtained, at low speed, for reductions of the butt width. Some variability in the traces was evident, but the effect was small, and could be the result of the change in the surface properties of the butt for each reduction in width. Typical traces are shown in Fig 8.27 (b).

(ii) Effect of Butt Length.

Traces were obtained using alternatively a standard long-butt needle and then a short-butt needle, as shown in Fig 3.2. Otherwise the traces were obtained under exactly similar conditions yet, apart from the normal trace variation that occurred between one needle and another, very little

difference apparently occurred.

(iii) The Effect of the Yarn upon the Cam-Force.

The results in Fig 8.28 (b), show a typical set of results for the effect of the yarn upon the cam force. Trace number 1 was obtained using a 0.406 mm (0.016 in) needle knitting under the conditions specified in Fig 8.28 (a). The needle head was removed and another set of results were obtained, see trace number 2 on Fig 8.28 (b). The effect that the yarn has upon the cam-force can be seen from the subtraction of traces 1 and 2. The precise effect of the yarn on the cam-force is discussed in more detail in section 9.8.2. Trace number 4 on Fig 8.28 (b) shows a 0.443 mm (0.0175 in) needle fitted in the same trick as previously used with the 0.406 mm needle.

8.6 Summary of Results.

A brief summary of the experimental results is given below :-

(i) Stitch-draw. (section 8.5.1)

As stitch-draw was increased, the yarn-force and cam-force increased non-linearly in the region where the new loop was being drawn. When the depth of draw was changed from 0.0628 in to 0.1077 in the cam-force rose from 180 gf to 540 gf, while the yarn-force increased from 140 gf to 300 gf.

For a lower stitch-draw, where the small loops being cast-off had to stretch considerably in order to pass over the head of the needle, the cam-forces are high, and they increase very rapidly as the stitch-draw is further reduced. In fact when the draw depth was changed by only 0.004 in - i.e. from 0.0668 in. to 0.0628 in, the force increased from 120 gf to 210 gf in the region on the cam preceding the new loop being drawn.

(ii) Yarn-input tension (section 8.5.2)

As the input yarn tension, measured prior to the final feeder, was increased from 1.5 gf to 5.5 gf the peak vertical cam-force increased from 90 gf to 160 gf, while the yarn force increased from 50 gf to 118 gf.

(iii) Fabric take-down tension. (section 8.5.3)

The experimental results show that the yarn force is a twin-peaked plot. The effect of increasing the fabric take-down load was to increase the second peak and slightly decrease the first peak. When the total load was varied between 1,477 gf and 3,757 gf, the magnitude of the second peak increased from 69 gf to 83 gf.

The corresponding change in the cam-force in the region where the new loop was being drawn was negligible.

(iv) Machine speed. (sections 8.5.4 and 8.5.9)

As machine speed increased, the cam-force, depending upon certain parameters, also increased. The most important parameters, were, briefly :-

(a) The viscous resistance of the oil in the trick:- When the needle and the trick were soaked in oil the vertical cam-force increased from 100 gf at 35 ft/min to 200 gf at 180 ft/min.

and (b) Rate and application of oil :- Immediately after oiling, the cam-force was large at high speed, i.e. in the order of 200 gf for heavy oiling. The oil soon drained away and the vertical cam-force dropped to 100 gf, and this force was then virtually constant with speed. Machine speed had almost no effect upon the yarn-force. As the machine speed increased an impact, where the needle contacted the stitch-cam, grew considerably in magnitude.

(v) Needle thickness. (section 8.5.5)

When the needle thickness was increased from 0.394 mm (0.0155 in.) to 0.452 mm (0.0178 in.) the maximum vertical non-knitting cam-force rose from 56.6 gf to 127 gf. Although the cam-force is low for the thin needles, they tend to tip out of the tricks and foul the cams. Nominal trick width was 0.470 mm (0.0185 in.).

(vi) Clearance between the cylinder and cams. (section 8.5.6)

The cam-cylinder clearance was changed from 0.15 mm to 0.356 mm; this covers the range of clearances normally found on commercial machines. The effect of the change upon the cam-force was small; when the clearance was 0.15 mm the vertical cam-force was 161 gf, and when the clearance was 0.356 mm the force was 175 gf. In earlier measurements, as the cam was moved 3.04 mm away from the cylinder, then the cam-force increased from 138 gf to 285 gf.

(vii) Latch resistance to motion. (section 8.5.7)

A cam-force plot was obtained for a normal 0.443 mm (0.0175) in.) needle. The needle was then removed from the trick and the faces opposite the latch pivot squeezed slightly until a definite resistance to motion was felt in the latch. The maximum vertical cam-force before and after the squeezing was 169 gf and approximately 300 gf.

(viii) Effect of the resistance to needle motion in the Trick. (section 8.5.8)

Very wide variation in the force level were noted when traces were obtained for a needle first in one trick then another. In the example contained in section 8.5.8 the horizontal cam force increased from 112 gf to 168 gf.

(ix) Effect of the Temperature upon Cam-force.(section 8.5.10)

It was impossible to carry out a very thorough investigation. However, when the temperature was raised from 21 ^{o}C to 35 ^{o}C, very little difference in cam-force was noted.

(x) Variations in butt-width and butt-length.(section 8.5.11 (i) and (ii))

Appeared to have little effect upon the cam-force.

(xi) The force exerted on the cams when casting off a fairly tight stitch.(section 8.5.11 (iii))

The sample of results detailed in section 8.5.11 showed that for a stitch-draw of 1.70 mm the cam-force increased from approximately 80 gf when no yarn was being drawn into a loop to approximately 180 gf when an old loop was being cast-off.

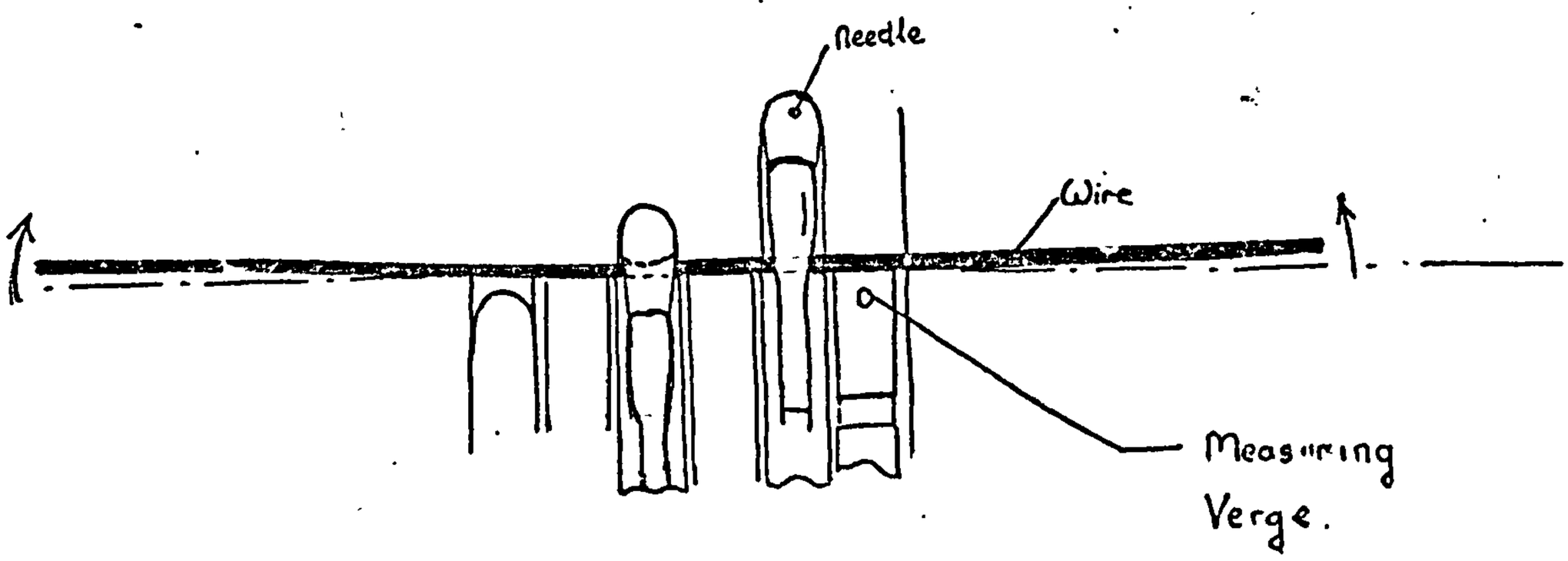

Oscilloscope trigger set to fire just when wire begins to rise. This sets the position of the verge with respect to the loop forming process.

SETTING OSCILLOSCOPE TRIGGER

FIG 8.1

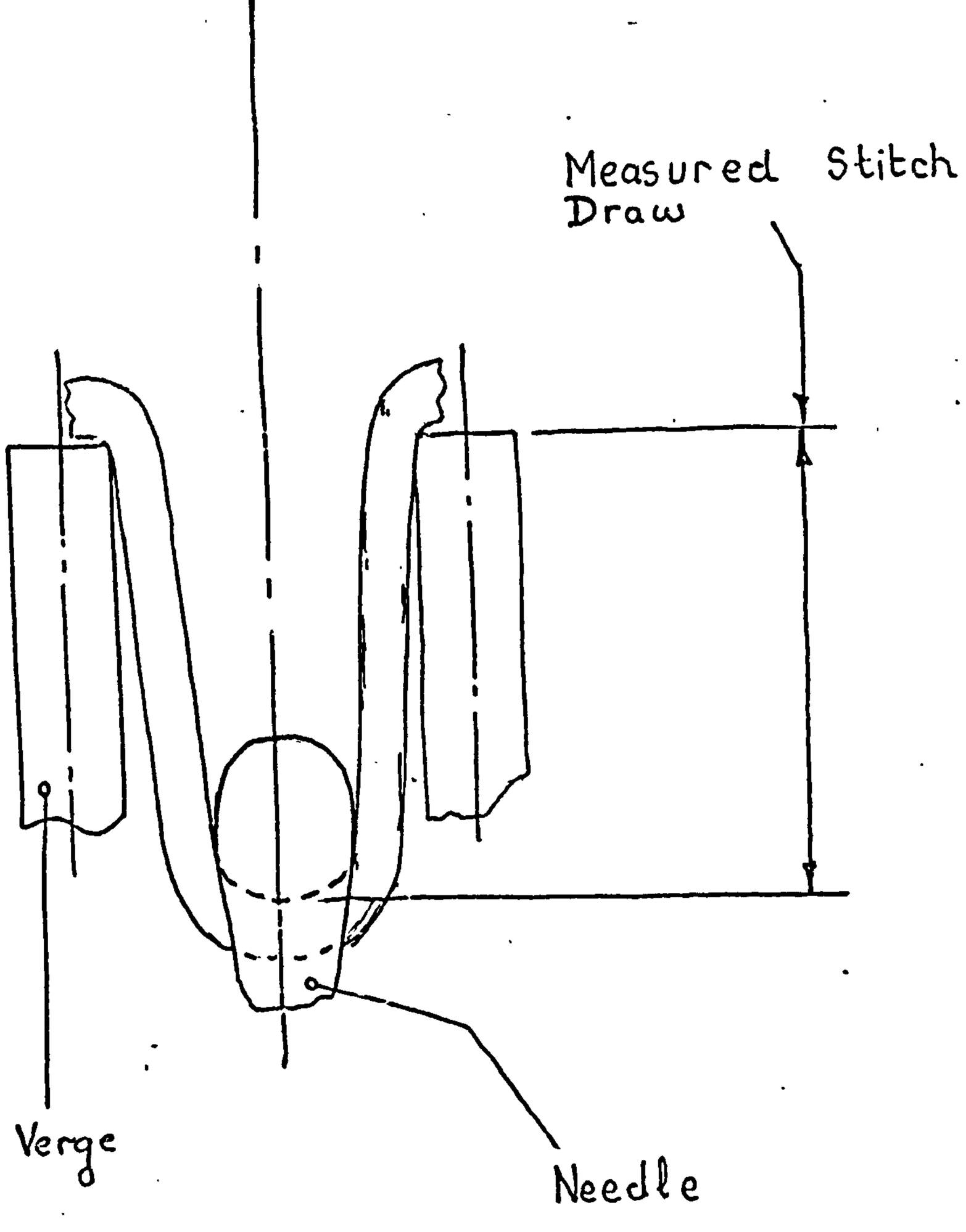

The Stitch-Draw. Fig 8.2

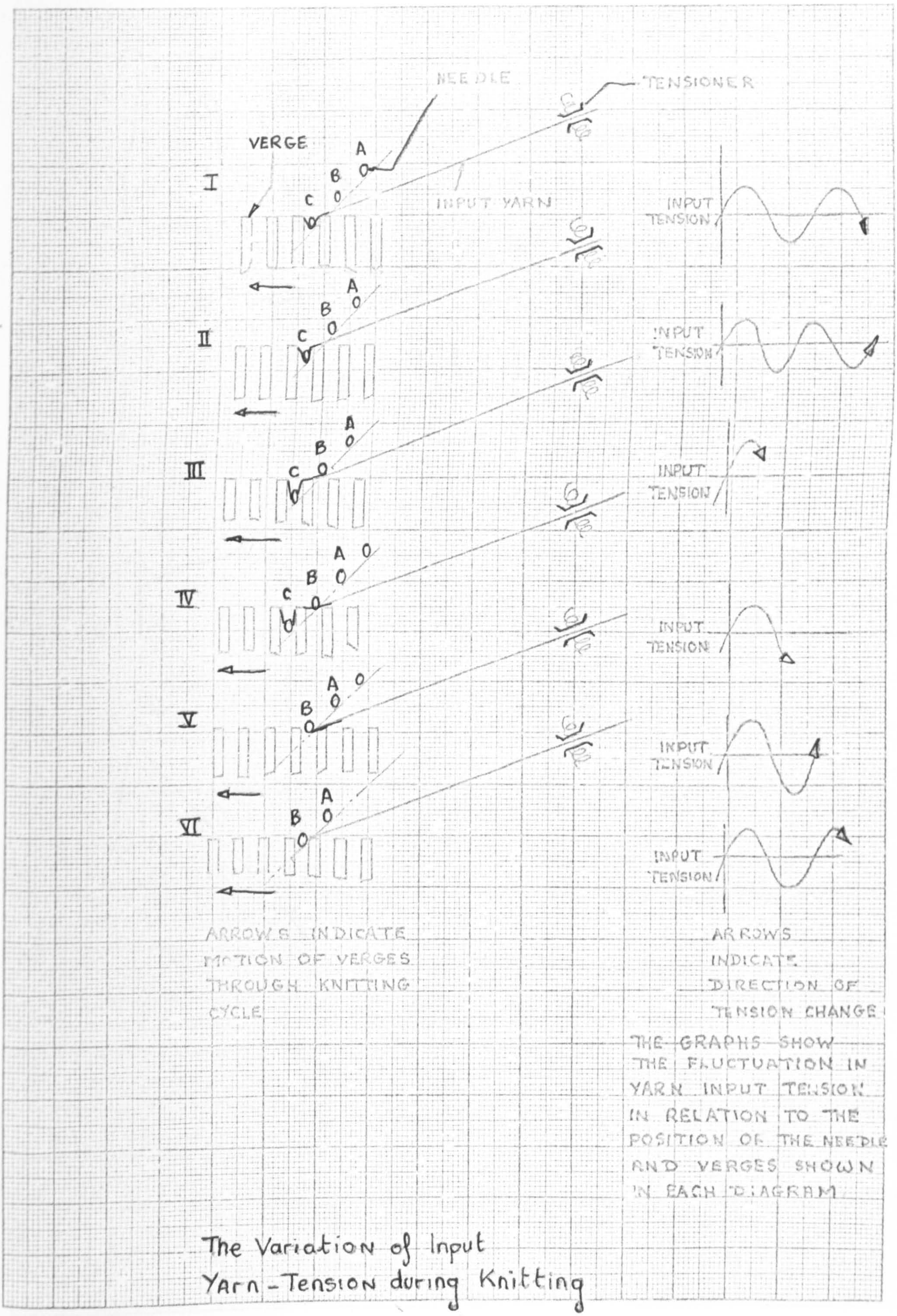

The Variation of Input Yarn-Tension during Knitting

FIG 8.3

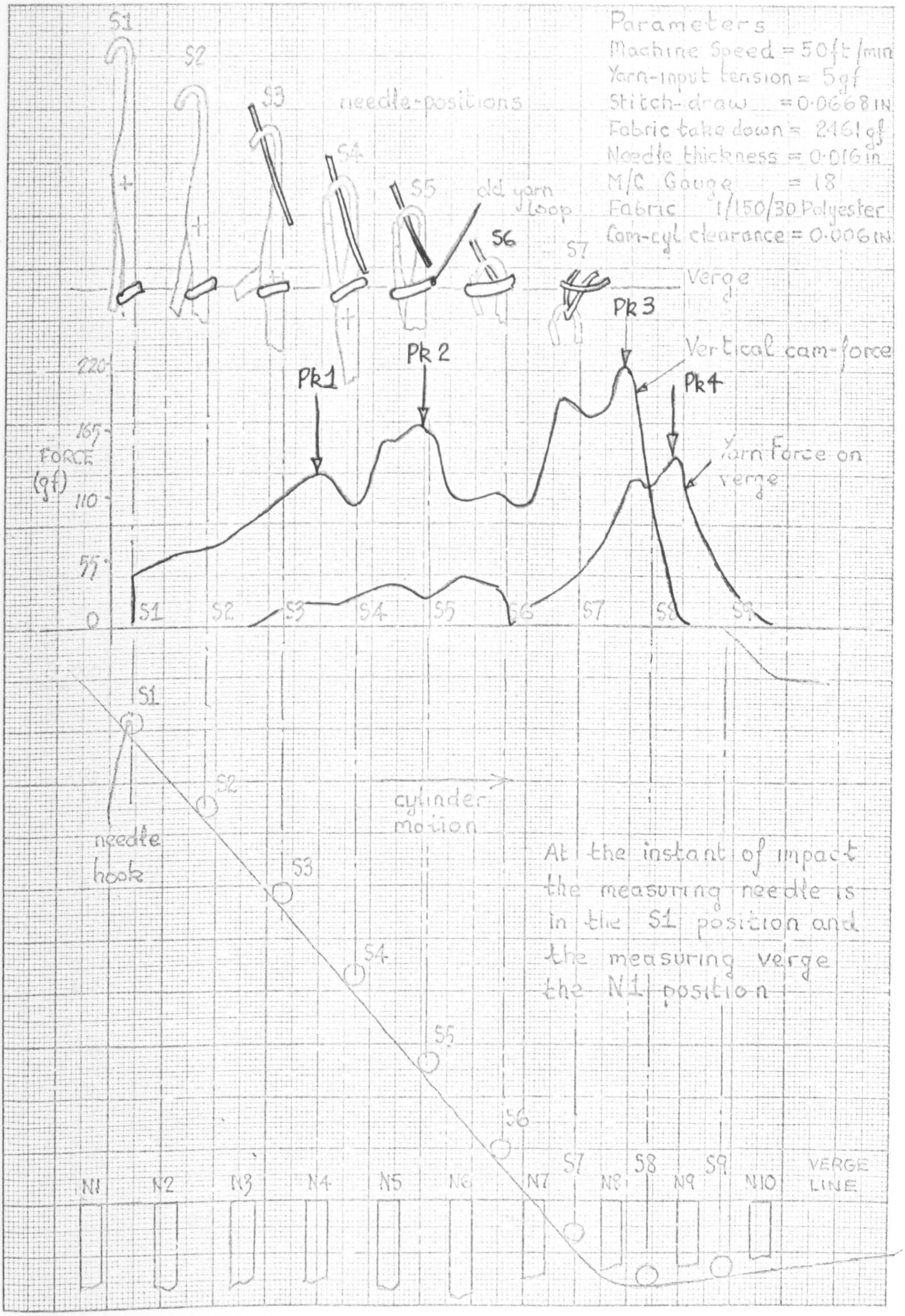

YARN-FORCE AND CAM-FORCE DURING KNITTING

FIG 8.4

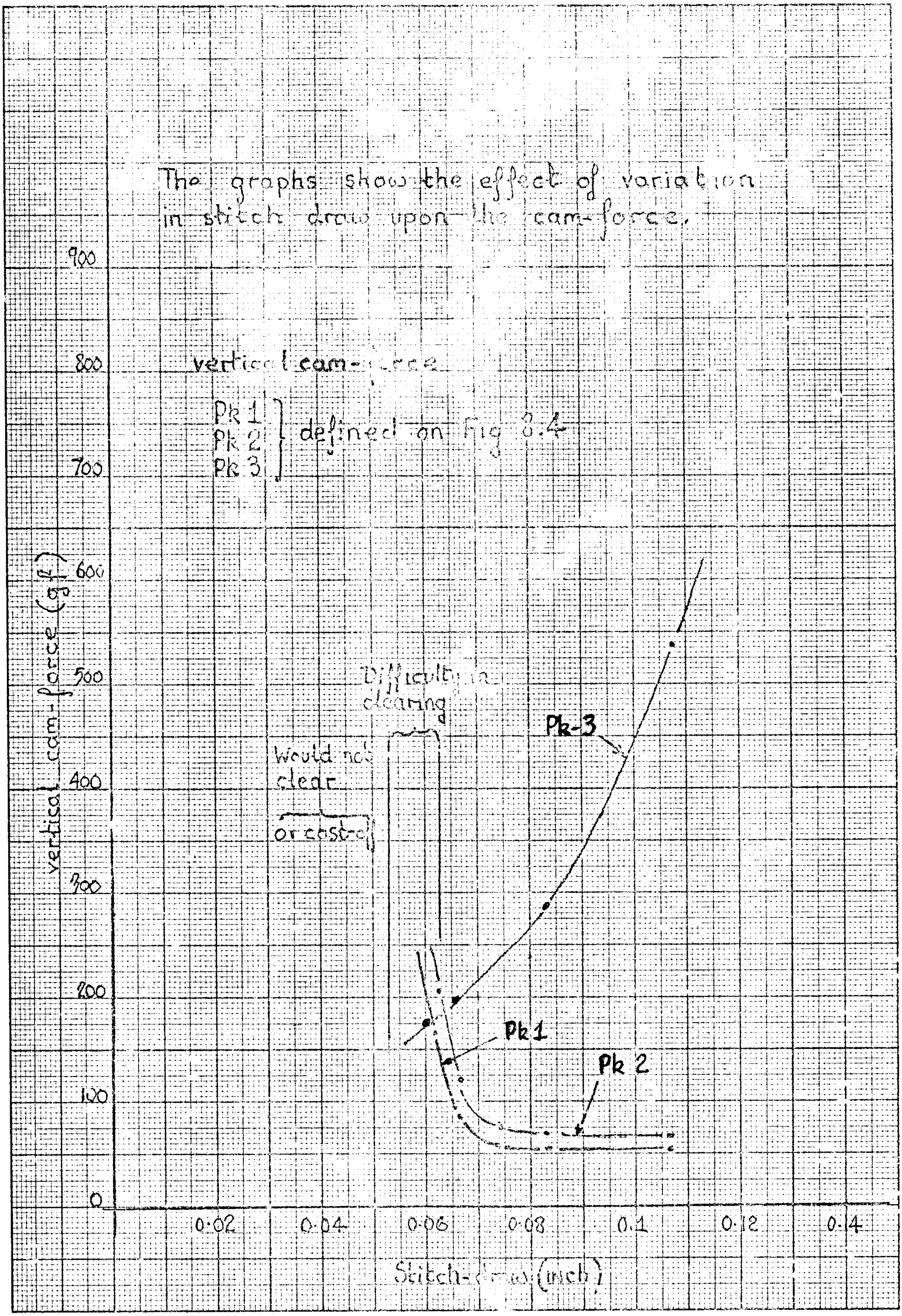

EFFECT of STITCH DRAW UPON CAM-FORCE. FIG 8.5

The graph shows the effect of variation in stitch-draw upon the yarn-force PK 4 defined in Fig 8.4.

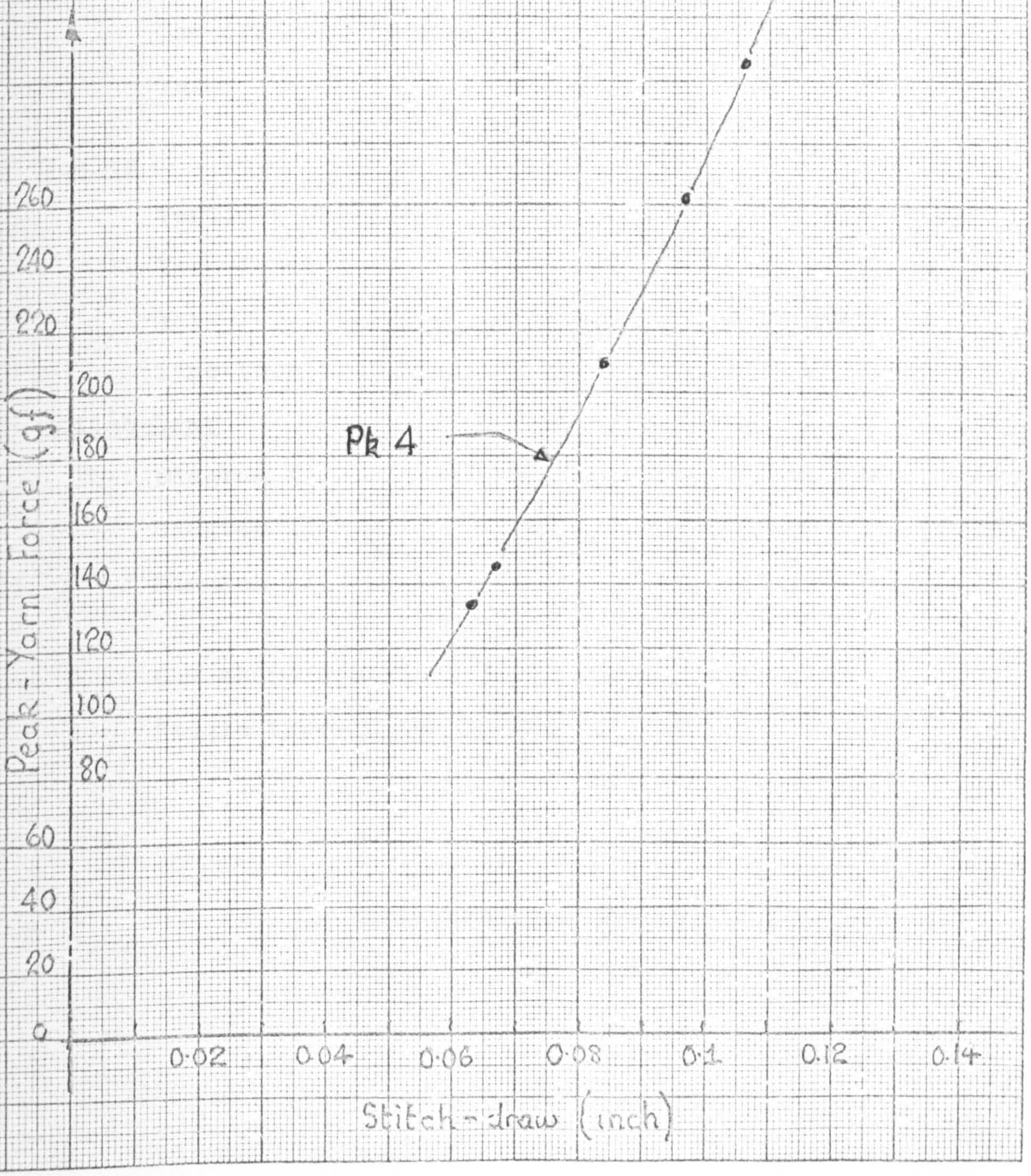

EFFECT of STITCH-DRAW UPON YARN-FORCE FIG 8.6

The Effect of the Depth of Stitch-Draw upon the Cam and Yarn-Force

Parameters

Yarn-input tension measured directly before entry into needles

Fabric take-down tension (overall) = 2,461 gf

Machine Speed = 50.0 ft/min (15.2 m/mi

Temperature = 22°C

Cam-cylinder spacing = 0.006 in. (0.15 mm) -

Yarn = 1/150/30 Bulked Polyester

Scales

Vertical Cam-force = 140 gf/ 10 mm

Yarn-force = 95 gf/10 mm

Yarn-input tension = 10 gf/10 mm

Time (horizontal scale) = 10 mS/8.5mm

Stitch-Draw

Diagram I = 0.063 in. (1.60 mm)

Diagram II = 0.067 in. (1.70 mm)

Diagram III = 0.108 in. (2.73 mm)

Cam shape see Fig 4.3

Needle type- 0.443 mm see Fig 3.2

Parameters for traces shown in Fig 8.7(b)

Fig 8.7(a)

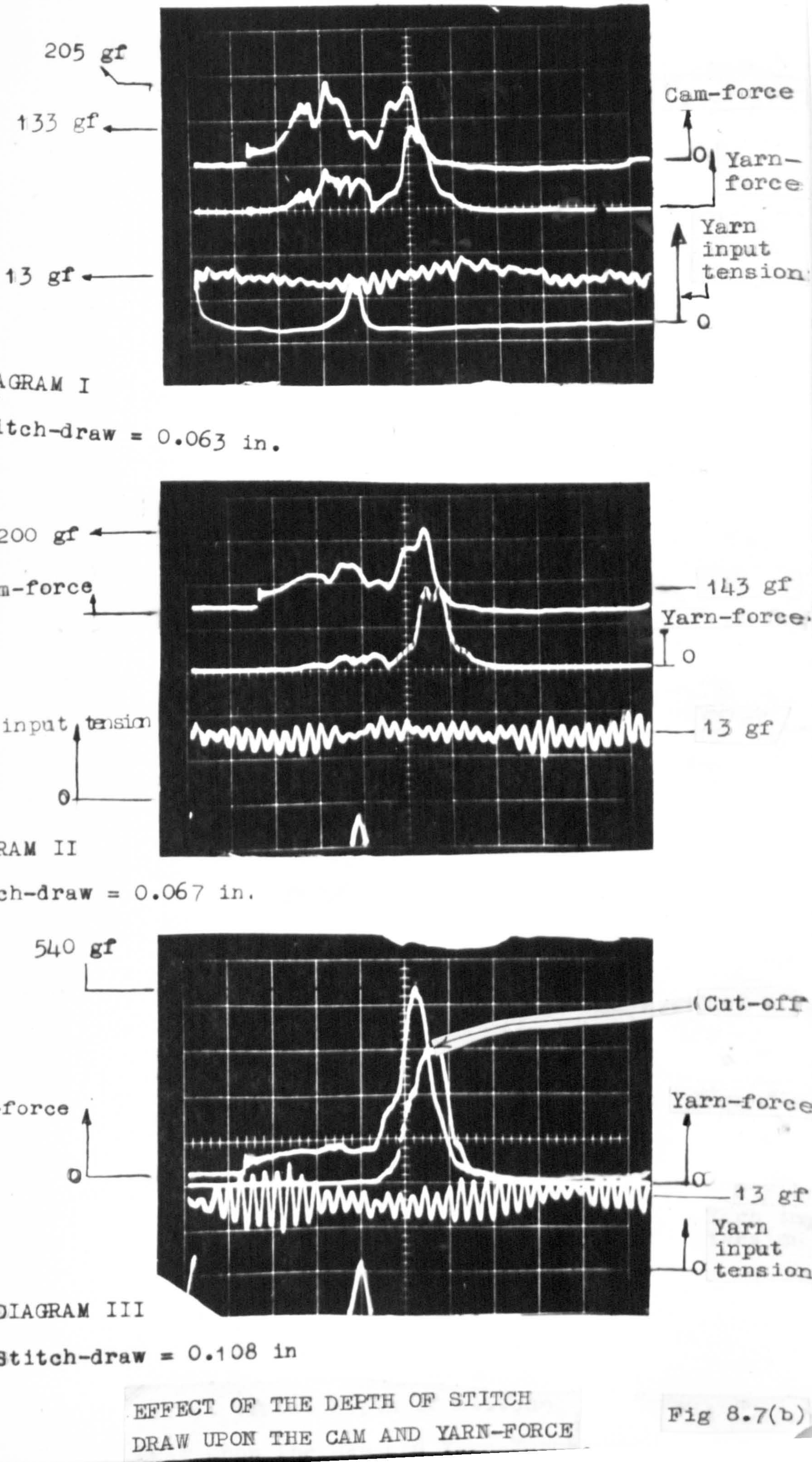

EFFECT OF THE DEPTH OF STITCH DRAW UPON THE CAM AND YARN-FORCE

Fig 8.7(b)

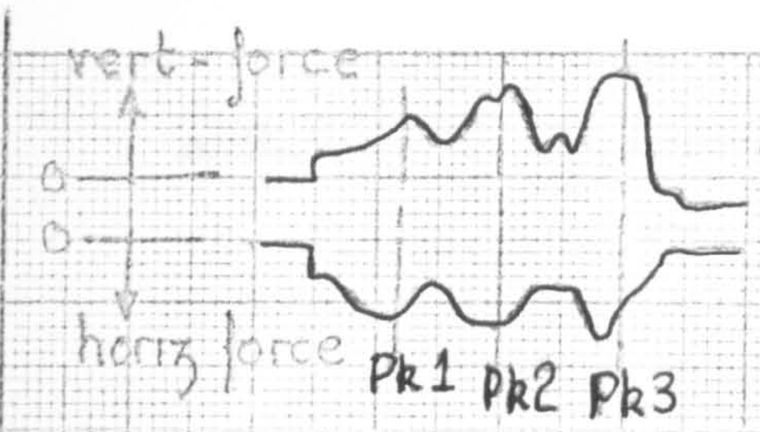

A typical cam-force trace.

Pk 1, 2 and 3 vertical cam-force and Pk 4 are defined in Fig 8.1. The relationship between horizontal and vertical peaks is shown above.

Pk 1 & 2 were substantially constant with input yarn tension hence only Pk 3 horiz and vert cam-force and Pk 4 are plotted.

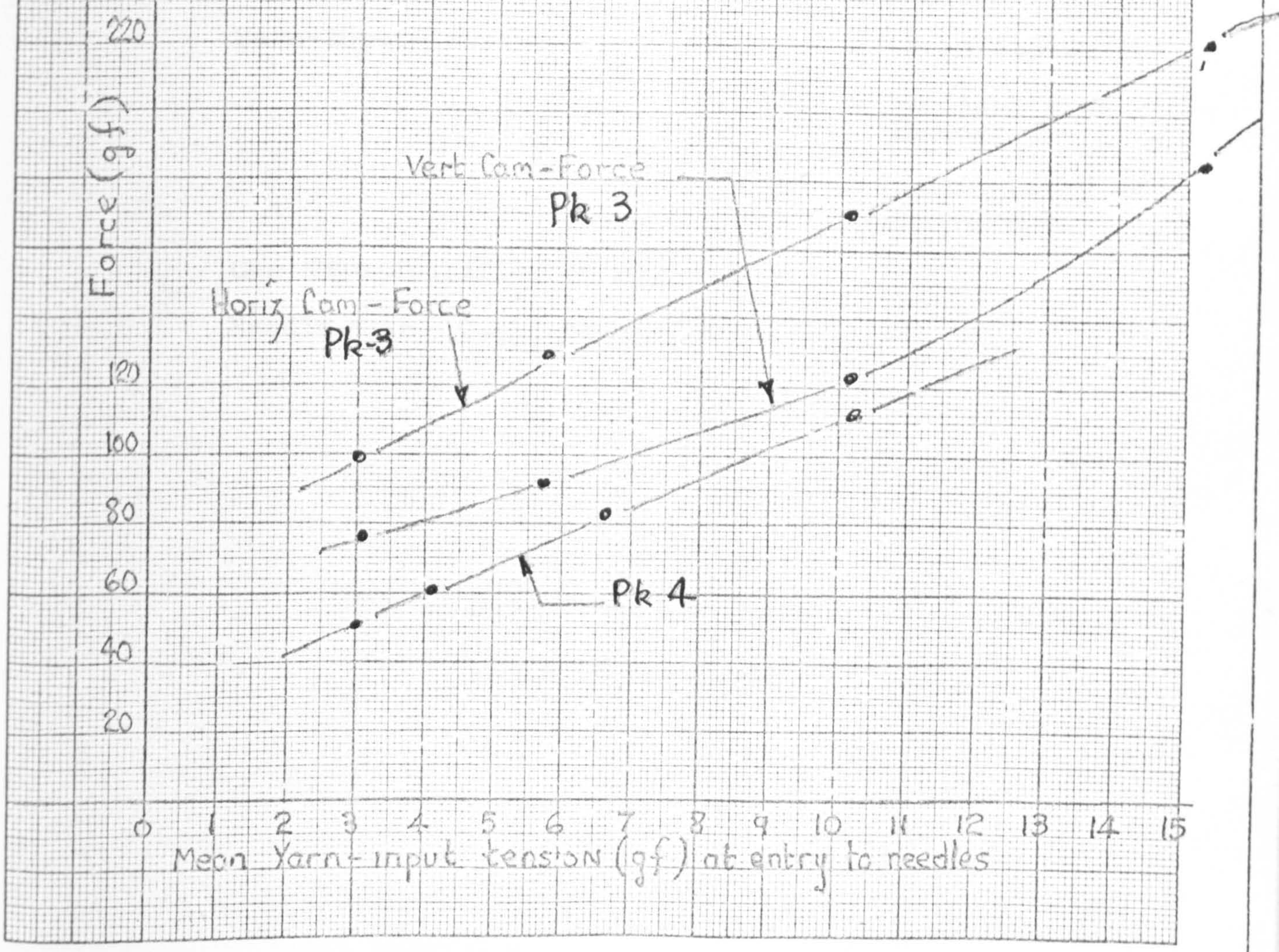

EFFECT OF INPUT YARN TENSION UPON CAM AND YARN FORCE

FIG 8.8

The Effect of Input Yarn Tension upon the Cam-Forces

Parameters

Fabric take-down-tension (overall) = 2,461 gf

Stitch-draw = 1.70 mm (0.067 in.)

Machine speed = 15.2 m/min (50 ft/min)

Temperature = 21 °C

Cam-cylinder clearance = 0.15 mm (0.006 in.)

Yarn = 1/150/30 Bulked polyester

Scales

Vertical Cam-force = 140 gf/10 mm (V)

Horizontal Cam-force = 140 gf/10 mm (V)

Yarn-input-tension = 10 mS/8.5 mm (H)

(V) = Vertically on photograph

(H) = Horizontally on photograph

Cam shape specified on Fig 4.3

Needle type - 0.443 mm see Fig 3.2

Parameters for traces shown in Fig 8.9(b)

Fig 8.9(a)

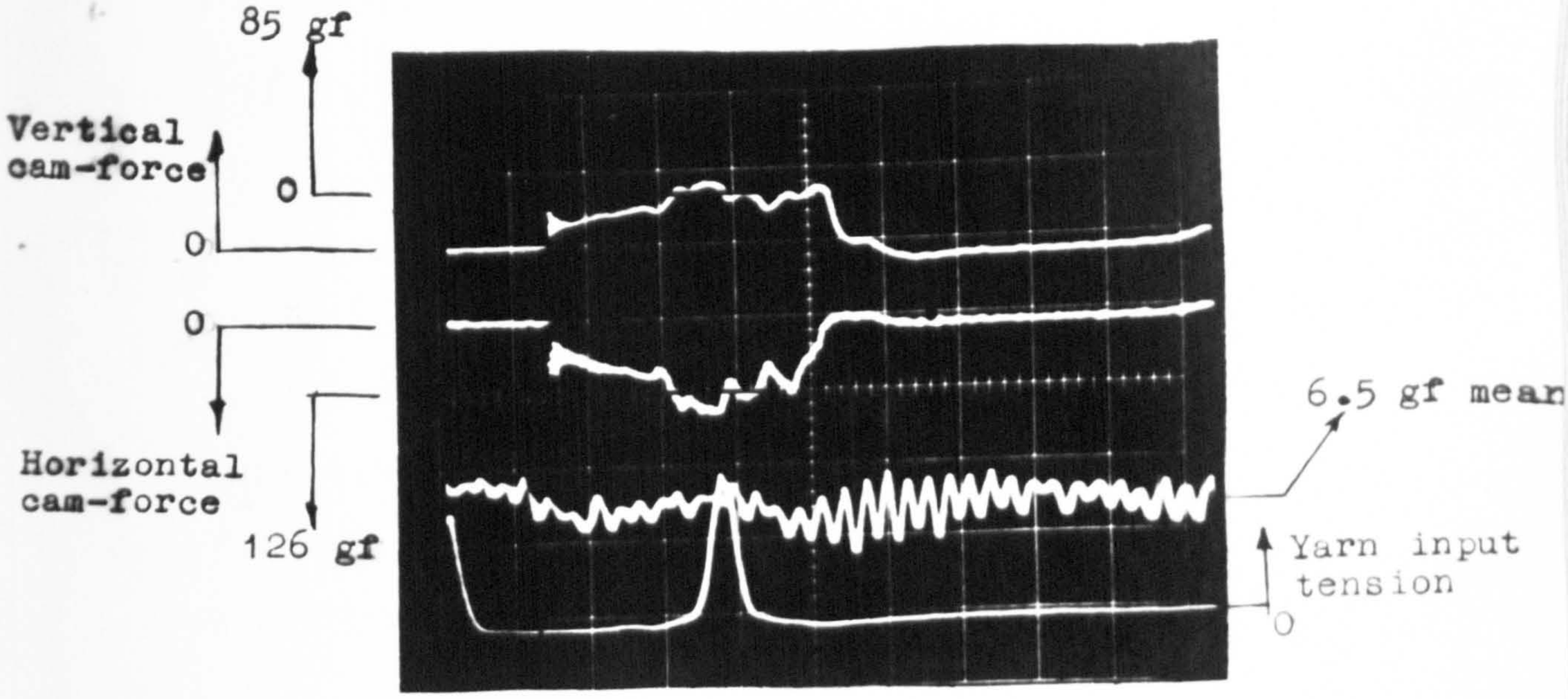

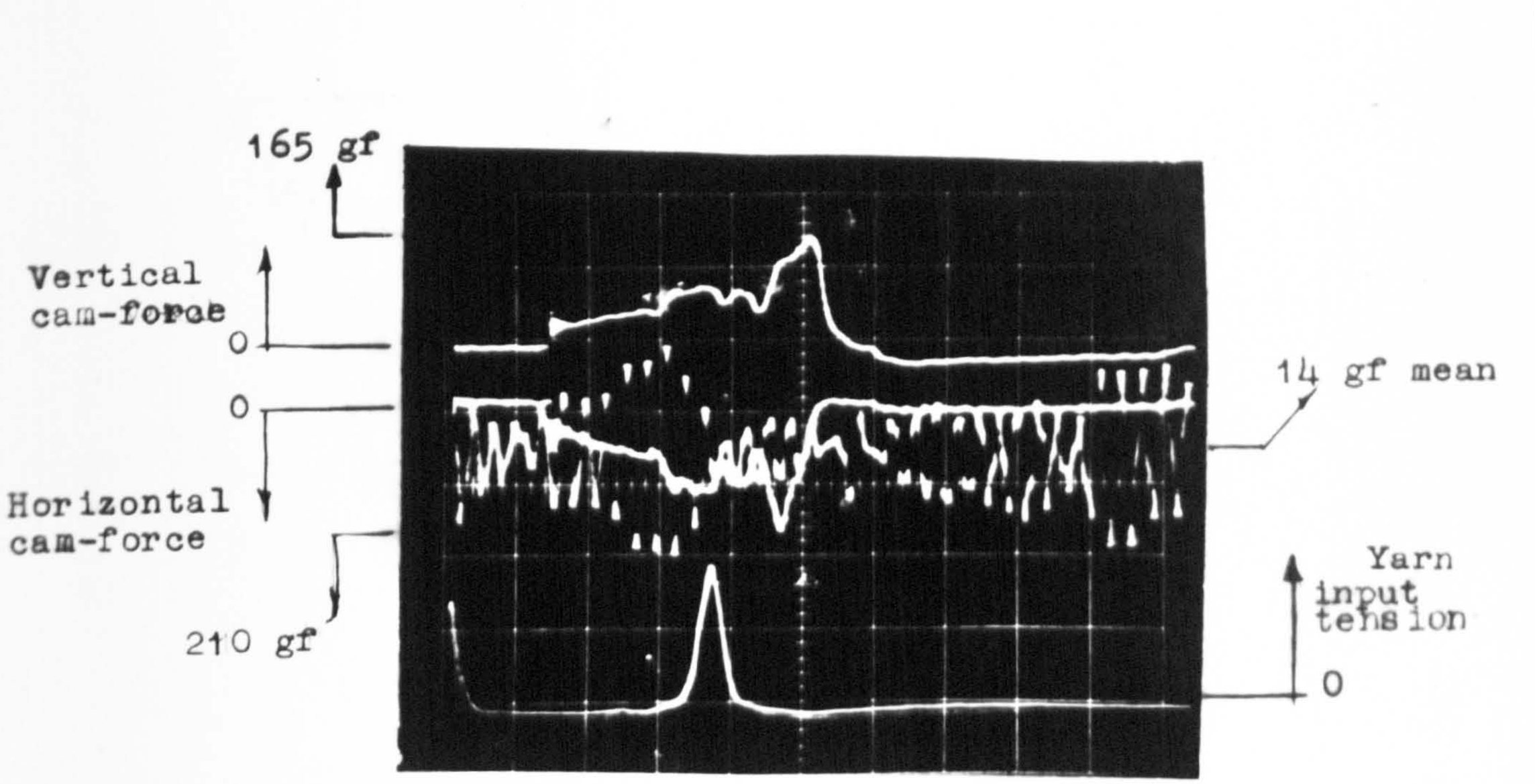

Effect of Yarn-input

Tension upon the Cam-forces

Fig 8.9(b)

The Effect of Input Yarn Tension upon the Yarn-Forces

Parameters

Fabric take-down-tension (overall) = 1,477 gf

Stitch-draw = 1.70 mm (0.067 in.)

Machine Speed = 8.24 m/min (27 ft/min)

Temperature = 26°C

New Yarn Bobbin

Yarn Type = 1/150/30 Bulked polyester

Scales

Yarn-force = 19.2 gf/10 mm (V)

Yarn-input-tension = 2 gf /10 mm (V)

Time (horizontal scale) = 5 mS/8.5 mm (H)

(V) = Vertically on photograph

(H) = Horizontally on photograph

Diagram I - 2 traces superimposed

Diagram II - 2 traces superimposed

Diagram III - 1 trace superimposed

Cam shape see Fig 4.3

Needle Type - 0.443 mm see Fig 3.2

Parameters for traces shown in Fig 8.10(b)

Fig 8.10(a)

DIAGRAM I

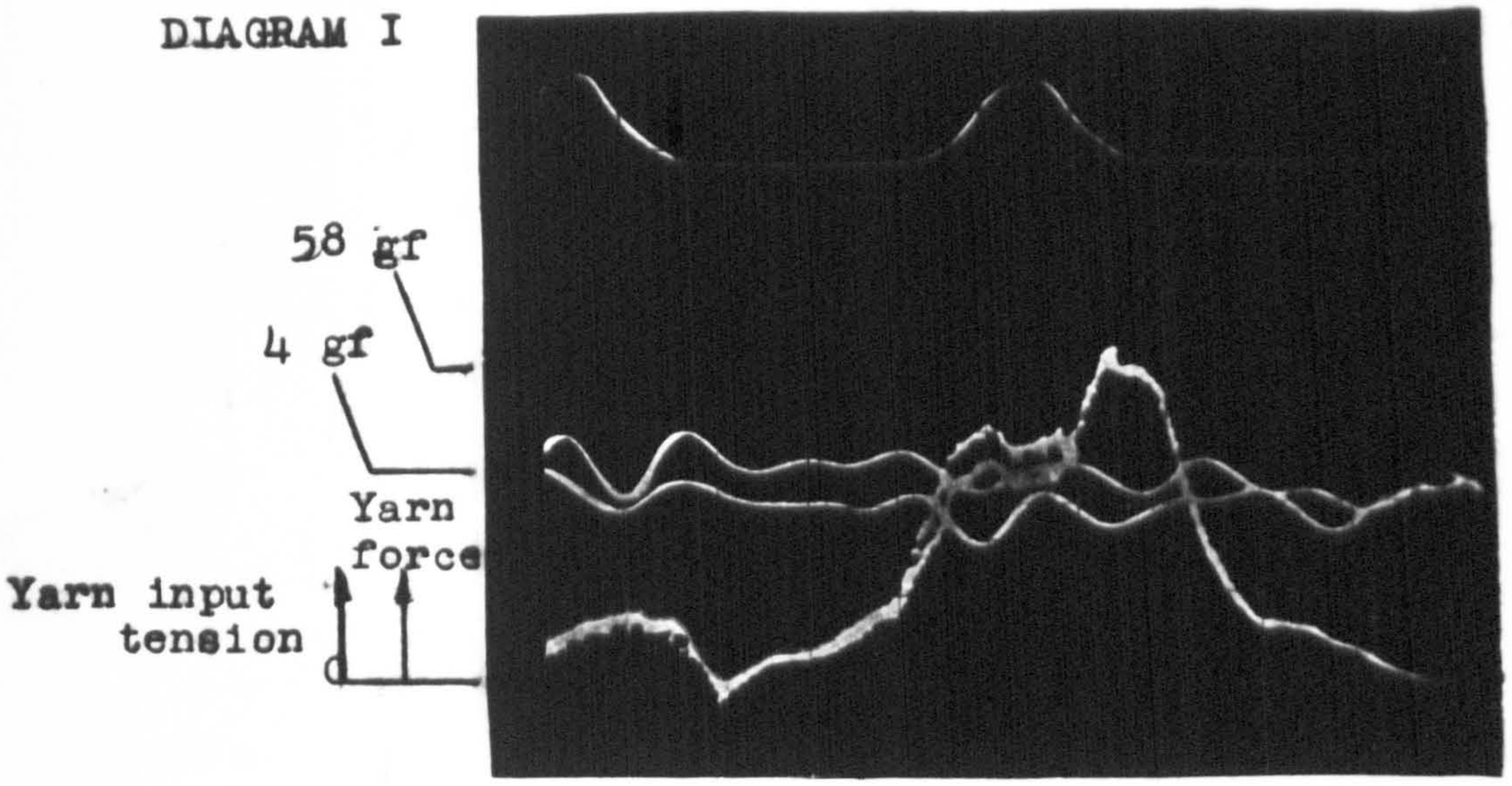

DIAGRAM II

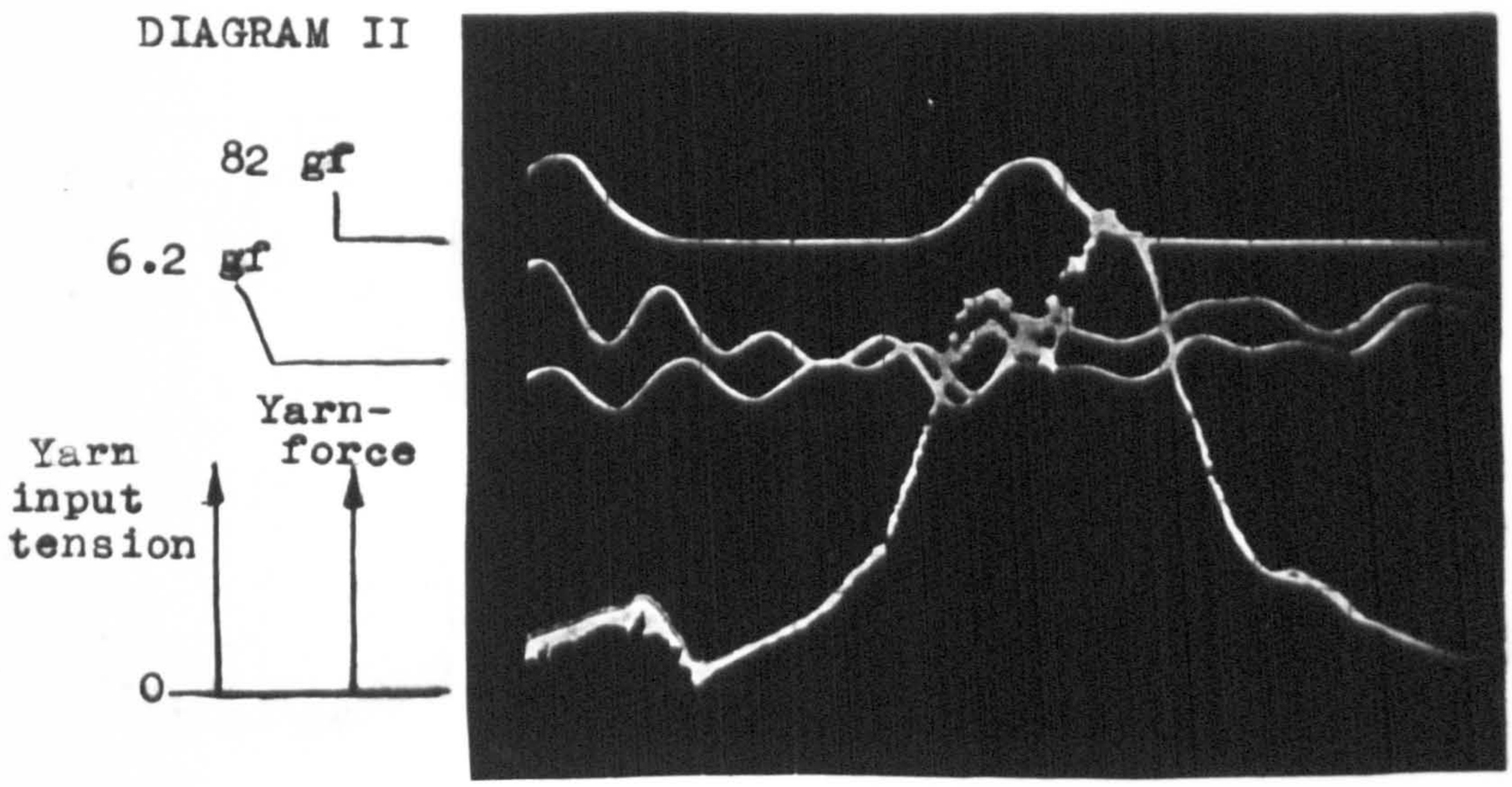

DIAGRAM III

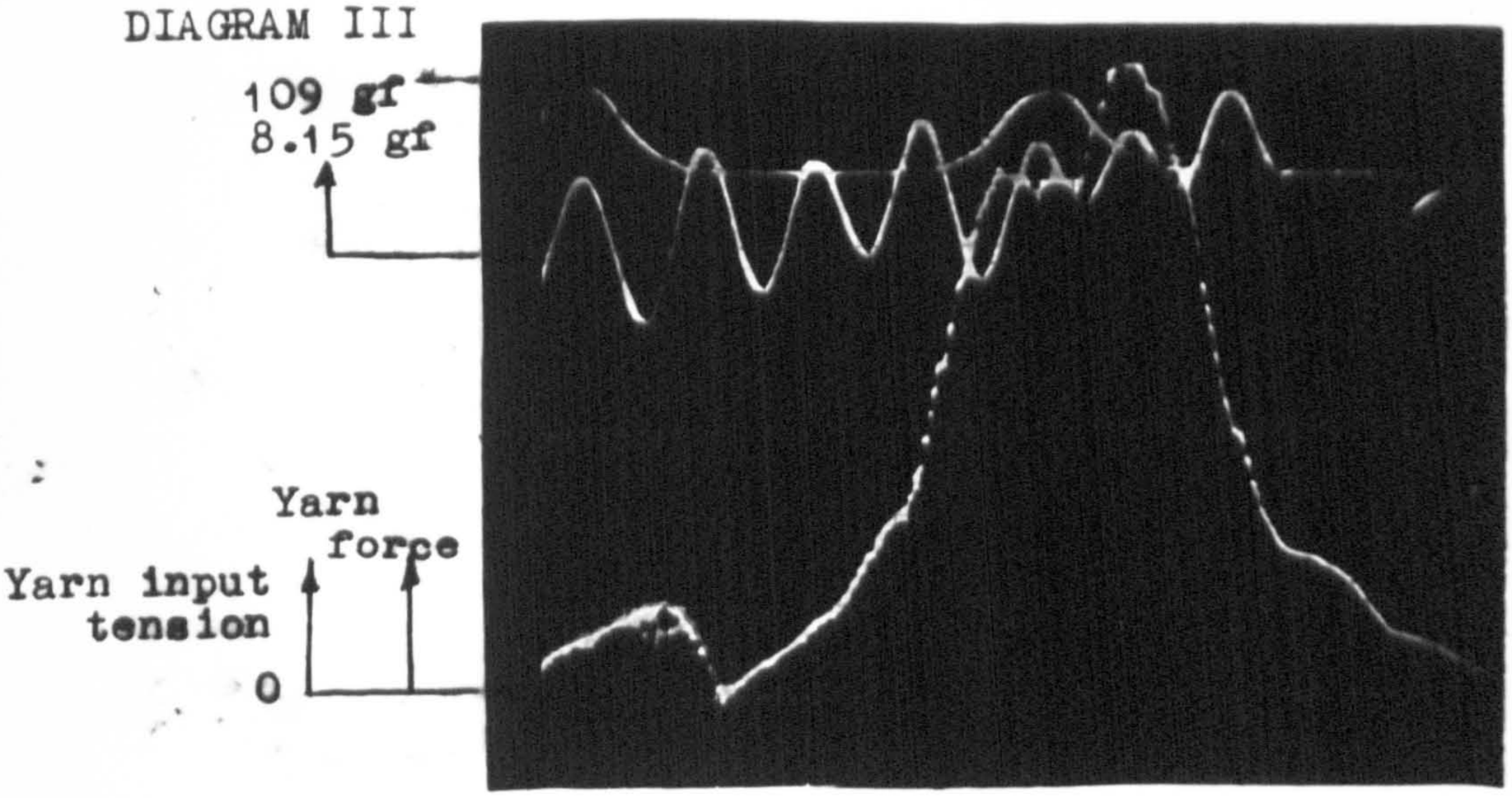

EFFECT OF INPUT YARN TENSION

UPON THE YARN-FORCE

Fig 8.10(b)

The Fabric load was equally distributed over 472 needles

The following peaks of horizontal cam-force are plotted.

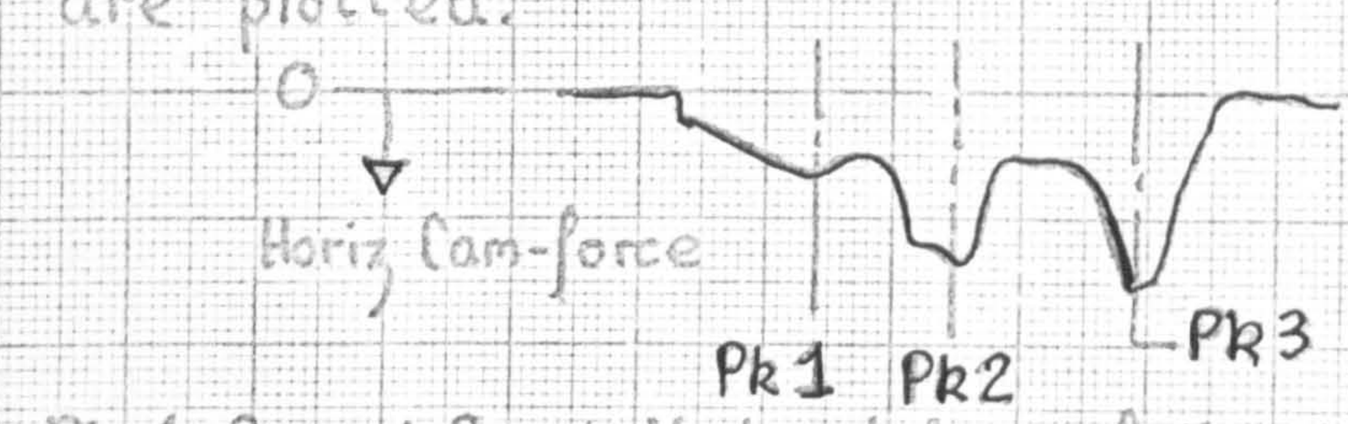

Pk 1, 2, and 3 of Vertical force followed similar trends to the horizontal peaks shown below.

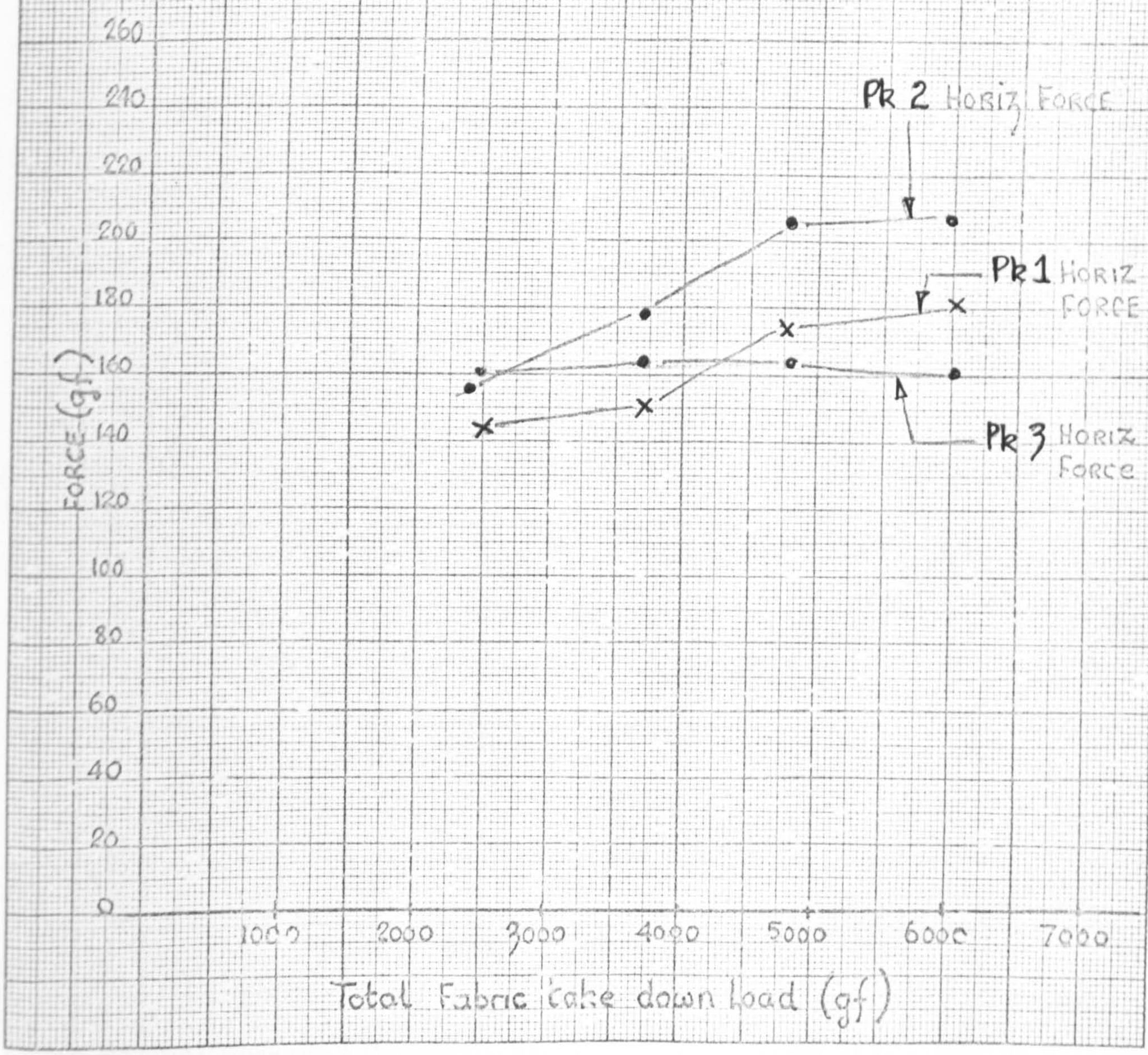

EFFECT OF FABRIC TAKE-DOWN TENSION UPON THE CAM AND YARN-TENSION FORCES

FIG 8.11

The following peaks of yarn-force are plotted

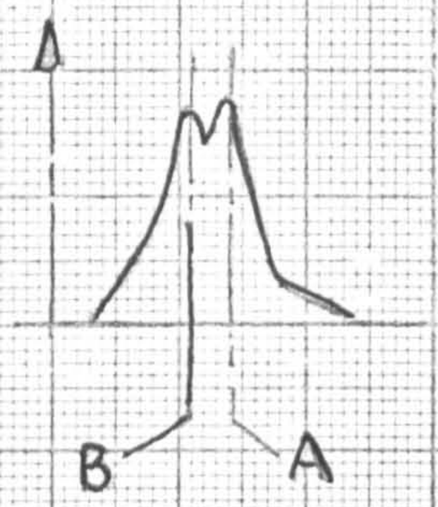

Typical yarn-force plot, On Fig 8.4 A, corresponds to Pk 4.

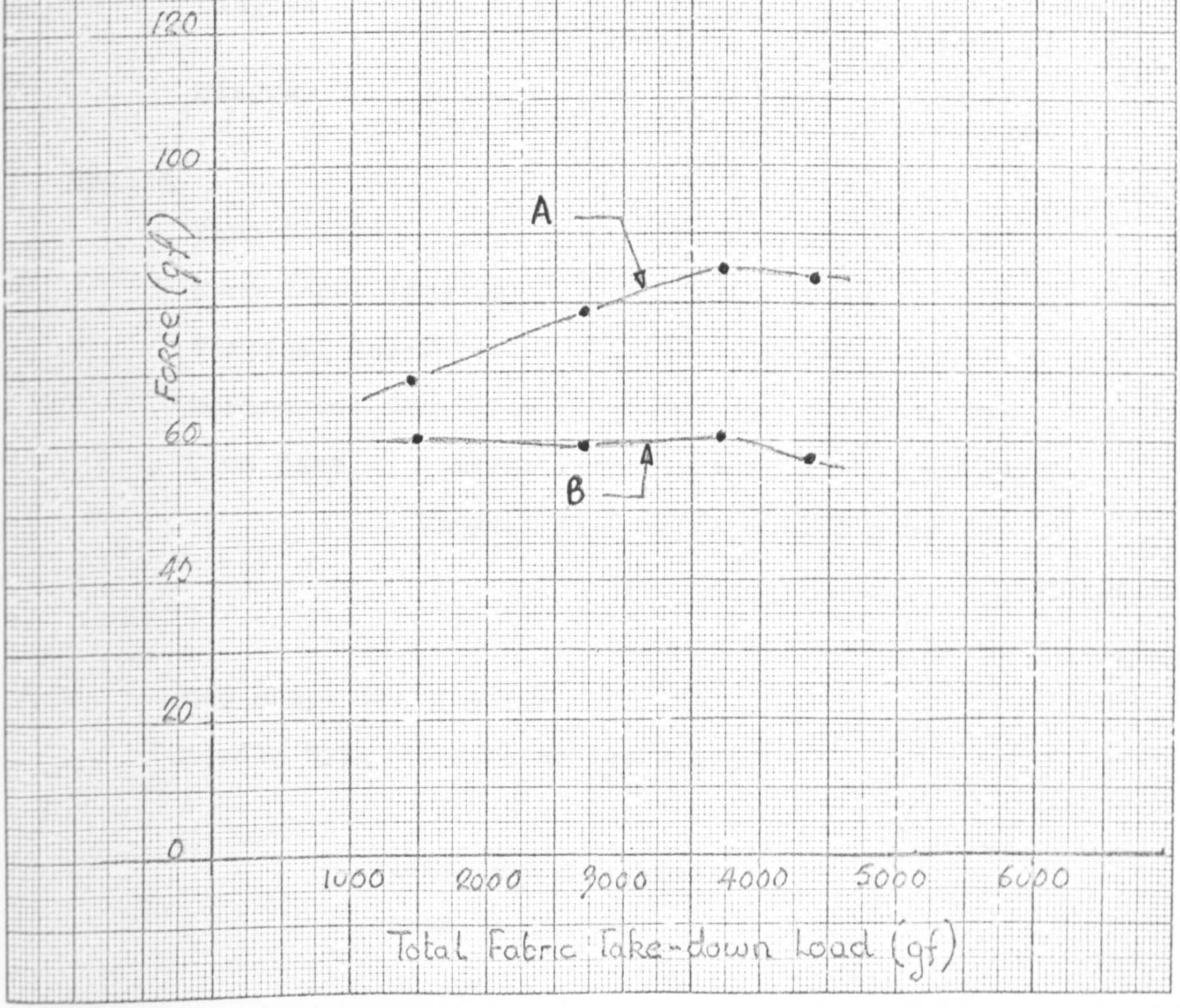

EFFECT OF FABRIC TAKE-DOWN TENSION UPON THE YARN-FORCES

FIG 8.12

Effect of the Fabric Take-Down Tension upon the Cam and Yarn-Forces

Parameters

Stitch-draw = 0.17 mm (0.068 in.)

Machine Speed
Diagram I = 15.2 m/min (50 ft/min)

Machine Speed
Diagram II and III = 6.1 m/min (20 ft/min)

Cam-cylinder spacing = 0.15 mm (0.006 in.)

Yarn = 1/150/30 Bulked Polyester

Diagram III 8 traces superimposed
Take-down tension= 4437 gf (overall)

Diagram II 8 traces uperimposed
Take-down tension= 1477 gf (overall)

Diagram I 1 trace
Take-down tension= 3693 gf (overall)

Scales

Yarn-force = 19 gf/10 mm (V)

Yarn-input tension = 5 gf/10 mm (V)

Vertical Cam-force =140 gf/10 mm (V)

Horizontal Cam-force =140 gf/10 mm (V)

Time base Diagram I = 10 mS/8.5 mm (H)

Diagram II = 5 mS/8.5 mm (H)

(V) = Vertically on photograph

(H) = Horizontally on photograph

Cam shape see Fig 4.3

Needle type – 0.443 mm see Fig 3.2

Parameters for traces
shown in 8.13(b)

Fig 8.13(a)

DIAGRAM I

Take-down tension 3693 gf

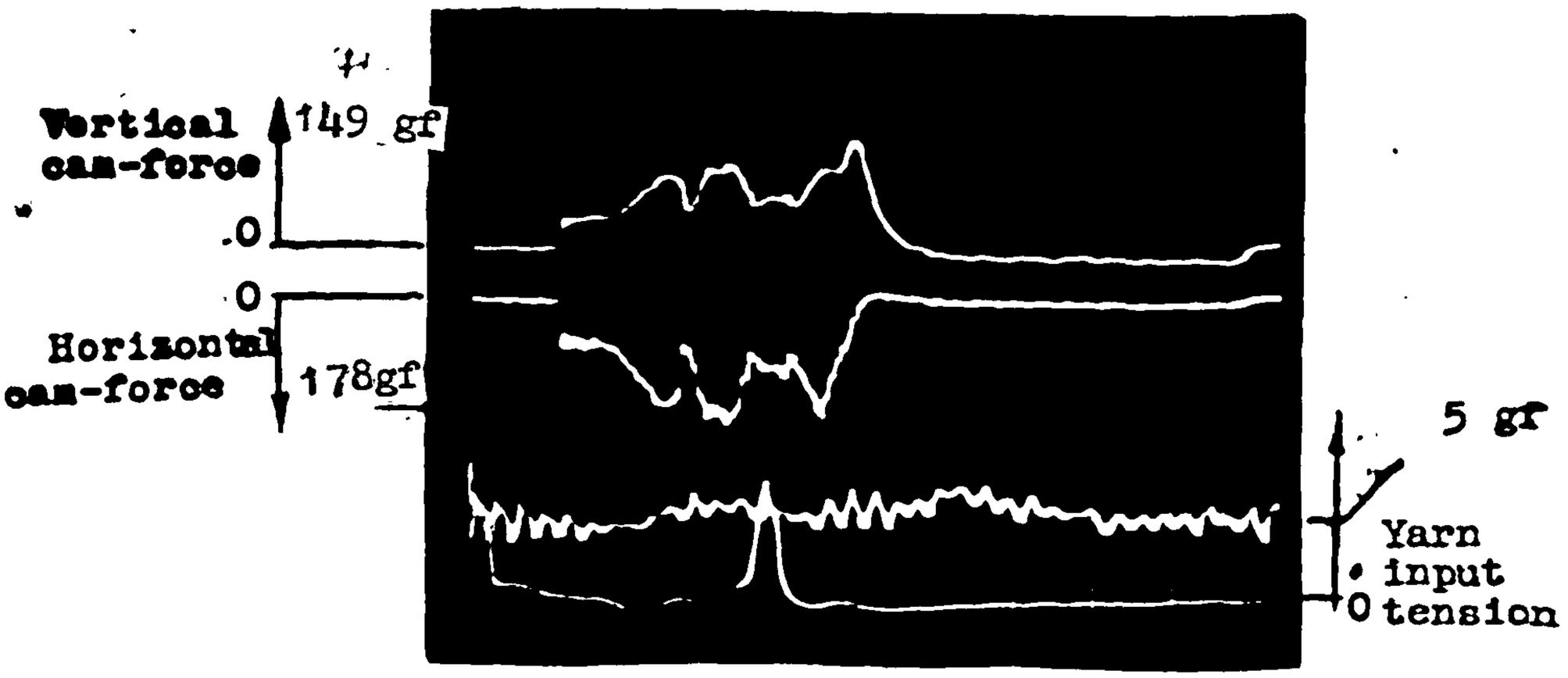

DIAGRAM II

Take-down tension 1477 gf

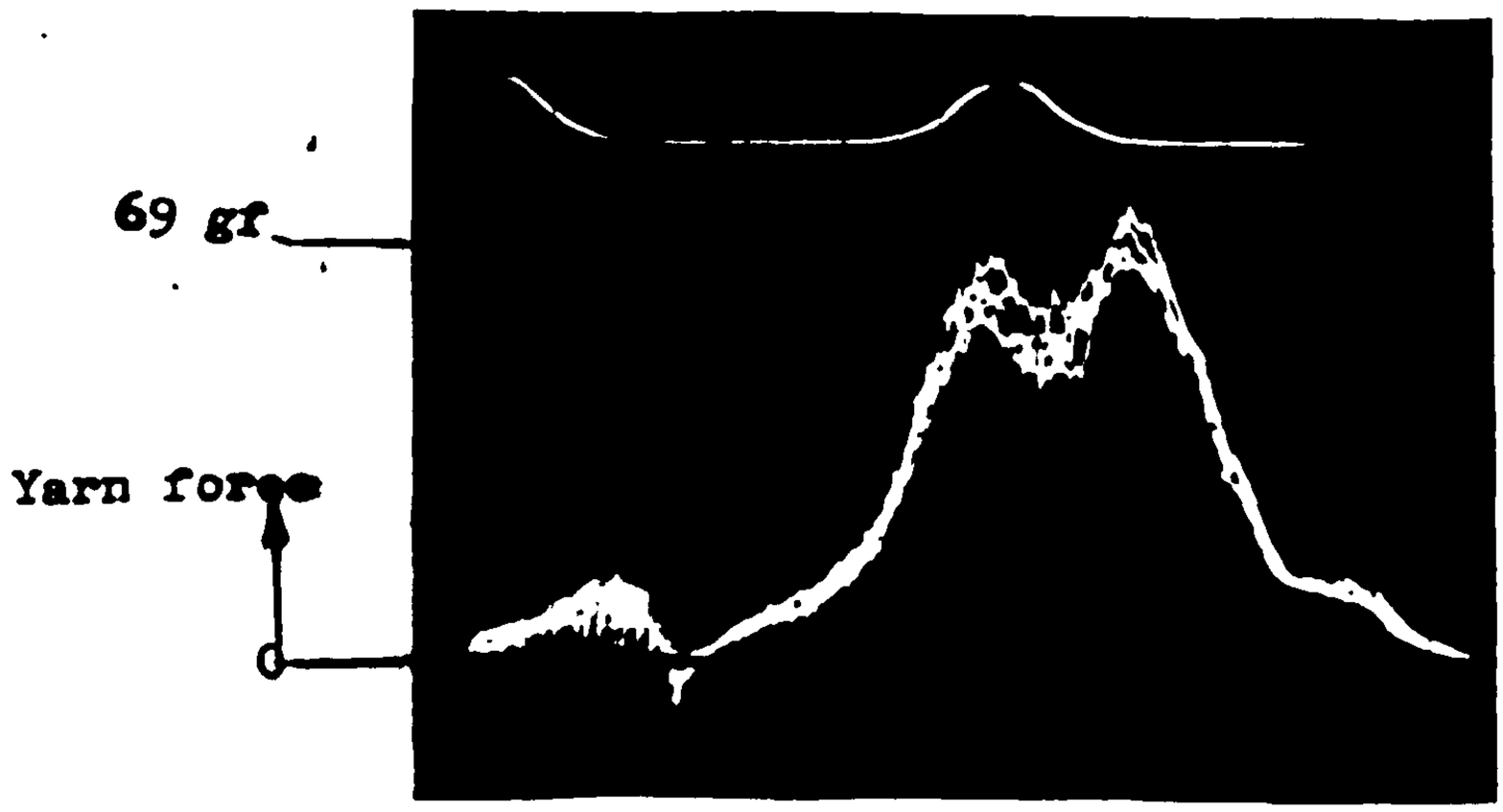

DIAGRAM III

Take-down tension 4437 gf

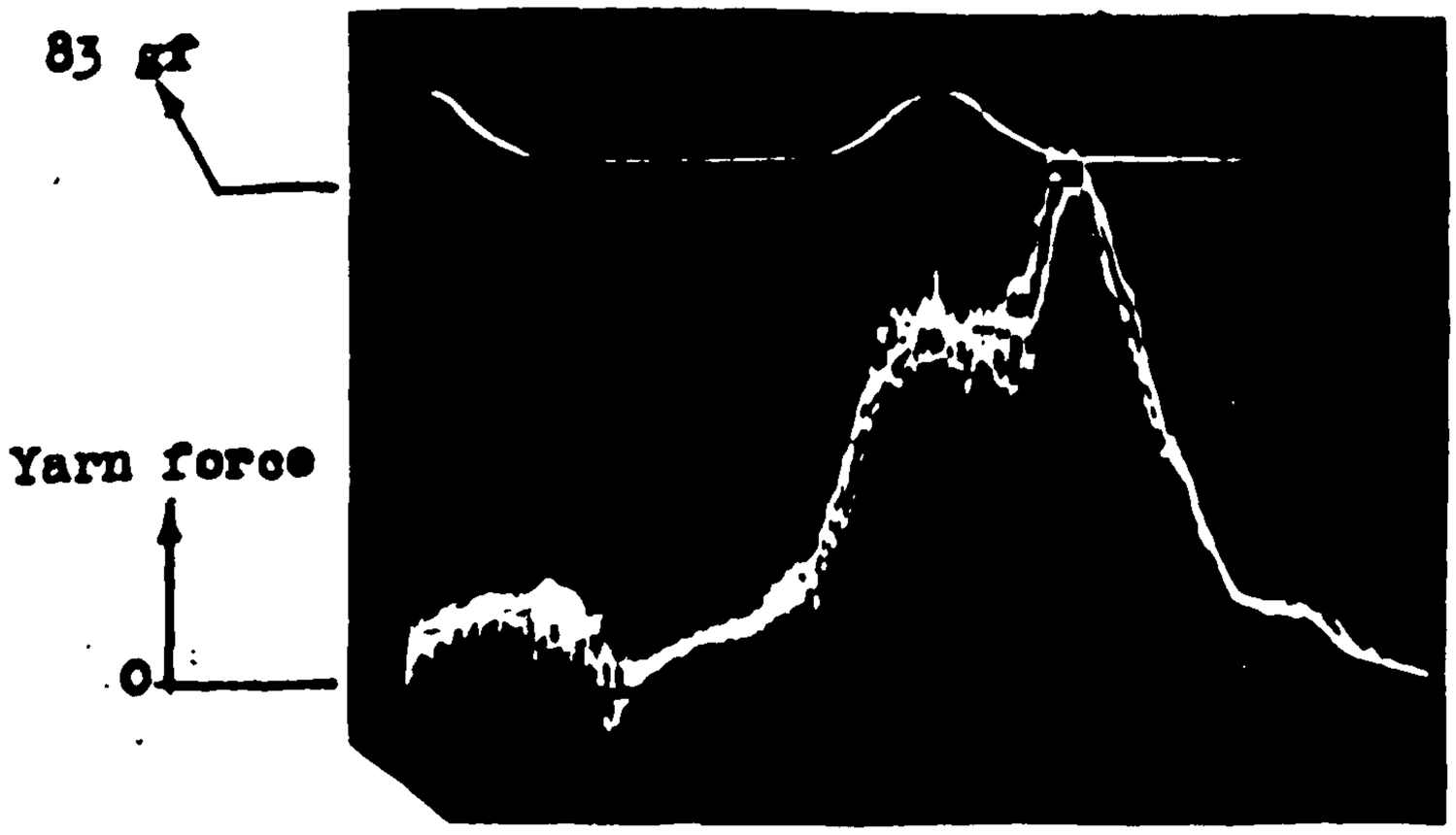

Effect of the Fabric Take-down Tension upon the Cam and Yarn Forces

Fig 8.13(b)

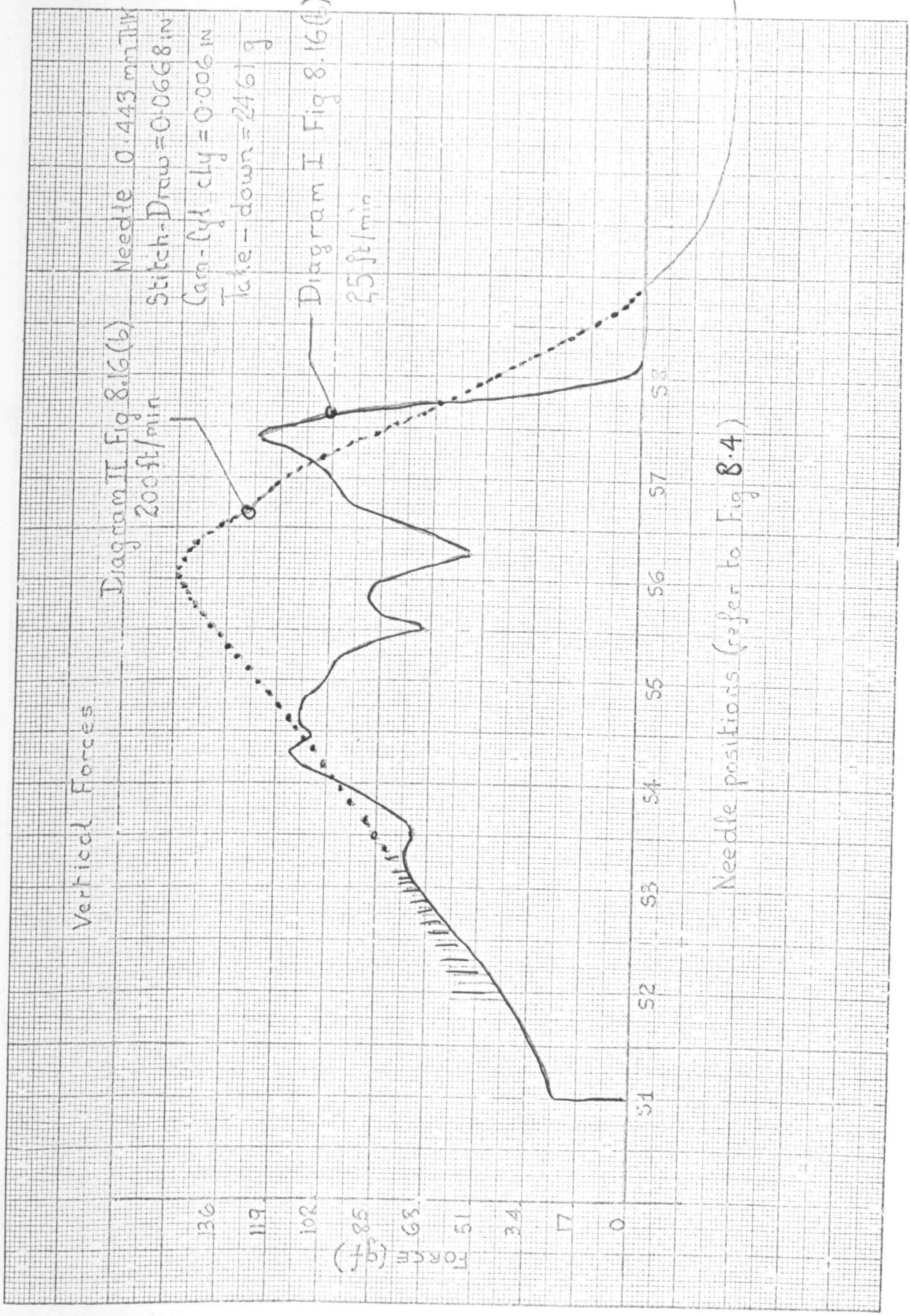

EFFECT OF MACHINE SPEED UPON THE VERTICAL CAM-FORCES

FIG 8.14

Vertical forces

(1) 0·016 IN (0·406mm) Needle, non-knitting, measured soon after heavy application of oil, Spotless B.N.O

(2) 0·0175 (0·443mm) Needle same conditions as (1)

(3) 0.0175 (0·443mm) Needle, knitting, some time after normal application of oil

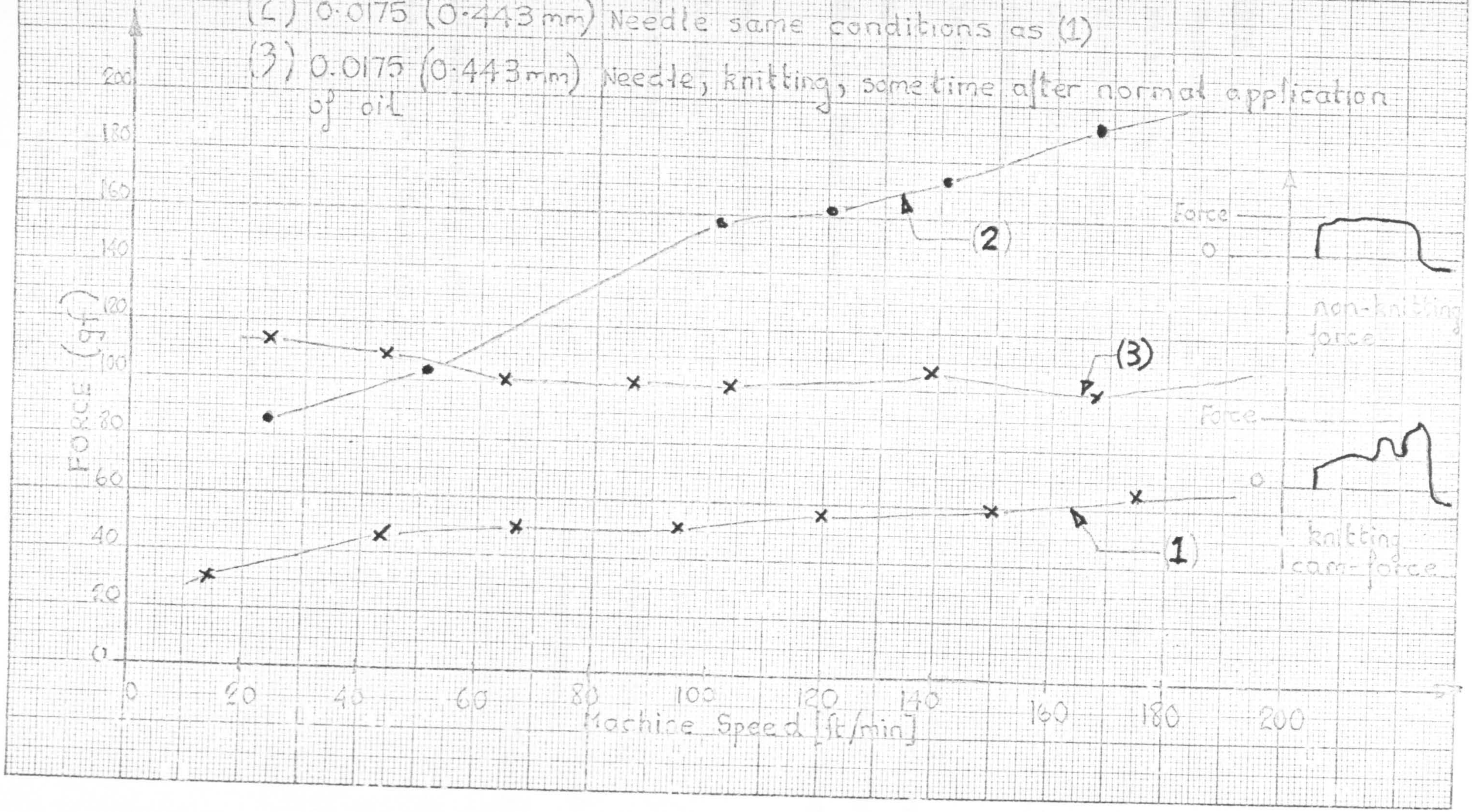

FIG 8.15

Effect of Machine Speed upon Cam-force

Parameters

Fabric take-down tension (overall) = 2,461 gf

Stitch-Draw = 0.17 mm (0.067 in.)

Yarn-Input Tension = 7 gf

Cam-Cylinder Clearance = 0.15 mm (0.006 in.)

Temperature = 21°C

Yarn = 1//150/30 Bulked Polyester

Machine Speed (Diagram I) = 7.5 m/min (24.7 ft/mir

Machine Speed (Diagram II) = 61 m/min (200 ft/min)

Scales

Vertical Cam-force = 140 gf/10 mm (V)

Horizontal Cam-force = 140 gf/10 mm (V)

Time-base = 10 mS/8.5 mm (H)

(V) = Vertical deflection on photograph

(H) = Horizontal deflection on photograph

Cam shape see Fig 4.3

Needle type - 0.443 mm see Fig 3.2

Parameters for the traces shown in Fig 8.16(b)

Fig 8.16(a)

DIAGRAM I

Machine Speed = 24.7 ft/min.

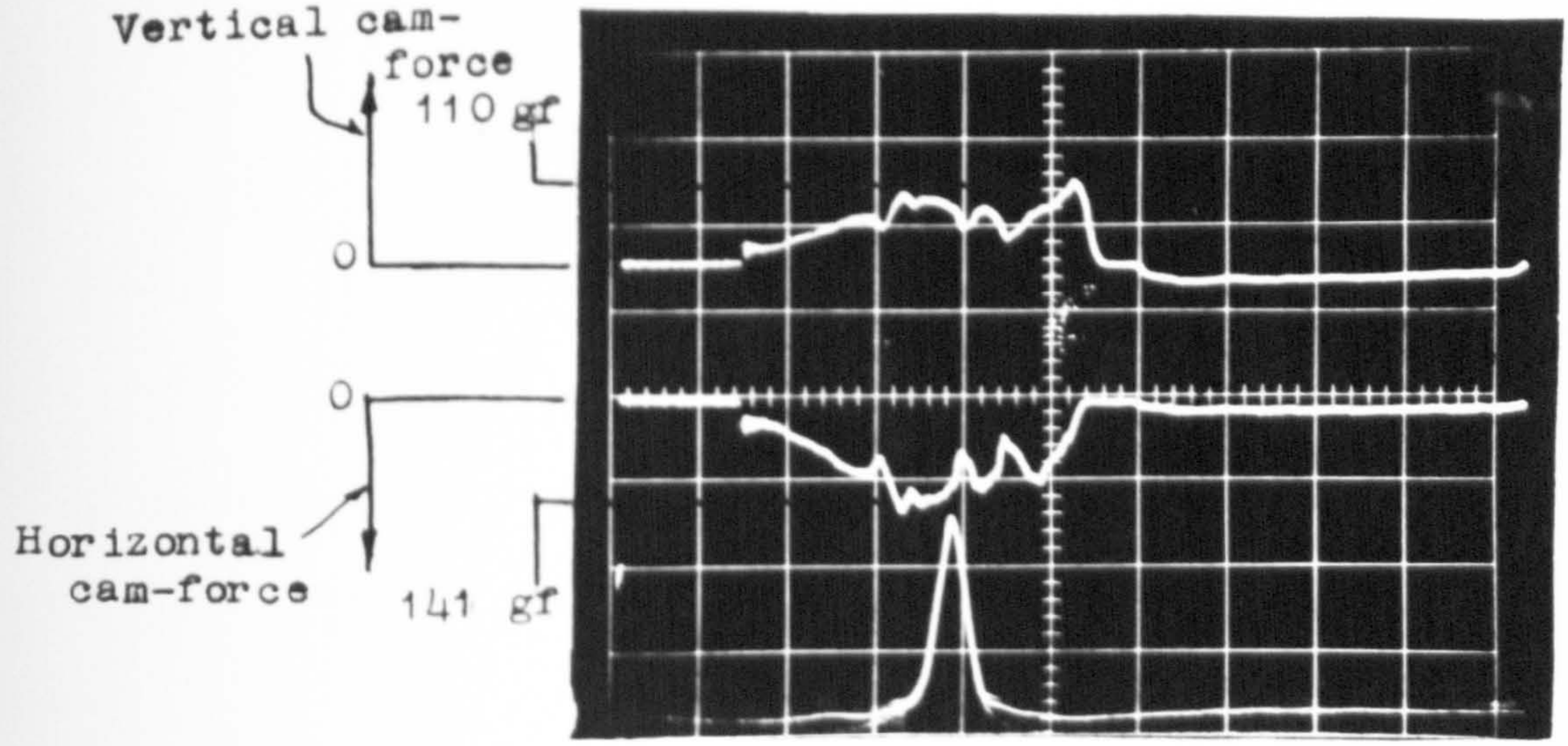

DIAGRAM II

Machine Speed = 200.0 ft/min.

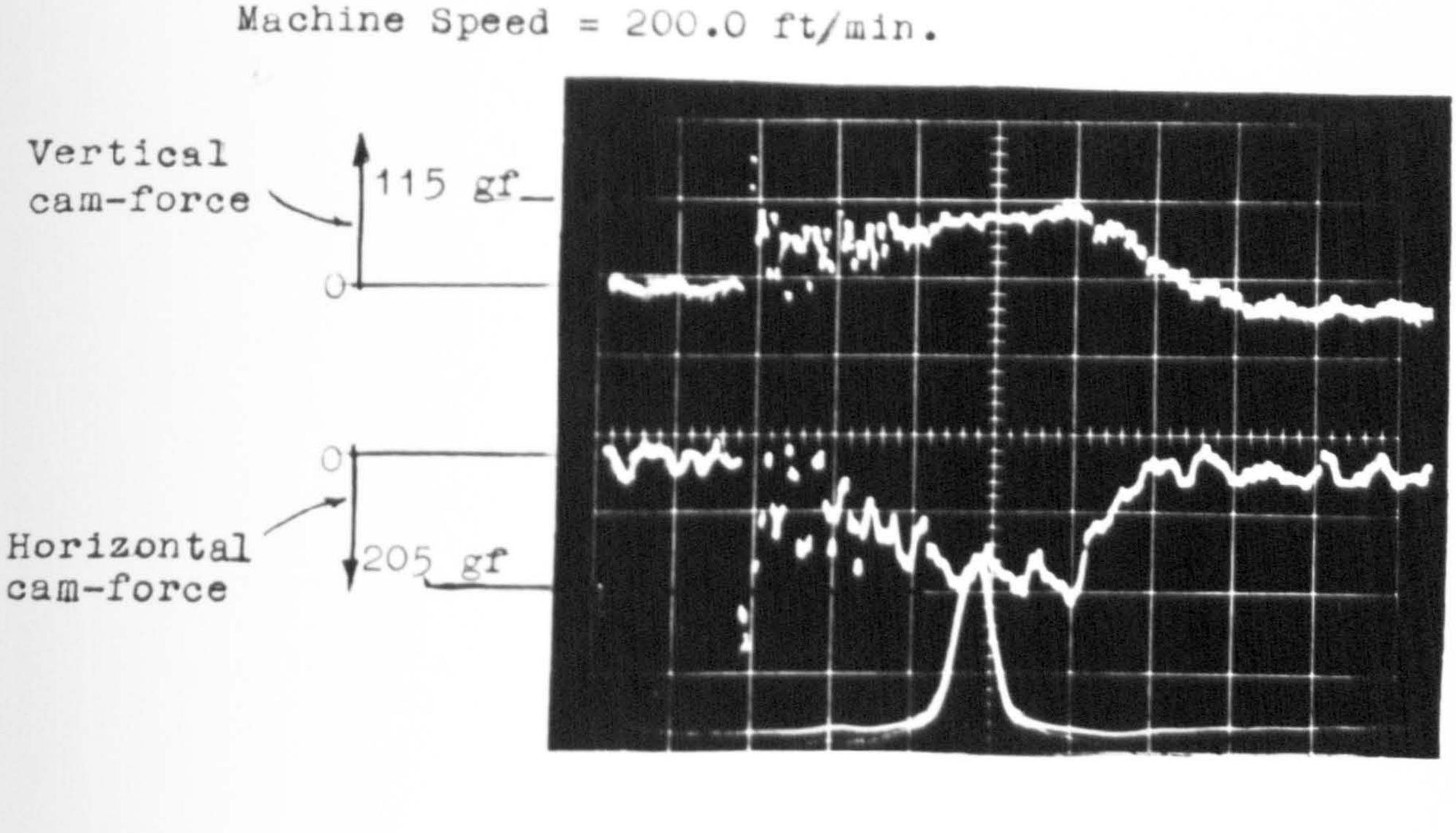

Effect of Machine Speed

Upon Cam-Force. Fig 8.16(b)

Effect of Machine Speed upon Yarn-Force

Parameters

Fabric take-down tension = 1,477 gf

Input Yarn Tension = Approx 8 gf (constant for all traces)

Stitch-Draw = 1.8 mm (0.067 in.)

Temperature = 25°C

Scales

Yarn-force = 19.2 gf//10 mm (V)

Diagram I — Speed = 6.1 m/min(20 ft/min)

10 traces superimposed

Time = 10 mS/8.5 mm (H)

Diagram II — 10 traces at 6.1 m/min (20 ft/min) at 10 mS/8.5 mm (H)

Superimposed upon 30 m/min (95 ft/min) at 2 mS/div

Diagram III — 1 trace at 61 m/min (200 ft/min) at 1 mS/8.5 mm (H)

(V) = Vertical scale deflection

(H) = Horizontal scale deflection

Cam shape see Fig 4.3

Needle type - 0.443 mm see Fig 3.2

Parameters for the traces shown in Fig 8.17(b)

Fig 8.17(a)

DIAGRAM I

100 gf

Yarn-force

0

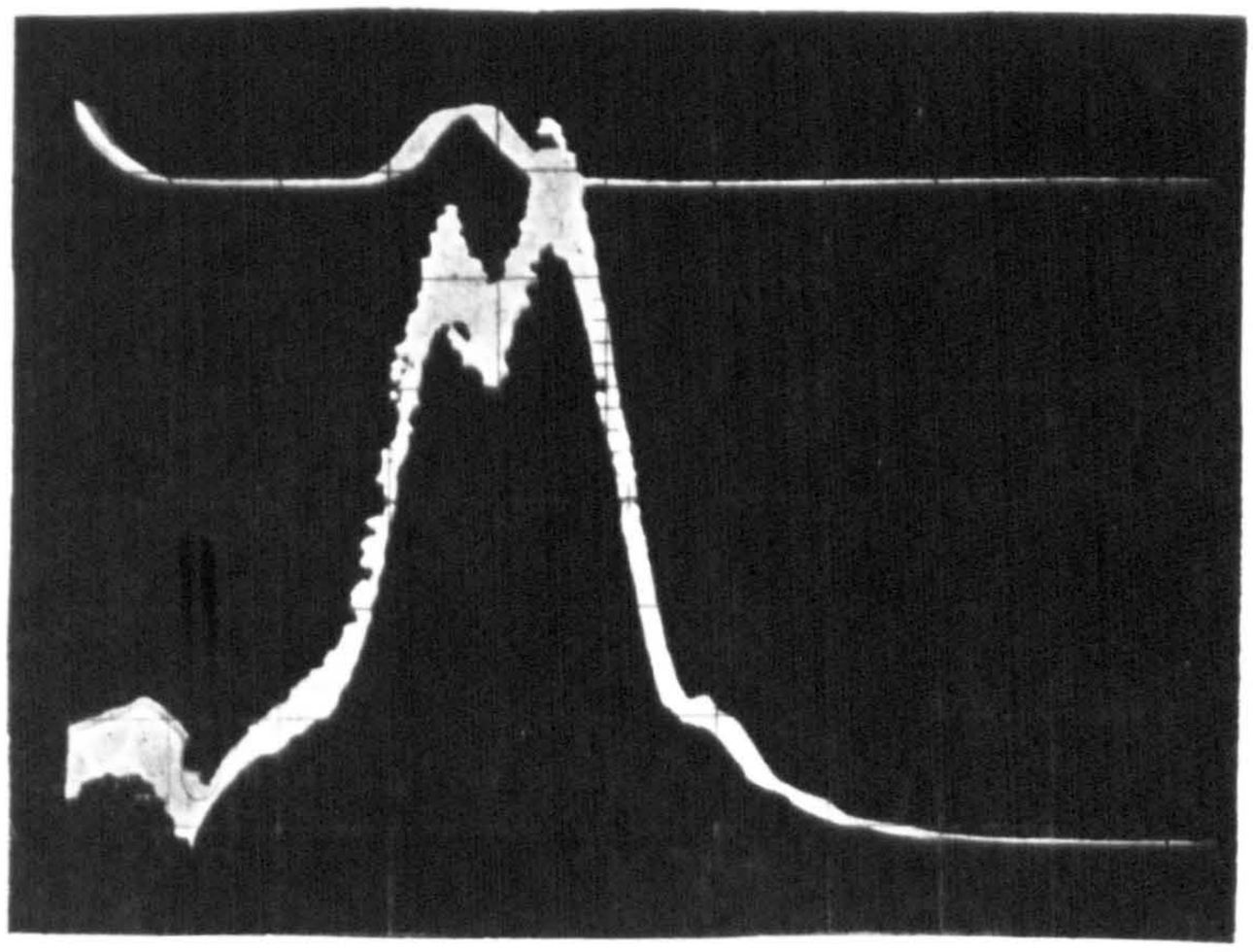

DIAGRAM II

100 gf

Yarn force

0

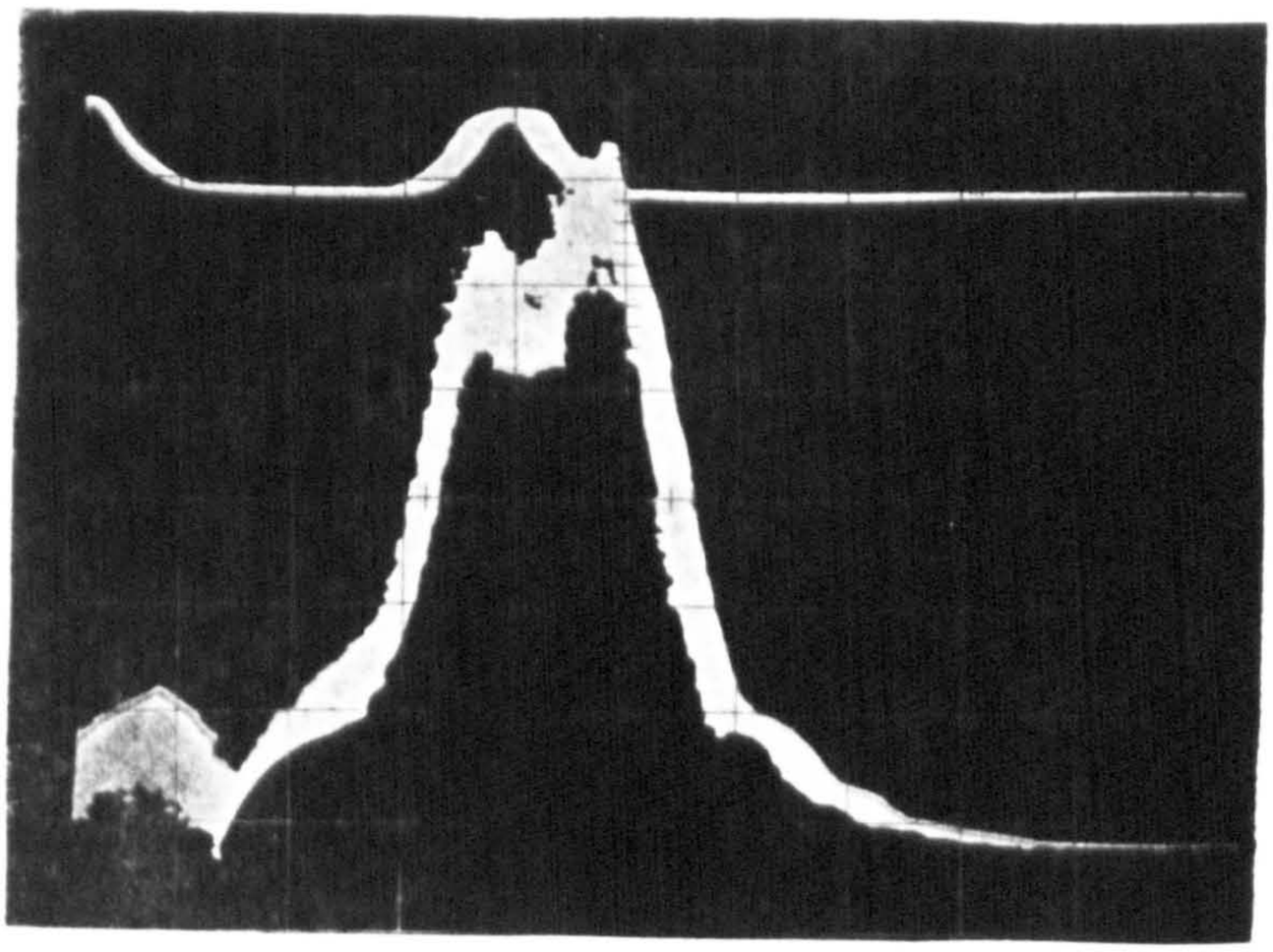

DIAGRAM III

100 gf

Yarn force

0

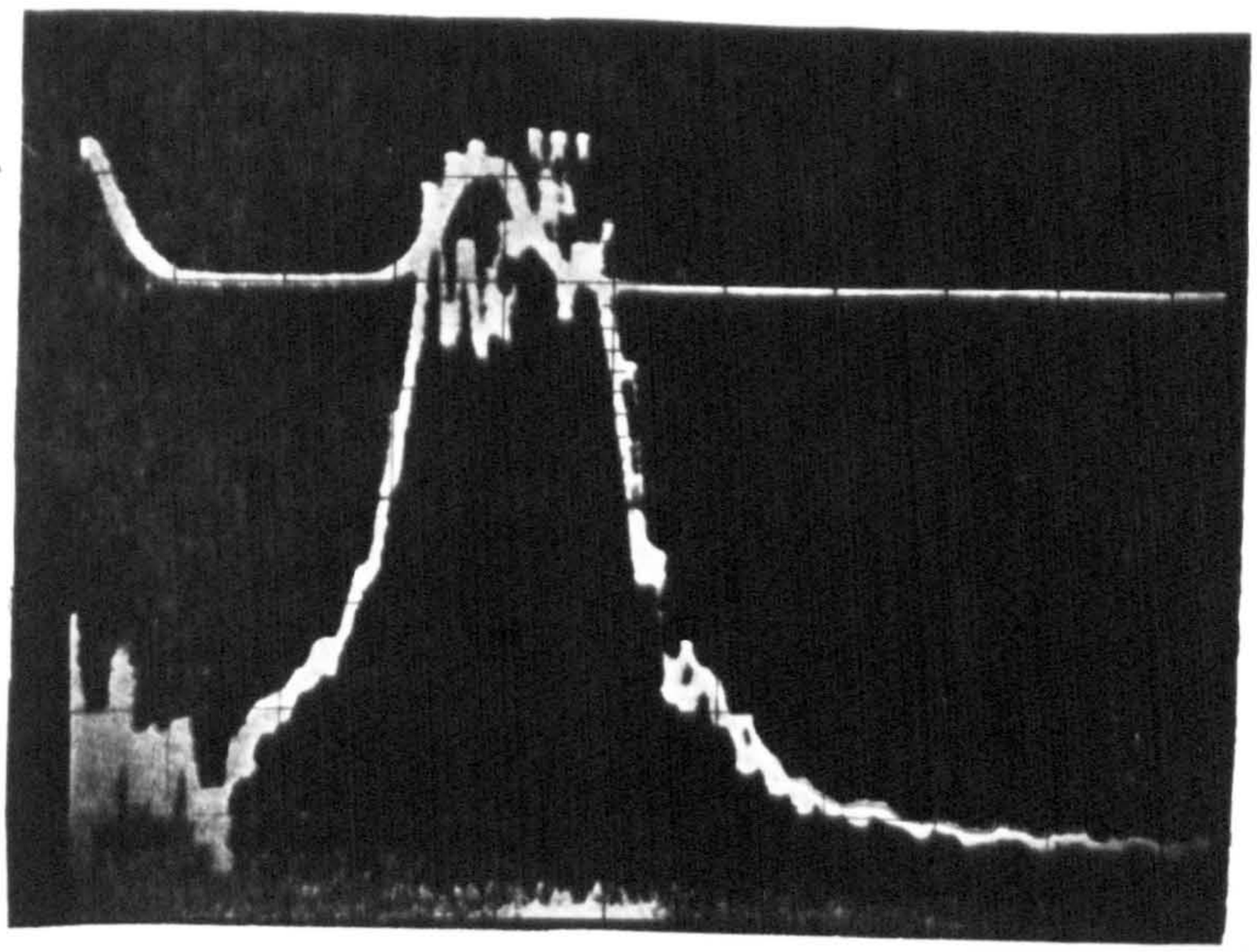

Effect of Machine Speed

Upon Yarn-force.

Fig 8.17(b)

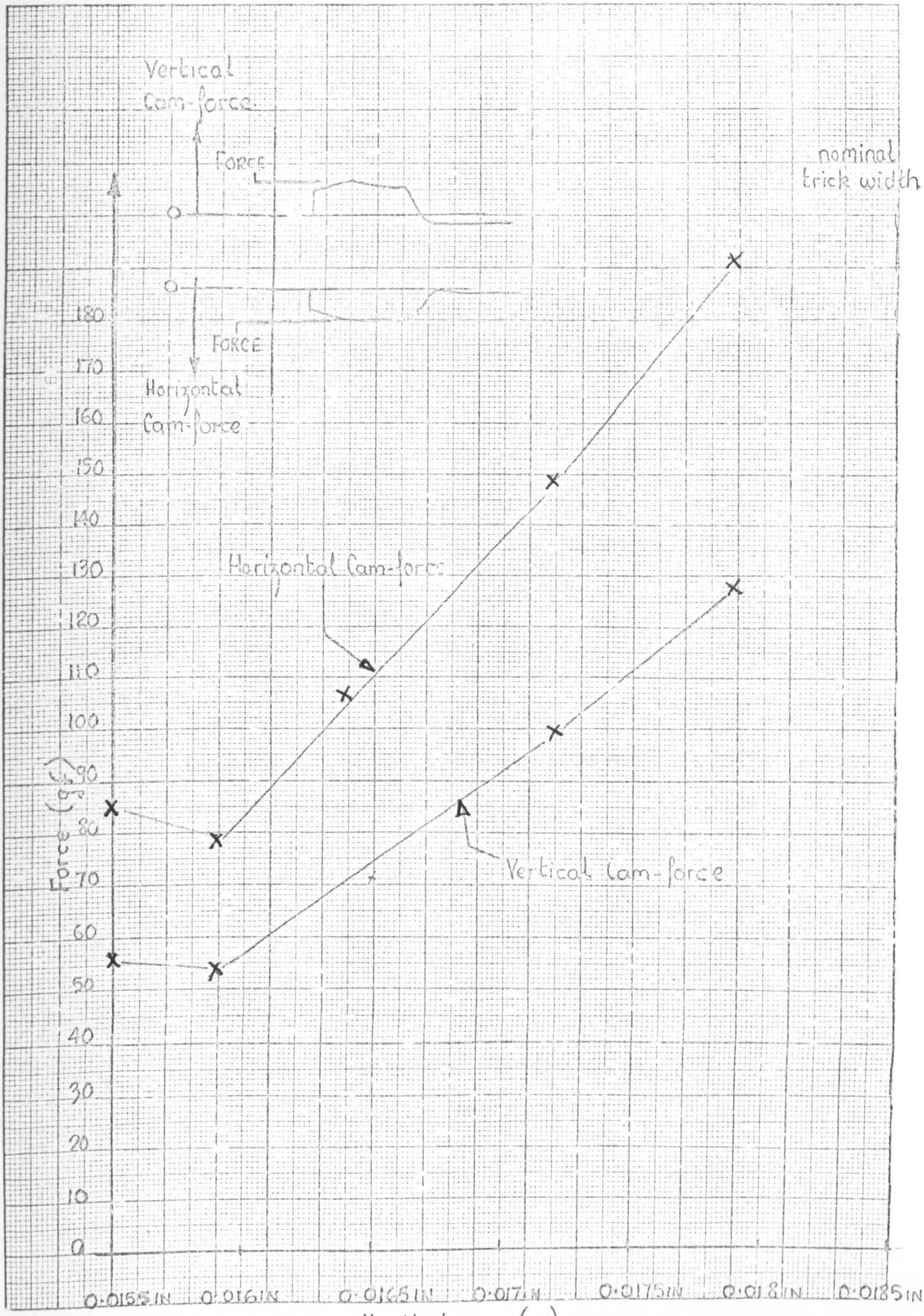

EFFECT OF NEEDLE THICKNESS UPON THE NON-KNITTING CAM-FORCE.

FIG 8.18

Effect of the Needle Thickness upon the Cam-Force

Parameters

Machine Speed = 15.25 m/min (50 ft/min)

Cam-Cylinder Clearance = 0.15 mm (0.006 in.)

Temperature = 21 °C

Nominal Trick Thickness = 0.47 mm (0.0185 in.)

Scales

Vertical Cam-force = 140 gf/10 mm (V)

Horizontal Cam-force = 140 gf/10 mm (V)

Time scale = 10 mS/8.5 mm (H)

(V) = Vertical photograph deflection

(H) = Horizontal photograph deflection

Diagram I - 0.452 mm (0.0178 in.) Needle in trick

Diagram II - 0.406 mm (0.0160 in.) Needle in trick

Cam shape see Fig 4.3

Parameters for the traces shown in Fig 8.19(b)

Fig 8.19 (a)

DIAGRAM I

0.0178 in. Needle.

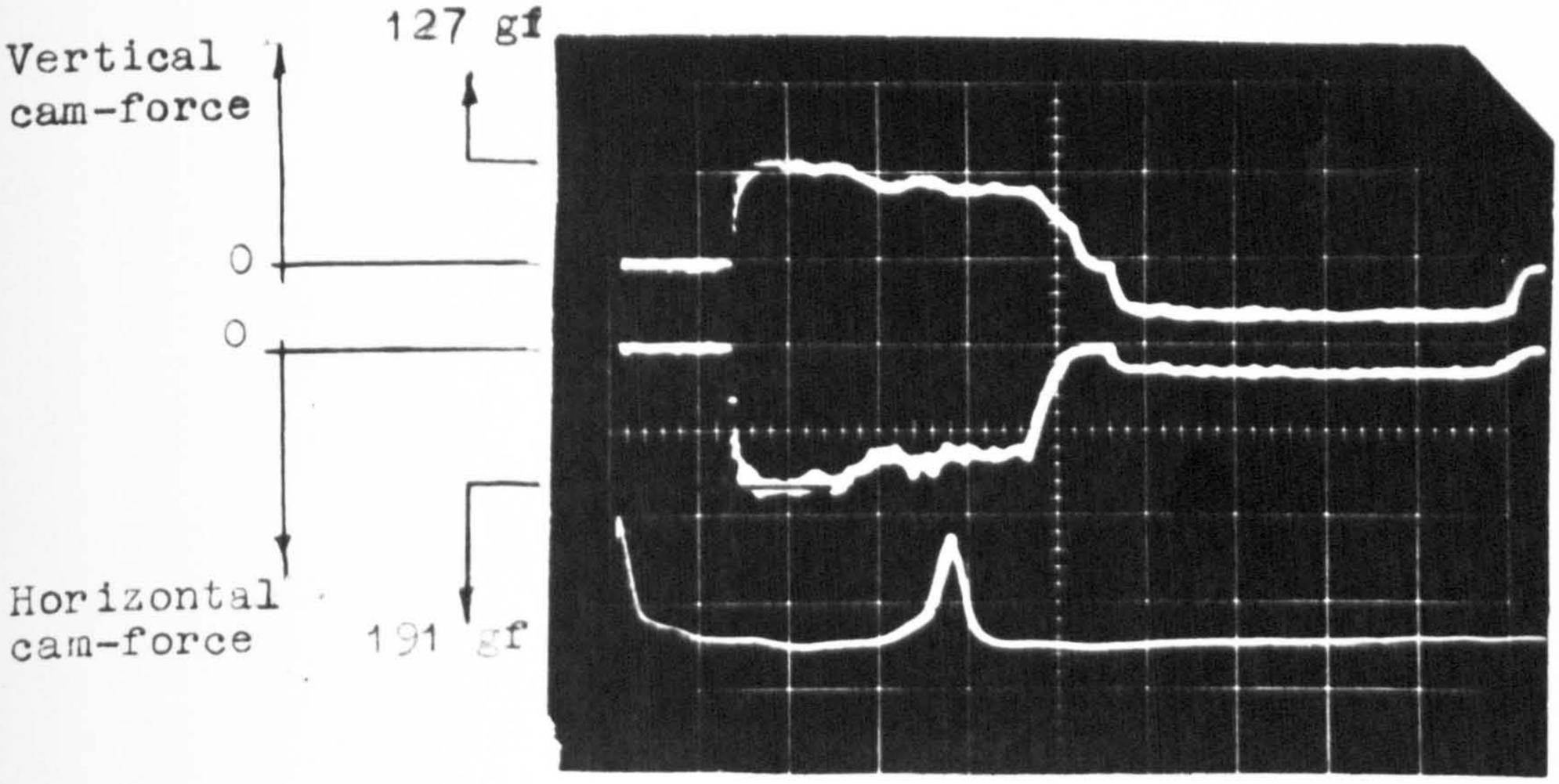

DIAGRAM II

0.016 in. Needle.

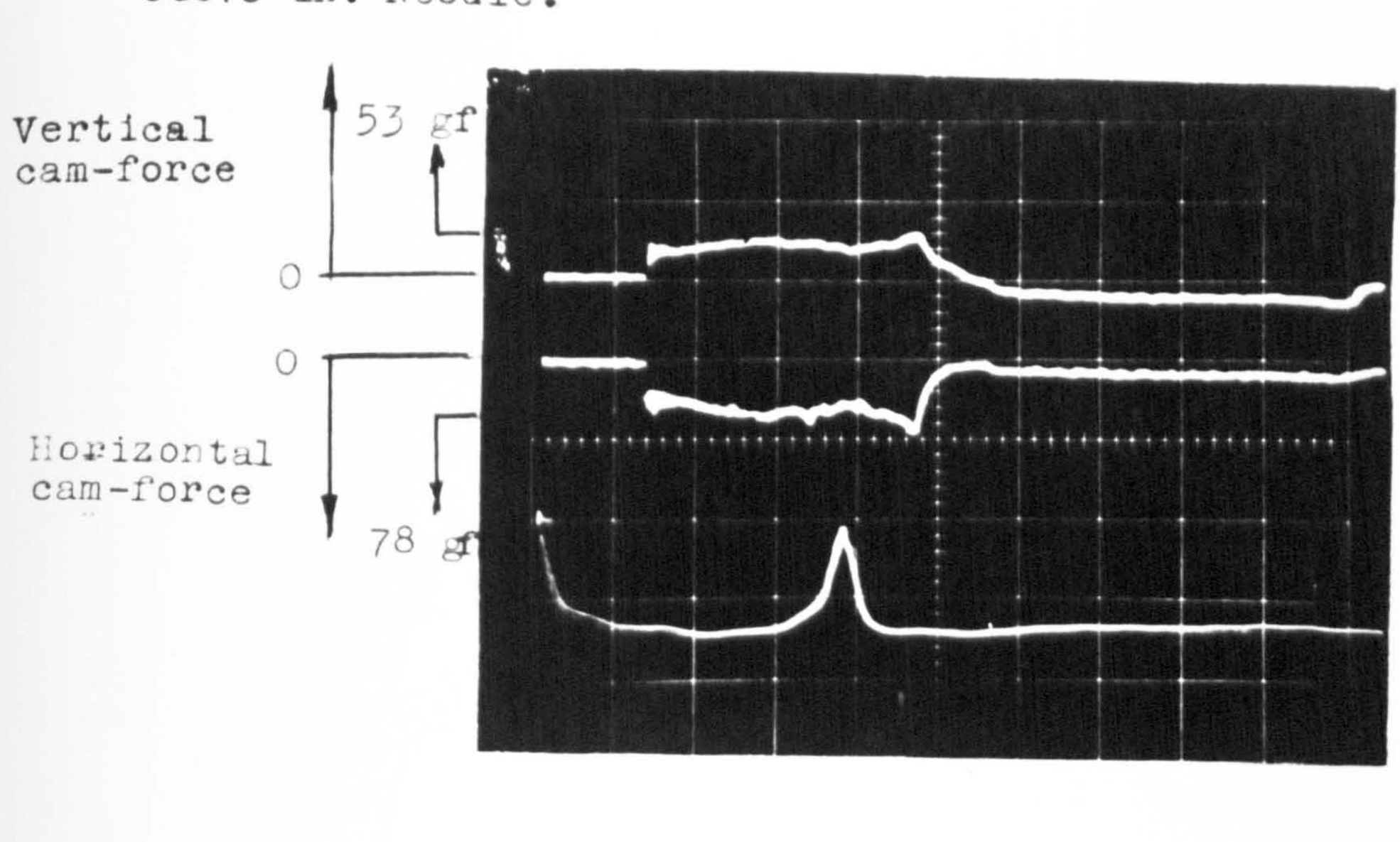

Effect of Needle Thickness upon the Non-Knitting Cam-Force.

Fig 8.19(b)

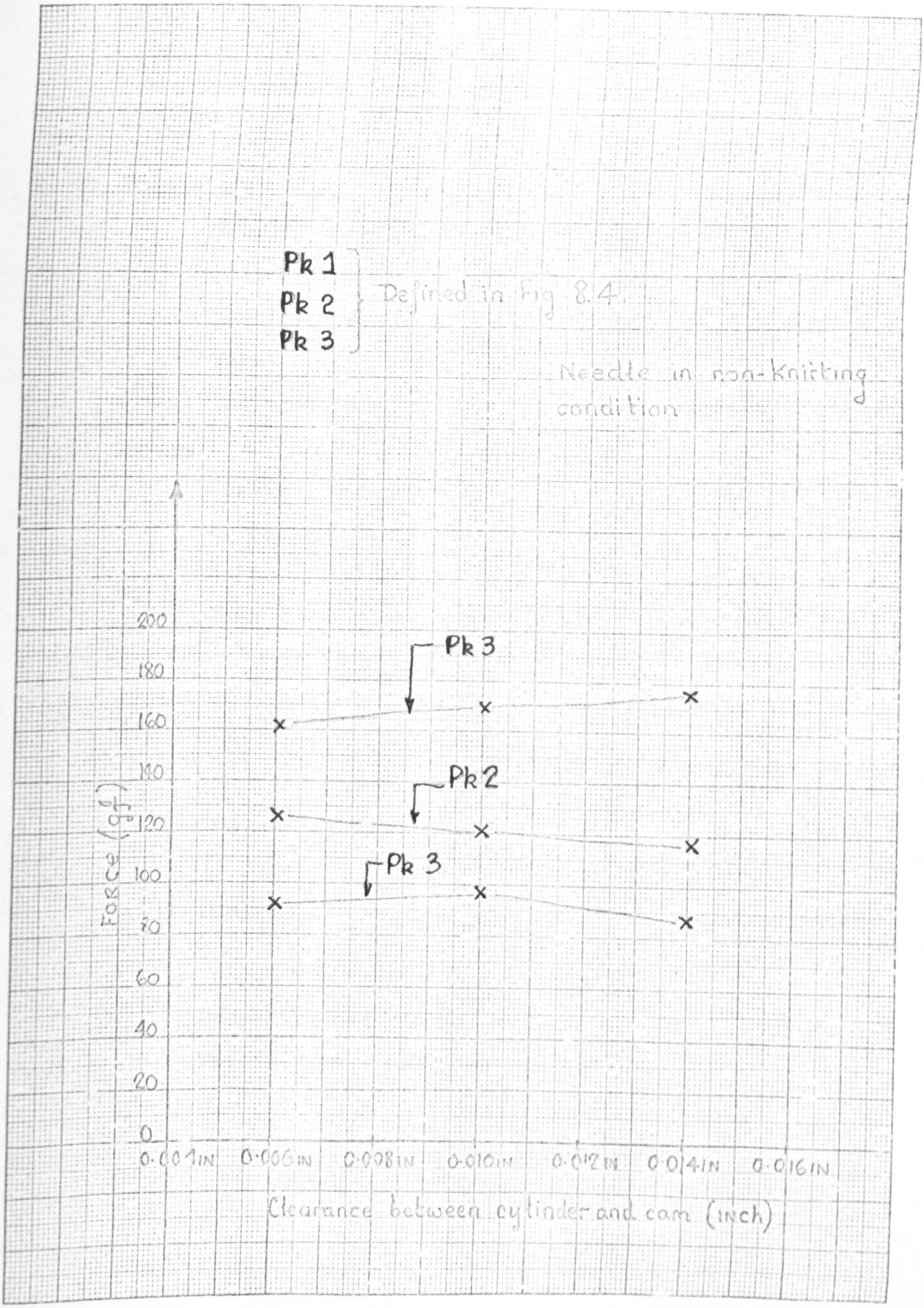

EFFECT OF THE CLEARANCE BETWEEN THE CYLINDER AND THE CAM UPON THE NON-KNITTING CAM-FORCE

FIG 8.20

Effect of the Clearance between the Cylinder and the Cams on the Cam-force

Parameters

Fabric take-down tension (overal)	= 2.461 gf
Stitch-draw	= 1.7 mm (0.067 in.)
Machine Speed	= 15.2 m/min (50 ft/mi
Yarn	= 1/150/30 Polyester
Temperature	= 21 °C

Scales

Vertical Cam-force	= 140 gf/10 mm (V)
Horizontal Cam-force	= 140 gf/10 mm (V)
Yarn-input tension	= 5 gf/10 mm (V)
Time	= 10 mS//8.5 mm (H)

(V) = Vertical photograph deflection.

(H) = Horizontal photograp deflection

Diagram I = Cam-Cylinder clearance 0.15 mm (0.006 in.)

Diagram II = Cam-Cylinder clearance 0.36 mm (0.014 in.)

Cam-shape see Fig 4.3

Needle type - 0.443 mm see Fig 3.2

Parameters for the traces shown in Fig 8.21(b)

Fig 8.21(a)

DIAGRAM I

Cam-Cylinder clearance 0.006 in.

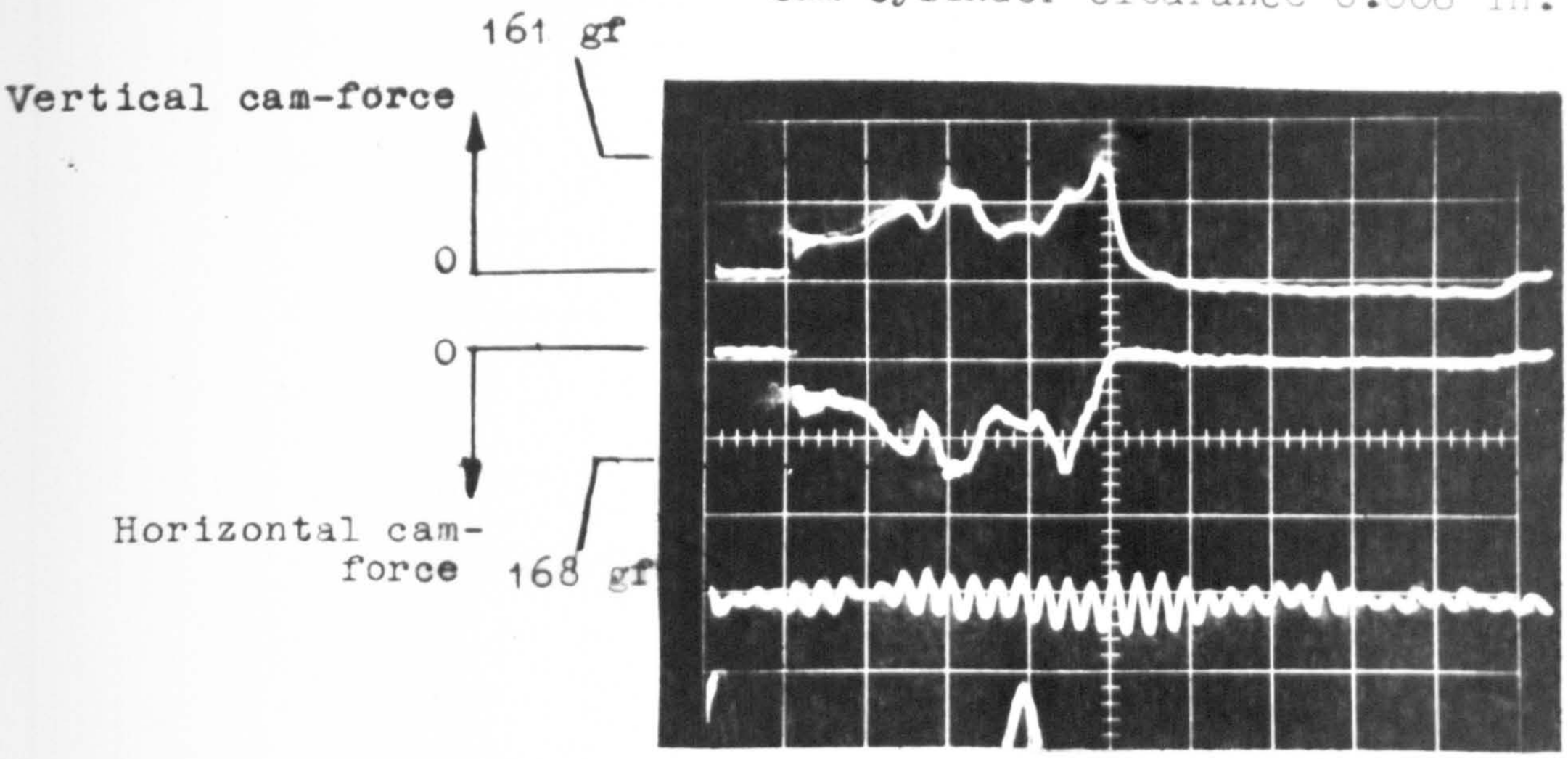

DIAGRAM II

Cam-Cylinder clearance).014 in.

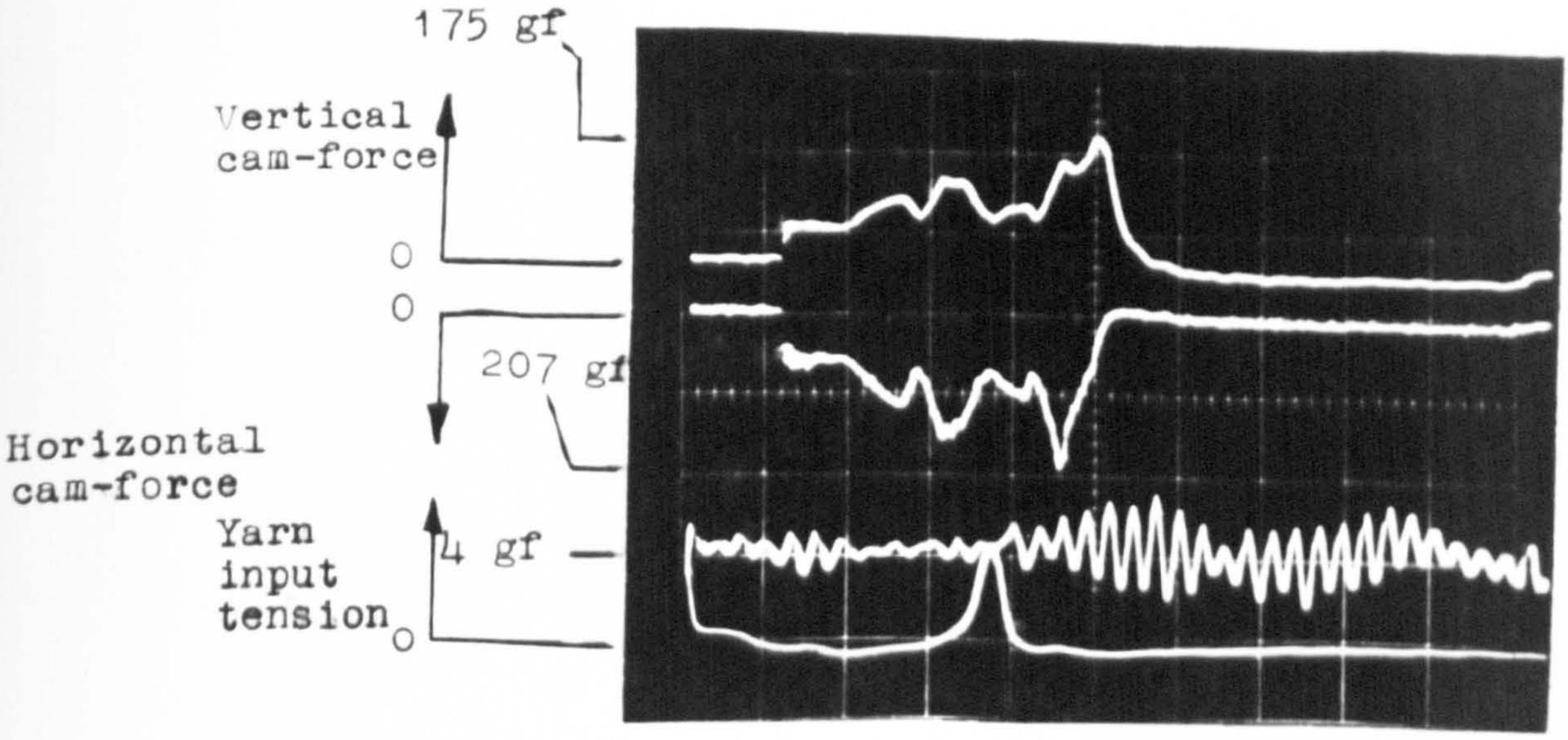

Effect of the Clearance between the Cylinder and the cams upon the cam force.

Fig 8.21(b)

Effect of the Latch Resistance to Motion upon the Cam-Forces and Yarn Forces

Parameters

- Fabric take-down tension = 2,461 gf
  Machine Speed = 15.2 m/min (50 ft/min)
  Stitch-draw = 0.17 mm (0.067 in.)
  Temperature = 21 °C
  Cam-cylinder clearance = 0.15 mm (0.006 in.)
  Yarn = 1//150/30 Bulked polyester

Scales

Vertical Cam-force = 140 gf//10 mm (V)
Yarn-force = 95 gf//10 mm (V)
Input Yarn Tension = 5 gf//10 mm (V)
Time = 10 mS/8.5 mm (H)

(V) = Vertical trace deflection

(H) = Horizontal trace deflection

Diagram II - with-stiffened latch motion

Diagram I - same needle as diagram II without stiffened latch motion

Cam-shape see Fig 4.3

Needle type - 0.443 mm see Fig 3.2

Parameters for the traces shown in Fig 8.22(b)

Fig 8.22(a)

DIAGRAM I

Needle without stiffened latch motion

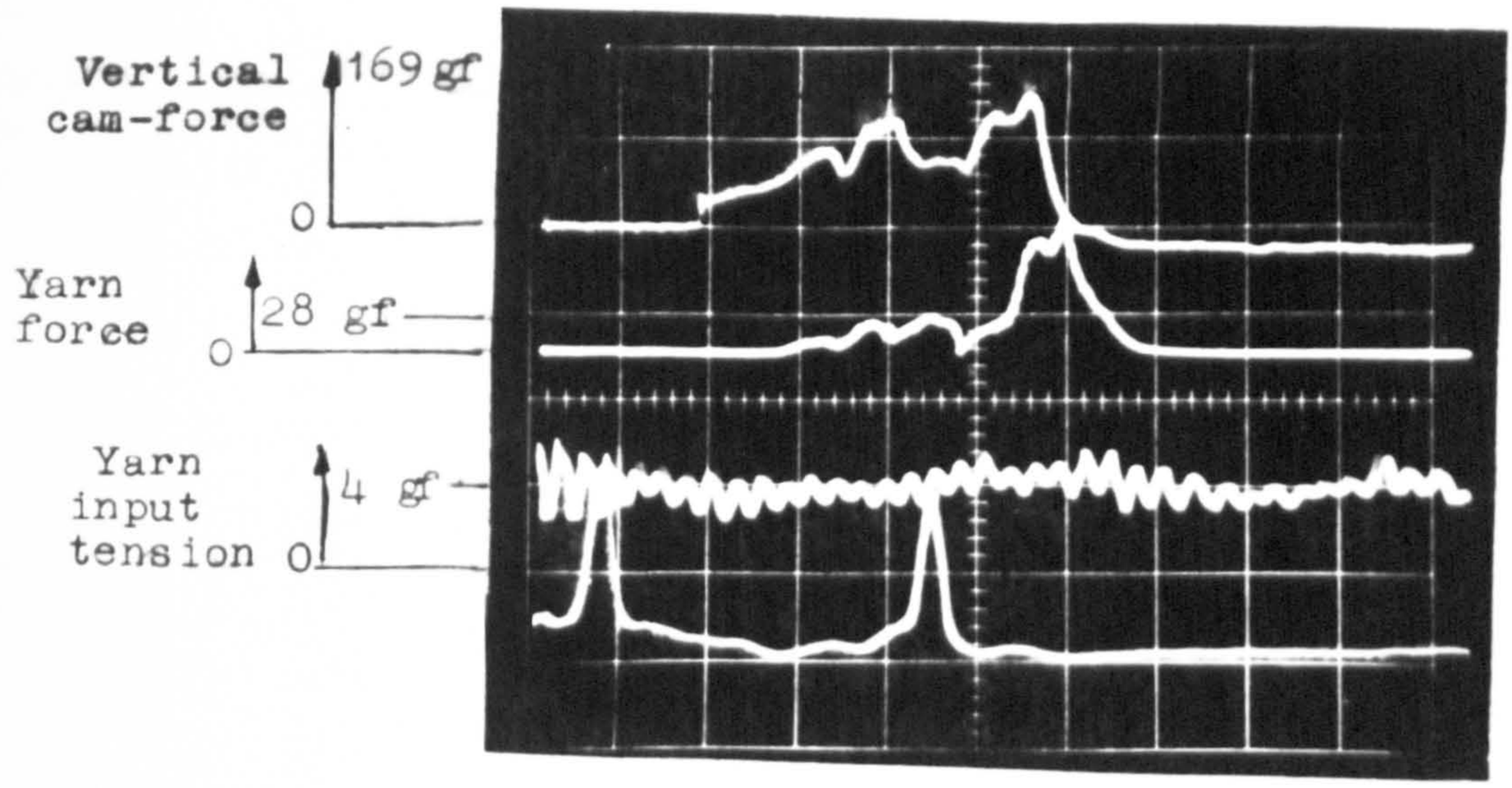

DIAGRAM II

Needle with Stiffened Latch Motion

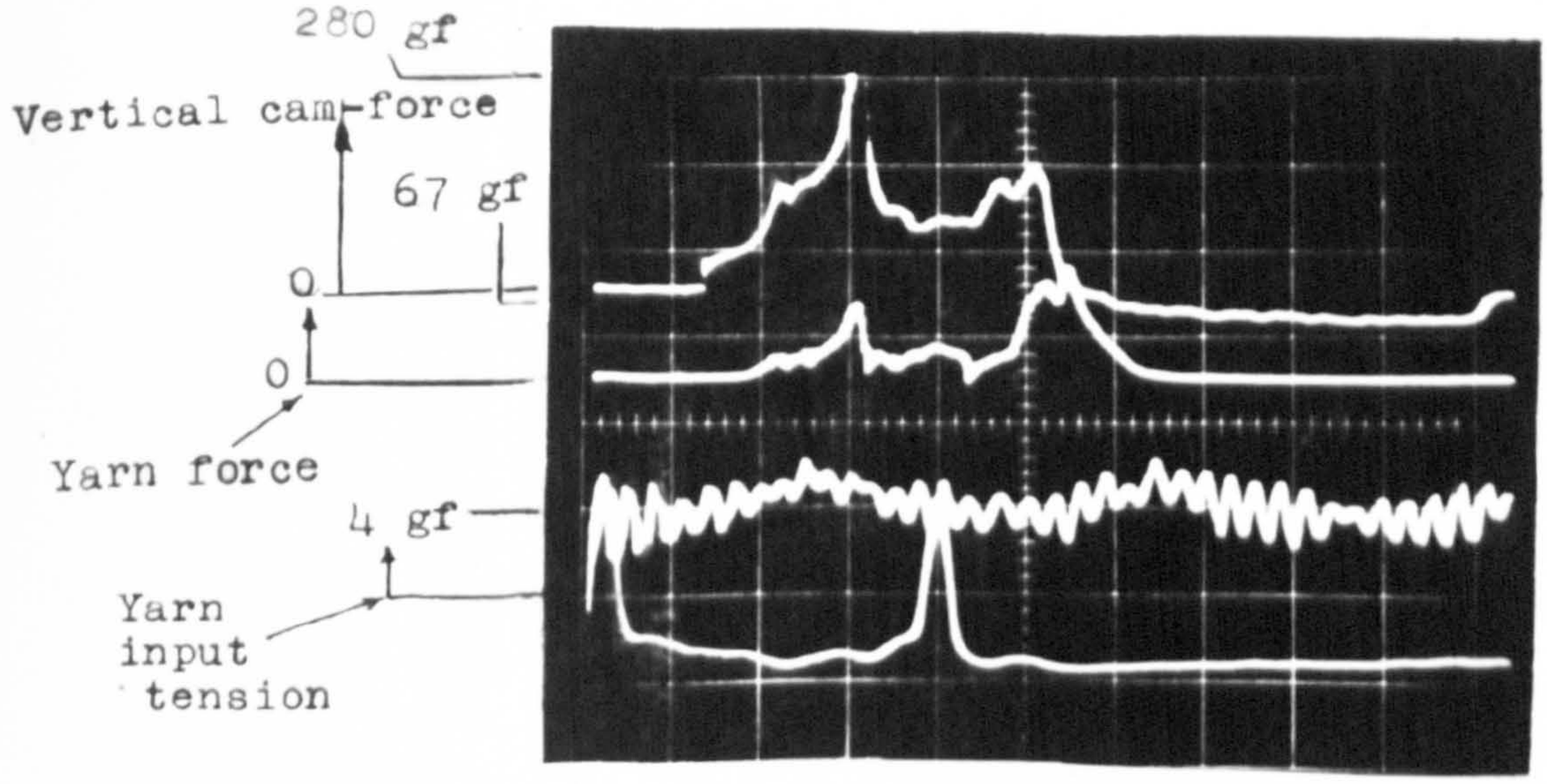

Effect of the Latch Resistance to Motion upon the Cam-Forces and Yarn-Forces.

Fig 8.22(b)

Effect of the Resistance to Needle Motion in the Trick

Parameters

Machine Speed = 15.2 m/min (50 ft/min)

Cam-cylinder clearance = 0.15 mm (0.006 in.)

Temperature = 22°C

Scales

Vertical Cam-force = 140 gf/10 mm (V)

Horizontal Cam-force = 140 gf/10 mm (V)

Time-scale = 10 mS/8.5 mm (H)

(V) = Vertical trace deflection

(H) = Horizontal trace deflection

Diagram I - Needle in free-trick

Diagram II - Needle in stiff-trick

Cam shape see Fig 4.3

Needle type - 0.443 mm see Fig 3.2

Parameters for the traces shown in Fig 8.23(b)

Fig 8.23(a)

DIAGRAM I

Needle in free trick

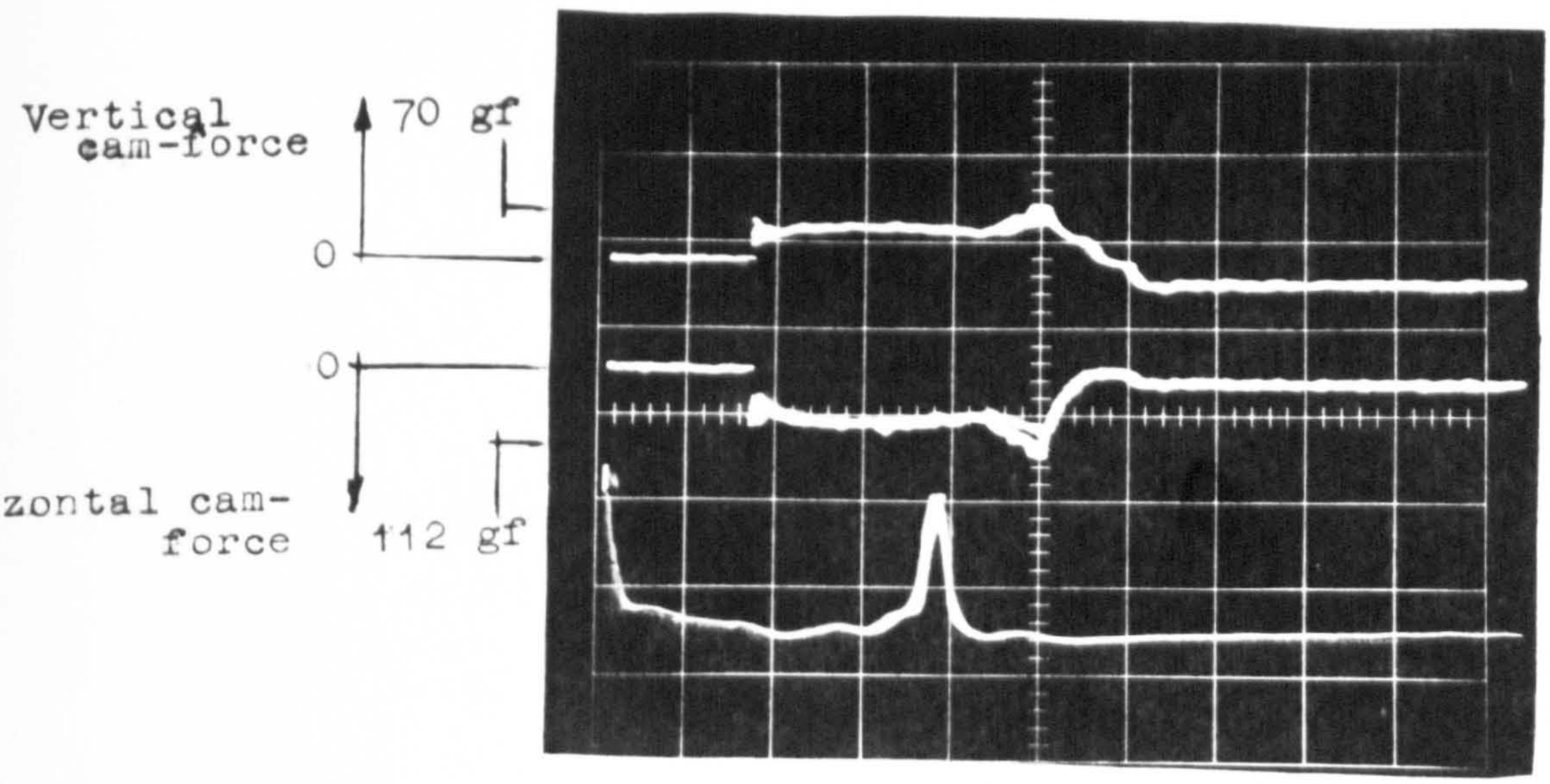

DIAGRAM II

Needle in stiff trick

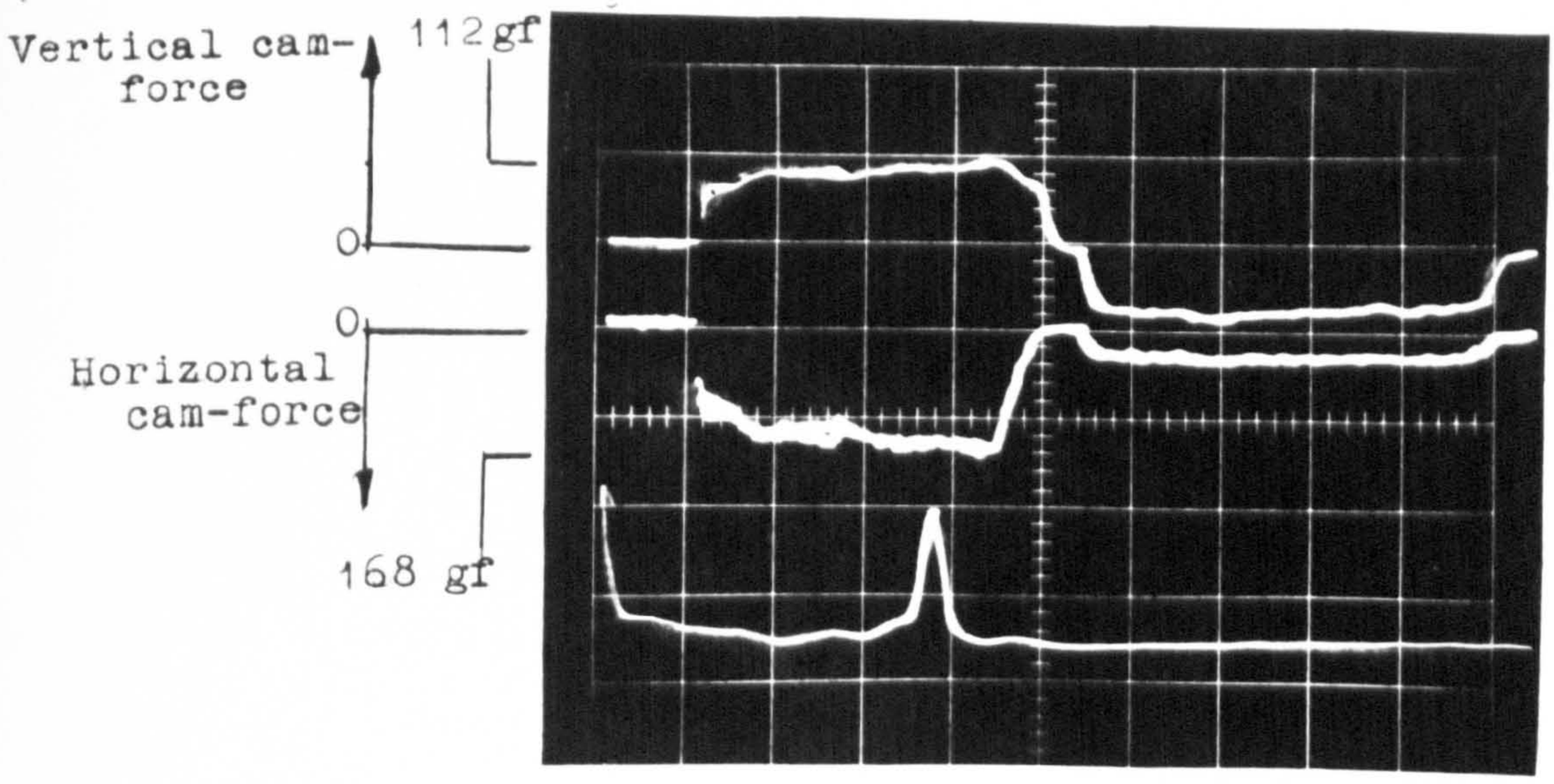

Effect of the Resistance to Needle Motion in the Trick.

Fig 8.23(b)

Effect of the Oil in the Trick

Parameters

Tricks soaked in Vickers Spotless B.N.O Oil

Cam-cylinder clearance = 0.15 mm (0.006 in.)

Temperature = 22°C

Scales

Horizontal Cam-forces = 140 gf/10 mm(V)

Vertical Cam-forces = 140 gf/10 mm (V)

Diagram I Machine speed = 7.6 m/min (25 ft/min)

Time = 10 mS/8.5 mm (H)

Diagram II Machine speed = 61 m/min (200 ft/min)

Time = 2 mS/8.5 mm (H)

(V) = Vertical scale deflection

(H) = Horizontal scale deflection

Cam shape see Fig 4.3

Needle type- 0.443 mm see Fig 3.2

Parameters for the traces shown in Fig 8.24(b)

Fig 8.24(a)

DIAGRAM I

Machine Speed 25 ft/min.

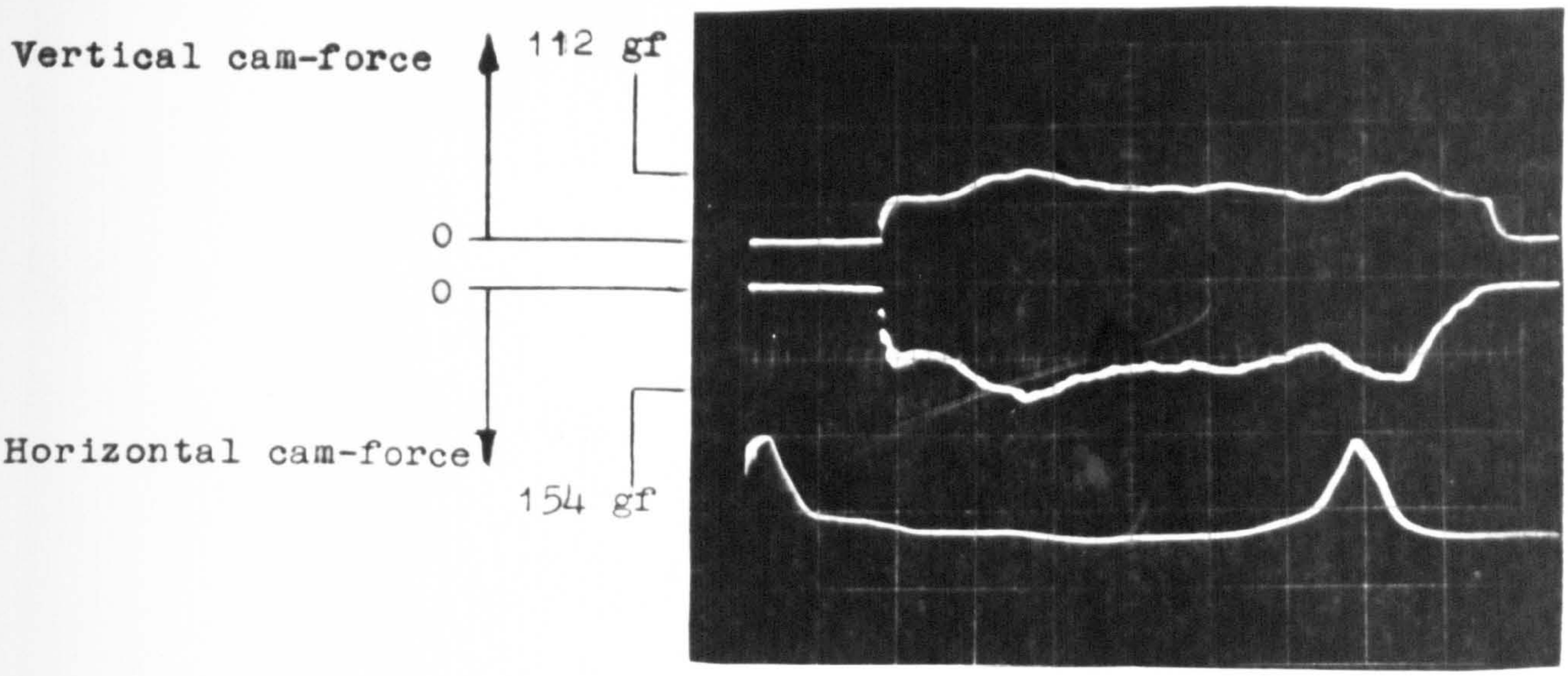

DIAGRAM II

Machine Speed 200 ft/min.

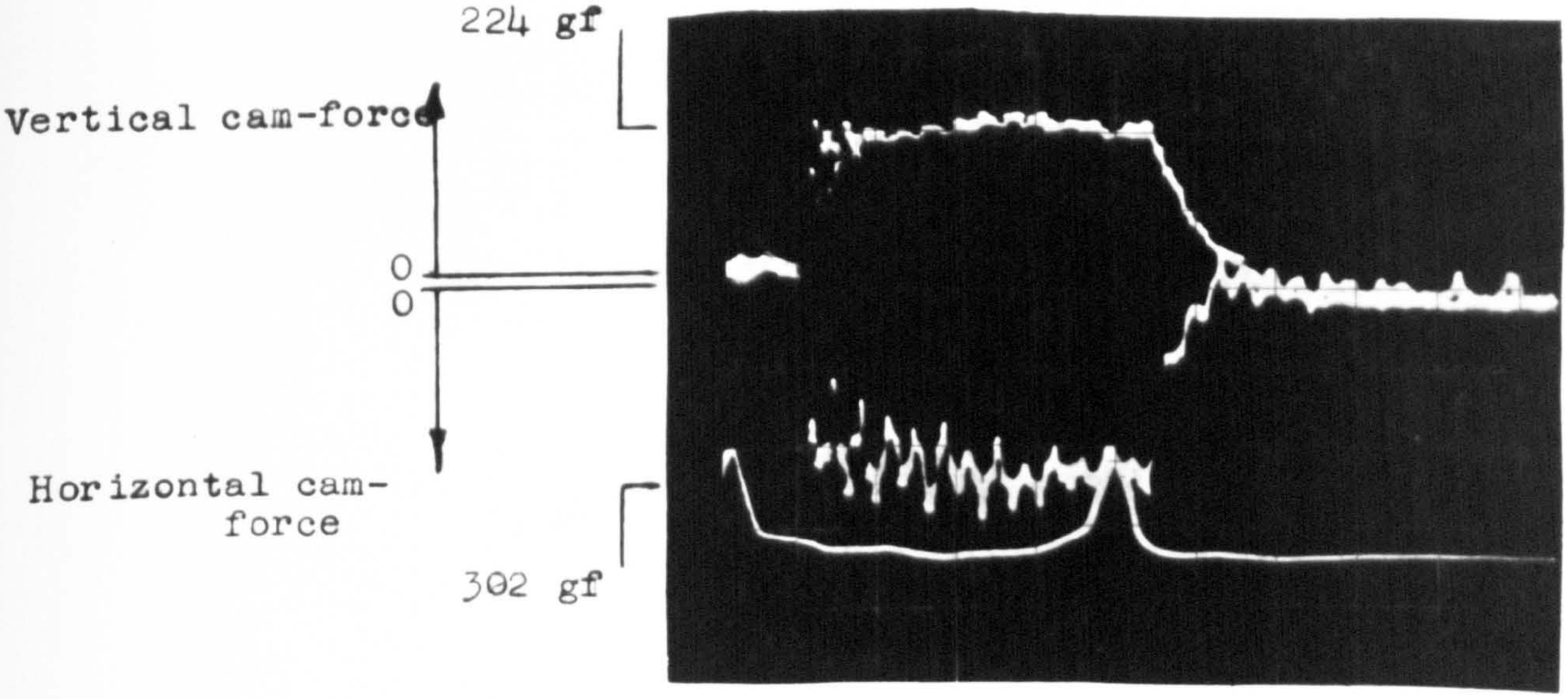

Effect of the Oil in the Trick

RELATIONSHIP BETWEEN CAM-FORCE AND MACHINE SPEED FOR TWO OILING CONDITIONS

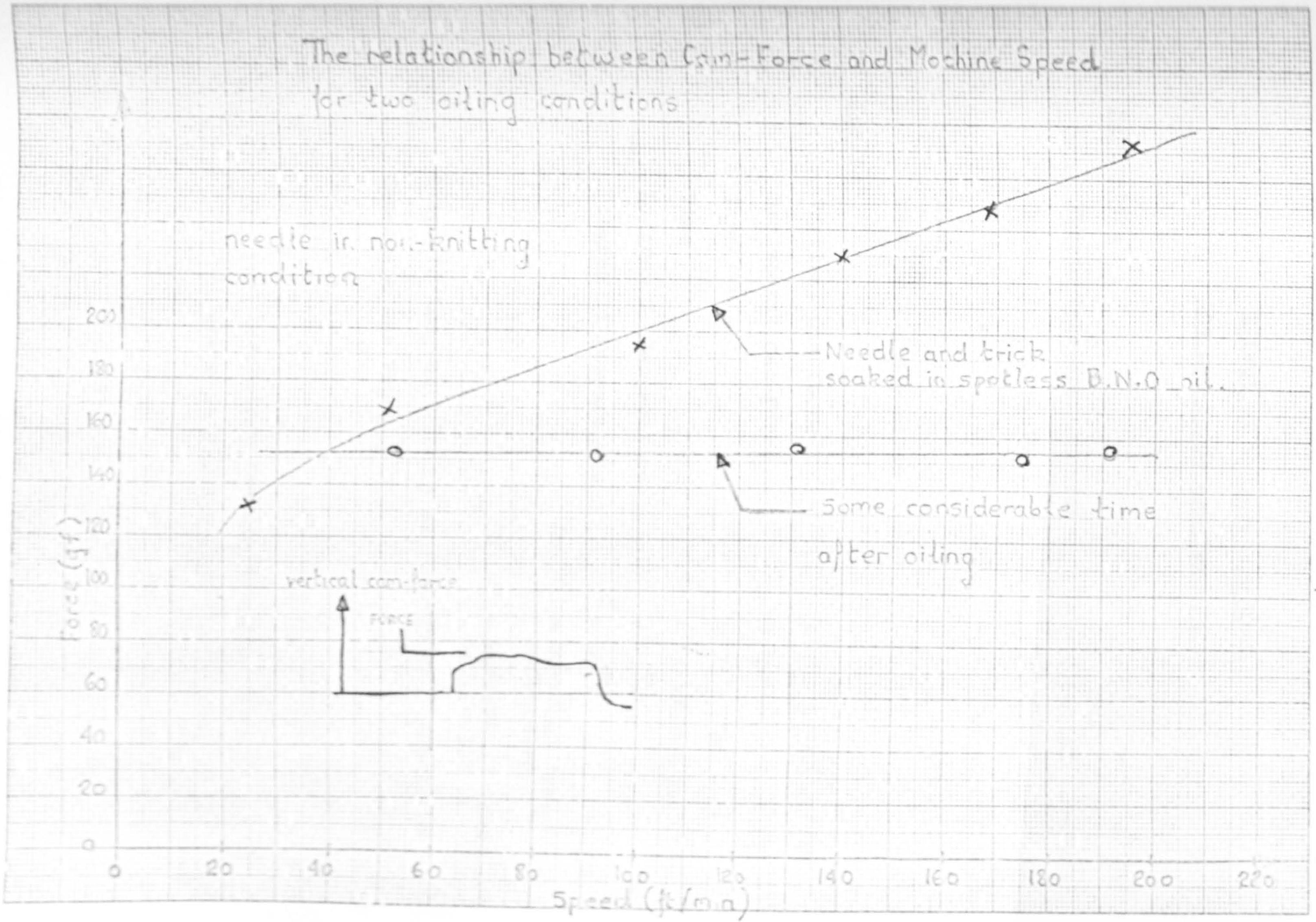

FIG 8.25

Effect of Temperature upon the Cam-Force and Yarn-Force

Parameters

Fabric take-down tension = 2,461 gf (overall)

Cam-cylinder spacing = 0.15 mm (0.006 in.)

Stitch-draw = 1.7 mm (0.067 in.)

Machine Speed = 15.2 m/min (50 ft/min)

Machine lightly-oiled

Scales

Vertical Cam-force = 140 gf/10 mm (V)

Horizontal Cam-force = 140 gf/10 mm (V)

Yarn force = 95 gf/10 mm (V)

Time = 10 mS/8.5 mm (H)

Diagram I Temperature = 23°C

Diagram II Temperature = 36°C

(V) = Vertical trace deflection

(H) = Horizontal trace deflection

Standard long-butt 0.443 mm (0.0175 in.) needle in trick.

Cam-shape see Fig 4.3

Parameters for the traces shown in Fig 8.26(b)

Fig 8.26(a)

DIAGRAM I

Temperature 23°C.

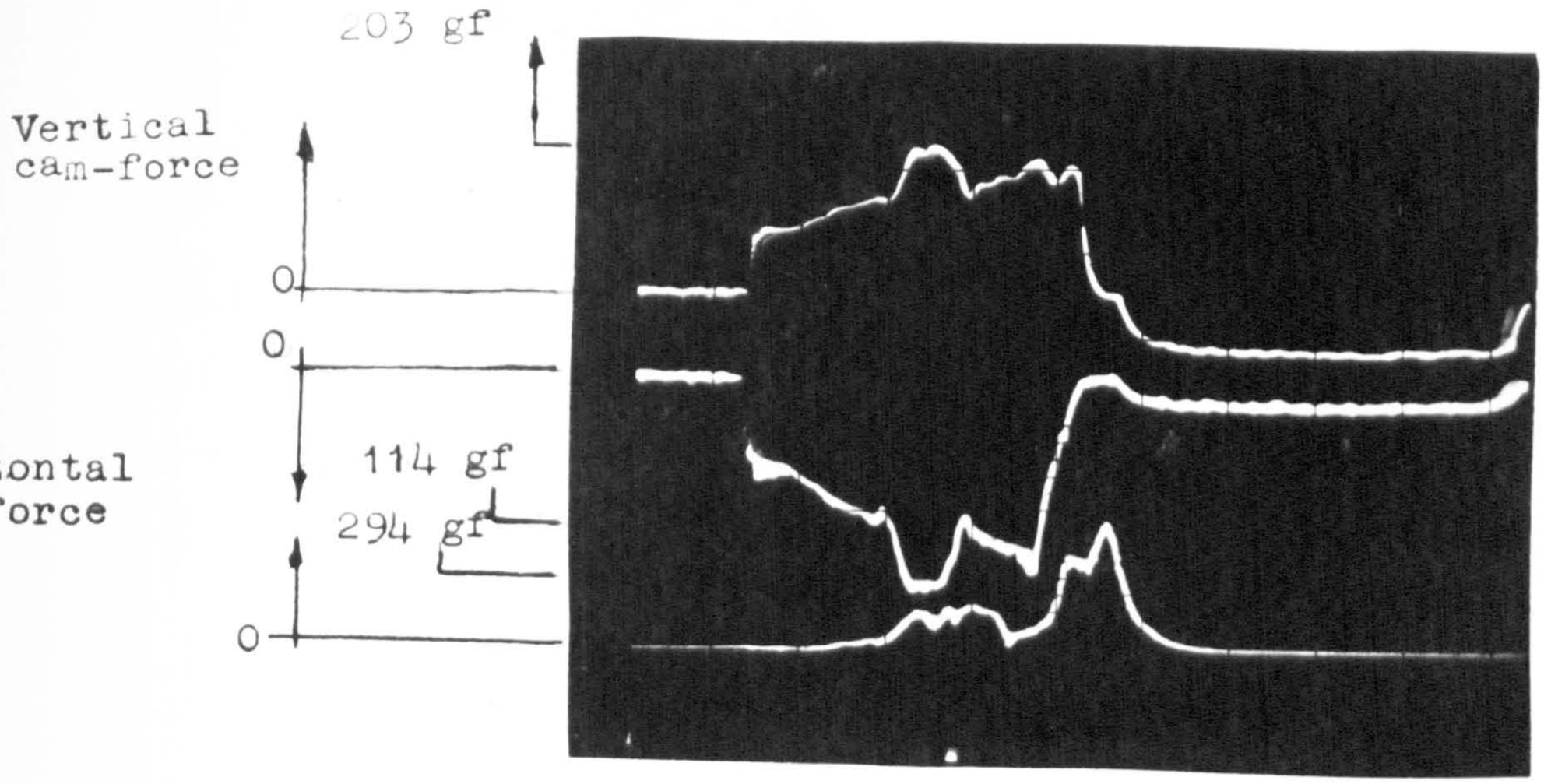

DIAGRAM II

Temperature 36°C.

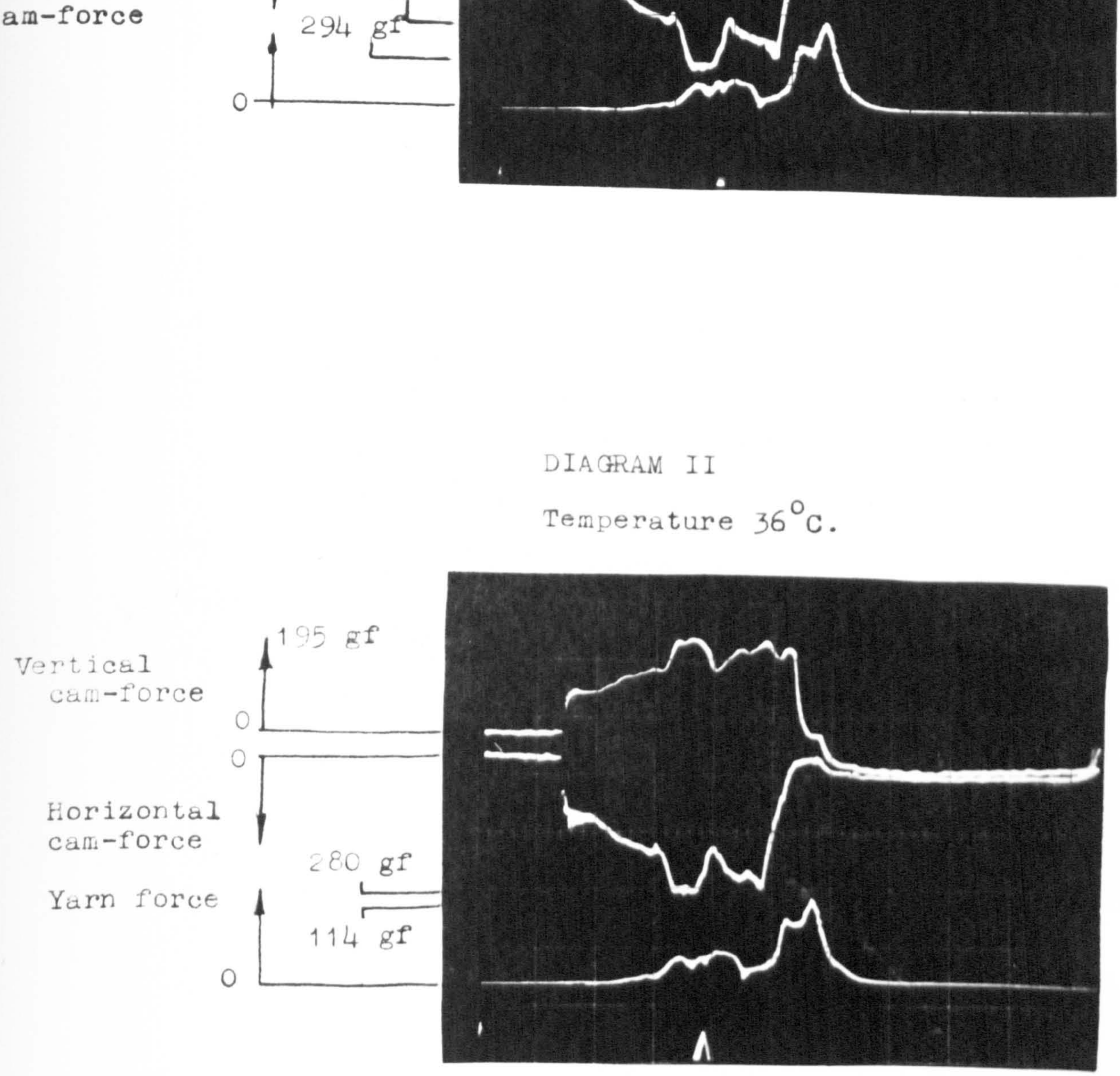

Effect of Temperature upon the Cam-Forces.

Fig 8.26(b)

Effect of Butt Width upon the Cam-Force

Parameters

Fabric take-down load (overall) = 2,461 gf

Stitch-draw = 1.7 mm (0.0668 in.)

Yarn = 1/150/30 Bulked polyester

Temperature = 22°C

Speed = 15.2 m/min (50 ft/min)

Scales

Cam-force (vertical) = 140 gf/10 mm (V)

Cam-force (Horizontal) = 140 gf/10 mm (V)

Yarn-input tension = 5 gf/10 mm (V)

Time = 10 mS/8.5 mm (H)

(V) = Vertical trace deflection

(H) = Horizontal trace deflection

Diagram I - Butt width = 3.18 mm (0.125 in.)

Diagram II - Butt width = 2.79 mm (0.110 in.)

Diagram III - Butt width = 1.91 mm (0.075 in.)

Cam shape see Fig 4.3

Needle type - 0.443 mm see Fig 3.2

Parameters for the traces shown in Fig 8.27(b)

Fig 8.27(a)

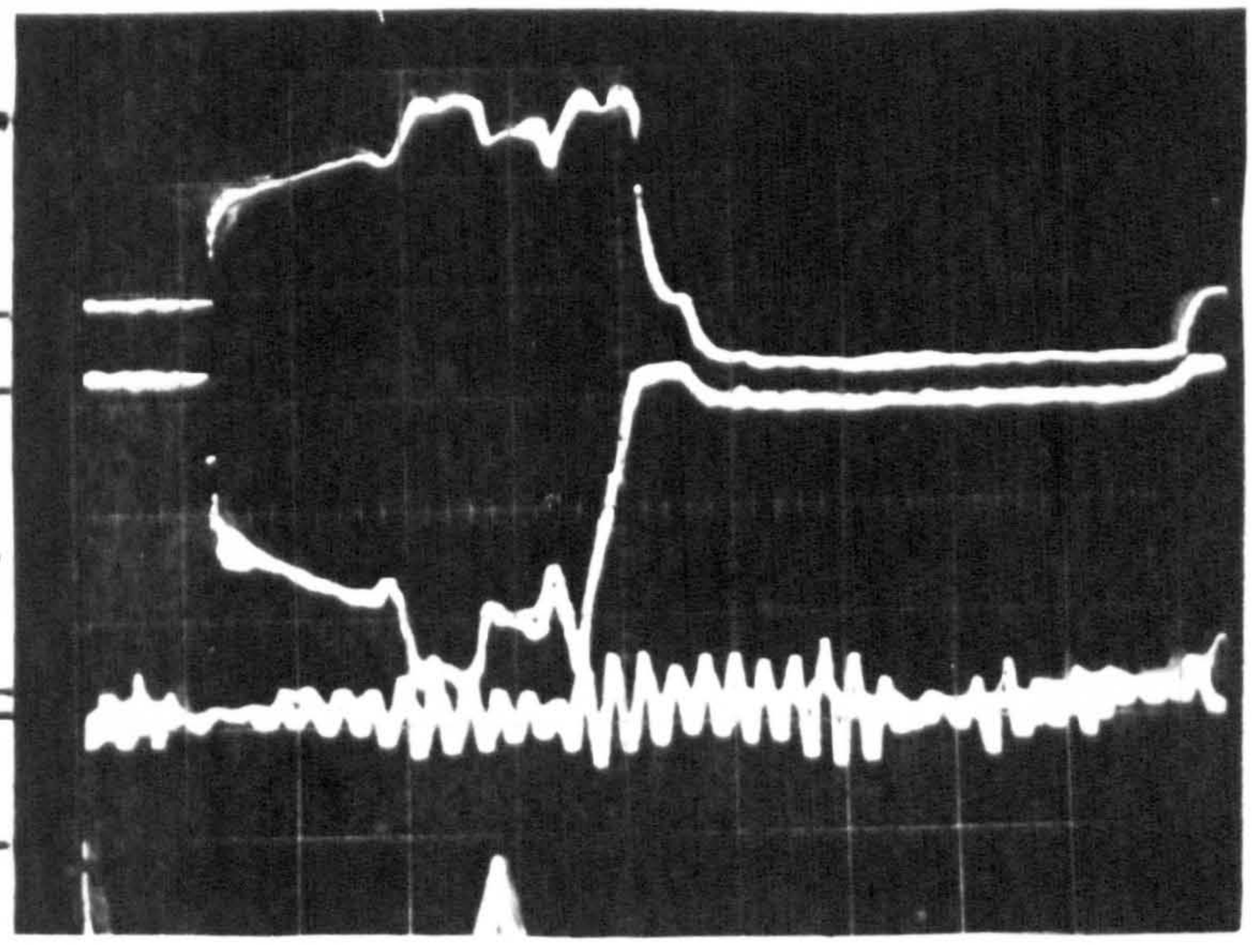

DIAGRAM I

Butt width 0.125 in.

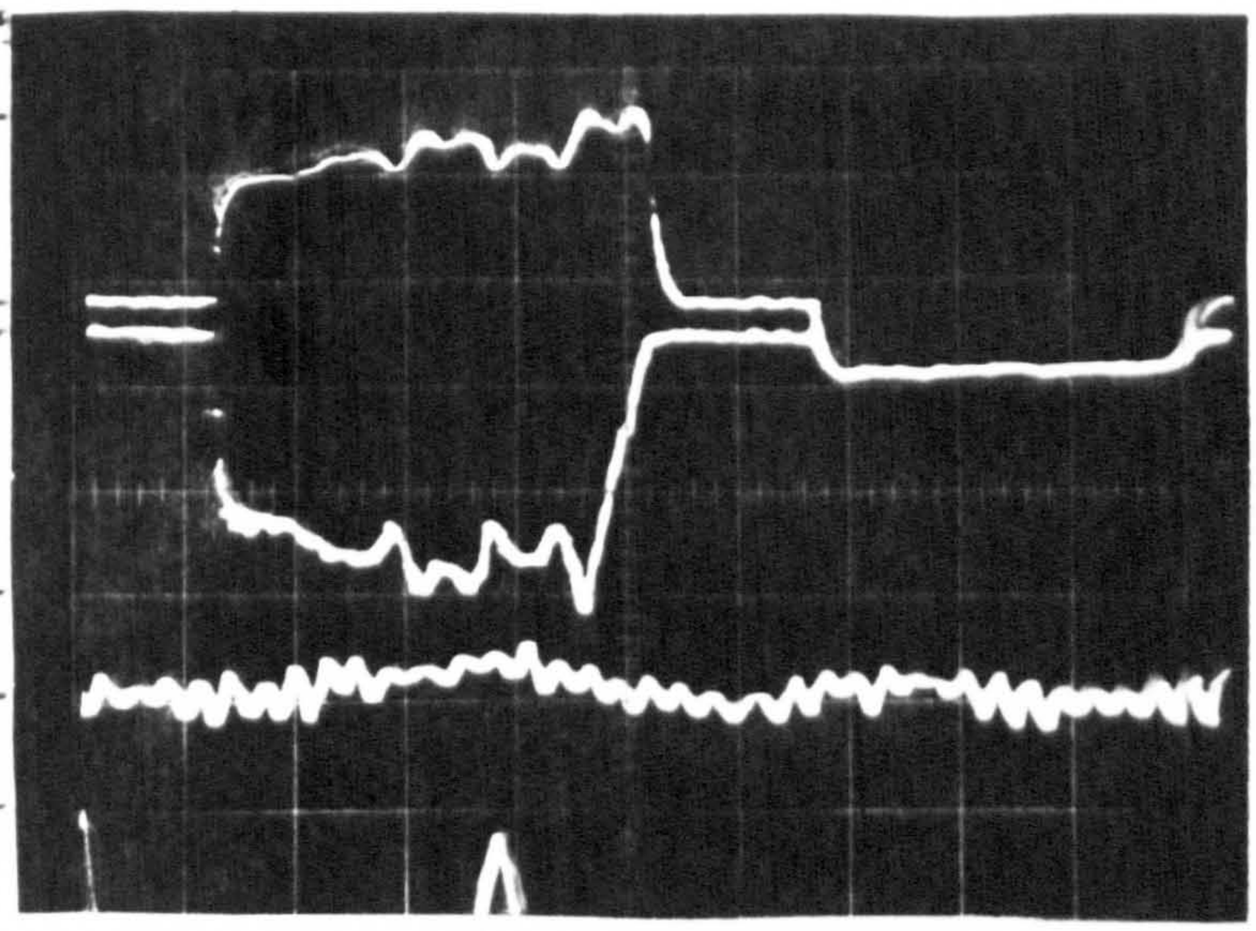

DIAGRAM II

Butt width 0.110 in.

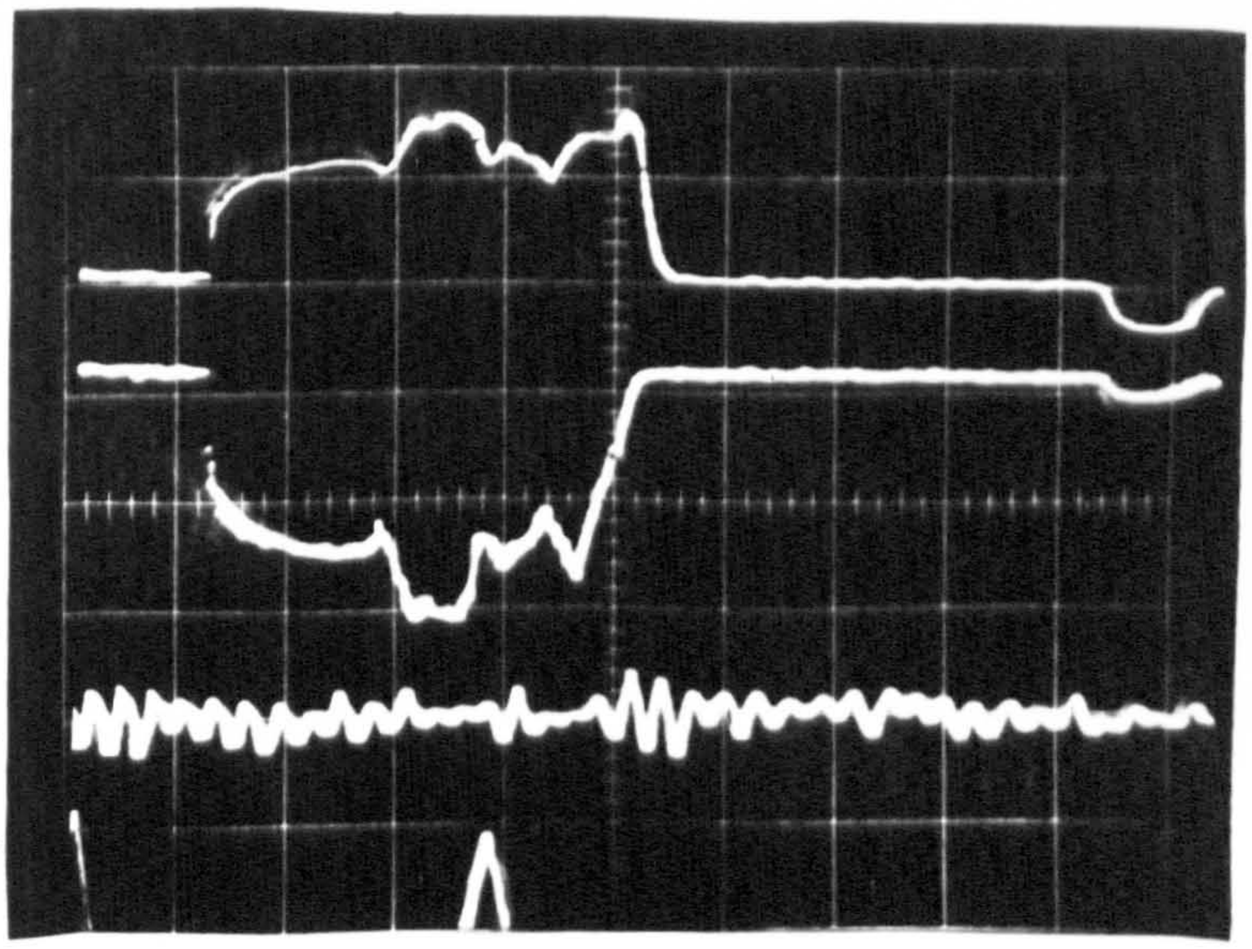

DIAGRAM III

Butt width 0.075 in.

Effect of Butt Width upon the Cam-Force.

Fig 8.27(b)

Effect of Yarn upon the Cam-Force

Parameters

Time for traces	= 10 mS/div = 1 div = 8.5 mm
Take-down tension	= 2,461 gf (Overall)
Cam-cylinder clearance	= 0.15 mm (0.006 in.)
Stitch-draw	= 1.7 mm (0.0668 in.)
Yarn	= 1/150/30 Bulked polyester
Yarn-input-tension	= 9 gf approx.
Machine speed	= 15.2 m/min (50 ft/min)

Cam shape see Fig 4.3

Parameters for the experimental results shown in Fig 8.28(b)

Fig 8.28(a)

(4) - 0·0175 IN (0·443mm) Needle IN same trick as traces (1) (2) and (3)

(3) - 0·016 IN (0·406mm) Needle holding two yarn loops

(2) - 0·016 IN (0·406mm) Needle with head removed shows forces required to overcome trick resistance

(1) - 0·016 IN (0·406mm) Needle - cam-force

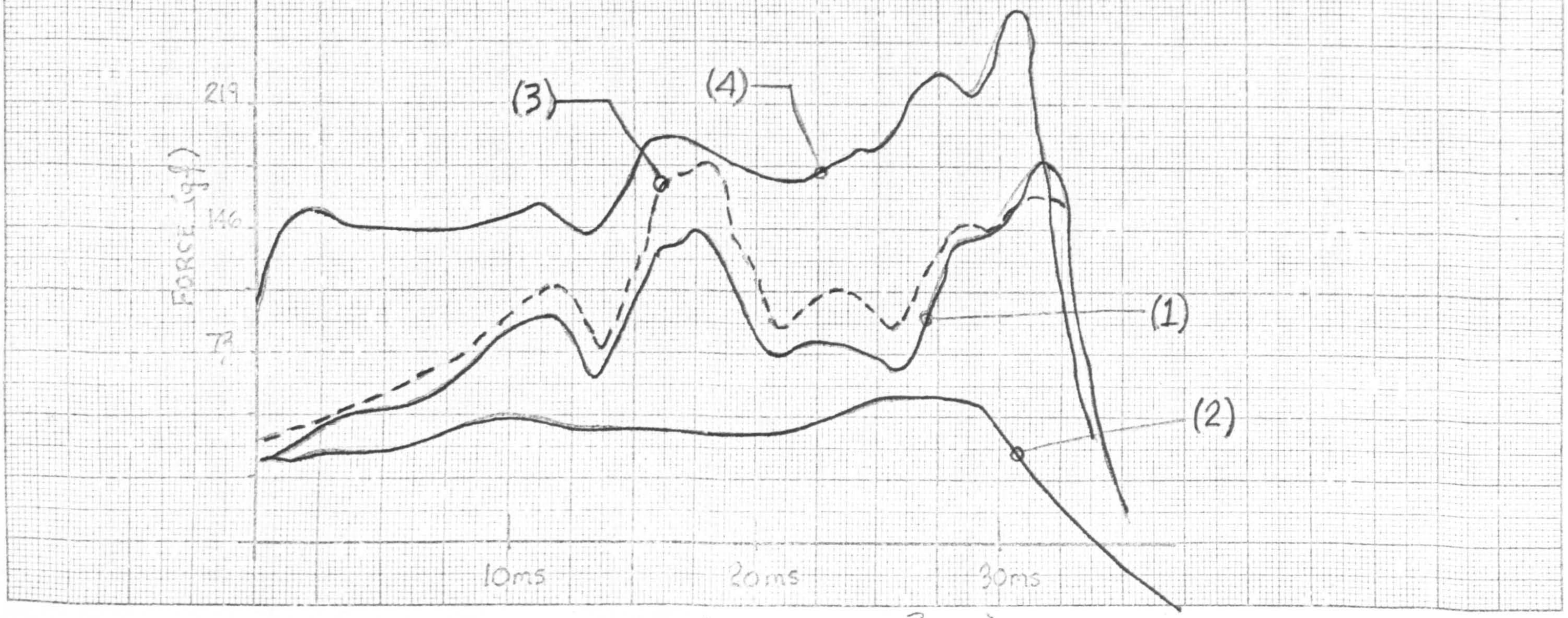

Fig 8·28(b)

CHAPTER 9

ANALYSIS OF FORCES PRESENT IN THE KNITTING OPERATION

9.1 Need for a Theoretical Analysis.

The objectives of the theoretical analysis are briefly detailed below :-

(i) To determine the important parameters, and the manner in which they affect the cam and yarn-force.

(ii) To predict the cam-force and yarn-forces under all knitting conditions.

9.2. Theoretical Analysis of forces between Cam and Needle during Normal Knitting.

Munden and Knapton[13,14,15,21,19] theoretically analysed the forces existing between the cams and needles during knitting. Fig 9.1 shows the various forces acting on a needle as it moves down the straight portion of the stitch-cam. From this diagram Knapton[13,14] derived an equation for the cam and needle reaction force, R, of the form :-

$$R = \frac{f(x) + \mu_1 Q - mg}{(1-\mu_1\mu_2)\cos\theta - (\mu_1 + \mu_2)\sin\theta} \quad . \qquad (16).$$

All the terms in the equation are defined in Fig 9.1.

Barth[30,48] carried out a more rigorous analysis taking account of the moments of the forces, but because Knapton's theory is relatively simple to use, it was decided, initially, to compare the experimental results detailed in chapter 8, to theoretical predictions based upon Knaptons analysis. If the comparison proved unsatisfactory then the

more detailed work of Barth would be used. Equation (16) derived by Knapton, could not be used in the form shown. Certain basic modifications had to be made to the equation so that it could satisfactorily account for some of the experimental results. Although the results are detailed in chapter 8, a brief reminder of their titles is given here as follows :-

(i) The increase in the force level as the clearance between the cylinder and the cams is increased (section 8.5.6).

(ii) The increase in the force level due to the addition of oil to the cylinder (section 8.5.9).

(iii) The variation in the force level when a needle is moved from one trick to another (section 8.5.8).

The theory was modified to take account of the above experimental variations. The revised cam-needle force relationship is shown in Fig 9.2.

The following equations can be derived :-

$$R_x = \frac{Sb}{a} \quad . \quad . \quad . \quad . \quad (17),$$

where $$R_x = R\sin\theta + \mu_2 R\cos\theta \quad . \quad . \quad . \quad (18),$$

$$R_y = \mu_1 S + F + P + \mu_1 R_k + \mu_1 Q + f(\alpha) - mg \quad (19),$$

$$R_y = R\cos\theta - \mu_2 R\sin\theta \quad . \quad . \quad . \quad (20),$$

and $$R_x + R_k = S \quad . \quad . \quad . \quad . \quad (21).$$

All the terms are defined in Fig 9.2.

Using equations (17) to (21) the following equation can be derived :-

$$R = \frac{F + F + \mu_1 Q + f(\alpha) - mg}{\cos\theta(1 - \alpha\mu_1\mu_2) - \sin\theta(\mu_2 + \alpha\mu_1)} \quad (22),$$

where $$\alpha = \frac{2a}{b} - 1 .$$

Equation (22) formed the basis for an initial examination of the experimental results.

9.2.1 <u>The Inertial Component of Force on the Curved Portion of the Cams.</u>

Equation (22) can only be used when the needle is moving down the cam at constant velocity i.e. when the needle is on a straight cam section. However, at circular terminations, or non-linear portions, an inertial force component exists, and equation (22) must be modified to include this component.

The inertial force acting on the needle has the form:-

$$T = m \frac{d^2y}{dt^2} \quad . \quad . \quad . \quad . \quad (23),$$

where m = needle mass,

T = accelerating force (vertical),

and $\frac{d^2y}{dt^2}$ = vertical accleration.

$$\frac{dy}{dt} = \frac{dy}{dx}\frac{dx}{dt} = v\frac{dy}{dx}$$

where v = cylinder peripheral speed,

and $\frac{dy}{dx}$ = cam slope.

Similarly $\frac{d^2y}{dt^2} = v^2 \frac{d^2y}{dx^2}$

where $\frac{d^2y}{dx^2}$ = first derivative of the slope with respect to

then $$T = mv^2 \frac{d^2y}{dx^2} \quad . \quad . \quad . \quad . \quad (24).$$

The experiments detailed in chapter 8 were carried out using the cam-profile, illustrated in Fig 4.3. As the needle passes round the radius at the bottom of the stitch-cam there will be a decelerating force. If it reaches such proportions

that the cam-needle reaction-force R becomes equal to zero; then separation will occur between the needle and stitch-cam. It will then move over towards the guard cam with possibly an impact at the point of contact.

On Fig 9.3. the following relationships are derived:-

$$\frac{dy}{dx} = \frac{x_c - x}{y - y_c}$$

$$\frac{d^2y}{dx^2} = -\left(\frac{(y - y_c)^2 + (x_c - x)^2}{(y - y_c)^3} \right) \quad . \quad . \quad . \quad (25),$$

combining equations (24) and (25) for the radial termination at the base of the stitch cam.

$$T = -mv^2 \left(\frac{(y - y_c)^2 + (x_c - x)^2}{(y - y_c)^3} \right) \quad . \quad (26).$$

9.2.2 Effect of the Oil in the Trick.

Black[29] showed that oil in the needle tricks was responsible for an increase in cam-force as the machine speed was increased. He showed that, for a Newtonian fluid, the drag force on the needle as it moved down a well lubricated trick was given by :-

$$F = A\rho \left(\frac{v \tan \theta}{d} \right) \quad . \quad . \quad . \quad (27),$$

where F = drag-force,
A = total wetted area of needle,
ρ = oil viscosity,
v = machine speed,
θ = cam angle,
and d = an equivalent parallel distance between needle and trick well.

Black[29] showed the effect of using various oils in the trick, namely that highly viscous oils lead to very large forces as speed is increased.

9.3 Estimation of Friction Parameters from Photograph Traces.

Before the theory derived in section 9.2 could be used to examine the experimental results, the coefficients of friction between the needle and the trick and between the needle and the cams had to be found. Bentley Machine Development had previously done some considerable unpublished work on friction, and their measurements of the coefficient of friction for a needle running down a lightly oiled cam μ_2 in Fig 9.2. varied from 0.11 to 0.14, and for a needle on a lightly oiled trick surface μ_1 in Fig 9.2 varied from 0.12 to 0.14.

An experiment was carried out to determine the coefficients of friction and check the values obtained by Bentleys. The experiments consisted of measuring the angle at which a sheet of lightly oiled cam material, and alternatively trick material, had to be tilted so that a block of needle material slid down the surface at constant velocity. Further details of both measurements is given in Fig 9.4. The coefficients of friction were measured for cam to needle μ_2 varying from 0.12 to 0.15, and trick to needle μ_1 from 0.11 to 0.14.

The coefficients of friction can also be determined from the traces obtained during the experiments detailed in sections 8.5.1 to 8.5.11.

Resolving the forces on the needle :-

$$R_x = R\left(\sin\theta + \mu_2\cos\theta\right) \quad \cdots \quad (28),$$

$$R_y = R\left(\cos\theta - \mu_2\sin\theta\right) \quad \cdots \quad (29),$$

where R_x = horizontal component of cam-needle reaction force,

R_y = vertical component of cam-needle reaction force,

R = cam-needle reaction force,

θ = cam-angle,

and μ_2 = cam-needle coefficient of friction.

From equations (28) and (29) the following equation can be derived :-

$$\mu_2 = \frac{\frac{R_y}{R_x} \tan\theta - 1}{\frac{R_y}{R_x} + \tan\theta} \quad \cdot \quad \cdot \quad (30).$$

The ratio of the horizontal and vertical forces was measured from the many photographic traces obtained during the experiments detailed in chapter 8, this value was then substituted in equation (30) and a mean figure for μ_2 equal to 0.135 was derived. It is possible to derive μ_1 from the theoretical equation (22); however, since the validity of the theory was actually being examined, this should not be used as a basis for deriving the coefficients.

From Bentley's figures and the experiments with the tilting table described above, and illustrated in Fig 9.4, a mean value for μ_1 of 0.125 was adopted; similarly a value for μ_2 of 0.135 was used. If a heavy addition of oil was applied to the trick or cams, then the coefficients of friction would have to be remeasured. Most of the experiments detailed in chapter 8 were carried out under conditions of light oiling.

9.4 Analysis of the Yarn Friction over the Verge and the Needle.

The apparatus detailed in Fig 7.4 was used to measure the friction build-up in tension as yarn passed over the needle and verge elements. The needle, verge, and yarn used in these friction measurements were the same as those used throughout the experiments detailed in chapter 8 and the experimental method used for measuring the friction was the same as that detailed in section 7.3.

The measurement and analysis was done as a final year undergraduate project by D.E. Smith[49] undertaken under the supervision of Professor G.R. Wray and the Author. He measured the input and output yarn tension over an element clamped in a vice, for a range of wrap-angles and yarn speeds. Early on in the work he found that small measurement errors were greatly amplified, and that those led to considerable inaccuracies when applied to the published theoretical formulae. He applied statistical analysis to the results, and derived an equation of the form :-

$$\frac{T_2}{T_1} = e^{K\theta^{\gamma}\left(r/T_1\right)^{1-n}} \quad . \quad . \quad . \quad . \quad (31),$$

where K = a constant dependent upon yarn speed,
and γ and n = constants,
r = bollard radius,
θ = wrap angle,
T_2 = outgoing yarn tension,
T_1 = ingoing yarn tension.

K has the form :-

$$K = Ae^{-\eta s} \quad . \quad . \quad . \quad . \quad (32),$$

where A and η are constants,
and s is the yarn speed.

The constants in equation (31) were measured as

n = 0.912 for the 0.559 mm thickness verge,
and n = 0.808 for the 0.432 mm and 0.330 mm thickness needles.

The variation of K with speed was found to be relatively small and, for the theoretical analysis detailed in section 9.6, it was considered permissable to treat K as a constant, i.e. :-

K = 0.628 for the 0.432 mm needles
and K = 0.493 for the 0.559 mm verge.
γ = 0.8052 for the 0.432 mm needles.
and γ = 0.553 for the 0.559 mm verge.

The close degree of correspondence between the

experimental values of input and output yarn tension over the verge, and the theoretical values derived from Smith's equation are shown on Figures 9.5 and 9.6.

9.4.1 Errors involved in using Amonton's Law.

The equation (31) derived by Smith is much more complex than the simple relationship derived by Amonton. For this reason it was important to determine how accurate Amonton's equation was, and if it could be used under the particular circumstances of this experimentation. Amonton's equation is expressed in the following well-known form :-

$$\frac{T_2}{T_1} = e^{\mu\theta} \quad . \quad . \quad . \quad . \quad . \quad (33),$$

where T_2 = output yarn tension,
T_1 = input yarn tension,
μ = yarn-steel coefficient of friction,
and θ = yarn wrap angle.

From equation (33) it can be shown that :-

$$\log_e\left(\frac{T_2}{T_1}\right) = \mu\theta \quad . \quad . \quad . \quad . \quad . \quad (34).$$

If equation (34) is plotted against θ, the wrap angle, a straight line of slope μ should be obtained, but the experimental results displayed in Fig 9.7 clearly show a divergence from Amonton's Law. If a mean straight line is drawn through the results on Fig 9.7 a typical value using this line would be :-

$$\text{when} \quad \theta = 160^\circ \quad \log_e\left(\frac{T_2}{T_1}\right) = 0.635.$$

However, on the graph the maximum error using the mean line, at $\theta = 160^\circ$ is when $T_1 = 60.0$ gf, then from the correctly plotted graph :-

$$\text{when} \quad \theta = 160^\circ \quad \log_e\left(\frac{T_2}{T_1}\right) = 0.475 \text{ for } T_1 = 60 \text{ gf}$$

Using this mean straight line approximation to the experimental results :-

then T_2 = 113 gf for T_1 = 60 gf

although the correctly plotted value was :-

T_2 = 96 gf T_1 = 60 gf

This clearly shows that Amonton's law is not strictly applicable for the prediction of knitting tensions.

9.4.2 Effect of the Old Yarn Loop and the Shape and Thickness of the Verge upon the Frictional Forces.

For the reasons given below it was decided that the author should re-examine Smith's results for the verge :-

(i) An examination of Smith's model of the verge showed that at the point where the yarn passed over it, it was thicker than the actual machine-verge i.e. 0.552 mm instead of an average figure of 0.443 mm. It was also noticed that the needle surface was rounded considerably more than what was considered to be the normal rounding of a machine verge due to wear. A microscope was used to examine the surface of the machine verges at the position where the yarn loops passed over them. It was found that the majority, including the verge transducer itself, were rounded due to wear only at the corners, the shape being as shown in Fig 9.8.

(ii) A close observation of the loop drawing process showed that the yarn passing over the verge also made contacts with the old yarn loop in the manner shown in Fig 9.8. The results obtained from Smith's yarn-friction apparatus (Fig.7.4) were unrepresentative because they

did not include the effect of this yam-to-yarn contact over the verge.

To test the effect of the old yarn loop, a model verge was made. Using a microscope the surface of the model verge was rounded to the same extent as the verges on the knitting machine. The model was also made to the same hardness and material as a machine verge, and is illustrated in Fig 9.9.

During the loop-forming process the majority of the wrap angles around the needles and verges approximate to 180^{o} except at the beginning of the knitting zone. It was difficult to achieve 180^{o} wrap on the friction apparatus due to mechanical interference between the measuring heads, and the closest angle that could be obtained was 173^{o}; this was considered, however, to be an adequate approximation to the practical angles.

An experiment showed that, for 173^{o} wrap, the tension increase as the yarn passed over the old loop and verge, was less than when it passed only over the verge. However, the tensions were considerably higher than those obtained by Smith for his verge. It was found that, when the experiment was repeated at wrap-angles below 160^{o}, the results with and without the old yarn loop around the verge were very similar. These results are graphically plotted in Fig 9.10.

The old yarn loop was removed and a series of experiments were undertaken to determine the effect of the surface shape of the verge upon the forces. These results are plotted in Fig 9.11. Although there was some variation in the traces it was clear that as the verge surface became more rounded the braking effect was reduced.

A series of experiments were carried out to examine the effect of verge thickness upon the friction forces. First, a series of results were obtained with a 0.600 mm thickness verge. It was then reduced in thickness and another set of results was obtained. A large number of different thickness verges were examined and the graphical results are shown in Fig 9.12. This experiment was difficult to control accurately, because the surface of each verge unavoidably changed slightly after each successive reduction in thickness. The experiments suggest that as thickness is increased the braking effect is lessened, and this is contrary to that predicted by the equation (31) derived by Smith. It is possible, however, that the results may not be representative due to the inevitable difference in the surfaces after each reduction in thickness.

9.4.3 Conclusions to Yarn Friction Experiments.

A great many factors obviously influence the frictional build up in tension as yarn passes over the verge and needle elements, and it is impossible to derive an equation with anything but very limited application. It is obviously important to understand the mechanism of yarn friction and the parameters that influence it; however, for knitting measurements, where the primary interest in these frictional relationships is entirely directed to forming a basis for further examination of the loop-forming process, then more worthwhile results could probably be achieved by building a simple yarn-friction testing device. Thus, a range of measurements could be carried out under realistic conditions and the friction results from the experimental graphs could be used as a basis for examining the loop formation.

The results of Smiths work, and subsequent experiments

conducted by the author, showed that for the particular test yarn passing over the verges and needles, Amonton's law was not accurate; approximately 10% error occurred when predicting the frictional increase in tension for the example in section 9.4.1.

An interesting result was the effect of the verge surface in that a rounded edge offered less frictional resistance; consequently, if the vertge top was rounded to the same extent as the needle, then the frictional resistance should be much less than at present. In practice, the measurements indicated that the build-up in tension over the machine verge shaped as in Fig 9.8 was considerably higher than that on the needle.

The effect of the yarn-loop being cast-off over the needle head seemed to cushion the effect of the verge corners at wrap angles approaching 180^{o}. When the old loop was round the verge, see Fig 9.9, the output tensions were lower than when there was no old yarn loop. The cushioning effect of the old loop disappeared as the wrap angle became less than 160^{o}. Results obtained when the needle thickness was increased showed a reduction in force level; this was contrary to that expected from the equation(31) derived by Smith. However, the experiment was subject to a possible error because it was difficult to control the surface properties accurately after each reduction in thickness.

9.5 Comparison between the theoretical prediction of Cam-force and the Experimental Results.

If the yarn input to the needles is withdrawn the needles still pass through the cam system without drawing a loop. Equation(22) can then be simplified by making $f(x) = O$:-

Therefore :-

$$R = \frac{F + P + \mu_1 Q - mg \pm mv^2\left(\frac{d^2y}{dx^2}\right)}{\cos\theta\,(1 - \alpha\mu_1\mu_2) - \sin\theta\,(\mu_2 + \alpha\mu_1)}. \qquad (35),$$

The nomenclature in equation (35) is defined in Fig 9.2.

The inertial term analysed in section 9.2.1 is positive for needle acceleration and negative for needle deceleration.

For a needle running in a trick which contains very little oil, the viscous resistance F is negligible. If the impact point is close to the cylinder then α is very nearly equal to 1.

Equation (35) can then be further simplified :-

$$R = \frac{P + \mu_1 Q - mg \pm mv^2\left(\frac{d^2y}{dx^2}\right)}{\cos\theta\,(1 - \mu_1\mu_2) - \sin\theta\,(\mu_1 + \mu_2)} \qquad (36)$$

A good approximation to $P + \mu_1 Q - mg$ can be made by measuring the force required to pull the needle vertically in the trick so that it moves at a constant slow upward velocity. A standard 0.443 mm needle was fitted in a dry machine trick. A length of yarn was then tied to the needle hook and the yarn was pulled steadily, raising the needle in its trick. The tension in the yarn was measured using a calibrated Rothschild head, whose output was passed to the Tektronix oscilloscope. As the needle was pulled steadily upwards, the yarn tension, and hence the force required to lift the needle, was displayed on the oscilloscope screen. The photographic trace of the results is shown by Diagram I in Fig 9.13, and from this the value of $P + \mu_1 Q - mg$ was measured; for the 0.443 mm needle under test it was equal to 46 gf. A trace was then taken of the vertical and horizontal cam-forces under the conditions of no yarn in the hook and very little oil in the trick, and this is shown in Fig 9.13, Diagram II.

Initially, when the needle is on the linear portion of the cam $m v^2 \left(\frac{d^2y}{dx^2}\right) = 0$ Equation (36) was evaluated under the following conditions :-

$$\mu_2 = 0.135,$$
$$\mu_1 = 0.125,$$
$$\theta = 49^{\circ},$$
and $$P = 46 \text{ gf}.$$

From the calculation the following values were determined :-

Reaction force, R,	= 101 gf,
Horizontal Component of Reaction force, R_x,	= 85 gf,
Vertical Component of Reaction force, R_y,	= 56 gf.

The calculation was then extended to account for the needle motion around the radial portion at the base of the stitch-cam. A greatly enlarged accurate drawing was made of the radial portion, and a reproduction of essential parts of this is shown in Diagram I Fig 9.14. The larger diagram was subdivided into a number of small intervals and the reaction force R in units of gf was evaluated for each interval using the equation :-

$$R = \frac{46 - mv^2\left(\frac{(y-y_c)^2 + (x_c - x)^2}{(y-y_c)^3}\right)}{(0.983)\cos\theta - (0.26)\sin\theta} \quad .(37).$$

A typical trial solution is shown below

at $V = 8.92$ in/sec (0.27 m/sec)
$m = 0.67$ g
$r = 0.0625$ in. (1.6 mm)
and $\theta = 30^{\circ}$.

then $R = \frac{46 - 3.62}{0.721} = 58.7$ gf

and the vertical component of R = 47 gf
and the horizontal component of R = 36 gf

A theoretical plot of the cam-force was drawn and a reproduction of this drawing is also shown in Fig 9.14, superimposed over a typical experimental result. The experimental plot is an enlargement of the trace shown in diagram II of Fig 9.13. The experimental and theoretical results agreed closely both on the linear portion and the radial portion of the cams.

Further work concerning the radial cam termination is contained in section 23.2.

The work was further extended using the 0.406 mm needle. This needle was fitted in the same trick as originally used with the 0.443 mm needle and was very free, $P + \mu_1 Q - mg$ was measured at 22 gf only.

The theoretical results, together with a typical experimental result for the 0.406 mm needle are shown in Fig 9.16. The traces are again of closely similar forms.

At the particular conditions of the test, when there was no yarn in the hook and very little oil in the trick, the experimental and theoretical results corresponded very closely for both thicknesses of needle, and it was considered that the possibility, suggested in section 9.2, of a further extension of the theory using Barth's[30,48] analysis was unnecessary.

9.5.1 Effect of Moving the Impact Point Radially away from the Cylinder.

For the particular situation when the needle is not drawing a loop of yarn and there is little oil in the trick, equation (37) can be expressed in the form shown below :-

$$R = \frac{P + \mu_1 Q \pm mv^2\left(\frac{d^2y}{dx^2}\right) - mg}{\cos\theta\,(1 - \propto\mu_1\mu_2) - \sin\theta\,(\mu_2 + \propto\mu_1)} \quad . \qquad (38).$$

All the terms are defined in Fig 9.2 and section 9.2.1. If attention is confined to the linear portion of the cam, then $mv^2\left(\frac{d^2y}{dx^2}\right) = 0$ and equation (38) can be restated in the form :-

$$R = \frac{A}{\cos\theta\,(1 - \propto\mu_1\mu_2) - \sin\theta\,(\mu_2 + \propto\mu_1)} \quad . \qquad (39),$$

where $A = P + \mu_1 Q - mg$.

The reaction force R approaches infinity when :-

$$\cos\theta\,(1 - \propto\mu_1\mu_2) - \sin\theta\,(\mu_2 + \propto\mu_1) = 0.$$

Reorganising this expression,

R tends to infinity when $\propto = \frac{1 - \mu_2 \tan\theta}{\mu_1(\mu_2 + \tan\theta)}$ (40).

Using the friction values derived in section 9.3 i.e. $\mu_1 = 0.125$ and $\mu_2 = 0.135$, and using a 49^0 cam angle, equation (39) then reduces to the form shown below :-

$$R = \frac{A}{0.554 - 0.105\propto} \quad . \quad . \quad . \qquad (41).$$

In equation (22) $\propto$ had the form shown below :-

$$\propto = \frac{2a}{b} - 1$$

and $a = b + \lambda$

where λ = cam cylinder clearance,

and therefore $\propto = 1 + \frac{2\lambda}{b}$

b = 0.124 in. for a standard 0.443 mm needle.

Fig 9.17 is a graph of reaction force R against the cam-cylinder clearance, which clearly shows that as the cam is moved away from the cylinder the cam-force increases.

Experimental results detailed in section 4.6.4 showed that horizontal cam-force increased from 265 gf to 490 gf when the cam-cylinder clearance was increased from 0.15 mm to 3.05 mm. Since the experiment detailed in section 4.6.4 was carried out to very similar parameters to those used for the theoretical results detailed on the graph in Fig 9.17, the theory clearly shows a close correlation to experimental results. The force nearly doubles when changing the clearance from 0.15 to 3.05 mm. There is also agreement with the results obtained in section 8.5.6. The experimental results showed that a movement of 0.15 mm to 0.30 mm produced very small differences in the force level, and as can be seen the theoretical change in cam force shown in Fig 9.17 is only form 2.27A to 2.35A, (where A is the defined parameter for equation(39), such a slight difference would be difficult to observe on a photographic trace.

9.6 Comparison between the Theoretical Prediction of Yarn-Force and the Experimental Results.

A close observation of the loop-formation process using a sensitive magnifying glass showed that the effect of the old loop was to increase the wrap-angles around the needle heads and verges, and to necessitate the new yarn being formed into a loop having to pass over the old yarn loop. This is illustrated in more detail in Fig 9.8, and a discussion of the effect of the old yarn loop on the friction forces is detailed in section 9.4.2.

Using the experimental parameters specified in Fig 8.7(a),

three stages were drawn of the loop formation process, each showing the measuring verge advanced to the right by one-third of the needle pitch, assuming that the yarn is being supplied from the left. These three diagrams are reproduced in Fig 9.18. The yarn tensions over the needles were calculated using the results obtained from Smith's[49] report as detailed in section 9.4. The expression specified for a 0.443 mm needle was :-

$$\frac{T_2}{T_1} = e^{K\theta^{\gamma}(r/T_1)^{1-n}} \quad \ldots \quad (42)$$

where $n = 0.808$,
$K = 0.628$,
and $\gamma = 0.805$.

For the tension build up over the verge, the graphs in Fig 9.10 were used. The output tension for wrap-angles that were not graphically plotted on Fig 9.10, were obtained by interpolation, using the graphical results nearest to the desired wrap angle. The method used to calculate the tensions through the loop-forming process is illustrated by the example below :-

Initially, the analysis was confined to diagram (C) in Fig 9.18. If, as an initial hypothesis, it was considered that the yarn was robbed from needle positions IX and XII; then, the available yarn would be more than that required by needle VI to form a loop, and the yarn would have to flow over needle VI to the left, i.e. towards the supply direction. However, calculating the yarn tensions over the elements from the supply direction, it quickly became obvious that the tension near needle VI was far too low for it to be capable of robbing yarn from needles IX and XII, due to the large number of needle and verge contacts. This hypothesis had to

be revised since the cam-slope at needle position IX was one-half of the slope at needle position VI, and therefore needle XII was only capable of supplying half the yarn requirements of needle VI to form its loop. The needle in position VI must thus draw yarn from both the supply and the back-robbing directions. A quick calculation of the tension build-up on the supply side verified that this hypothesis of the loop-drawing process was plausible. However, it was still necessary to define the predicted tensions around needle position VI, for example, in diagram (C) of Fig 9.18 the predicted tensions were 60 gf on the supply side, and 95 gf on the robbed side. The latter tension value of 95 gf on the robbed side is not immediately obvious and it is therefore necessary to offer a lengthier explanation. When a large number of diagrams were drawn there was always at least one in which the tensions could easily be determined throughout the process. Thus in Fig 9.18 it was easier to determine the tension in diagram (A), since it could be considered that motion over verge 7 has just stopped, this defining the output tension for needle position VII; from this, the tensions could be evaluated throughout the process, and the position when the yarn-tension dropped to the take-down value, known as the release point[22], could also be determined. Once the tensions were defined on one of the diagrams and especially when the release point was known, it was possible to predict the tensions on the other diagrams. For example, as the verge moved between positions 10 and 11 in diagram(A), the tension on the output side of the verge changed from 51.5 gf to 7 gf. The verge positions 11 and 12 in diagrams (B) and (C) were equally spaced between positions 10 and 13,

and it was therefore possible to approximate the yarn tension on the output side of the verges at 11 and 12 by proportioning the tensions according to the verge distance from the original position 10. Obviously this provided only approximate tension values; however, once these were known, using the flow directions in diagram (B) and (C) and the position of the release point in diagram (A) they could be improved to suit the dynamic conditions of each diagram. There was no other obvious method of calculating the tensions throughout the loop forming process, and although the method used was quite quick and easy there were basic difficulties in calculating the tensions; these are detailed below :-

(i) The verges differed slightly in shape due to their differing amounts of wear. It was therefore doubtful that the frictional relationship for the tension build-up should be the same for every verge.

(ii) The method of determining the yarn-flow was approximate and took little account of yarn-stretch.

(iii) The analysis was dependent upon the fact that the needle accurately followed the cam-profile, defined by the drawing (Fig 4.3).

Figure 9.19 shows the experimental yarn-tension plot, which is an enlargement of the trace shown in Diagram (II) Fig 8.7 (b) of section 8.5.1. Superimposed upon the experimental plot are the theoretical forces on the verge evaluated from the yarn-tension shown on Fig 9.18. The method of evaluating the vertical force on the verge was to add the tensions on each yarn arm acting on the verge and correct these for their angular disposition.

The theoretical and experimental plots showed a close

similarity in shape. However, one trace was displaced with respect to the other, since it was impossible to predict with any precision the position of the verges and needles, at which the first verge, just contacted the yarn and began to register a force, an error of merely a few thousandths of an inch leads to an apparently large displacement between the two traces. The close similarity between the traces proved that the major component of the tension increase occurred as the yarn passed over the verges. It was also obvious that the tension dropped to the take-down value within two verge-pitches of the bottom of the stitch-cam.

The input yarn-tension was measured using a Rothschild head. Since the head had a braking effect upon the yarn, the tension output from the Rothschild, and the input into the needles was corrected using the calibration graph shown in Fig 7.5. The input tensions in Fig 9.18 were adjusted for the force fluctuation which had previously been analysed on Fig 8.3. For example on diagram (B) Fig 9.18, needle II has just snatched the yarn and the input tension is therefore high at 23 gf.

The input yarn tensions on Fig 9.18 may seem generally high; however, friction measurements carried out on the final guide illustrated in Fig 7.2 (a) indicated that the tension built up more than double the value over the final guide. The measurements were obtained by clamping the guide in the vice of the friction apparatus, Fig 7.4, yarn being then run through the guide at typical angles, and the input and output tension measured using the Rothschild heads. It was found that 13 to 15 gf mean level output tension was compatible with an input yarn tension of only 4.5 to 5 gf. The implication of the measurements were that although the feeder input

tension may be low the actual tension input to the needles could be much higher. The analysis was repeated under similar conditions to the earlier example, except that the stitch-draw was increased to 2.74 mm. One of the diagrams showing the theoretical yarn-flow and tension throughout the loop forming process is shown in Fig 9.20. The experimental and theoretical plots are superimposed and shown on Fig 9.21. During the experiments it was noticed that the transducer verge tended to cut-off before reaching the high force levels. Allowing for the cut-off the close degree of similarity between the theoretical and experimental traces is clearly demonstrated.

The analysis was again repeated under similar conditions as in Fig 9.18, except that the take-down tension was increased. One of the diagrams showing the yarn flow direction and the tensions in each yarn arm is given in Fig 9.22, and the experimental and theoretical plots are shown superimposed in Fig 9.23. The shape of the theoretical plot did not correspond very well to the experimental plot, especially in the region of the second peak. The method of analysis was very susceptible to small errors, for example, if instead of a change of 5 to 6.5 gf over verge 3 in Fig 9.22, the actual tension increase was 5 to 8 gf then the diagrams, Fig 9.22, would be modified and the shape of the theoretical plot would become that indicated at (2) in Fig 9.23.

The method of analysis was subject to considerable errors and approximations, but it was difficult to see how any other method could be used. Taking due allowance for the difficulties, a fairly close approximation was achieved. The interesting features of the traces are the clear demonstration of robbing-back, the rapidity at which the

tension falls-off after the base of the stitch cam, and the very much larger proportion of the braking force imposed by the verge upon the yarn, rather than that by the needle.

9.7 Effect of Oil upon the Cam-Force.

In section 9.2.3 Black's theory[29] for the viscous resistance of the oil was examined. The expression he derived had the form :-

$$F = Mv \quad . \quad . \quad . \quad . \quad . \quad (43),$$

$$M = \frac{A\rho \tan\theta}{d} \quad . \quad . \quad . \quad (44).$$

Extensive work on the effect of oil was not carried out in this project, and for further analysis, especially concerning the effect of oil viscosity, Black's thesis[29] should be referred to. However, an experiment (section 8.5.9 and Fig 8.25) was carried out examining the effect of the machine speed upon the cam force after a heavy soaking with Vickers Spotless B.N.O. Oil. The experiment showed a linear relationship that agreed with the prediction contained in equation (43), assuming M does not vary with machine speed.

9.8 Effect of the Yarns Presence upon the Cam-Force.

There was a considerable difference between the measured cam-force when the needles were knitting a yarn and when they were passing through the cams without knitting a yarn. When the yarn was being pulled into a loop there was a force exerted on the cam by the yarn tension acting on the needle hook. As the stitch-draw increased the force increased rapidly and soon became very large compared to the trick forces. However, when small stitches were being drawn, a force which seemed closely related to the shape of the needle head grew in magnitude as the stitch was further reduced in size. The only possible explanation was that the small loop

being cast-off had to expand and stretch to pass over the needle head. The cam-force during loop-formation, and the effect of the needle head shape upon the force is detailed in the following two sections.

9.8.1 Effect of the Yarn upon the Cam-Force during Loop Formation.

The equation derived in section 9.2 for the cam needle force, R, had the form :-

$$R = \frac{F + P + \mu_1 Q - mg + f(x) \pm mv^2\left(\frac{d^2y}{dx^2}\right)}{\cos\Theta\left(1 - \alpha\mu_1\mu_2\right) - \sin\Theta\left(\mu_2 + \alpha\mu_1\right)} \quad . \qquad (45).$$

When the cam-cylinder clearance is small and only a small amount of oil is added to the trick then equation (45) can be simplified to the following form :-

$$R = \frac{P + \mu_1 Q - mg + f(x) \pm mv^2\left(\frac{d^2y}{dx^2}\right)}{\cos\Theta\left(1 - \mu_1\mu_2\right) - \sin\Theta\left(\mu_1 + \mu_2\right)} \quad .$$

Using the same needle and trick as used in the examination detailed in section 9.5. The equations for R in units of grammes force can be written in the form shown below:-

$$R = \frac{46 - mv^2\left[\frac{(y-y_c)^2 + (x_c-x)^2}{(y-y_c)^3}\right] + f(x)}{\cos\Theta\left(1 - \mu_1\mu_2\right) - \sin\theta\left(\mu_1 + \mu_2\right)} \quad . \qquad (46).$$

The yarn-force $f(x)$ exerted upon the needle during loop formation was obtained from the theoretical tension shown in Fig 9.18 and the inertial term was calculated for a machine speed of 10 in/sec (0.25 m/sec). In Fig 9.24 diagram (A) shows the yarn-force component of the reaction-force defined by equation (47):-

$$\frac{f(x)}{\cos\Theta\left(1-\mu_1\mu_2\right)-\sin\Theta\left(\mu_1+\mu_2\right)} \quad \ldots \quad (47).$$

Diagram (B) in Fig 9.24 shows the non-knitting cam-force defined by equation (48) :-

$$\frac{46-mv^2\left(\frac{\left(y-y_c\right)^2+\left(x_c-x\right)^2}{\left(y-y_c\right)^3}\right)}{\cos\Theta\left(1-\mu_1\mu_2\right)-\sin\Theta\left(\mu_1+\mu_2\right)} \quad \ldots \quad (48).$$

Diagram (A) and Diagram (B) were added and the resulting curve is shown at Diagram (C). Superimposed upon Diagram (C) is a reproduction of the trace of experimental cam-force, diagram II Fig 8.7 (b), obtained under similar conditions as the theory. When compared the theoretical and experimental predictions agree closely. Other calculations carried out at different machine speeds also showed a close correspondence to experimental results.

9.8.2 <u>During Casting-Off over the Needle Head.</u>

When small yarn loops are being knitted, considerable force is exerted by the yarn upon the cams during the loop casting-off stage of the knitting process. For a stitch-draw of 1.70 mm and using a 0.443 mm standard needle, the clearance between a yarn loop and the needle shank, when the needle was at the yarn clearing height was measured by inserting a thin steel shim betweeen the shank and the loop. The clearance was measured as approximately 0.03 mm. If this yarn loop stretched as though it were a closed loop, i.e. in a similar manner to an elastic band, then the maximum amount of stretch in the loop of yarn as it passed over the head would

be approximately 23%.. A simple extension under load test for the yarn was carried out by hanging loads on a length of yarn, and this showed that when the extension approached 9% the yarn broke, and therefore the analogy with the elastic band is not true. Using a magnifying glass, a close examination of the fabric showed that some of the loops adjacent to the loop-forming region were slightly distorted, suggesting that robbing back occurs to allow for the casting off of a tight loop. A diagram of the loop structure is shown in Fig 9.25.

It was almost impossible to determine the tension in the yarn as it stretched over the needle head; but it was possible to relate the shape of the needle head to the force exerted upon the stitch cams by the cast-off loop.

Two traces of the cam-force were obtained, one with no yarn fed to the needle, and the other during normal knitting. The results on the first trace were subtracted from the trace for normal knitting. The diagram showing the subtracted force is given in Fig 9.26. The shape of the subtracted cam-force can be related to the yarn motion over the needle shank as demonstrated in Fig 9.26.

(i) The force increases as the yarn stretches in passing from position 1 to 9.

(ii) At position 10, the yarn relaxes a small amount as it contacts the decreasing thickness section just after the latch pivot.

(iii) At position 11 there is a sudden rise in tension as the loop is further stretched in passing over the latch. At position 11 the yarn is bent at such a large angle that the force required to draw the needle through the yarn is also large.

(iv) At positions 12, 13, and 14 the stretch continues, but the acute angle of the yarn decreases. The force tends to level out.

(v) As the loop continues stretching over the latch, a point is reached where the needle, just ahead of the needle shown in Fig 9.26 casts-off its loop. A quantity of low tension yarn is then available and this relaxes the tension in the highly stretched yarn passing over the latch.

(vi) As the yarn continues stretching, more yarn is robbed from the cast-off loop and this lowers the tension in the yarn being cast-off the needle shown in Fig 9.26.

The above work led to some interesting conclusions concerning the design of the needle head. It is generally considered that the width of the head restricts the size of the loop that can be knitted. However, by successful design it should be possible to produce a needle head that allows very small loops to be knitted. An idea for a needle head design untilising controlled robbing of yarn from the cast-off loop is detailed in chapter 10. As machine speed was increased the successive peaks tended to flatten out as shown in Figs 8.15 and 8.17 (b) in section 8.5.4. A possible explanation of this flattening of the cam-force trace could be the effect of yarn inertia. At high speed there is insufficient time for loop relaxation.

Conclusions to this chapter and this section of the work are given in chapter 10.

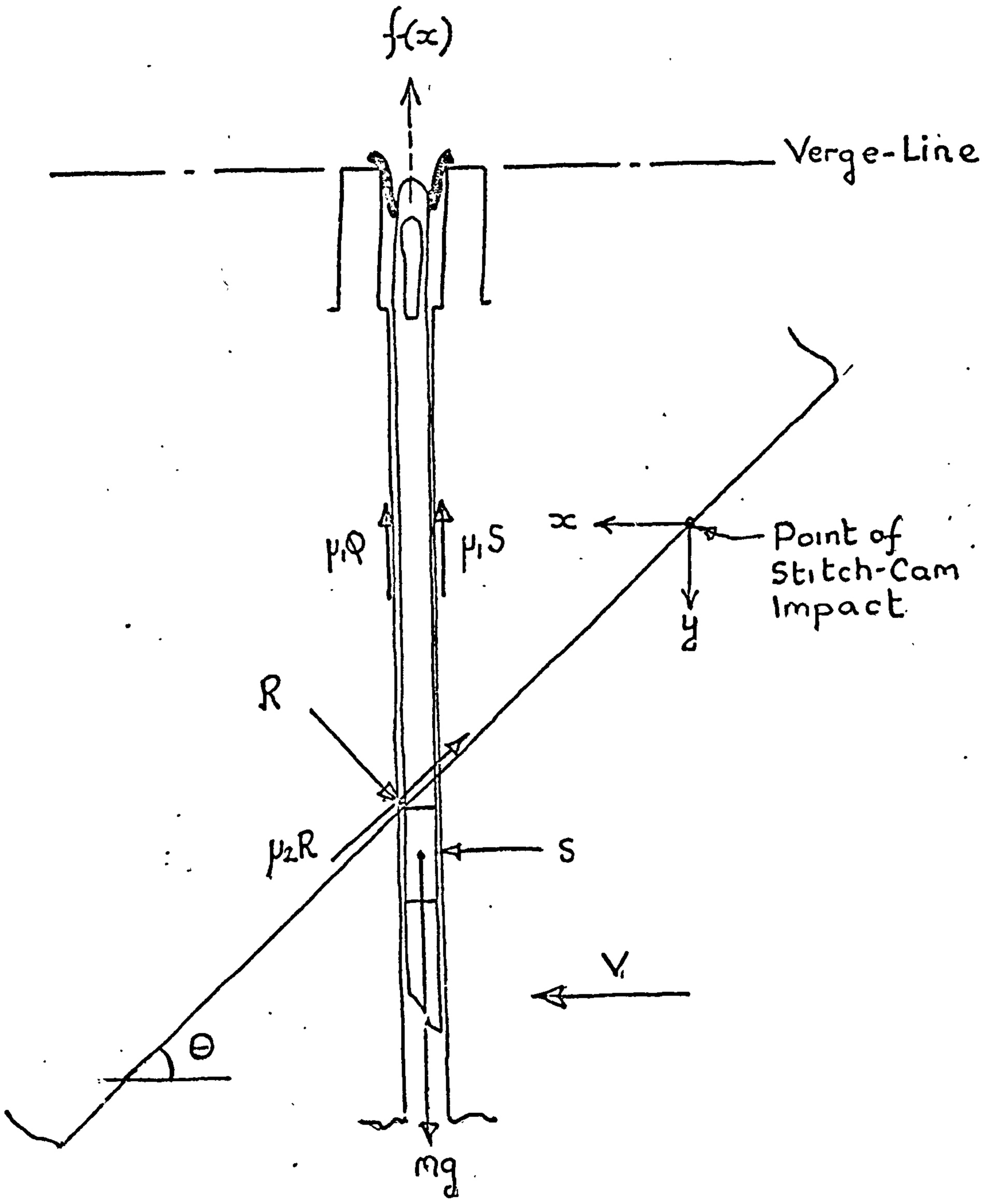

V = machine peripheral speed
f(x) = vertical component of yarn-force
Q = band-spring force.
S = side-reaction-force
μ_1 = coefficient of friction (trick to needle)
μ_2 = coefficient of friction (cam to needle)
mg = needle weight.
R = cam-needle reaction force.
θ = cam-angle.

FORCES ON NEEDLE AS IT MOVES DOWN STITCH-CAM.

FIG 9.1

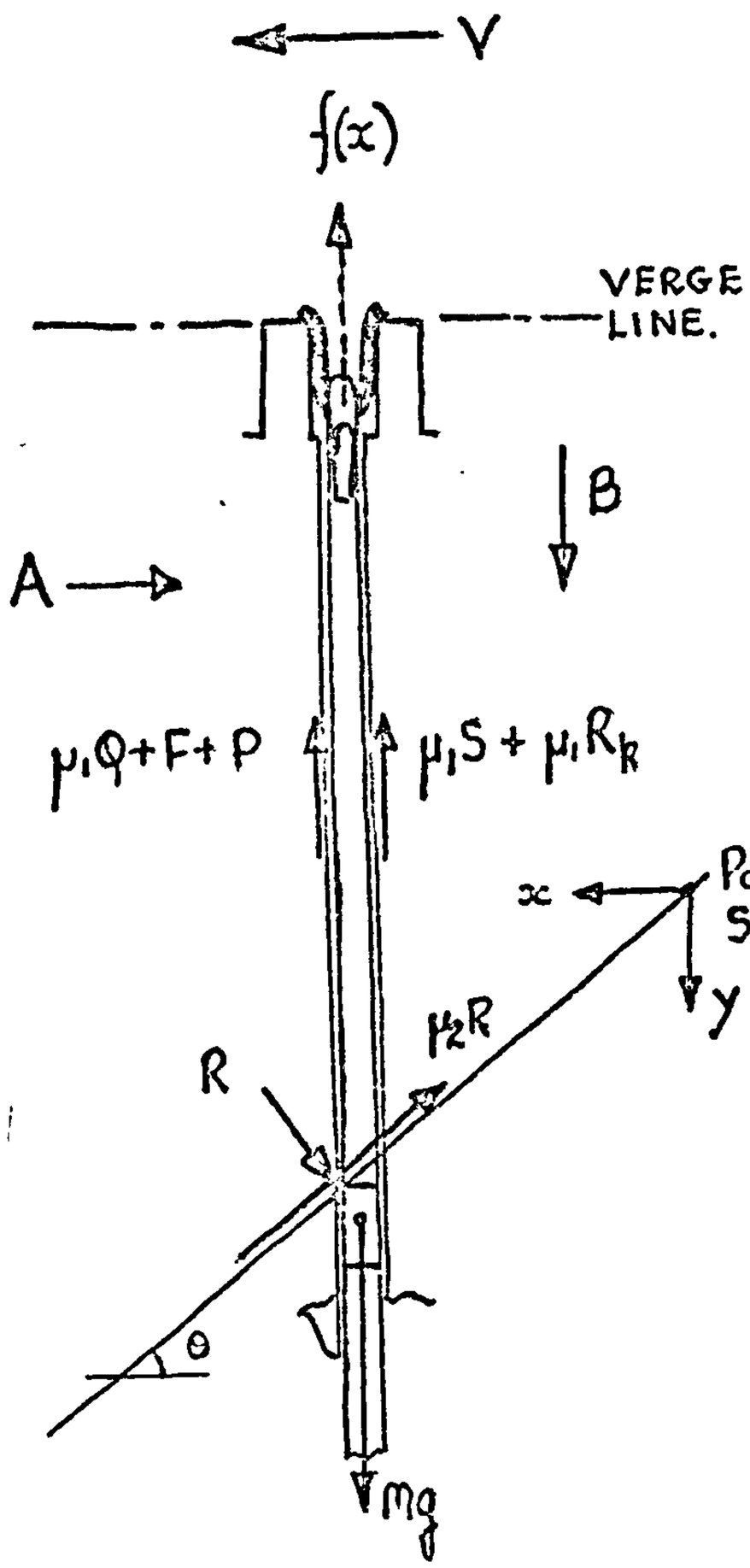

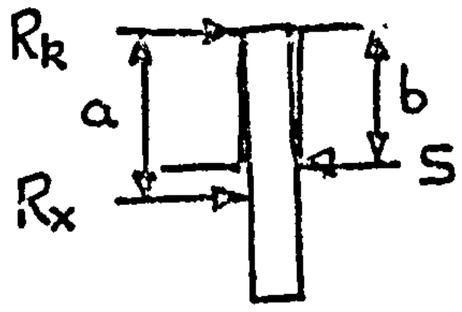

VIEW-B.

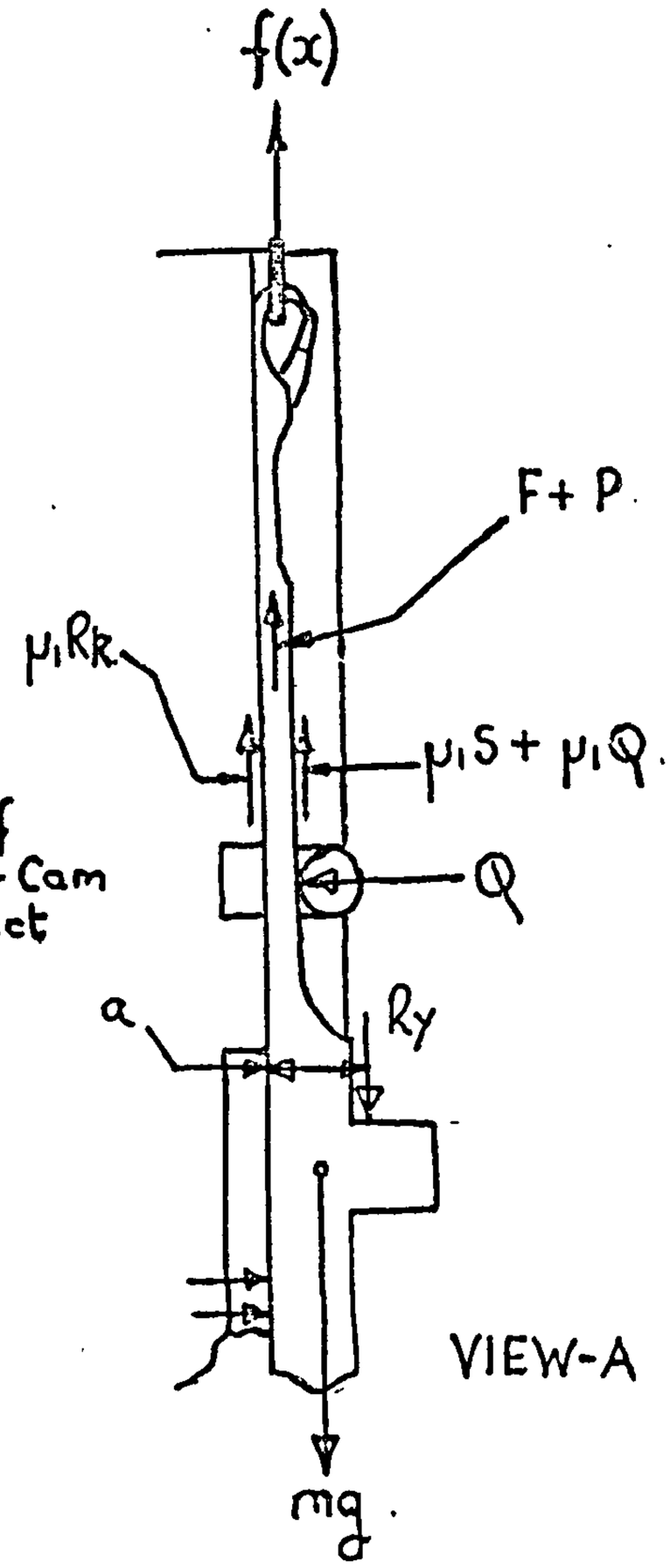

F = viscous-drag from oil.
P = trick-clamping force.
S = side reaction force
μ_2 = coefficient of friction (cam to needl
μ_1 = coefficient of friction (trick to needl
R = cam-needle reaction force.
R_x = horizontal component of R
R_y = vertical component of R.
R_k = side reaction force.
mg = needle weight.
a = reaction-force R moment arm
b = reaction-force S moment arm
Q = band-spring force.
V = machine peripheral speed

θ = cam angle
f(x) = yarn force

FIG 9.2

FORCES ON NEEDLE MOVING DOWN THE STITCH-CAM. (revised diagram)

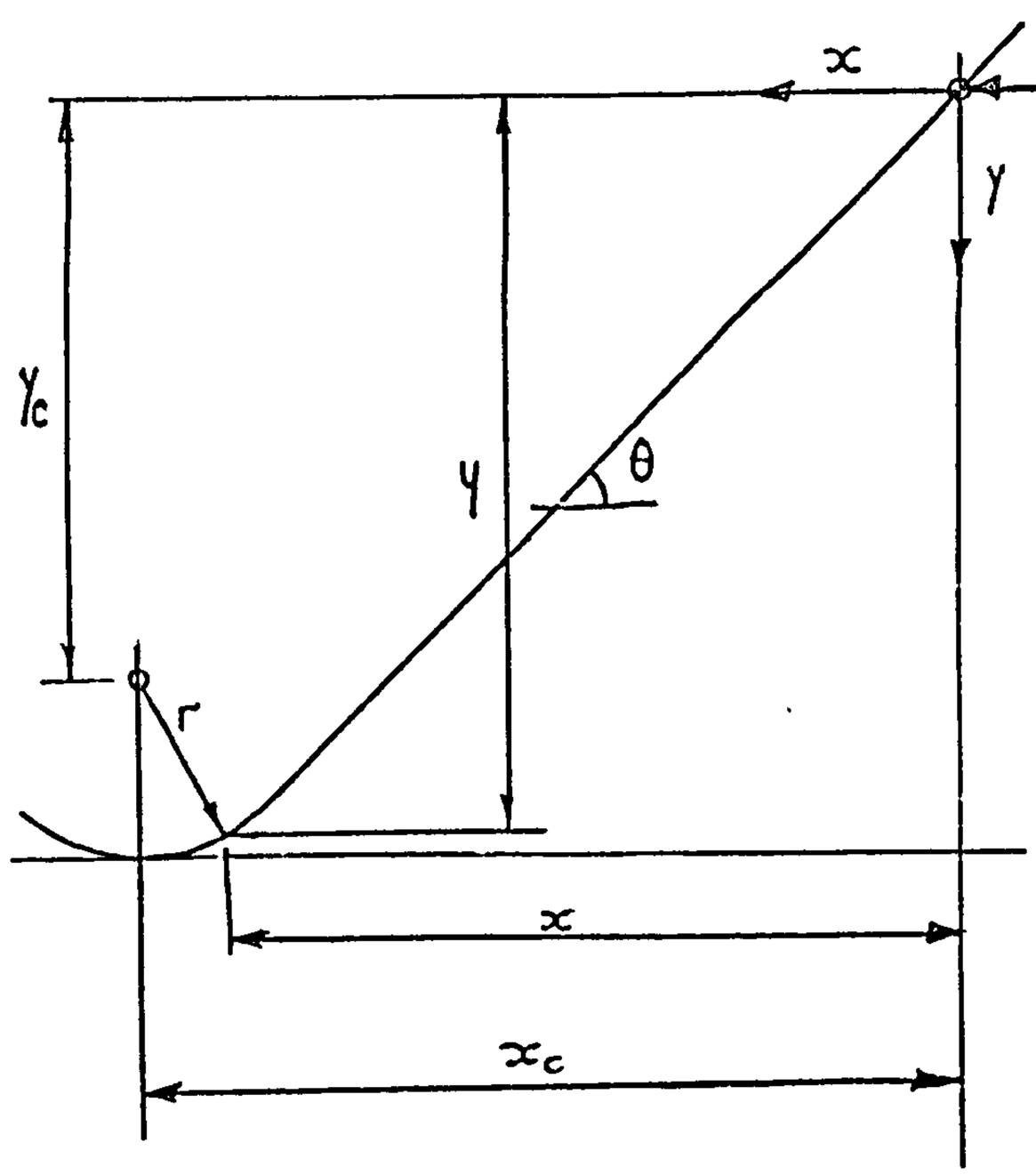

Using co-ords defined in Fig 9.2

On radial portion

$$(y - y_c)^2 + (x_c - x)^2 = r^2$$

$$\frac{dy}{dx} = \frac{(x_c - x)}{(y - y_c)}$$

$$\frac{d^2y}{dx^2} = -\frac{[(y - y_c)^2 + (x_c - x)^2]}{(y - y_c)^3}$$

$$\frac{d^2y}{dt^2} = -v^2 \left[\frac{(y - y_c)^2 + (x_c - x)^2}{(y - y_c)^3} \right]$$

CO-ORDINATES FOR RADIAL CAM - TERMINATION

FIG 9.3

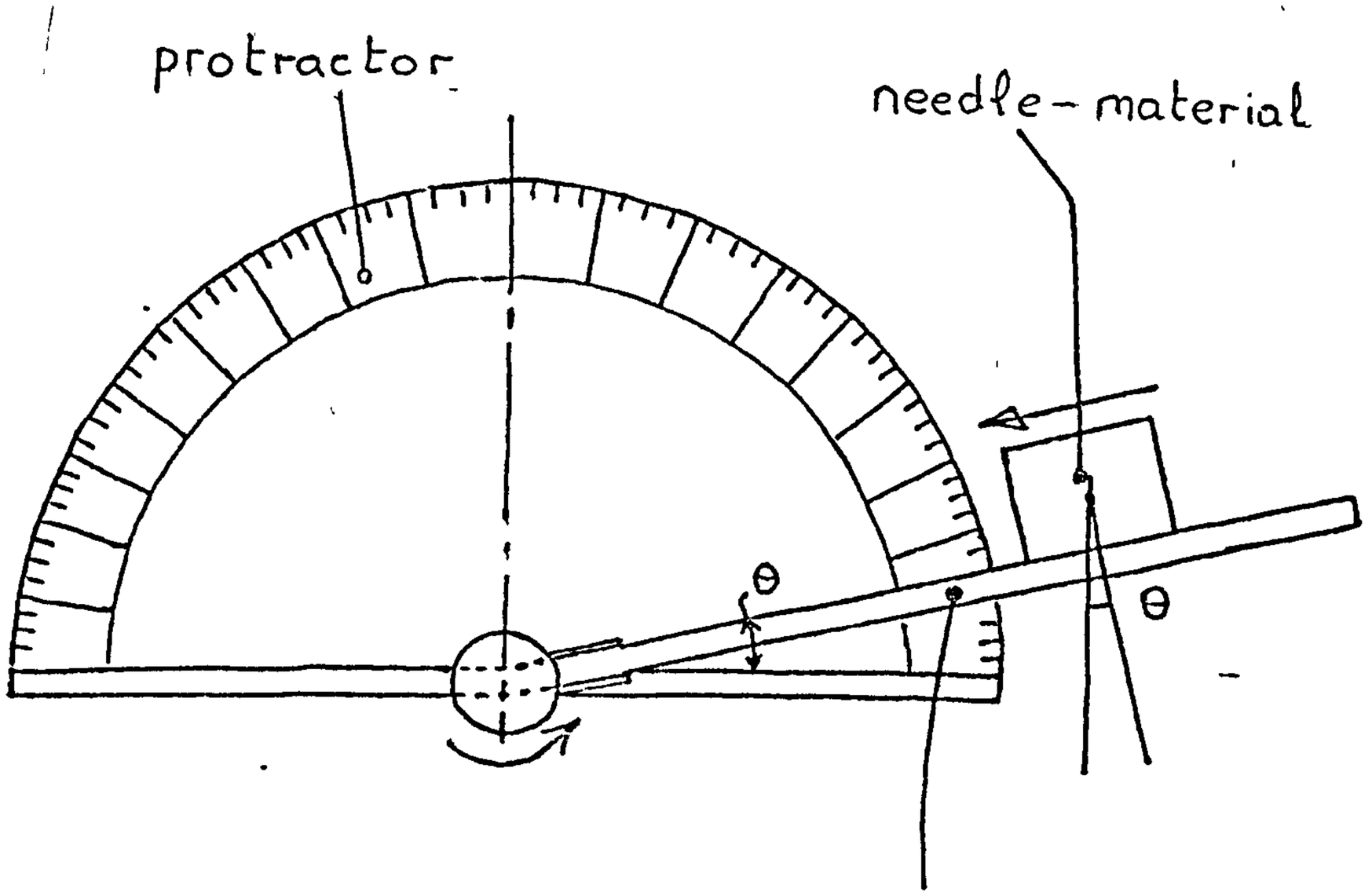

cam - material surface - polished - lightly oiled
trick - material surface - unpolished - smooth - oiled.
needle - material surface - polished.

MEASURING THE COEFFICIENTS OF FRICTION.

FIG 9.4

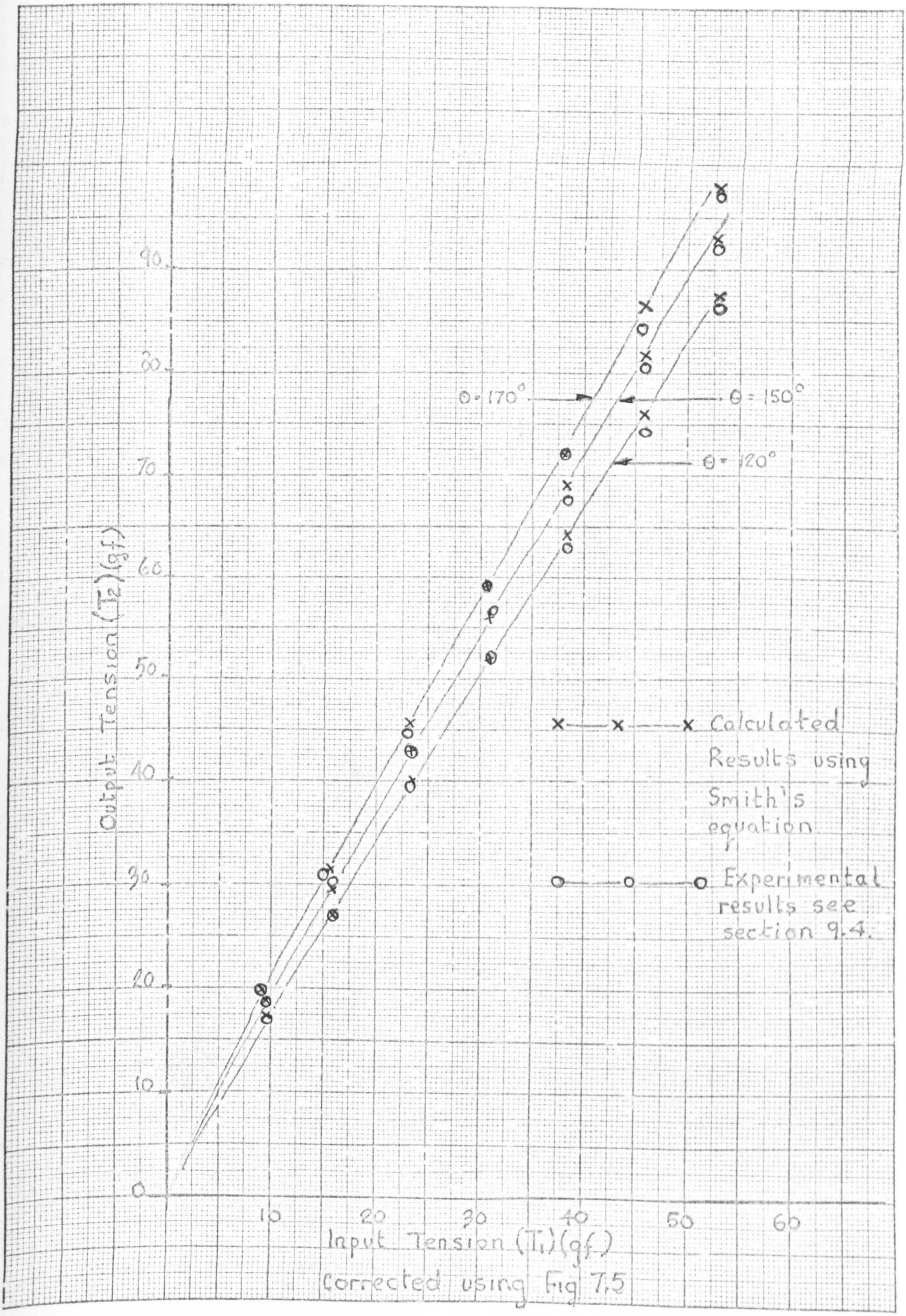

CALCULATED RESULTS OVER 0.559 mm VERGE

FIG 9.5

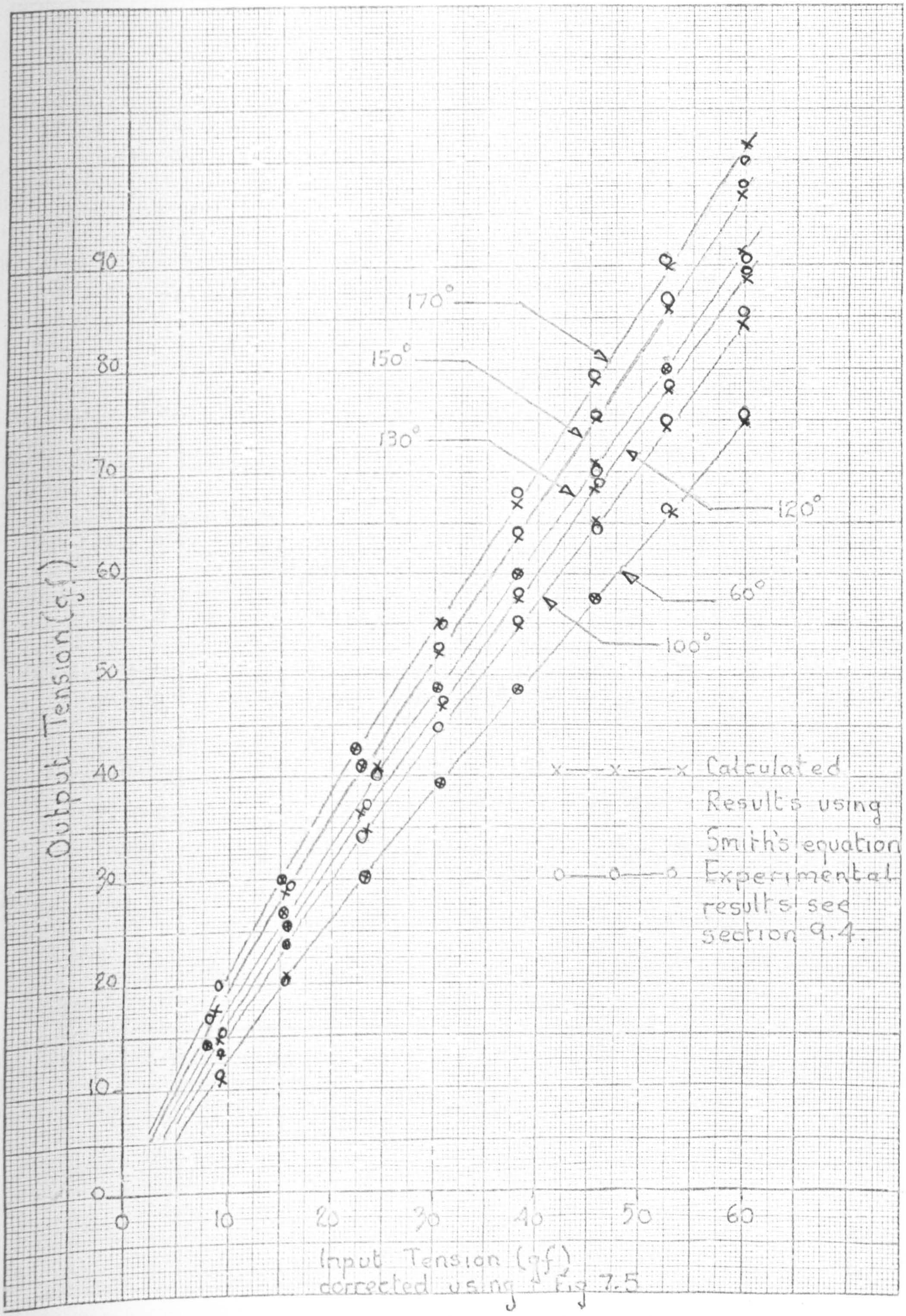

YARN INPUT AND YARN OUTPUT TENSIONS
CALCULATED RESULTS OVER 0.432 mm NEEDLE

FIG 9.6

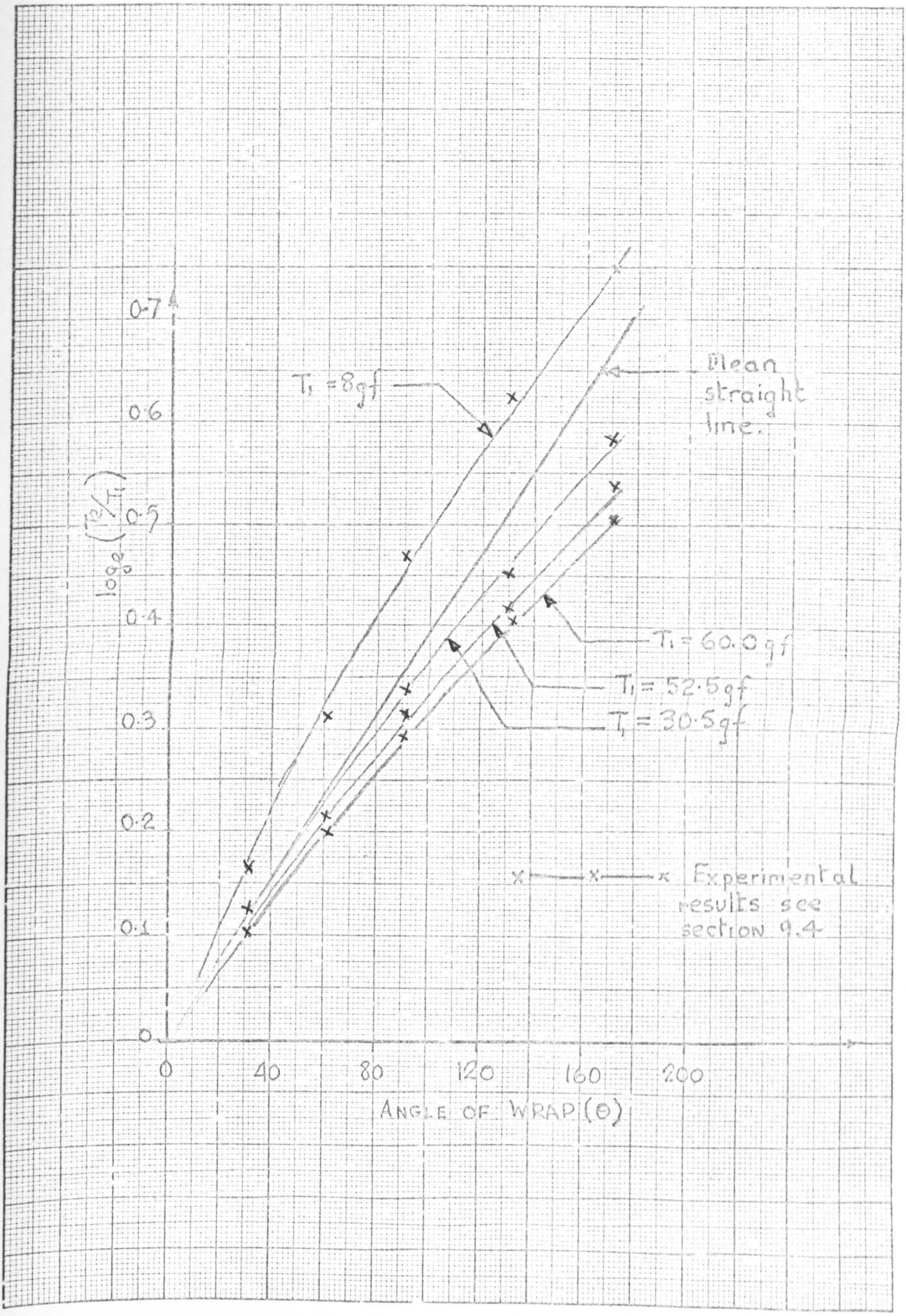

$\log_e\left(T_2/T_1\right)$ AGAINST ANGLE OF WRAP FOR 0.432mm NEEDLE

FIG 9.7

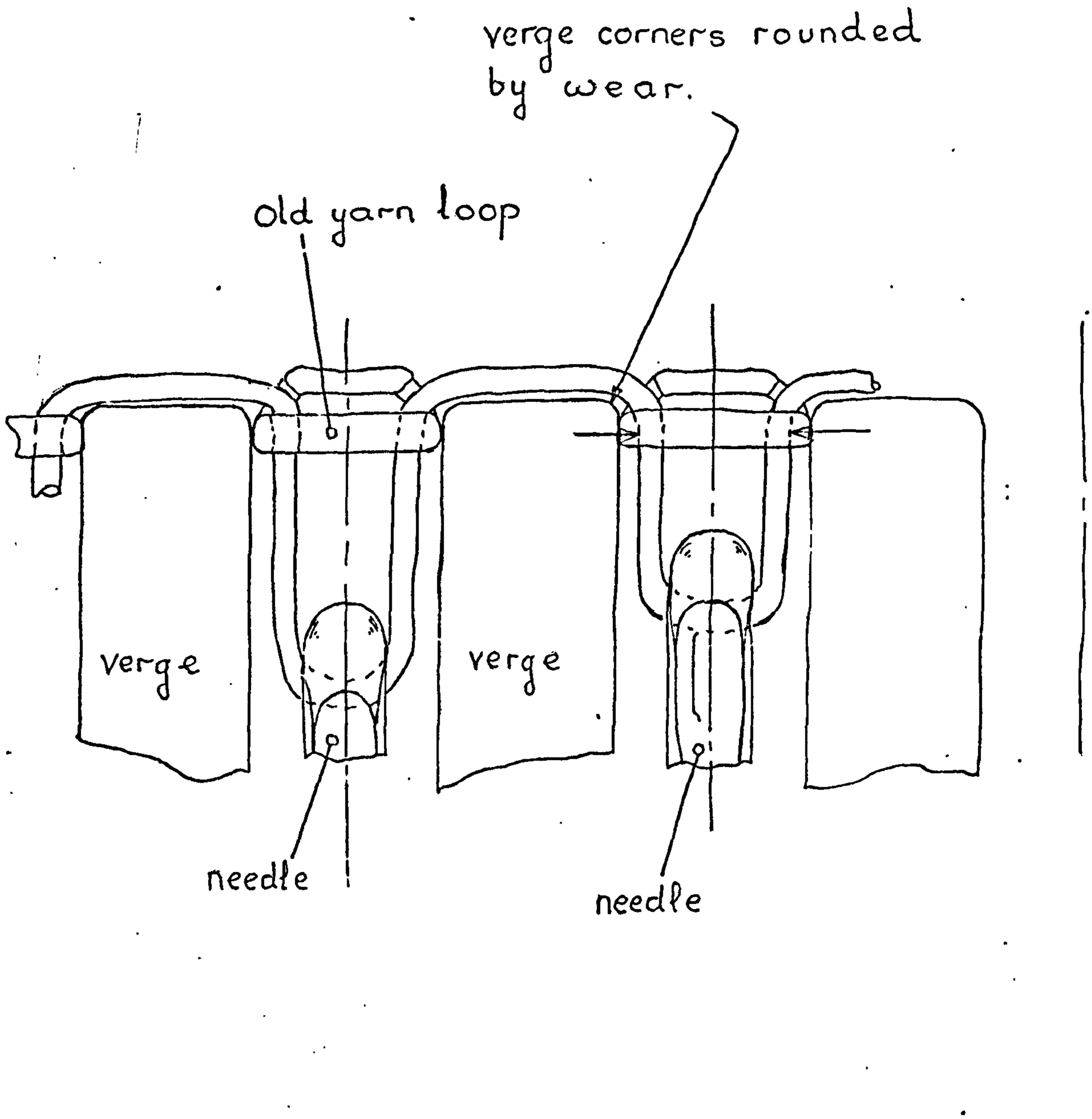

THE EFFECT OF THE OLD-YARN-LOOP UPON STITCH FORMATION.

FIG 9.8

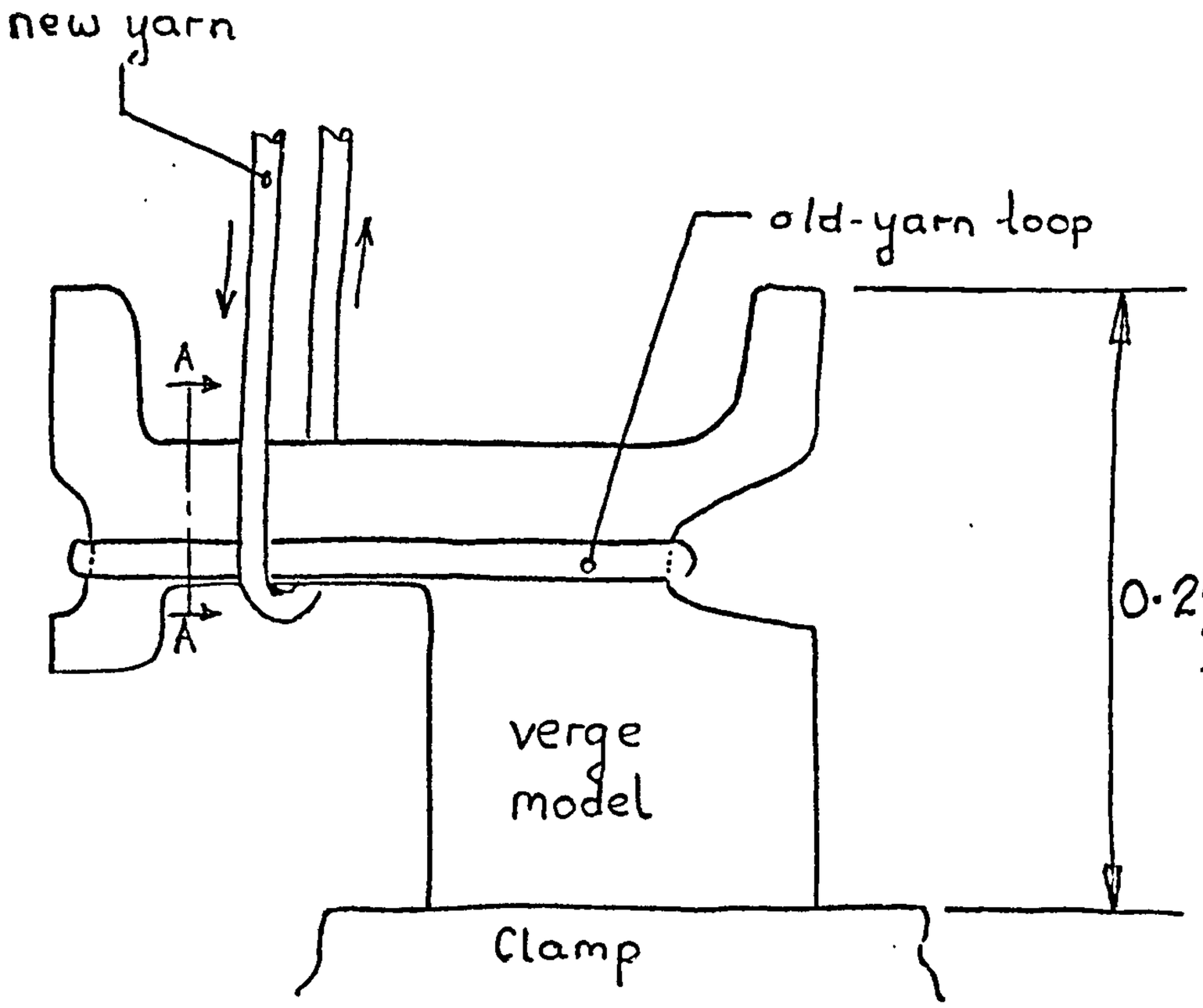

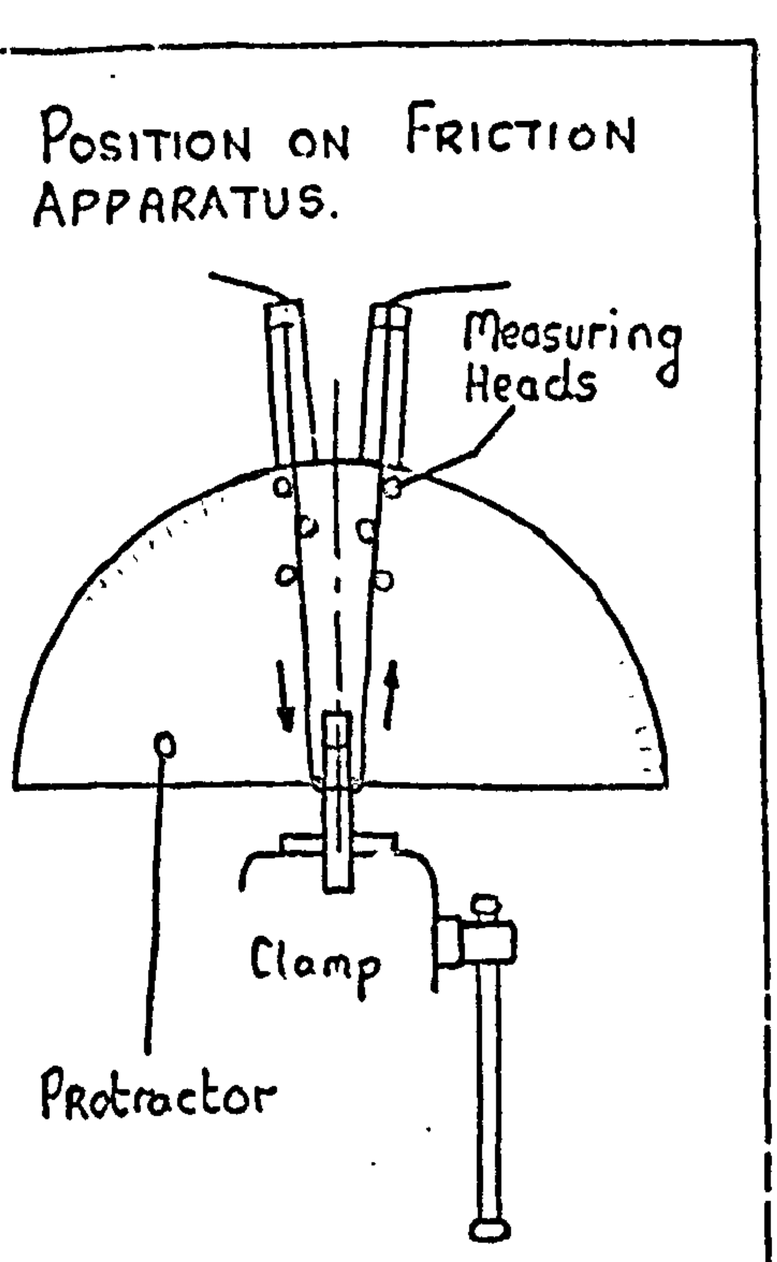

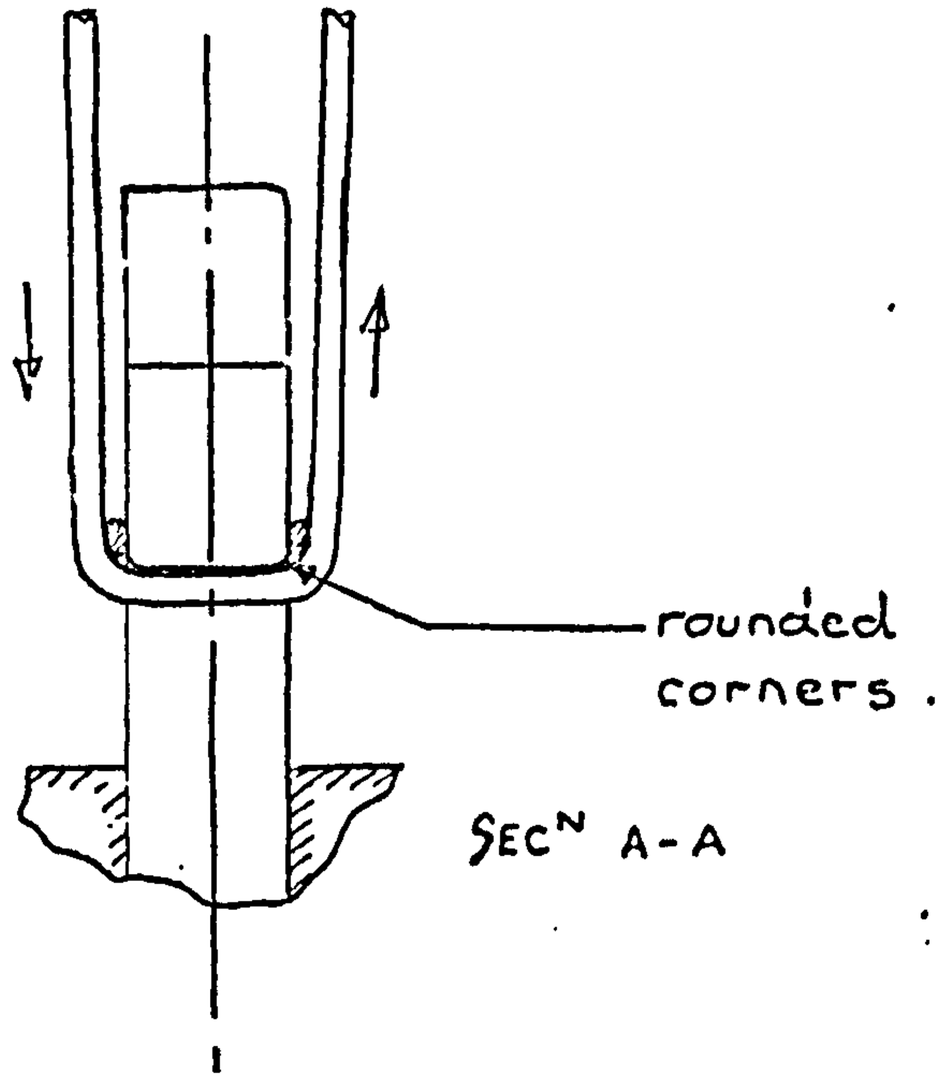

THE VERGE MODEL USED FOR FRICTION MEASUREMENTS.

FIG 9.9

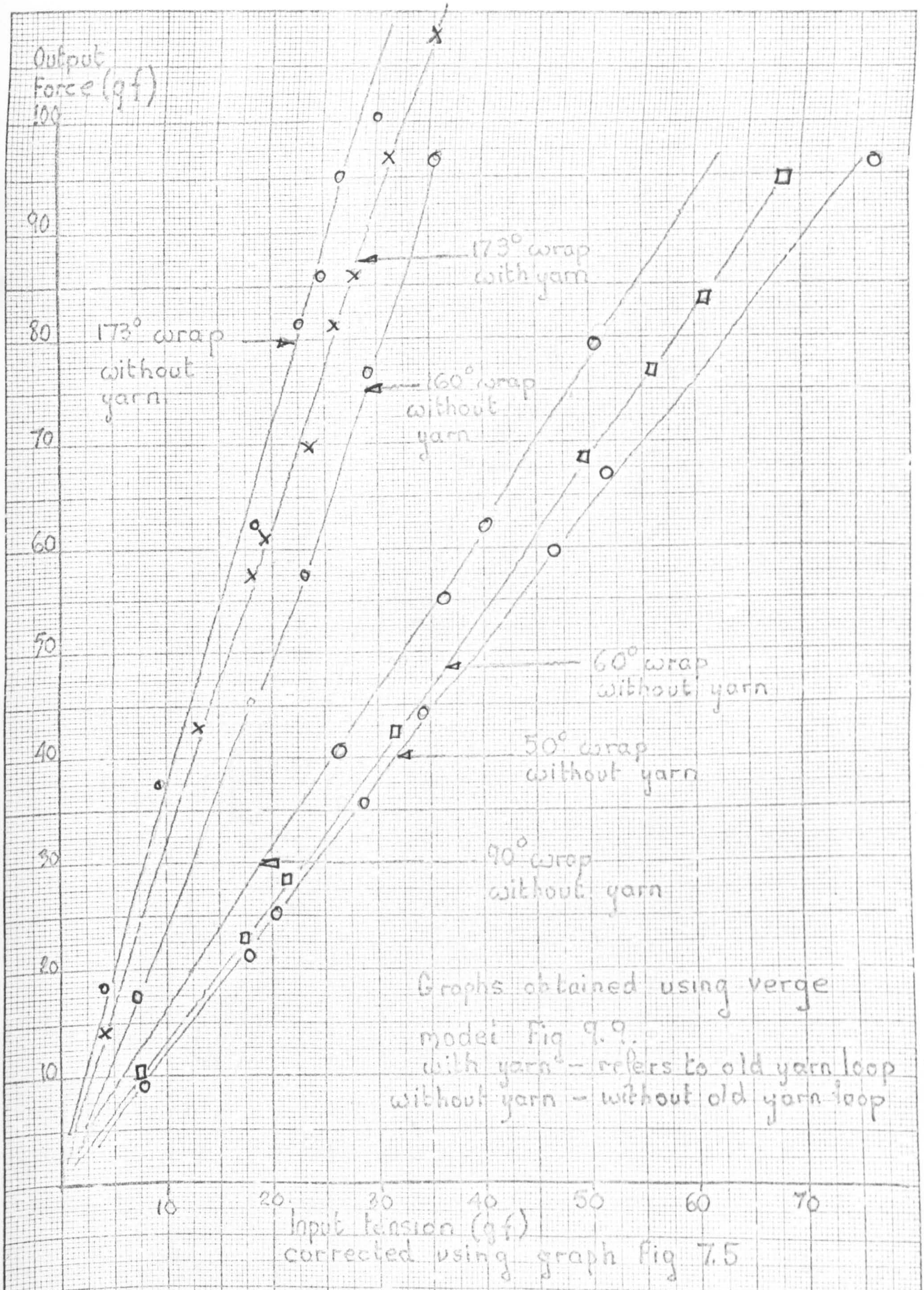

YARN TENSIONS OVER MODEL VERGE SHOWN IN FIG 9.9 FIG 9.10

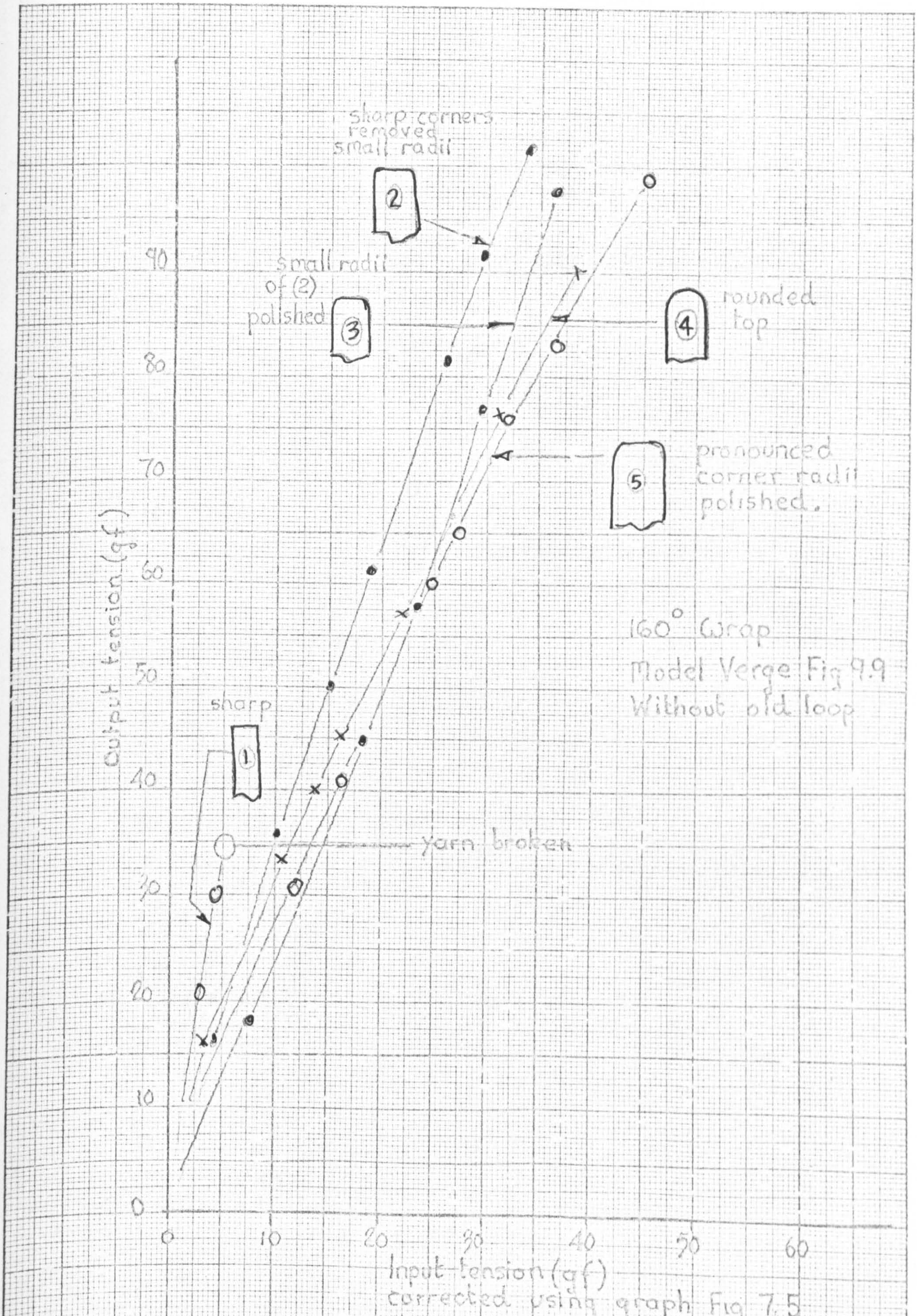

EFFECT OF VERGE SURFACE UPON YARN TENSIONS FIG 9.11

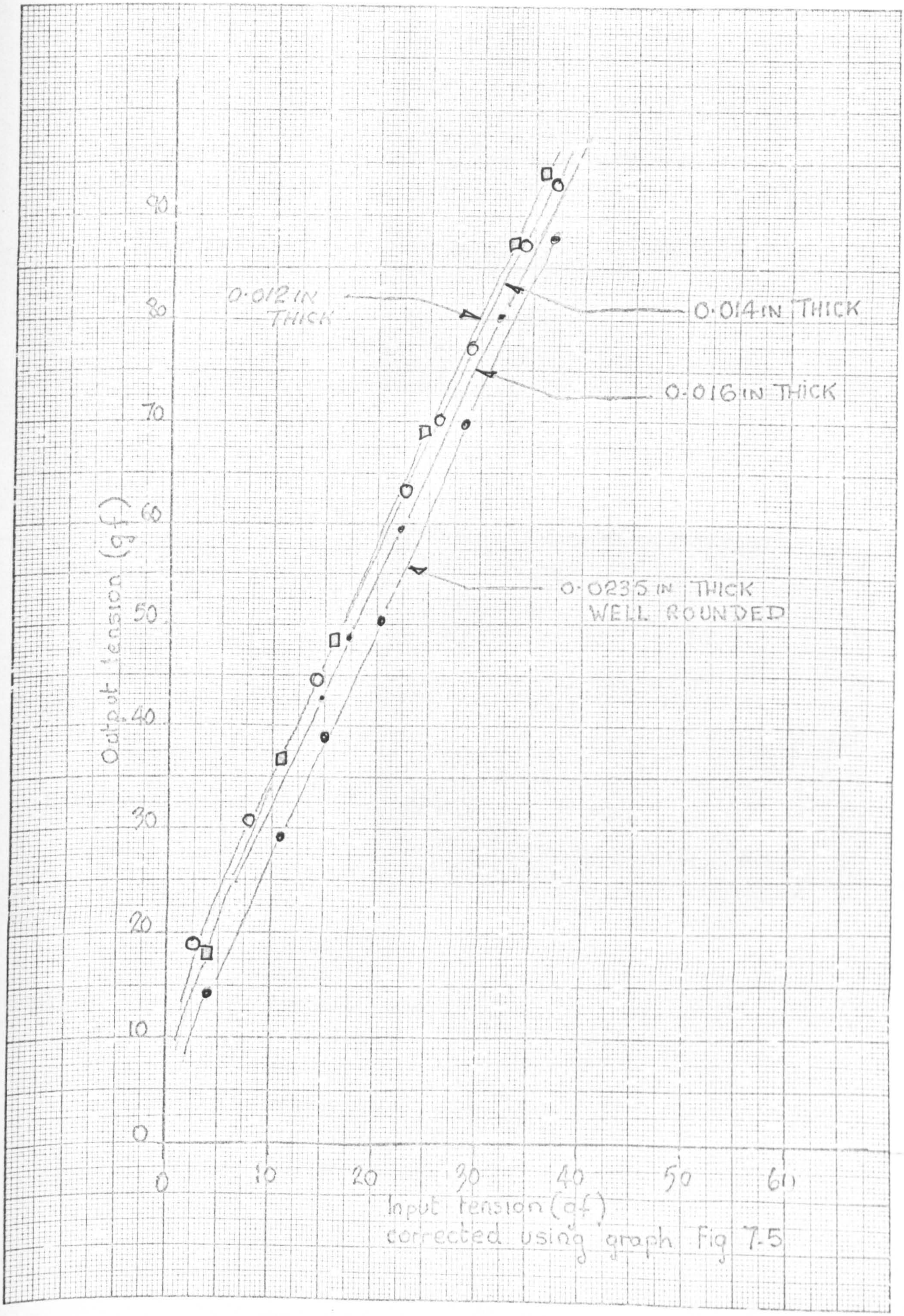

EFFECT OF VERGE THICKNESS UPON YARN TENSIONS

FIG 9.12.

DIAGRAM I

Measurement
of $P + 4^{Q} - mg$

46 gf

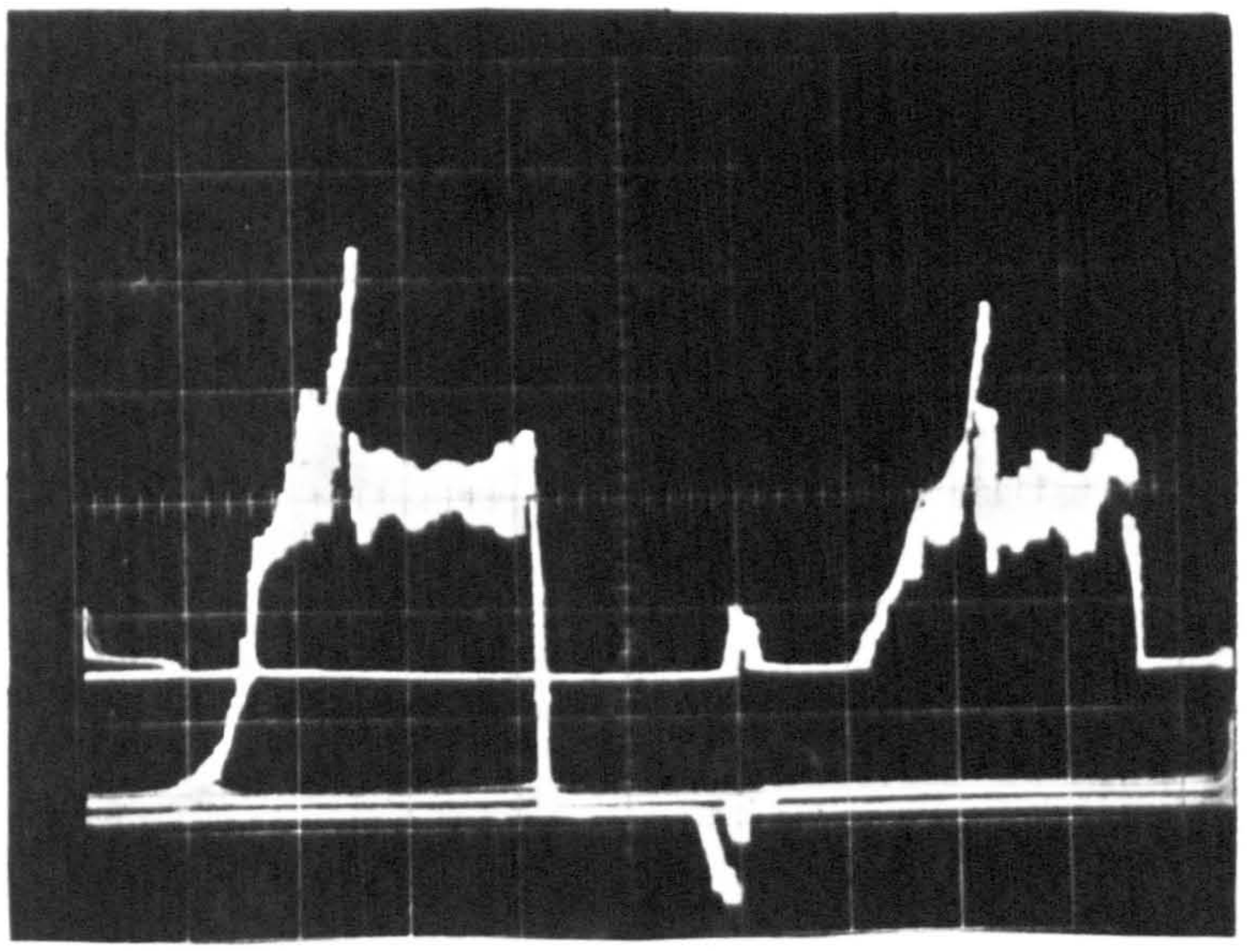

DIAGRAM II

Vértical cam-force

60 gf

0

0

85 gf

Horizontal cam-force

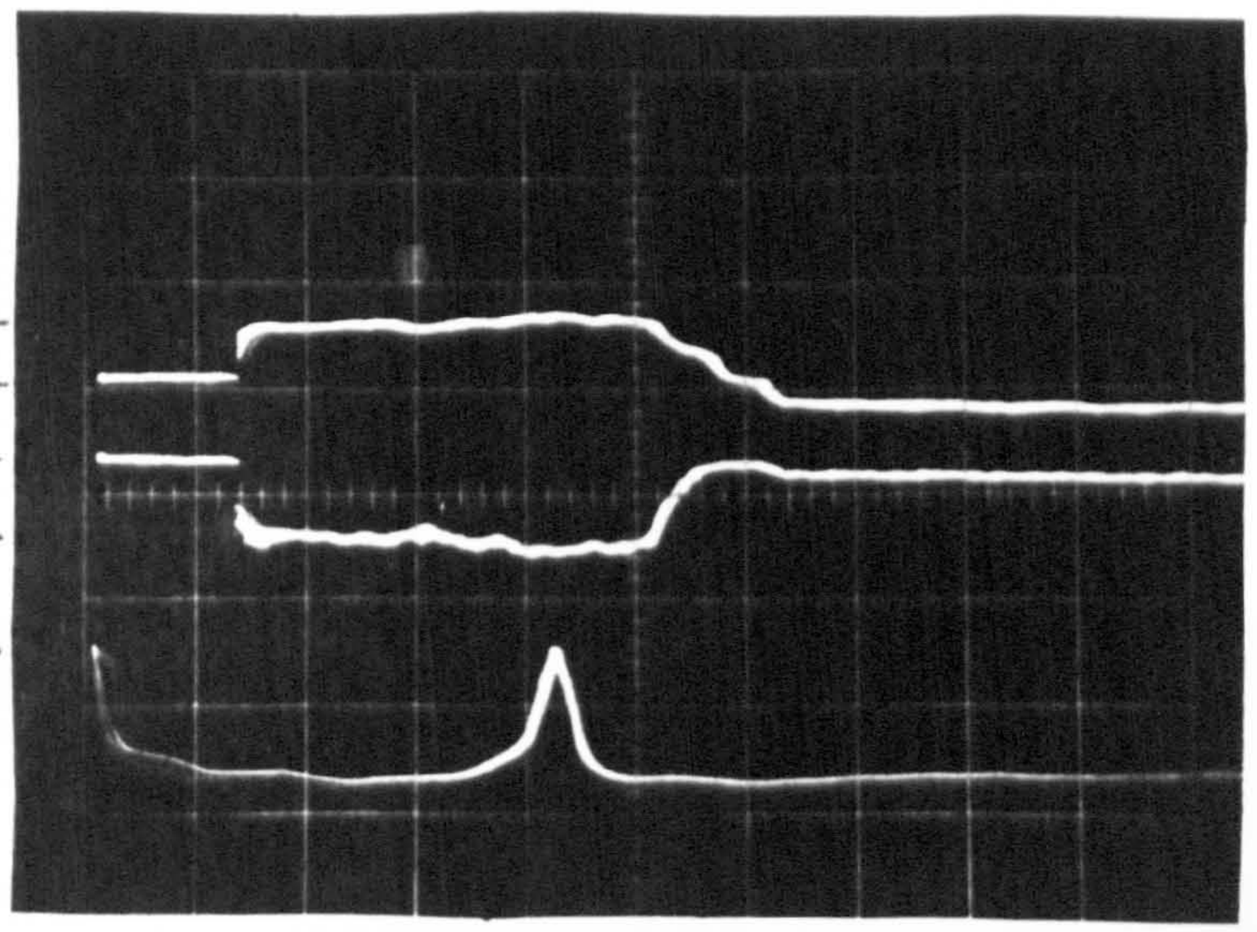

Parameters for Diagram II

Horizontal Calibration = 140 gf/10 mm.
Vertical Calibration = 140 gf/10 mm.
Time-scale = 10 mS/8.5 mm.
Speed = 8.92 in/sec (13.6 m/min)
Cam-cylinder clearance = 0.15 mm (0.006 in.)
Standard .0175 in. needle in trick.
Cam-profile Fig 4.3

MEASUREMENT OF CAM-FORCE
FOR THEORETICAL COMPARISON

Fig 9.13

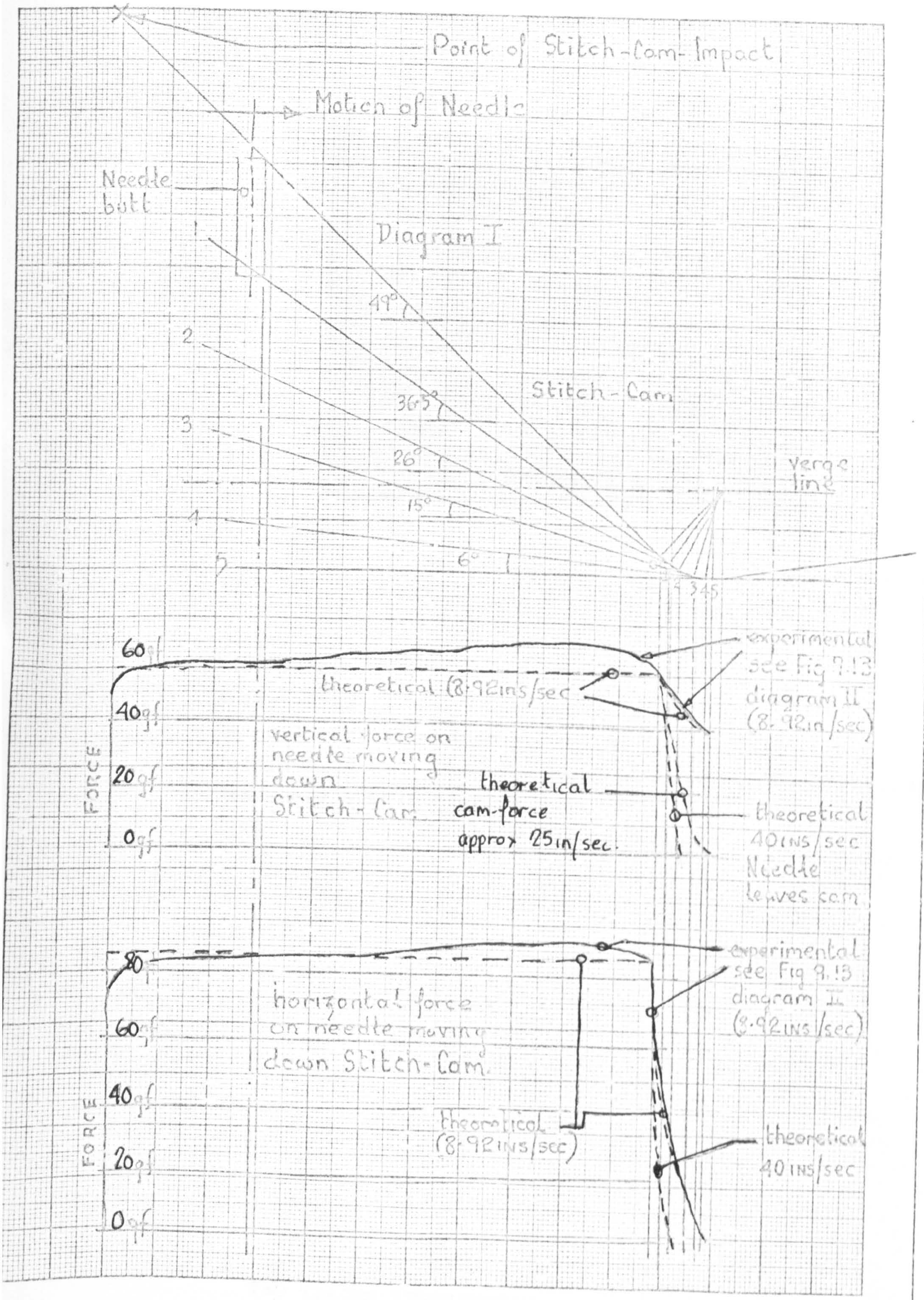

CAM-FORCE - (THEORETICAL COMPARISON)

FIG 9.14.

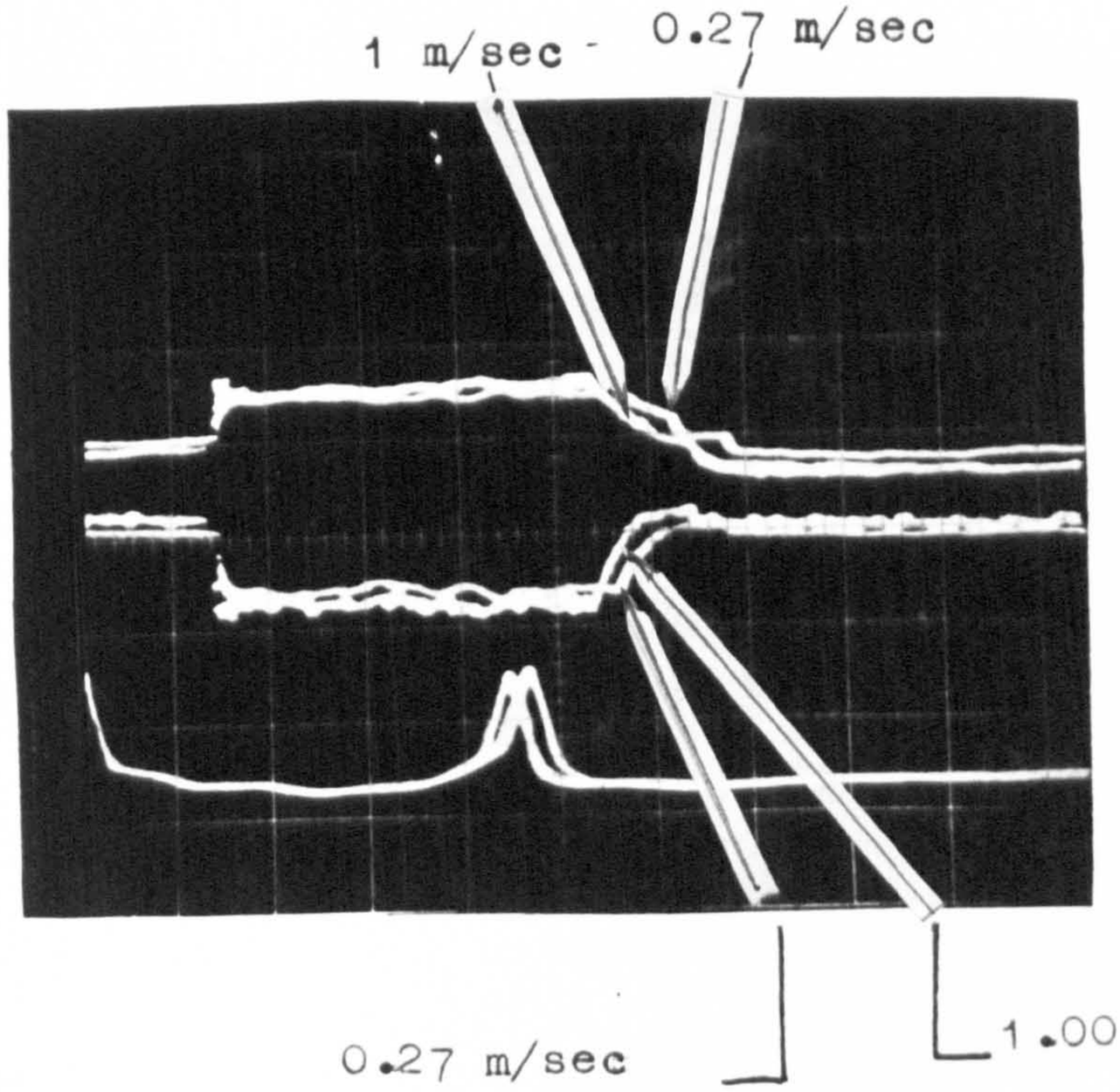

Parameters

Stitch-draw	= 1.7 mm (0.067 in.)
Cam-cylinder clearance	= 0.15 mm (0.006 in.)
Needle-type	= 0.443 mm (0.0175 in.)Standard.
Cam shape specified on	Fig 4.3
Time	= 10. mS/8.5 mm.

TWO TRACES SUPERIMPOSED ONE
AT 1.00 m/sec AND ONE AT 0.27 m/sec.

Fig 9.15

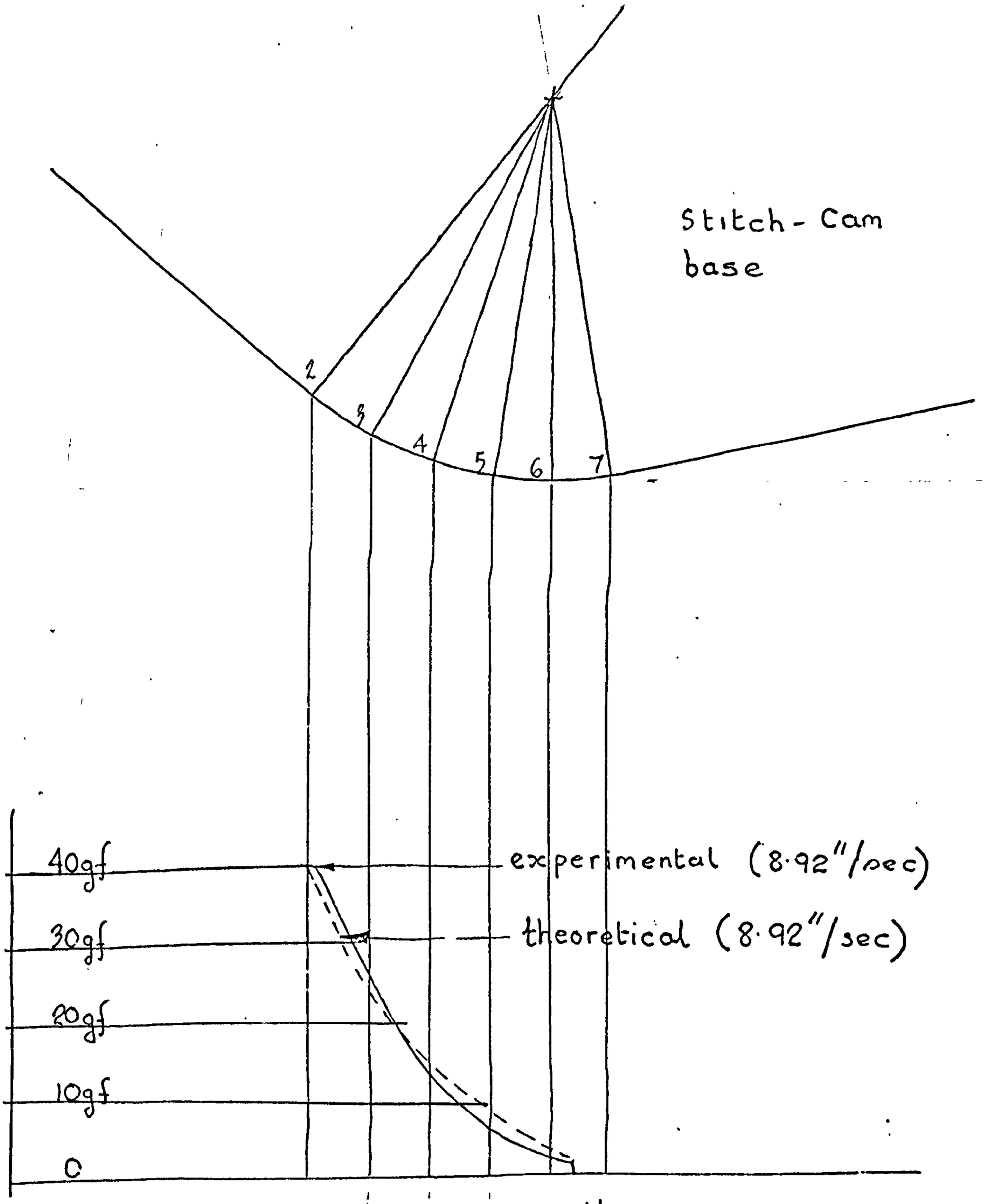

Horizontal force on needle moving down Stitch - Cam.

CAM - FORCE (THEORETICAL COMPARISON) USING 0·406 mm (0·016") NEEDLE

FIG 9.16

$$A = P + \mu_1 Q - mg$$

where P = trick clamping force
μ_1 = coefficient of friction trick to needle
Q = band-spring force
mg = needle weight.

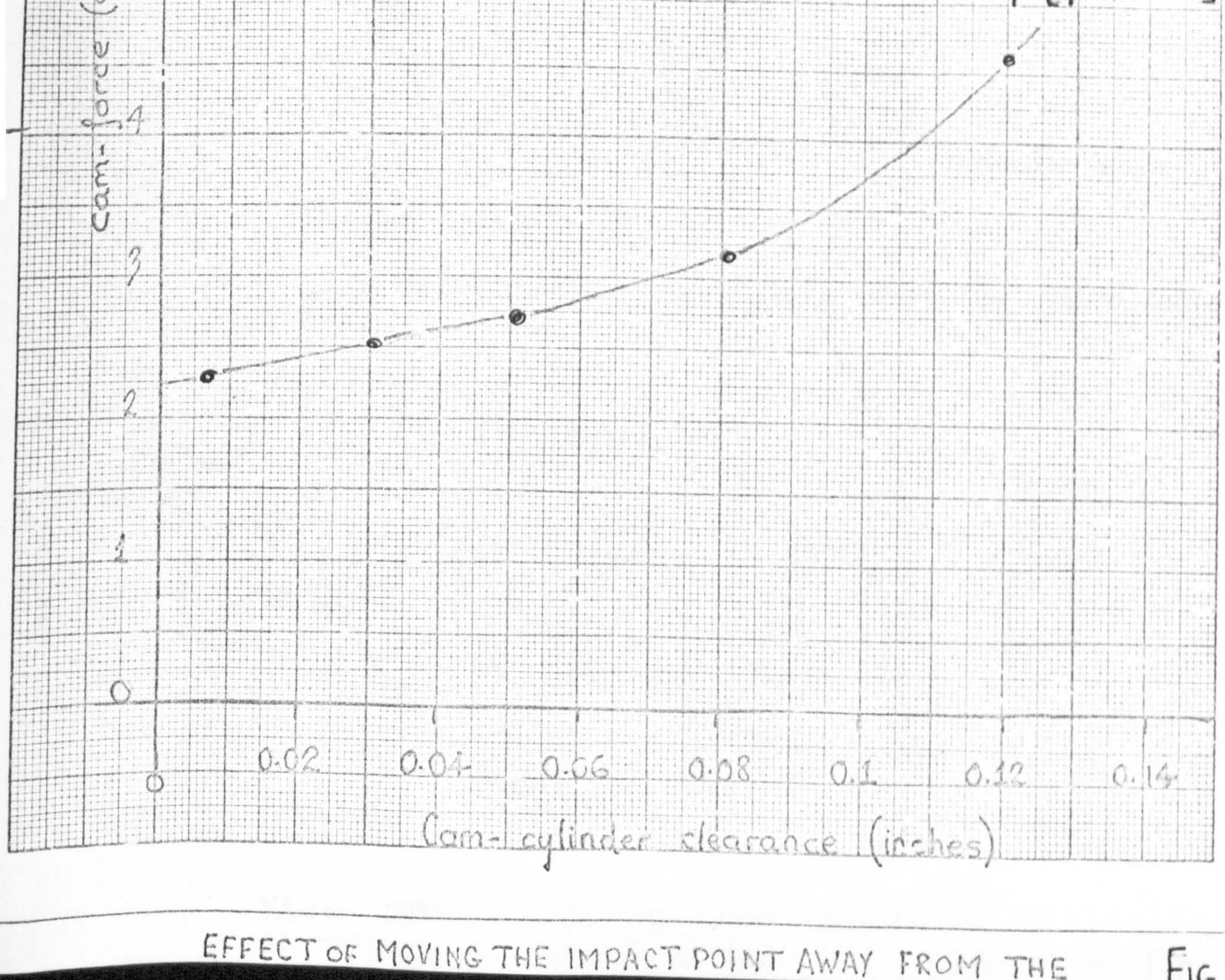

EFFECT OF MOVING THE IMPACT POINT AWAY FROM THE

FIG 9.17

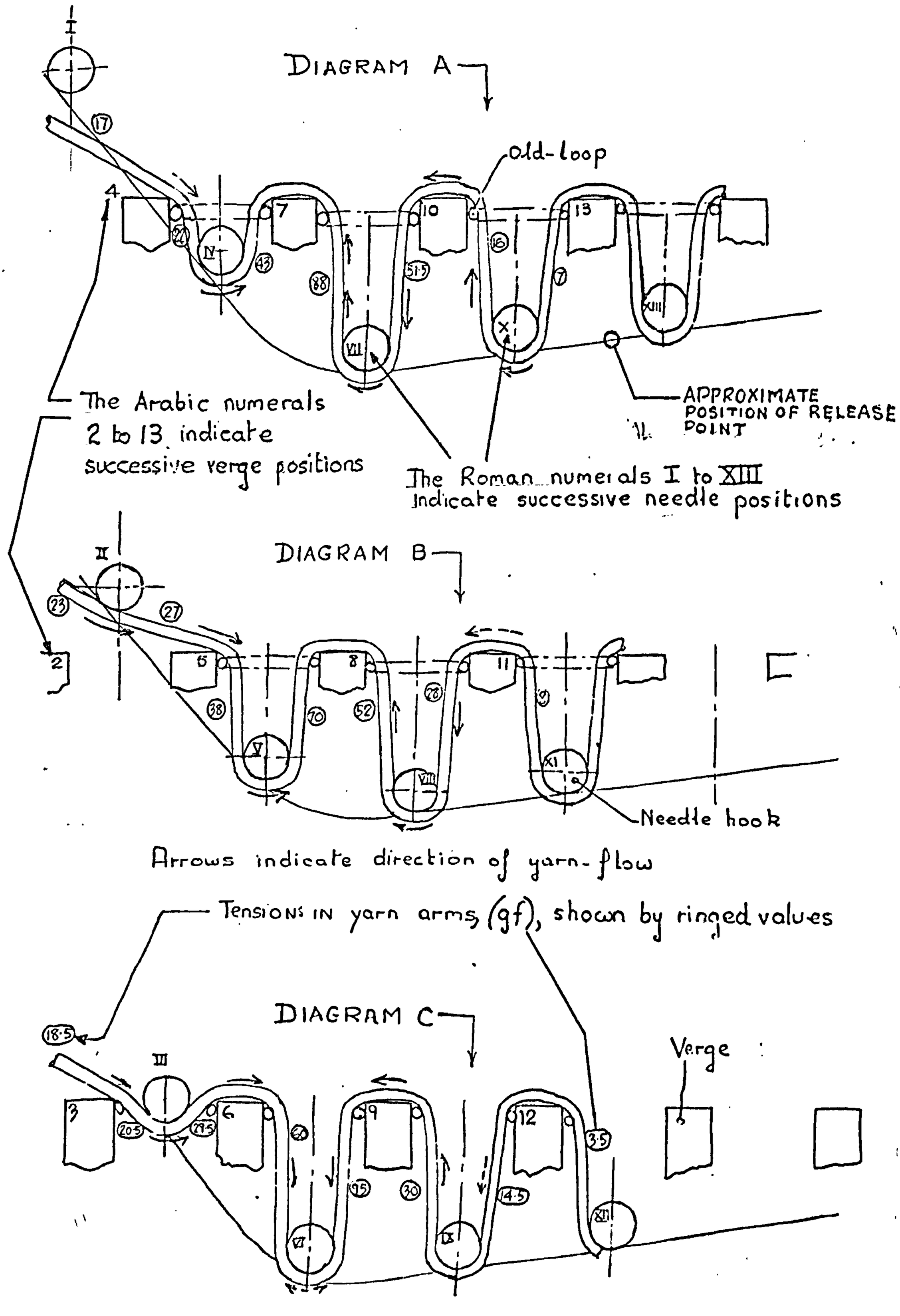

YARN-TENSIONS DURING LOOP FORMATION.
IN SUCCESSIVE STAGES OF ONE-THIRD VERGE PITCH FIG 9.18

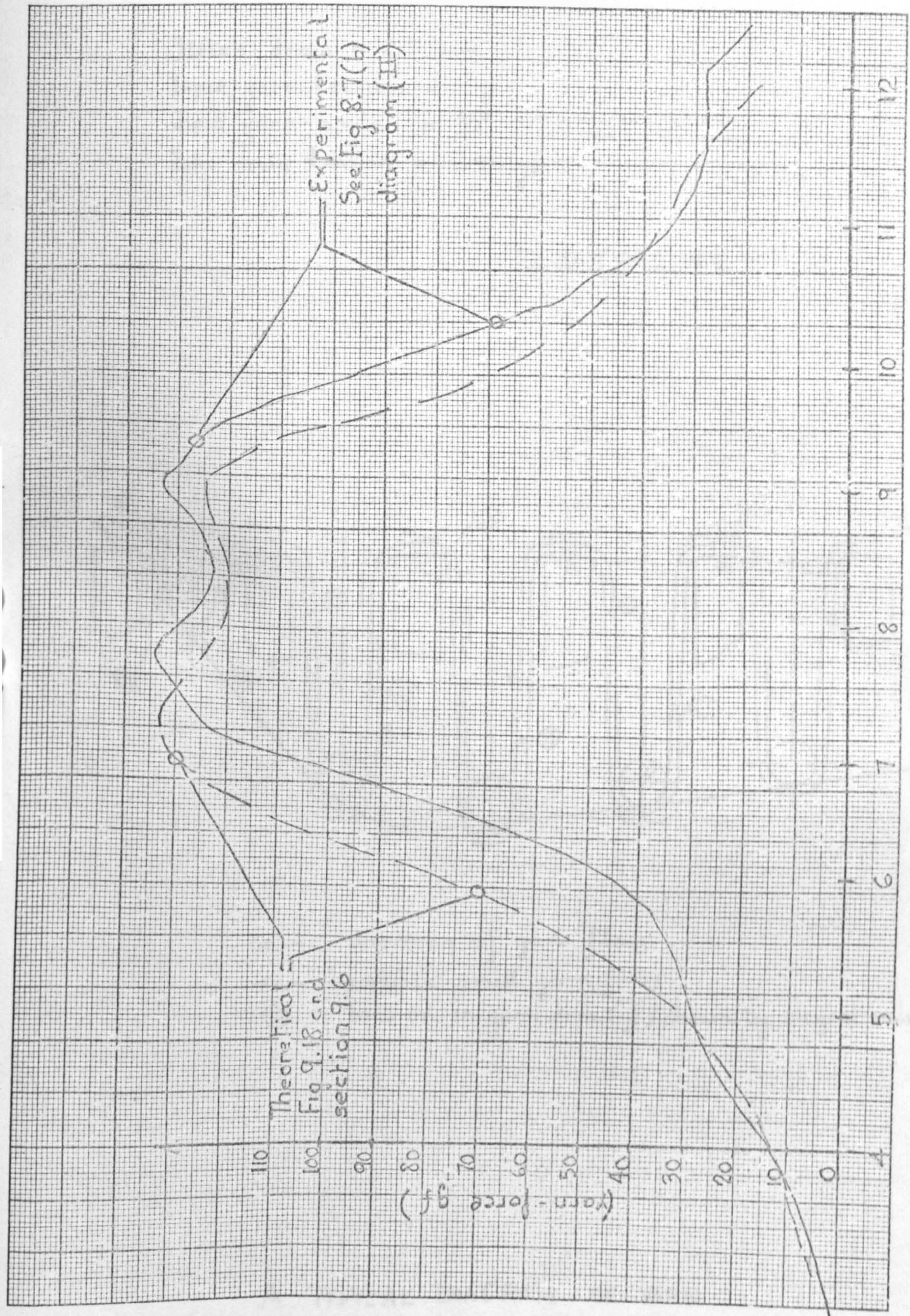

STITCH - DRAW = 0.067 IN

YARN - FORCE ON VERGE DURING LOOP FORMATION

FIG 9.19

Stitch-draw = 2·74mm
Input yarn-tension = 13gf
Input yarn-angle = 30°
Take down tension = 2,461gf.

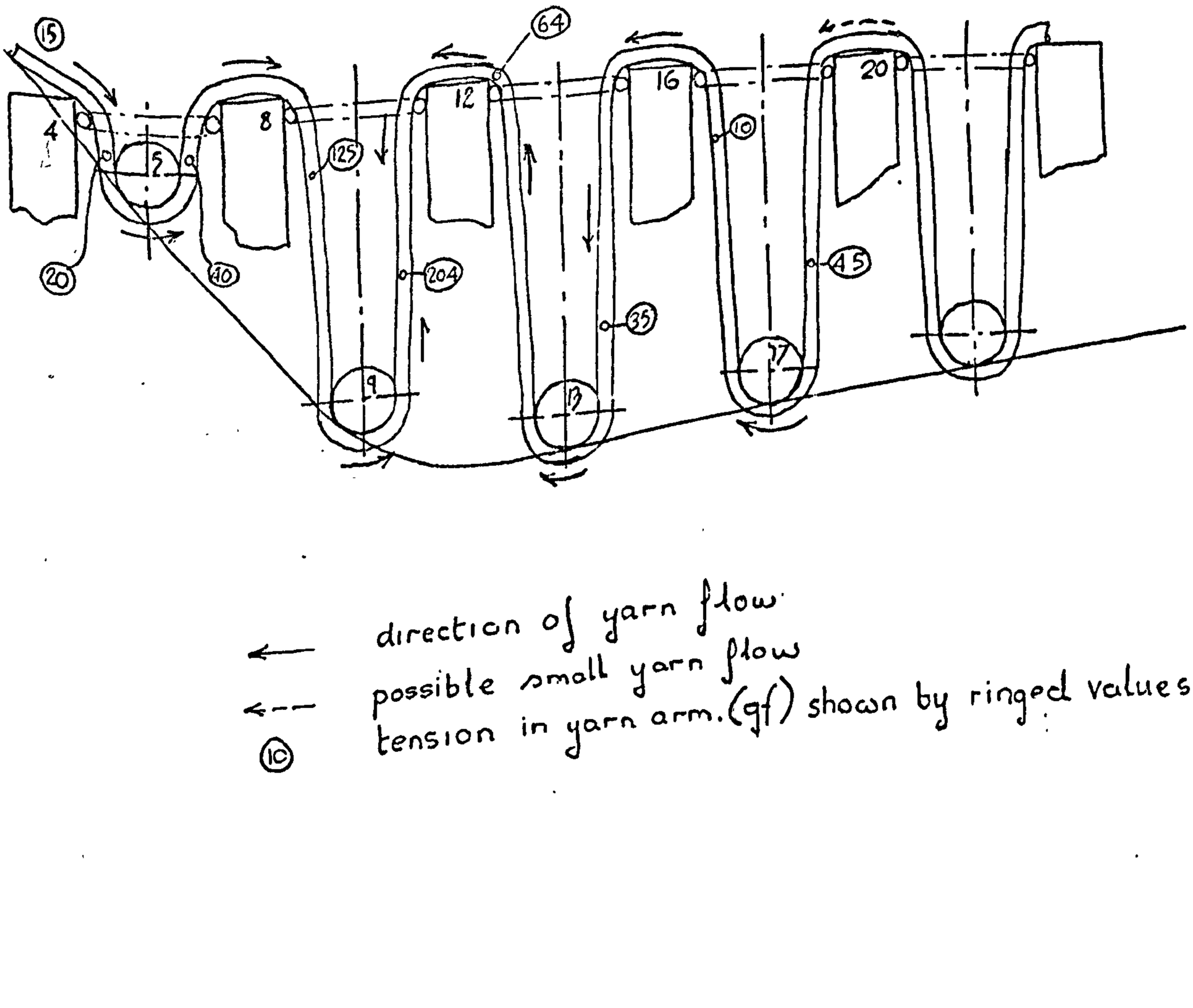

A TYPICAL DIAGRAM OF YARN TENSION DURING LOOP FORMATION

FIG 9.20

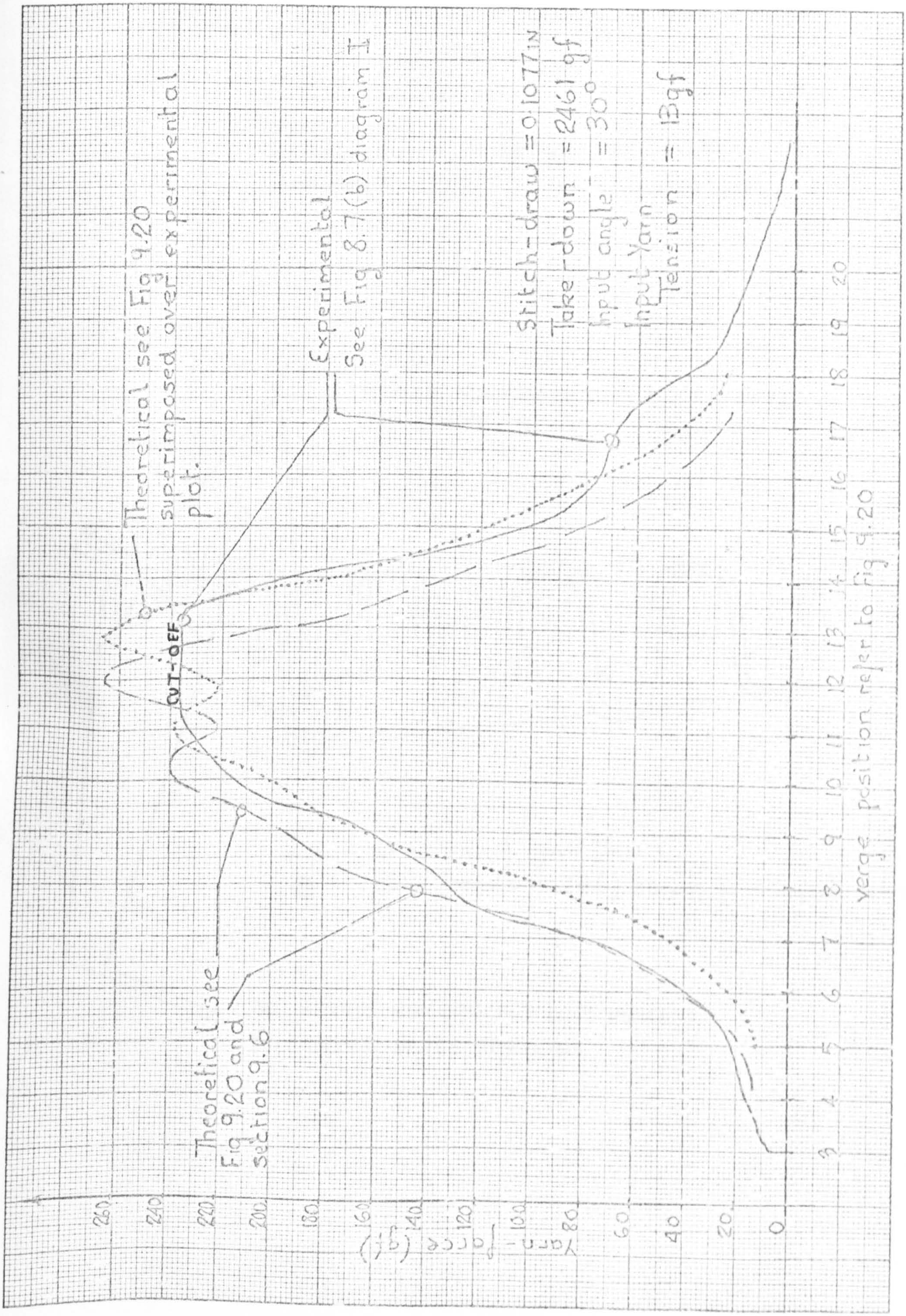

YARN-FORCE ON VERGE DURING LOOP FORMATION
STITCH-DRAW = 0.1077 IN.

FIG 9.21

Stitch-draw = 1·7mm
Input tension = 5gf
Take-down = 4.437 gf
Input angle = 30°

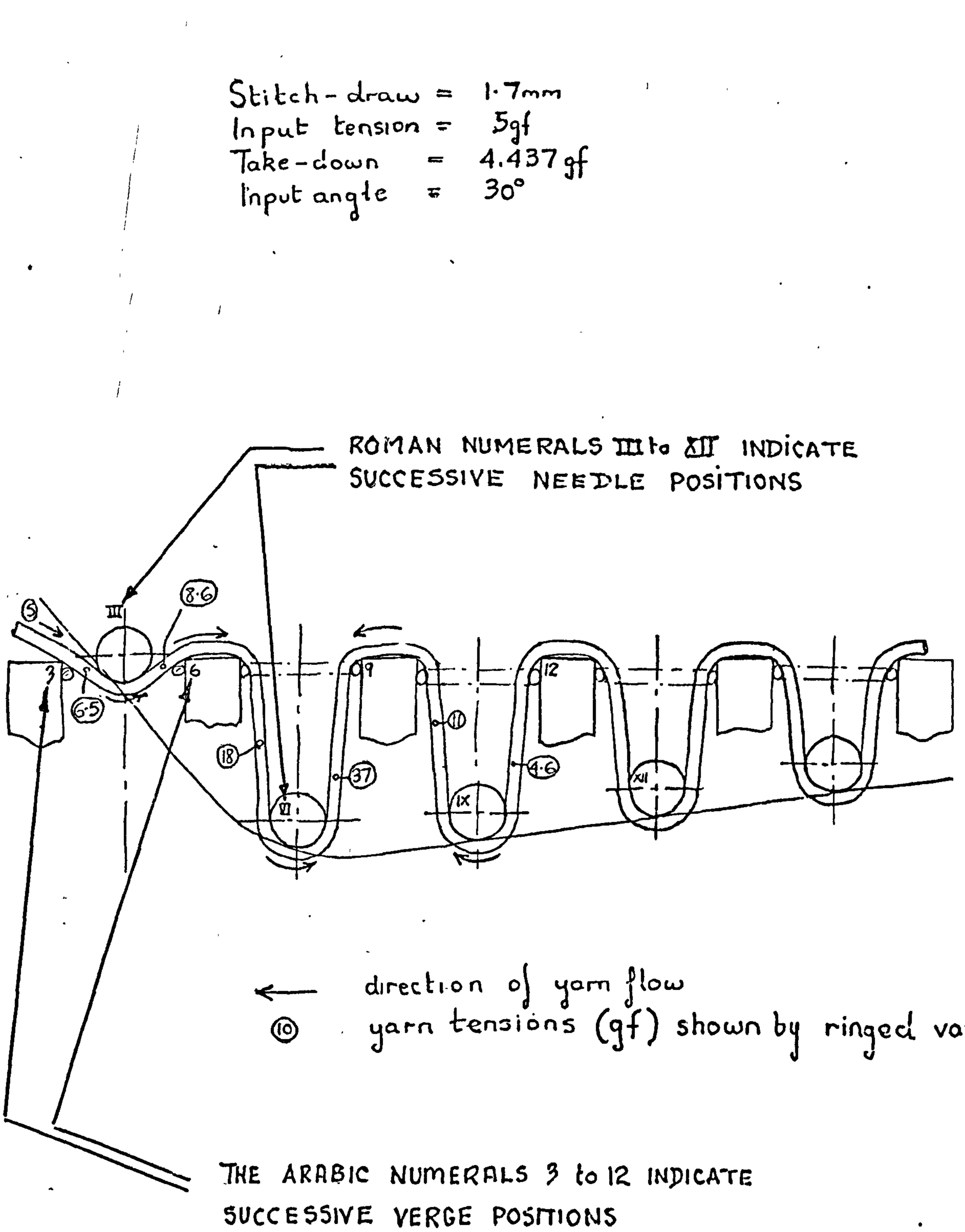

A TYPICAL DIAGRAM OF YARN TENSION DURING LOOP FORMATION.

FIG 9.22.

YARN-FORCE ON VERGE DURING LOOP FORMATION
STITCH-DRAW = 0.067 IN YARN-INPUT TENSION 5gf

Stitch draw=0.067 IN
Input-tension= 5gf
Take-down = 1437 gf
Input angle = 30°

Experimental See Fig 8.13 (b) diagram III

(2)

Theoretical Fig 9.22 and section 9.6

Yarn tension (gf)

100
90
80
70
60
50
40
30
20
10
0

3 4 5 6 7 8 9 10 11 12 15

Verge position refer to Fig 9.22

Fig 9.23

THEORETICAL CAM-FORCE (IN REGION OF LOOP FORMATION COMPARED) TO EXPERIMENTAL RESULTS

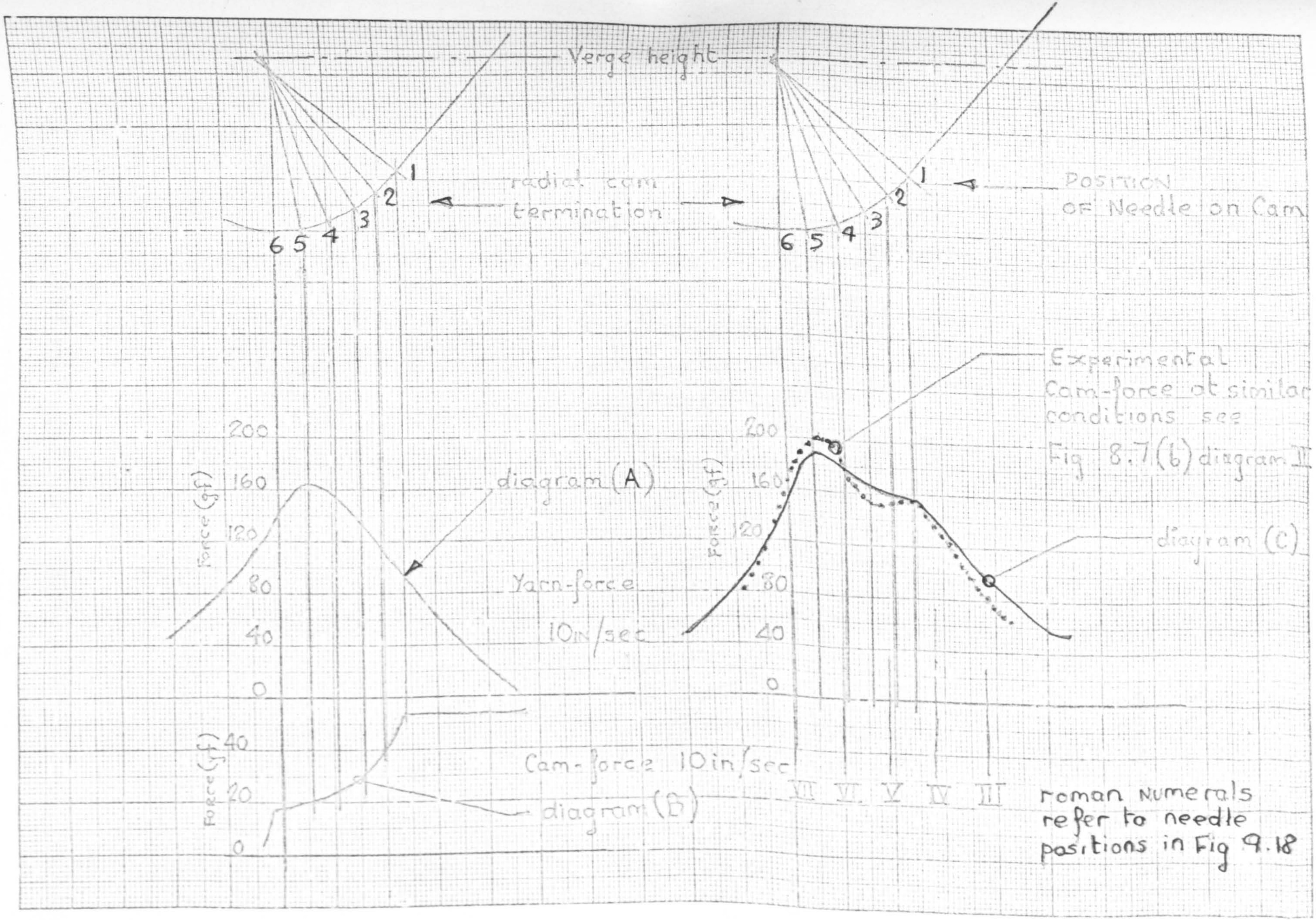

Fig 9.24

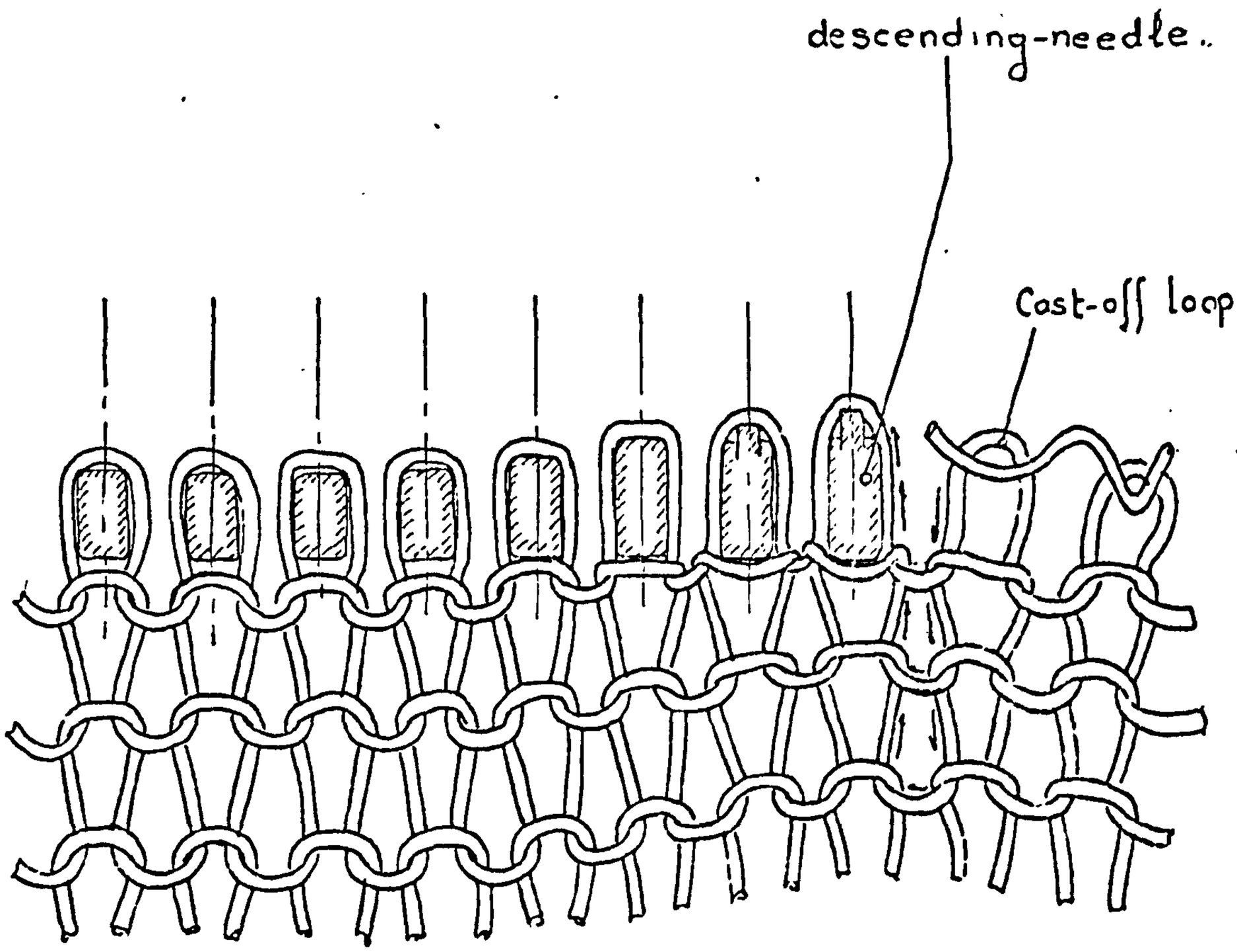

CASTING - OFF A TIGHT LOOP.

Fig 9.25

Test on 0·443 mm needle.
Stitch - draw = 1·7mm.
Yarn - input tension =
Fabric take-down tension =

Traces shown are reproduced from the photographs.

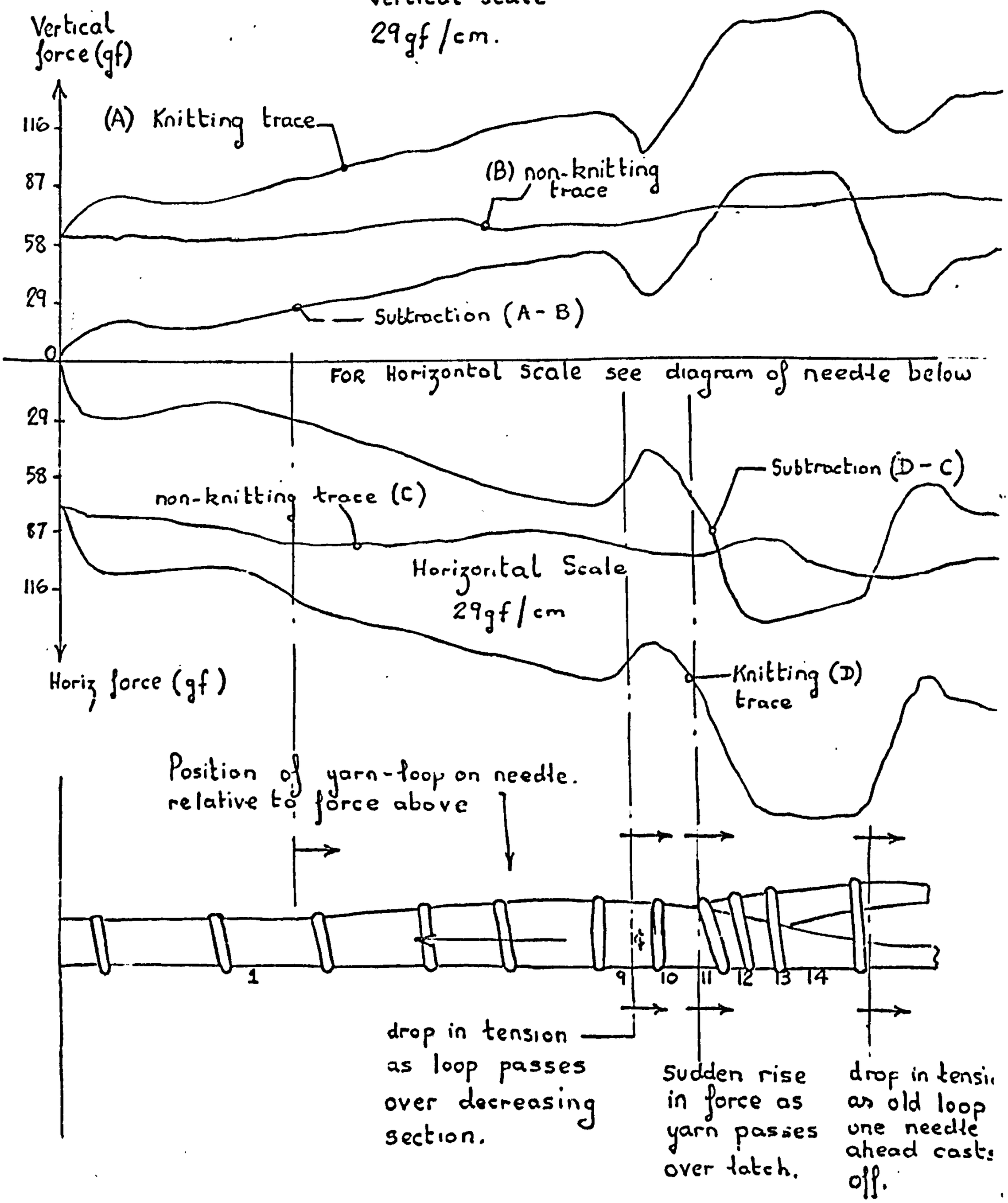

Expansion of Loop over Needle Head.

FIG 9.26

CHAPTER 10

CONCLUSIONS TO PART (C)

10.1 Brief Summary of some of the Important Results Contained in Chapter 9.

A theoretical analysis by Knapton[13,14] was used as a basis for the derivation of a cam-force equation(22) in section 9.2. Predictions from the analysis were compared to the experimental results detailed in chapter 8, and a reasonably close degree of similarity was found, as detailed in section 9.5.

A friction testing apparatus shown in Fig 7.4 was built to examine the tension build-up as the yarn passed over the needle and verge elements. From the experimental results detailed in section 9.4, equations(31) and(32) were derived. Subsequent experiments, also described in section 9.4, demonstrated how the verge shape and surface texture could greatly influence the frictional tension-build-up. It was concluded that, due to the complexity in deriving and using equations(31)and (32)and to their limited range of application, it would be better to build a simple friction testing device for the majority of the work requiring a knowledge of the frictional tension increase. Apparatus similar to that shown in Fig 7.4 could be used to measure the tension increase under representative conditions, rather than rely on an equation with limited application.

The theoretical prediction of yarn-tension during the loop-drawing process was carried out using an iteration technique based upon conservation of yarn-flow. Although difficulties were found in using the technique, the theoretical

solutions showed a reasonably good degree of similarity when compared to the experimental results. The experimental and theoretical comparison is covered more fully in section 9.6.

Experimental results aimed at determining the effect of the stitch-draw, see Fig 8.7 (b) and section 8.5.1, showed that the cam-force was considerable when casting-off a tight loop. The analysis in section 9.8.1 showed that it was possible to relate the shape of the cam-force trace to the shape of the needle head, but a prediction of force magnitudes was not carried out due to the difficulty in determining the yarn tensions in the old loop when expanding over the head.

10.2 Recommendations Resulting from the Analysis carried out in Chapter 9.

The experimental results shown by Figures 8.16 (a) and 8.16 (b) demonstrated that, as machine speed increased, the cam-force changed little in magnitude unless oil was applied to the trick. However, at higher machine speeds, an impact at the instant the needle contacted the stitch-cam became more prominent, and it grew in magnitude as the speed was further increased. The cam-force transducer Mark III, used throughout the experiments detailed in chapter 8, did not have a natural frequency sufficiently high to display the impact accurately, and another form of high natural frequency transducer would be required. This is discussed more fully in chapters 11 and 12. At this stage of the work it was considered likely that the magnitude of the impact force would be considerably higher than the slower changing cam-force recorded by the transducer MarkIII, and subsequent experiments, detailed in chapters 14 and 15, confirmed this view. It was unlikely that a reduction in the slower varying cam-force, analysed in chapter 9, would lead to a

reduction in the needle damage at the head and butt.

However, there were other reasons for reducing the cam-forces, especially at high speed, namely :-

(i) To minimise the frictional heat generated at high speed.

(ii) To minimise cam-wear; this is especially important when non-linear cams are used.

The factors, formulated in equation(22) section 9.2, that control the cam-force magnitude are summarised below :-

(i) The application of relatively large amounts of highly viscous oil at irregular intervals can lead to severe needle damage due to the sudden increase in the cam-force; this could be especially damaging at high machine speeds. A better system would be the application of equally distributed low viscosity oil.

(ii) Lower cam-forces are achieved when the cam-cylinder clearance is a minimum.

(iii) The experiments detailed in section 8.5.8 showed that the trick properties were highly variable. Variation in the trick-resistance to motion is undesirable, because it leads to non-uniformity in stitch-formation, as is discussed later in this section. However, under normal machine operating conditions, tricks are inevitably bound to be damaged, and it is impossible to ensure trick uniformity on conventional machines.

(iv) The cam-forces are very dependent upon the cam-angles and the friction coefficients. From equation(22) in section 9.2.1 it can be seen that,

when $\cos\theta\left(1-\alpha\mu_1\mu_2\right) = \sin\theta\left(\mu_2+\alpha\mu_1\right)$,

then the reaction-force between the cam and needle

theoretically becomes infinite and needle damage is unavoidable. If the cam-cylinder clearance is small, then α is very nearly equal to 1, and, using the values for the friction coefficients defined in section 9.3, the angle that theoretically leads to infinite cam-force is evaluated below :-

$$\tan\theta = \frac{1 - \mu_1\mu_2}{\mu_1 + \mu_2} \quad . \quad . \quad . \quad (49),$$

where $\mu_1 = 0.125$ and $\mu_2 = 0.135$,

and $\theta = 75^\circ$

Obviously, to avoid high cam force magnitudes, the camangles must be considerably less than 75°.

(v) As the needle thickness in the trick was reduced, the trick resistance to needle motion decreased, and the cam-force became considerably smaller in magnitude. However, the incidence of needle damage caused by it protruding from the trick and fouling the cams increased considerably as the needle thickness was reduced.

Variation in trick resistance to needle motion leads to non-uniformity in stitch formation. The magnitude of the inertial force is controlled by the needle mass and the cam-profile. When the needle-cam reaction force reduces to zero, the needle leaves the stitch-cam and moves over to the guard-cam. The trick resistance is a large component of the reaction force and, since it is variable from one trick to another, then the reaction force is also variable. The exact position at which the inertial force cancels out the reaction force will be different for each needle in each trick; this means that particular needles will lose contact with the cams at different positions. Since the subsequent needle motion is very dependent upon trick resistance, none of the needles

strike the guard cam at exactly the same point. The resulting variation in needle motion means that the stitch formation process is slightly different for each needle; this leads to stitch non-uniformity. A number of obvious methods can be used to eliminate the non-uniformity as detailed below :-

(i) The use of closed cam-tracks. The tracking must be designed for minimum clearance when the needle passes around the bottom of the stitch-cam.

(ii) The use of flat-bottomed cams. If the clearance between the stitch-cam and the guard-cam is minimised to just allow the needle to pass through the flat region, then all the needles must follow the same path and the stitch formation process is identical for all the needles.

(iii) Design of the cam-termination to produce a controlled inertial force. The profile can be designed so that, even with the minimum trick-resistance to motion, the needle will not leave the cam until a precise position is reached.

(iv) A positive yarn-feed system can be used to control the amount of yarn fed to each needle during loop formation.

The design of cams using the results obtained from chapters 8 and 9 and from chapters 14 to 21 inclusive, is carried out in considerably more detail in chapter 23.

A major factor that could have contributed to variation of the yarn-tension traces was the variation in the input yarn-tension. It is important that the yarn input tension is low because this reduces the loop-drawing forces. Kopel[32] states that it is important that the input tension is controlled at a constant low value.

A reduction of the loop drawing forces could be achieved

by rounding off the surface of the verge as this would result in a decrease in the frictional tension build-up over it. It was shown, during the analysis detailed in section 4.4.2, that the major limitations to the knitting of very small stitches were in the shape of the needle head and in the stretch of the old loop as it passed over the head. When the old loop had reached a precise position on the latch, the needle one verge-pitch further into the loop formation process had cast-off its loop and consequently made available some yarn which relieved the tension in the loop expanding over the latch. A tentative proposal for the design of a needle head to minimise the force required to cast-off the old-loop is shown in Fig 10.1. On this needle, the major component of yarn stretch occurs when the needle one pitch further into the loop-formation process has already cast off its loop.

Further work concerning the design of the needle, and utilising the results obtained in chapters 8,9 and 14 to 21, will be given in chapter 24.

10.3 Possible Improvements in the Measuring Apparatus.

The verge yarn-force transducer worked very well and no improvement in design was considered necessary. The beam of the cam-force transducer Mark III was a separate component fitted into the supporting bracket but, to simplify the manufacturing procedure, it was considered more advantageous to make the beam and bracket as one part. The material used for the cam-force transducer was steel; a better material would have been aluminium, since a beam could then be manufactured with the same strain sensitivity as a steel beam but with a higher natural frequency due to the decreased mass. However, the improvement in the natural frequency would not be very large because the cams at the end of the

beam have a much larger effect upon the frequency than has the beam material.

The above suggestions for improvements to the cam-force transducer were used in the design of the impact transducer detailed in chapter 13.

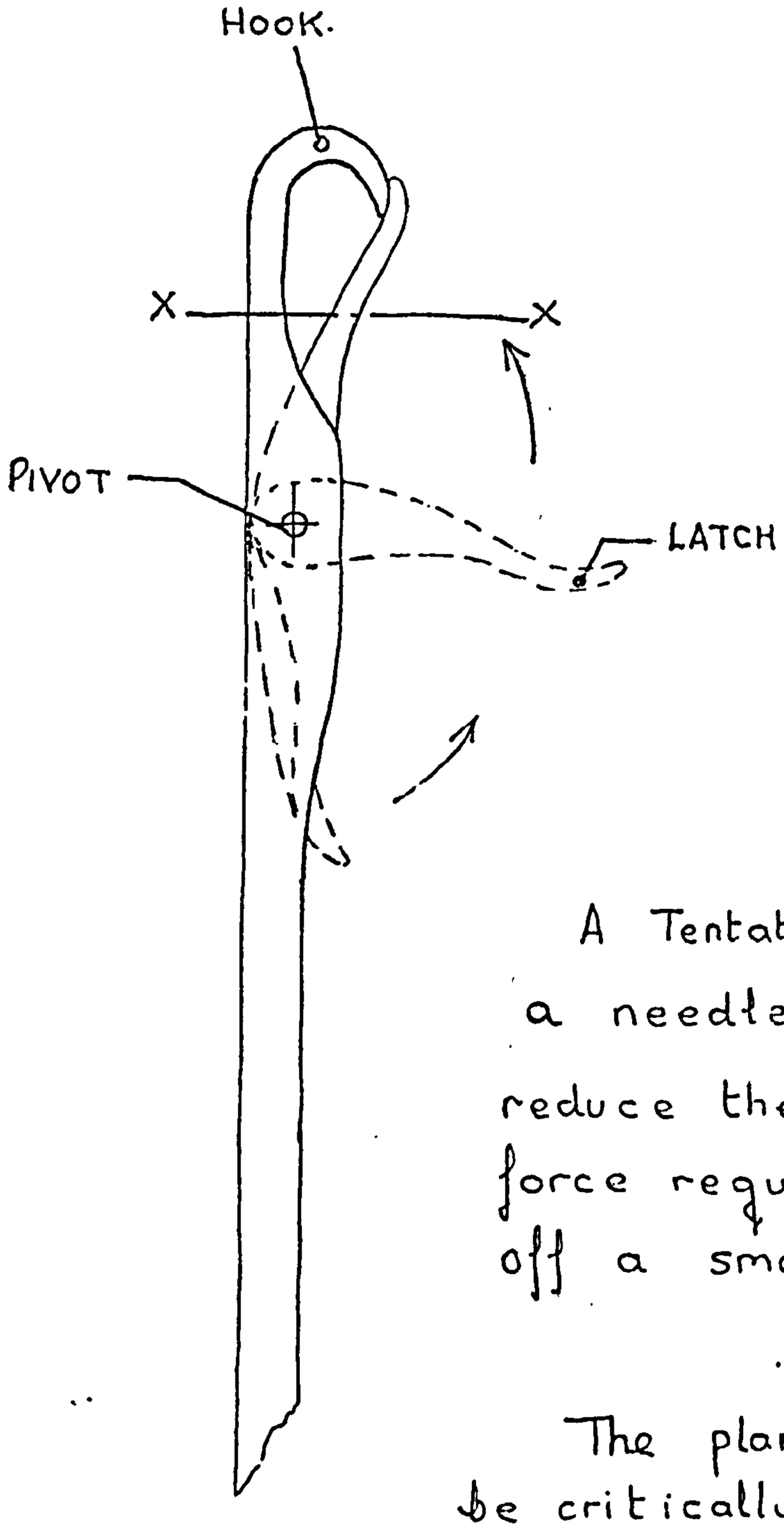

A Tentative suggestion for a needle design to reduce the high cam-force required to cast-off a small yarn loop.

The plane X-X must be critically chosen so that the yarn from the cast-off loop of the needle one pitch further into the loop forming process can be robbed to relieve the tension in the expanding loop after X-X.

NEEDLE DESIGN. FIG 10.1